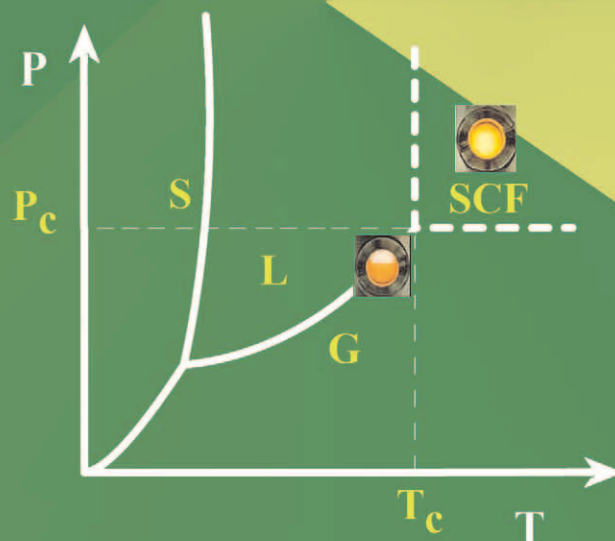
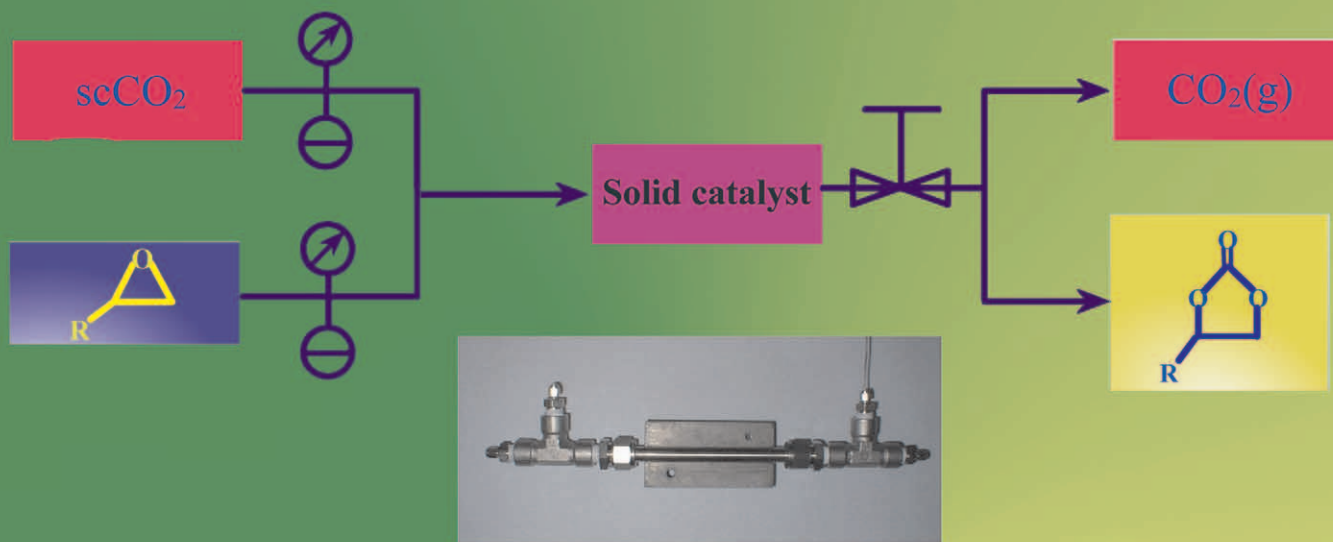


Green Chemistry

Cutting-edge research for a greener sustainable future

www.rsc.org/greenchem

Volume 7 | Number 7 | July 2005 | Pages 481–560



ISSN 1463-9262

RSC | Advancing the
Chemical Sciences

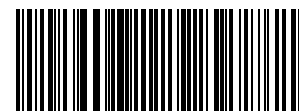
Anlian Zhu *et al.*
Aldol reactions without solvent using
an ionic liquid as catalyst

Xingfa Ma *et al.*
Water soluble poly(aniline) and its
potential application in gas sensors

Chinese Science

COVER ARTICLE

Ya Du *et al.*
Ion exchange resins as catalysts
for propylene carbonate synthesis



1463-9262(2005)7:7;1-9



JEM

Journal of Environmental Monitoring

Comprehensive, high quality coverage of multidisciplinary, international research relating to the measurement, pathways, impact and management of contaminants in all environments.

- Dedicated to the analytical measurement of environmental pollution
- Assessing exposure and associated health risks
- Fast times to publication
- Impact factor: 1.186
- High visibility - cited in MEDLINE



IN THIS ISSUE

ISSN 1463-9262 CODEN GRCHFJ 7(7) 481–560 (2005)

In this issue...

New editorial board member:
Professor Buxing Han



Chemical biology articles published
in this journal also appear in the
Chemical Biology Virtual Journal:
www.rsc.org/chembiol



Cover

Cyclic carbonates have been produced on an industrial scale for over 40 years. The reaction depicted uses supercritical carbon dioxide as both reagent and solvent, and insoluble ion exchange resins as catalysts.

Image reproduced by permission of Liang-Nian He from *Green Chem.*, 2005, 7(7), 518.

CHEMICAL TECHNOLOGY

T25

Chemical Technology highlights the latest applications and technological aspects of research across the chemical sciences.

Chemical Technology

July 2005/Volume 2/Issue 7

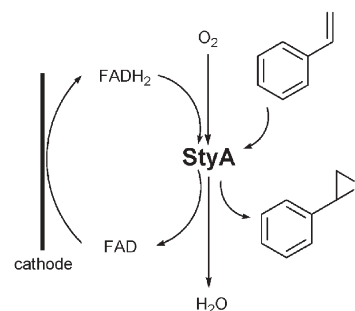
www.rsc.org/chemicaltechnology

HIGHLIGHT

489

Highlights

Markus Hölscher reviews some of the recent literature in green chemistry.



EDITORIAL STAFF

Editor

Harpal Minhas

Assistant editors

Nina Athey-Pollard, Merlin Fox, Katie Gibb

News writer

Markus Hölscher

Publishing assistant

Jackie Cockrill

Team leader, serials production

Stephen Wilkes

Technical editors

Katherine Davies, Christopher Ingle, Kathryn Lees

Administration coordinator

Sonya Spring

Editorial secretaries

Lynne Braybrook, Rebecca Gotobed, Julie Thompson

Publisher

Adrian Kybett

Green Chemistry (print: ISSN 1463-9262; electronic: ISSN 1463-9270) is published 12 times a year by the Royal Society of Chemistry, Thomas Graham House, Science Park, Milton Road, Cambridge, UK CB4 0WF.

All orders, with cheques made payable to the Royal Society of Chemistry, should be sent to RSC Distribution Services, c/o Portland Customer Services, Commerce Way, Colchester, Essex, UK CO2 8HP. Tel +44 (0) 1206 226050; E-mail sales@rscdistribution.org

2005 Annual (print + electronic) subscription price: £795; US\$1310. 2005 Annual (electronic) subscription price: £715; US\$1180. Customers in Canada will be subject to a surcharge to cover GST. Customers in the EU subscribing to the electronic version only will be charged VAT.

If you take an institutional subscription to any RSC journal you are entitled to free, site-wide web access to that journal. You can arrange access via Internet Protocol (IP) address at www.rsc.org/ip. Customers should make payments by cheque in sterling payable on a UK clearing bank or in US dollars payable on a US clearing bank. Periodicals postage paid at Rahway, NJ, USA and at additional mailing offices. Airfreight and mailing in the USA by Mercury Airfreight International Ltd., 365 Blair Road, Avenel, NJ 07001, USA.

US Postmaster: send address changes to Green Chemistry, c/o Mercury Airfreight International Ltd., 365 Blair Road, Avenel, NJ 07001. All despatches outside the UK by Consolidated Airfreight.

PRINTED IN THE UK

Advertisement sales: Tel +44 (0) 1223 432243; Fax +44 (0) 1223 426017; E-mail advertising@rsc.org

Green Chemistry

Cutting-edge research for a greener sustainable future

www.rsc.org/greenchem

Green Chemistry focuses on cutting-edge research that attempts to reduce the environmental impact of the chemical enterprise by developing a technology base that is inherently non-toxic to living things and the environment.

EDITORIAL BOARD

Chair

Professor Colin Raston,
Department of Chemistry
University of Western Australia
Perth, Australia
E-mail clrastron@chem.uwa.edu.au

Scientific editor

Professor Walter Leitner,
RWTH-Aachen, Germany
E-mail leitner@itmc.rwth-aachen.de

Professor Joan Brennecke,
University of Notre Dame, USA

Professor Steve Howdle, University of Nottingham, UK

Dr Janet Scott, Centre for Green Chemistry, Monash University, Australia

Dr A Michael Warhurst,
WWF, Brussels, Belgium

Professor Tom Welton,
Imperial College, UK
E-mail t.welton@ic.ac.uk

Professor Roshan Jachuck,
Clarkson University, USA
E-mail rjachuck@clarkson.edu

Dr Paul Anastas, Green Chemistry Institute, USA
Email p_anastas@acs.org

Professor Buxing Han, Chinese Academy of Sciences
Email hanbx@iccas.ac.cn

Associate editor for the Americas

Professor C. J. Li, McGill University, Canada
E-mail cj.li@mcgill.ca

INTERNATIONAL ADVISORY EDITORIAL BOARD

James Clark, York, UK

Avelino Corma, Universidad Politécnica de Valencia, Spain

Mark Harmer, DuPont Central R&D, USA

Makoto Misono, Kogakuin University, Japan

Robin D. Rogers, Centre for Green Manufacturing, USA

Kenneth Seddon, Queen's University, Belfast, UK

Roger Sheldon, Delft University of Technology, The Netherlands

Gary Shelldrake, Queen's University, Belfast, UK

Pietro Tundo, Università ca Foscari di Venezia, Italy

Tracy Williamson, Environmental Protection Agency, USA

INFORMATION FOR AUTHORS

Full details of how to submit material for publication in Green Chemistry are given in the Instructions for Authors (available from <http://www.rsc.org/authors>). Submissions should be sent via ReSource: <http://www.rsc.org/resource>.

Authors may reproduce/republish portions of their published contribution without seeking permission from the RSC, provided that any such republication is accompanied by an acknowledgement in the form: (Original citation) – Reproduced by permission of the Royal Society of Chemistry.

© The Royal Society of Chemistry 2005. Apart from fair dealing for the purposes of research or private study for non-commercial purposes, or criticism or review, as permitted under the Copyright, Designs and Patents Act 1988 and the Copyright and Related Rights Regulations 2003, this publication may only be reproduced, stored or transmitted, in any form or by any means, with the prior permission in writing of the Publishers or in the case of reprographic reproduction in accordance with the terms of

licences issued by the Copyright Licensing Agency in the UK. US copyright law is applicable to users in the USA.

The Royal Society of Chemistry takes reasonable care in the preparation of this publication but does not accept liability for the consequences of any errors or omissions.

Ⓢ The paper used in this publication meets the requirements of ANSI/NISO Z39.48-1992 (Permanence of Paper).

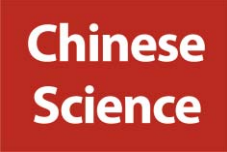
Royal Society of Chemistry: Registered Charity No. 207890

EDITORIALS

491

Chemical Science in China

Articles from China are showcased across RSC journals this month, in recognition of the growing importance of Chinese research in the Chemical Sciences.



492

New board member: Professor Buxing Han

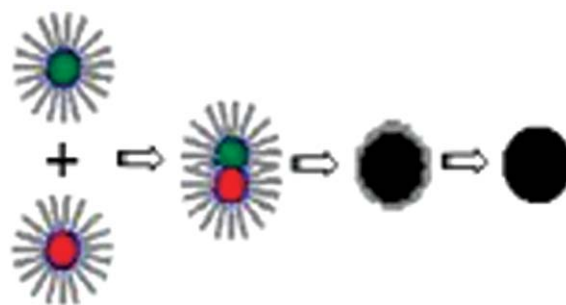
PAPERS

493

Synthesis of the high-surface-area $Ce_xBa_{1-x}MnAl_{11}O_y$ catalyst in reverse microemulsions using inexpensive inorganic salts as precursors

Fei Teng,* Ping Xu, Zhijian Tian,* Guoxing Xiong,* Yunpeng Xu, Zhusheng Xu and Liwu Lin

The $Ce_xBa_{1-x}MnAl_{11}O_x$ catalysts are synthesized in reverse microemulsions using inexpensive inorganic salts as precursors, which have high surface area and high activity for methane combustion.

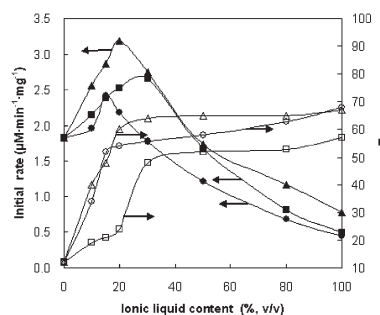


500

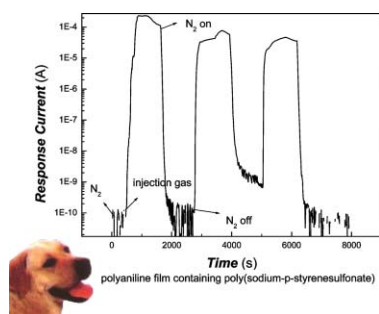
Markedly improving lipase-mediated asymmetric ammonolysis of D,L-*p*-hydroxyphenylglycine methyl ester by using an ionic liquid as the reaction medium

Wen-Yong Lou, Min-Hua Zong,* Hong Wu, Ruo Xu and Ju-Fang Wang

A comparative study was made of lipase-catalyzed asymmetric ammonolysis of D,L-*p*-hydroxyphenylglycine methyl ester (D,L-HPGME) with ammonium carbamate as the ammonia donor in nine ionic liquids (ILs) and four organic solvents.



507

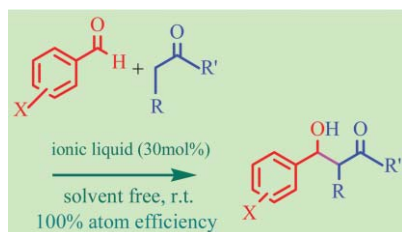


Preparation of water soluble poly(aniline) and its gas-sensitivity

Xingfa Ma,* Mang Wang, Hongzheng Chen, Guang Li, Jingzhi Sun and Ru Bai

The poly(aniline) film forming technology was improved *via* inducement effects of poly(sodium-*p*-styrenesulfonate). The composite film has good gas-sensitivity and reproducibility. It has a potential application on artificial olfaction.

514

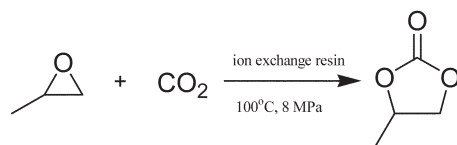


Direct aldol reactions catalyzed by 1,1,3,3-tetramethylguanidine lactate without solvent

Anlian Zhu, Tao Jiang,* Dong Wang, Buxing Han, Li Liu, Jun Huang, Jicheng Zhang and Donghai Sun

Direct aldol reactions can be conducted using ionic liquid [TMG][Lac] as a recyclable catalyst without any solvent. This is a new and greener process to β -hydroxyl ketones.

518

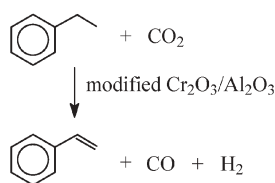


Organic solvent-free process for the synthesis of propylene carbonate from supercritical carbon dioxide and propylene oxide catalyzed by insoluble ion exchange resins

Ya Du, Fei Cai, De-Lin Kong and Liang-Nian He*

The process described here represents a simple, ecologically safer, cost-effective route to cyclic carbonates with high product quality, as well as easy product recovery and catalyst recycling.

524



Effect of modifiers on the activity of a $\text{Cr}_2\text{O}_3/\text{Al}_2\text{O}_3$ catalyst in the dehydrogenation of ethylbenzene with CO_2

Xingnan Ye, Yinghong Yue, Changxi Miao, Zaiku Xie, Weiming Hua* and Zi Gao

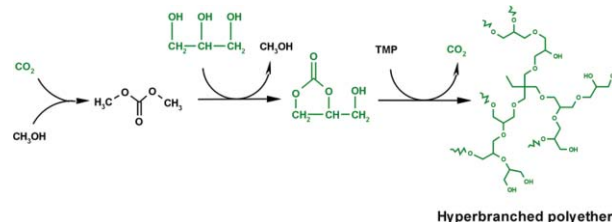
We report a novel and highly active catalyst system for the oxidative dehydrogenation of ethylbenzene to styrene using CO_2 as a mild oxidant.

529

Hyperbranched aliphatic polyethers obtained from environmentally benign monomer: glycerol carbonate

Gabriel Rokicki,* Paweł Rakoczy, Paweł Parzuchowski and Marcin Sobiecki

The synthesis of hyperbranched polyethers from environmentally acceptable monomer—glycerol carbonate—is presented. Glycerol carbonate was obtained from benign starting materials: glycerol and dimethyl carbonate.

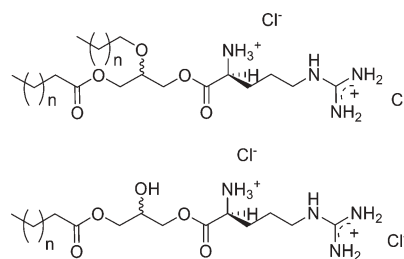


540

Biological properties of arginine-based glycerolipidic cationic surfactants

Noemí Pérez,* Lourdes Pérez, M. Rosa Infante and M. Teresa García*

In recent years, environmental concerns have provided the driving force to develop biodegradable surfactants with low toxicity. Here, we investigate the biodegradability and aquatic toxicity of new cationic arginine based surfactants.



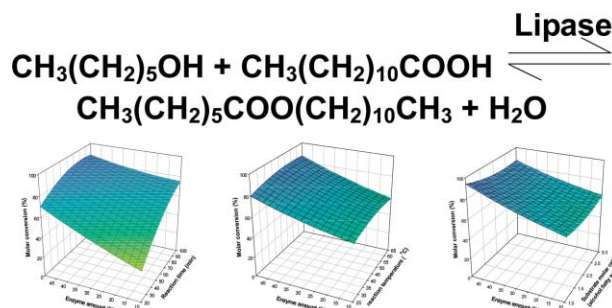
Mono and diglycerides from arginine

547

Optimal lipase-catalyzed formation of hexyl laurate

Shu-Wei Chang, Jei-Fu Shaw, Kun-Hsiang Yang, Ing-Lung Shih, Chih-Han Hsieh and Chwen-Jen Shieh*

Hexyl laurate, used as an emollient in the cosmetic industry, is commercially produced by chemical synthesis. This paper shows that hexyl laurate can be prepared readily with high molar conversion using lipase catalysis in *n*-hexane.



552

A novel highly active biomaterial supported palladium catalyst

Mark J. Gronnow, Rafael Luque, Duncan J. Macquarrie and James H. Clark*

An expanded starch supported palladium catalyst which is highly active in Suzuki, Heck and Sonogashira reactions has been developed. The biodegradable naturally occurring starch has proven to form and stabilise palladium nanoclusters.




AUTHOR INDEX

- | | | | |
|------------------------|----------------------------|-----------------------|-----------------------|
| Bai, Ru, 507 | Infante, M. Rosa, 540 | Rakoczy, Paweł, 529 | Xie, Zaiku, 524 |
| Cai, Fei, 518 | Jiang, Tao, 514 | Rokicki, Gabriel, 529 | Xiong, Guoxing, 493 |
| Chang, Shu-Wei, 547 | Kong, De-Lin, 518 | Shaw, Jei-Fu, 547 | Xu, Ping, 493 |
| Chen, Hongzheng, 507 | Li, Guang, 507 | Shieh, Chwen-Jen, 547 | Xu, Ruo, 500 |
| Clark, James H., 552 | Lin, Liwu, 493 | Shih, Ing-Lung, 547 | Xu, Yunpeng, 493 |
| Du, Ya, 518 | Liu, Li, 514 | Sobiecki, Marcin, 529 | Xu, Zhusheng, 493 |
| Gao, Zi, 524 | Lou, Wen-Yong, 500 | Sun, Donghai, 514 | Yang, Kun-Hsiang, 547 |
| García, M. Teresa, 540 | Luque, Rafael, 552 | Sun, Jingzhi, 507 | Ye, Xingnan, 524 |
| Gronnow, Mark J., 552 | Ma, Xingfa, 507 | Teng, Fei, 493 | Yue, Yinghong, 524 |
| Han, Buxing, 514 | Macquarrie, Duncan J., 552 | Tian, Zhijian, 493 | Zhang, Jicheng, 514 |
| He, Liang-Nian, 518 | Miao, Changxi, 524 | Wang, Dong, 514 | Zhu, Anlian, 514 |
| Hsieh, Chih-Han, 547 | Parzuchowski, Paweł, 529 | Wang, Ju-Fang, 500 | Zong, Min-Hua, 500 |
| Hua, Weiming, 524 | Pérez, Lourdes, 540 | Wang, Mang, 507 | |
| Huang, Jun, 514 | Pérez, Noemí, 540 | Wu, Hong, 500 | |

FREE E-MAIL ALERTS

Contents lists in advance of publication are available on the web *via* www.rsc.org/greenchem - or take advantage of our free e-mail alerting service (www.rsc.org/ej_alert) to receive notification each time a new list becomes available.

* Indicates the author for correspondence: see article for details.

 Electronic supplementary information (ESI) is available *via* the online article (see <http://www.rsc.org/esi> for general information about ESI).

ADVANCE ARTICLES AND ELECTRONIC JOURNAL

Free site-wide access to Advance Articles and the electronic form of this journal is provided with a full-rate institutional subscription. See www.rsc.org/ejs for more information.

ReSource

Lighting your way through the publication process

A website designed to provide user-friendly, rapid access to an extensive range of online services for authors and referees.

ReSource enables **authors** to:

- Submit manuscripts electronically
- Track their manuscript through the peer review and publication process
- Collect their free PDF reprints
- View the history of articles previously submitted

ReSource enables **referees** to:

- Download and report on articles
- Monitor outcome of articles previously reviewed
- Check and update their research profile

Register today!

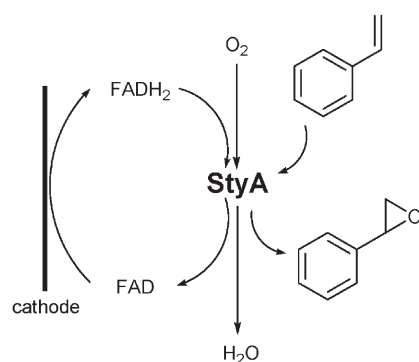
Highlights

DOI: 10.1039/b507076g

Markus Hölscher reviews some of the recent literature in green chemistry

Biocatalytic asymmetric epoxidation with electrochemical regeneration of monooxygenase

The interest in asymmetric synthesis using enzymes as catalysts has been growing steadily in recent years and a large area is still to be exploited. The reduction of O_2 in asymmetric epoxidations using monooxygenases is one of the fields in which interesting progress is occurring. Advantageously, oxygen is catalytically incorporated with high regio- and stereoselectivities under environmentally benign reaction conditions into many organic substrates. Unfortunately the monooxygenase catalyzed epoxidation suffers from dependence on cofactors and reducing equivalents; e.g. the expensive and unstable NAD(P)H cofactor has to be supplied in monooxygenase catalyzed reactions. Furthermore undesired oxidative side-reactions are inherent drawbacks. In a modified approach Schmid and coworkers from the Swiss Federal Institute of Technology replaced the NADH/NAD⁺ reducing couple and the reductase component StyB from styrene monooxygenase (StyAB) by an electrode, which was used as a cathode to regenerate the FAD/FADH₂ couple which reduces the oxygenase component StyA.¹

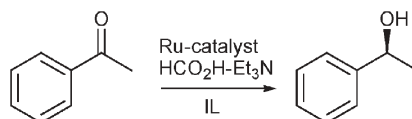


They found *trans*- β -methyl styrene to be epoxidized to practically enantiopure (1*S*,2*S*)-1-phenylpropylene oxide. Very high ee values were also obtained for

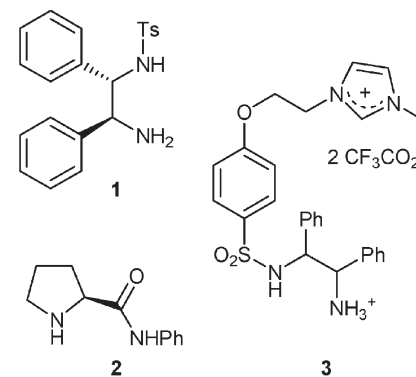
some other vinyl aromatic compounds (98.1 to 99.5%). Additionally, the electro-enzymatic reaction was much slower than the one with the native enzyme, showing a StyA activity of only 35.5 U g⁻¹ (compared to 2100 U g⁻¹ for the native system; 1 U g⁻¹ translates to a turnover frequency of 0.047 min⁻¹). It was assumed that the ratio of the cathode area to reaction volume has a large influence on the activity and that by increasing this ratio activities could be enhanced significantly. Undesired oxidative quenching during the regeneration cycle is also responsible for the low activities. However, increasing the aeration rate led to much higher StyA activities of up to 178.7 U g⁻¹. As a result the minimization of a complex native system to the oxygenase component and electrochemical reduction of its flavin prosthetic group is an interesting addition to the toolbox of asymmetric oxidation of organic substrates.

Enantioselective transfer hydrogenation with recyclable ruthenium catalysts in ionic liquids

An interesting alternative to the hydrogenation of ketones with molecular hydrogen to obtain optically active secondary alcohols is the transfer hydrogenation of ketones. An azeotrope of formic acid and triethyl amine is often used as hydrogen source leading to the production of CO₂ during the reaction. Ohta and coworkers from the Kyoto Pharmaceutical University investigated the performance and recyclability of different ruthenium catalysts containing chiral ligands in transfer hydrogenations of various acetophenones using ionic liquids (ILs) as solvents.²



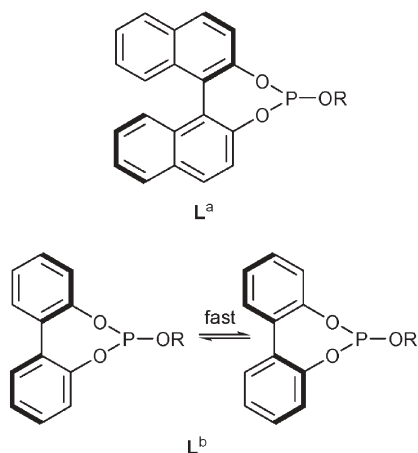
It was shown that the ruthenium catalyst containing ligand **1** developed by Noyori, Ikariya and coworkers led to high ee values with moderate to quantitative conversions when IL [bmim][PF₆] was used as the solvent, whereas ligand **2** resulted in moderate activity and enantioselectivity. In an attempt to develop new ligands well suited for this reaction and for use in ILs, imidazolium salt **3** was synthesized and tested in transfer hydrogenations of acetophenone in comparison with ligand **1**. Both catalyst systems yielded ee values varying between 92 and 93% ee in five consecutive runs, however, the catalyst system with ligand **1** lost a considerable part of its activity, whereas the competitor ligand **3** showed better results up to the fourth cycle, which is probably related to better immobilization in the IL.



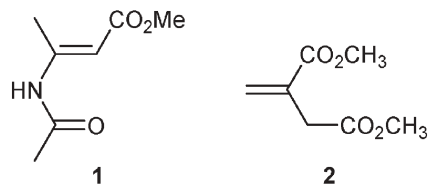
Combinatorial ligand optimization for asymmetric olefin hydrogenations using mixtures of monodentate P-compounds

A few years ago monodentate P-ligands were introduced to asymmetric Rh-catalyzed hydrogenation of olefins, breaking the dogma that only bidentate P-ligands would supply the necessary spatial features required for enantioselectivity. In addition to being interesting in itself, this fact opened the way to tackle the search for the best ligands by a

combinatorial approach. Reetz and Li from the Max Planck Institute of Coal Research utilized this strategy while expanding it to the application of mixtures of configurationally stable and unstable monodentate P-ligands.³ Upon mixing the precursor complex $[\text{Rh}(\text{cod})(\text{L}^a)_2]\text{BF}_4$ with ligand L^b a complex catalyst mixture is formed which contains three different species: $[\text{Rh}(\text{cod})(\text{L}^a\text{L}^a)]^+$, $[\text{Rh}(\text{cod})(\text{L}^b\text{L}^b)]^+$, and $[\text{Rh}(\text{cod})(\text{L}^a)(\text{L}^b)]^+$. Among these the hetero combination $[\text{Rh}(\text{cod})(\text{L}^a)(\text{L}^b)]^+$ is present in two diastereomeric forms, since only ligand L^a is configurationally stable, whereas ligand L^b changes its configuration rapidly on the NMR time-scale even at low temperatures.



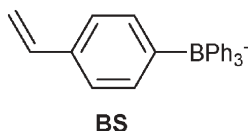
Screening experiments using BINOL derived phosphite ligands L^a and different phosphites L^b showed that optimum combinations can be found reaching ee values up to 98% in hydrogenations of β -acylaminoacrylate **1** with conversions of 100%. Also, dimethyl itaconate **2** can be hydrogenated using a different ligand combination yielding ee values up to 94%.



In addition to the theoretical interest in detailed mechanistic investigations, systems of this kind also have practical implications as the ligand system partly contains cheap achiral components.

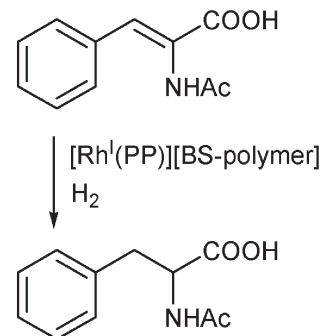
Noncovalent anchoring of cationic homogeneous catalysts on polystyrene based latices

Many immobilization strategies for homogeneous catalysts rely on the covalent anchoring of the complexes at a given support, whereas noncovalent anchoring *e.g.* via electrostatic interactions has not gained much interest yet. In order to avoid complex syntheses to introduce ionic substituents to ligands, Mecking, Vogt and coworkers contributed an inverse approach in which cationic homogeneous catalysts are anchored noncovalently to the anionic groups present in specially synthesized polystyrene latices.⁴ At first they synthesized a polymerizable triphenylstyrylborate anion (BS), which was copolymerized with styrene, divinylbenzene and a PEO macromonomer to yield colloidal stable polymer latices.



These materials could be reacted with $[\text{Rh}(\text{dppp})(\text{cod})]\text{BF}_4$ (dppp = bis

(diphenylphosphino)-propane, cod = cyclooctadiene) resulting in cation exchanged polymers with the $[\text{Rh}(\text{dppp})]^+$ ion being present in an amount of *ca.* 25% of the theoretical latex capacity. As a test reaction α -acetamidocinnamic acid was hydrogenated in batch experiments showing turnover frequencies (TOF) of *ca.* 30 h^{-1} for five of six consecutive runs without loss of activity, with the TOF in the first run being somewhat lower.



The activity obtained is about five times lower than that of the corresponding non-immobilized catalyst system, however this approach might open interesting alternatives for immobilizing homogeneous catalysts.

References

- 1 F. Hollmann, K. Hofstetter, T. Habicher, B. Hauer and A. Schmid, *J. Am. Chem. Soc.*, 2005, **127**, 6540–6541.
- 2 Ikuo Kawasaki, Kazuya Tsunoda, Tomoko Tsuji, Tomoko Yamaguchi, Hiroki Shibuta, Nozomi Uchida, Masayuki Yamashita and Shunsaku Ohta, *Chem. Commun.*, 2005, 2134–2136.
- 3 M. T. Reetz and X. Li, *Angew. Chem.*, 2005, **117**, 3019–3021.
- 4 R. Sablong, J. I. van der Vlugt, R. Thomann, S. Mecking and D. Vogt, *Adv. Synth. Catal.*, 2005, **347**, 633–636.

Chemical Science in China

DOI: 10.1039/b507557m

Articles from China are showcased across RSC journals this month, in recognition of the growing importance of Chinese research in the Chemical Sciences.

This month we are proud to feature articles from China across the covers of Royal Society of Chemistry (RSC) journals and magazines. The number of submissions from China to our journals has increased dramatically, from a few hundred papers in 1995 to now over 20% of our total submissions (Fig. 1). This increase reflects the growth and strength of chemical research in China.

In recognition of the growing importance of Chinese research, groups from the RSC, including the Director of Publishing, Editorial Director and journal Editors, recently visited over 30 of the most important Universities and Institutes in China.

RSC visits

✈ Beijing	✈ Hong Kong
✈ Changchun	✈ Nanjing
✈ Dalian	✈ Shanghai
✈ Fuzhou	✈ Shenyang
✈ Guangzhou	✈ Tianjin
✈ Hangzhou	✈ Wuhan
✈ Hefei	✈ Xiamen

The focus of these visits was to strengthen links with Chinese institutions and improve our understanding of chemical research in China. Research is developing at an impressive pace: Funding is increasing, as are the numbers of researchers at all levels, and there is a substantial investment in new buildings and research facilities. Research output will clearly continue to grow at a fast pace and to increase in importance. There is commitment from Universities and Institutes in China to increase the quality of research and articles published in international journals, and there is wide success in meeting this goal. The RSC is enthusiastic to support this through working with authors and our unbiased editorial

policies and procedures. We strongly encourage submission of the highest quality work from China. To aid authors our *Information for Authors* and *Ethical Guidelines* for publishing in RSC journals are available from our web site in Chinese (visit <http://www.rsc.org/resource>).

The cover of *Green Chemistry* features an article by Liang-Nian He and colleagues from Nankai University, Tianjin, China. Cyclic carbonates have been produced on an industrial scale for over 40 years, and demand is increasing. The group has developed a process for the production of carbonates employing supercritical CO₂. Traditional catalysts are replaced with ion exchange resins, and the CO₂ acts as both a reagent and solvent, providing an environmentally-benign and inexpensive process.

Higher Education in China is the focus of the lead article in this August's issue of *Chemistry World*. The article describes how the university system and funding operate and also how the education system has been reformed since the end of the Cultural Revolution. The article is

also available from the web: <http://www.chemistryworld.org>

2005 is the year of *UK-China Partners in Science*, encouraging links and collaborations between the UK and China in science, technology and innovation (<http://www.uk.cn/science>). For several years the RSC has been collaborating with Charlesworth China for the production of some of our leading journals. Charlesworth typeset articles in Beijing, contributing towards our fast publication times by preparing proofs overnight on our European timeframe.

Many thanks to the hosts who welcomed the groups from the RSC to their institutions and particular thanks to Professor Xue Long Hou (Shanghai Institute of Organic Chemistry), Professor Henry Wong (Chinese University of Hong Kong and *ChemComm* Editorial Advisory Board member) and Professor Daoben Zhu (Institute of Chemistry, Chinese Academy of Sciences and *Journal of Materials Chemistry* Associate Editor for China).

Harp Minhas, Editor

Robert Parker, Editorial Director

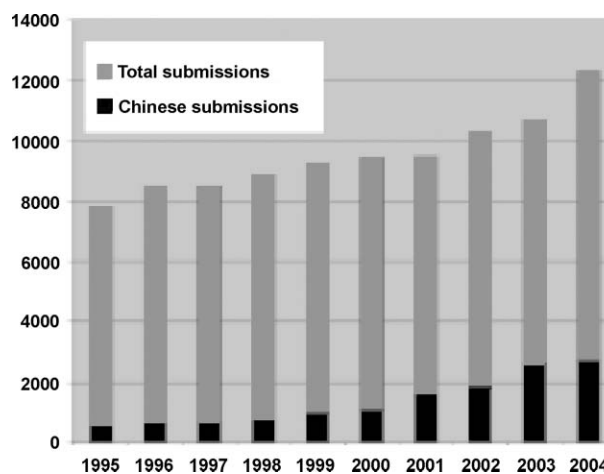


Fig. 1 Number of articles submitted to all RSC journals by year (total and Chinese submissions).

New board member: Professor Buxing Han

DOI: 10.1039/b506481n



Buxing Han was born in 1957. He completed a BS in chemical engineering in 1982 (Hebei University of Science and Technology, Shijiazhuang), an MS in inorganic chemistry in 1985 (Applied Institute of Chemistry, Chinese Academy of Sciences, Changchun) and a PhD in physical chemistry from the Institute of Chemistry of the Chinese Academy of Sciences in Beijing in 1988. After a year as an Assistant Professor at the Institute of Chemistry, he took up a post-doctoral position in the Department of Chemical Engineering at the University of Saskatchewan, Canada. He returned to the Institute of Chemistry of the Chinese

Academy of Sciences in 1991 and was promoted to Associate Professor in the same year. He has been a full Professor since 1993.

His research group has 35 members including staff, post-docs and students. Principal areas of research include studying physicochemical properties of supercritical fluids and ionic liquids, and their applications in chemical reactions, material science, and extraction and fractionation.

Buxing Han has published 290 papers, 21 patents and has given invited lectures at more than 10 international conferences.

Synthesis of the high-surface-area $Ce_xBa_{1-x}MnAl_{11}O_y$ catalyst in reverse microemulsions using inexpensive inorganic salts as precursors

Fei Teng,^{*ab} Ping Xu,^a Zhijian Tian,^{*a} Guoxing Xiong,^{*b} Yunpeng Xu,^a Zhusheng Xu^a and Liwu Lin^{ab}

Received 10th November 2004, Accepted 18th March 2005

First published as an Advance Article on the web 12th April 2005

DOI: 10.1039/b417229a

The high-surface-area $Ce_xBa_{1-x}MnAl_{11}O_y$ ($x = 0, 0.1, 0.2, 0.3$) catalysts were synthesized in the nonionic reverse microemulsion (ME), using the inorganic salts as the reactants. The supercritical drying (SCD) and conventional oven drying (CD) methods were used to remove the water in hydrogels, respectively. The $Ce_xBa_{1-x}MnAl_{11}O_y$ samples were characterized by N_2 -adsorption, transmission electron microscopy (TEM), TGA-DTA, and X-ray powder diffraction (XRD). The effects of the microemulsion composition, the drying method, the calcination temperature and the introduction of Ce on the catalysts were investigated. The results showed that the morphology of the catalyst was controlled by the microemulsion microstructure; and the homogeneity of the precursor was improved effectively by the reverse microemulsion method and the supercritical drying method. Due to the high homogeneity of the precursors, the initial formation temperature of the hexaaluminate phase decreased to lower than 1100 °C. The $BaMnAl_{11}O_{19}$ catalyst had high surface area ($72.4 \text{ m}^2 \text{ g}^{-1}$) and high catalytic activity ($T_{10} = 445 \text{ °C}$) for methane combustion. When Ce was introduced, the $Ce_xBa_{1-x}MnAl_{11}O_y$ catalyst ($x = 1$) had the higher activity ($T_{10} = 430 \text{ °C}$) than that of the $BaMnAl_{11}O_{19}$ one due to a synergetic effect between Ce and Mn.

1. Introduction

Catalytic combustion is an environmental-friendly technology, which can effectively reduce the emissions of CO and NO_x . Up to now, one of the main challenges in this field is to select and prepare excellent catalytic materials with high thermal stability and high activity at high temperature.^{1,2} Hexaaluminates are good catalysts for methane combustion due to their excellent thermal stability.³ Generally, hexaaluminates are synthesized by sol-gel, supercritical drying and coprecipitation methods.³⁻⁶ In 2000, Zarur and Ying⁷ prepared $CeO_2/BaAl_{12}O_{19}$ with the highest surface area *via* a reverse microemulsion-mediated sol-gel process, combining with freeze-drying and supercritical drying. However, since the alcoxides used in the sol-gel process are harmful and expensive, the preparation is not environmental-friendly and its cost is high. Besides, the hydrolyses of the alcoxides need to be carried out under very stringent conditions (moisture- and oxygen-free environment), so the preparation is difficult to operate. In addition, for the coprecipitation route, the homogeneity of the obtained precursor is poor; the conglomeration of the particles can not be avoided, while upon calcination at high temperature (above 1200 °C), the particles sinter very severely. Therefore, the activity of the catalyst synthesized by this method is low.

Herein, the nanostructured $Ce_xBa_{1-x}MnAl_{11}O_y$ ($x = 0, 0.1, 0.2$ and 0.3) catalysts were synthesized in the nonionic reverse microemulsions, which consisted of polyoxyethylene (6) tridecyl alcohol ether, n-hexanol, cyclohexane and aqueous

solution. During the process, the nontoxic and inexpensive inorganic salts were used as the reactants, *e.g.*, $(NH_4)_2CO_3$, $Ba(NO_3)_2$, $Mn(NO_3)_2$, $Ce(NO_3)_3$, and $Al(NO_3)_3$. Therefore, the preparation is environmental-friendly and low-cost. Through nanostructure processing with the reverse microemulsion, the homogeneity of the precursors could be improved at a molecular-level, and the particle size could be effectively controlled in the nanoscale range. After drying in supercritical ethanol, the homogeneity of the precursors could be adequately maintained. The preparation promotes the formation of hexaaluminate crystallites at a low temperature. In this study, the effects of the microemulsion composition, the drying method, the calcination temperature and the introduction of Ce on the physicochemical properties of the catalysts were investigated.

2. Experimental

2.1. Preparation

The reverse microemulsion system used in this experiment consisted of polyoxyethylene (6) tridecyl alcohol ether ($C_{13}E_6$, MW = 464) (S), n-hexanol (CS), cyclohexane (O) and aqueous solution (W), which were employed as surfactant, cosurfactant, continuous phase and dispersed phase, respectively. In the experiment, the weight ratio of aqueous solution in the reverse microemulsion was designated as W_0 , *i.e.* $W_0 = (m_W/(m_W + m_{CS} + m_S + m_O))$, in which m_W , m_{CS} , m_S and m_O represent weight of W, CS, S and O, respectively.

During the preparation, two microemulsions were used, which had the same proportions of W, S, CS and O, but contained different aqueous solutions. One microemulsion contained a 1.0 mol L^{-1} $(NH_4)_2CO_3$ solution, which was

*tfwd@dicp.ac.cn (Fei Teng)
tianz@dicp.ac.cn (Zhijian Tian)
gxxiong@dicp.ac.cn (Guoxing Xiong)

designated as ME_a. The other contained a 0.5 mol L⁻¹ mixture solution of stoichiometric Ba(NO₃)₂, Mn(NO₃)₂, Ce(NO₃)₃ and Al(NO₃)₃, designated as ME_b. While the weight ratios of CS, S and O were kept constant (*i.e.* 1.2 : 3.5 : 13.5), the addition amount of aqueous solution was changed. The ME_a was stable at a W_0 value lower than 0.25, while the ME_b was stable even when the W_0 value was higher than 0.25. Therefore, the W_0 value was altered in the range 0.10 to 0.25. The Ce_xBa_{1-x}MnAl₁₁O_y ($x = 0, 0.1, 0.2, \text{ and } 0.3$) catalysts were prepared by the procedures outlined below.

At room temperature, the same volumes of ME_a and ME_b were mixed rapidly while vigorously stirring. The reaction continued for 5 h under stirring, and then the reacting mixture was aged for 24 h under ambient static conditions. After aging, acetone was added to demulsify the system, and the hydrogel was recovered by centrifugation. The hydrogel was washed sufficiently with deionized water and ethanol in sequence, and then dried by supercritical ethanol drying (SCD). The supercritical drying process was operated at 260 °C and 7.0–8.0 MPa for 2 h. The details of the drying method were described elsewhere.⁸ The precursor was calcined at 800, 1000, 1100 and 1200 °C in a muffle in air for 5 h, respectively. The precursor dried by the SCD method was designated as aerogel. The obtained Ce_xBa_{1-x}MnAl₁₁O_y catalyst was designated as C_x-SCD; namely, the BaMnAl₁₁O₁₉, Ce_{0.1}Ba_{0.9}MnAl₁₁O_y, Ce_{0.2}Ba_{0.8}MnAl₁₁O_y, and Ce_{0.3}Ba_{0.7}MnAl₁₁O_y catalysts were denoted as C₀-SCD, C₁-SCD, C₂-SCD and C₃-SCD, respectively.

In contrast with the SCD method, the synthesized hydrogels were dried using the conventional oven drying method (CD). The precursors were designated as xerogels, and the other procedures were the same as above. The Ce_xBa_{1-x}MnAl₁₁O_y ($x = 0, 0.1, 0.2, 0.3$) catalysts prepared by the CD method were designated as C₀-CD, C₁-CD, C₂-CD and C₃-CD, respectively.

2.2. Characterization

The samples were characterized by X-ray powder diffraction (XRD) on a Rigaku D/MAX-RB X-ray powder diffractometer, using graphite monochromatized Cu K_α radiation ($\lambda = 1.54178 \text{ \AA}$), operating at 40 kV and 50 mA. The spectra were scanned between 5° and 70° (2θ) at a scanning rate of 5° min⁻¹. A nitrogen adsorption isotherm was performed at 77 K and <10⁻⁴ bar on a Micromeritics ASAP2010 gas adsorption analyzer. Each sample was degassed at 350 °C for 5 h before the measurement. Surface area and pore size distribution were calculated by the BET (Brunauer–Emmett–Teller) and the BJH (Barrett–Joyner–Halenda) methods, respectively. The catalyst morphology was characterized with a JEOL model 200CX transmission electron microscope, using an accelerating voltage of 200 kV. The powders were dispersed in ethanol ultrasonically, and then the samples were deposited on a thin amorphous carbon film supported by copper grids. TGA and DTA were carried out on Pyris 1 TGA-7 thermogravimeter and DTA-7 (US Perkin-Elmer Co.), respectively. The catalyst particles (0.015 g) were heated from room temperature to 1300 °C at a rate of 10 °C min⁻¹ in an air stream. The flow rate of air was 30 mL min⁻¹.

2.3. Catalytic combustion of methane

The reaction of methane combustion was carried out in a conventional flow system under atmospheric pressure. The catalysts (1 mL, ~1.2 g) (20–40 mesh) were loaded in a quartz reactor (*i.d.* = 10 mm), packed with quartz beads on both top and bottom of the catalyst bed. A mixture gas of methane (1 vol%) and air (99 vol%) was fed into the catalyst bed at a gas hourly space velocity (GHSV) of 48 000 h⁻¹. The inlet and outlet gas compositions were analyzed by on-line gas chromatography, using a packed column of carbon molecular sieves and a thermal conductivity detector (TCD). These details have been described in the literature elsewhere.⁸ Here, T_{10} and T_{90} are used to express the catalyst activity, in which T_{10} and T_{90} represent the temperatures at 10% and 90% conversions of methane, respectively.

3. Results and discussion

3.1. The BaMnAl₁₁O₁₉ catalyst morphology

The effects of microemulsion composition (W_0) and drying method on the catalyst morphology were investigated. As observed in Table 1 and Fig. 1, the nanostructured BaMnAl₁₁O₁₉ catalysts with different morphologies, *i.e.* spherical, spindly and rodlike, were prepared at different W_0 values. On the basis of the TEM images of the precursors and electric conductivity of the system at different W_0 values,⁹ we could conclude that the catalyst morphology was strongly dependent on the microemulsion microstructure, which acted as a soft template. At a low W_0 value ($W_0 = 0.10$), the interaction among the reverse micelles was weak, and the reverse micelles maintained spherical morphology. However, at a high W_0 value ($W_0 = 0.25$), the interaction among the micelles was strong, and the regular spherical micelles could not be maintained. As a result, the spherical micelles would probably change into a rodlike or bicontinuous structure.¹⁰ The composition (W_0) of the reverse microemulsion predominated the micelle morphology. The particles nucleated, grew, and assembled within the reverse micelles with different morphologies, and the morphology of reverse micelles would be imprinted into the precursor particles. During the SCD process, the aggregation of the particles was effectively suppressed due to elimination of capillary tension of water. Therefore, the morphology of the precursor was perfectly maintained. After calcination, the BaMnAl₁₁O₁₉ catalyst maintained its precursor morphology owing to its specific anisotropic crystal structure.¹¹ As observed from Fig. 1b and Fig. 1c, the size of the CD catalyst was larger than that of the SCD one. The large spindly particles probably resulted from

Table 1 The particle shape and size of the BaMnAl₁₁O₁₉ catalysts

Catalyst ^a	W_0	Drying	Particle shape ^b	Particle size/nm ^b
(a)	0.10	SCD	Spherical	15–20
(b)	0.25	SCD	Rod-like	(5–10) × (100–200)
(c)	0.25	CD	Spindly	(50–100) × (400–500)

^a Corresponding to the catalysts in Fig. 1. ^b Calcination at 1200 °C for 5 h.

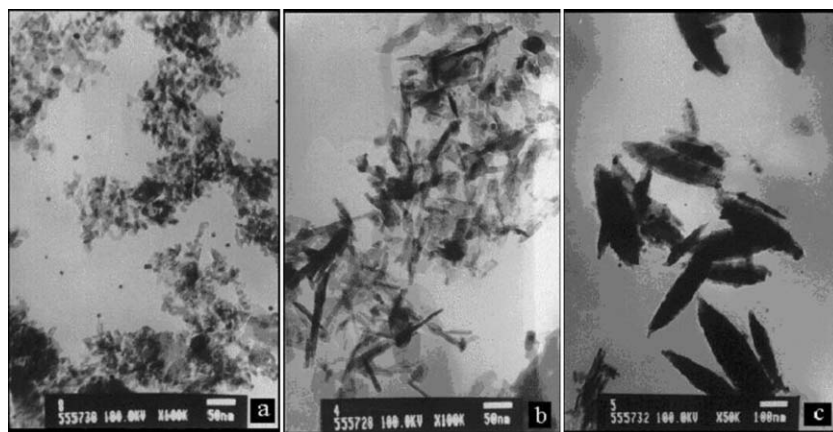


Fig. 1 TEM images of the $\text{BaMnAl}_{11}\text{O}_{19}$ catalysts prepared in the reverse microemulsions at different W_0 values. (a) $W_0 = 0.10$, SCD; (b) $W_0 = 0.25$, SCD; (c) $W_0 = 0.25$, CD. SCD—supercritical drying, CD—conventional oven drying; $W_0 = (m_W)/(m_W + m_{CS} + m_S + m_O)$, m_W , m_{CS} , m_S , m_O : the weights of aqueous solution (W), n-hexanol (CS), C_{13}E_6 (S) and cyclohexane (O), respectively.

the aggregation of the nanorods under the capillary tension of water during the conventional oven drying process.

3.2. Texture properties of the $\text{BaMnAl}_{11}\text{O}_{19}$ catalysts and their precursors

Texture properties of the samples are given in Table 2 and Figs. 2 and 3. The SCD catalyst shows an IV-type adsorption isotherm with H2-hysteresis loop, indicating that it gives rise to the crossed pores with narrow necks and wide bodies (often referred to as ‘inkbottle’ model mesopores).¹² The average pore size of the SCD catalyst is about 10 nm. Comparing curve 1 with curve 2 in Fig. 2, it is obvious that the collapsing of small pores and the contracting of large pores have occurred during calcination. The CD catalyst (IV-type isotherm curve, H3-type hysteresis loop) gives rise to the slit-shaped mesopores.¹² The average pore size of the CD catalyst is 30.5 nm, whose pore size distribution (PSD) is wide, suggesting that the CD sample sinter and agglomerate severely. The reason is that the xerogel contains more water and hydroxyls than the aerogel (proved by TGA-DTA in Fig. 4). Therefore, the surface area ($72.2 \text{ m}^2 \text{ g}^{-1}$) of the SCD catalyst is much higher than that ($43.3 \text{ m}^2 \text{ g}^{-1}$) of the CD one. The pore volume of the aerogel is twice that of the xerogel, indicating the contact area between particles for the SCD sample is smaller than that for the CD one. This means the crossed pores in the CD sample are easier to collapse than those in the SCD one.

Ishikawa *et al.*¹⁵ have reported that the contact area between particles was associated to the pore volume, and the sintering

Table 2 Effect of drying on the $\text{BaMnAl}_{11}\text{O}_{19}$ catalysts and their precursors prepared in the reverse microemulsions of $W_0 = 0.10$

Sample	Drying	SSA/ $\text{m}^2 \text{ g}^{-1}$ ^a	$V_{\text{pore}}/\text{mL g}^{-1}$ ^a	$d_{\text{pore}}/\text{nm}$ ^a
Xerogel	CD	264.5	0.32	9.5
Aerogel	SCD	325.9	0.78	15.5
$\text{BaMnAl}_{11}\text{O}_{19}$ ^b	CD	43.3	0.20	30.5
$\text{BaMnAl}_{11}\text{O}_{19}$ ^b	SCD	72.2	0.28	10.0

^a SSA: Specific surface area; V_{pore} : Pore volume; d_{pore} : Average pore size. ^b Calcined at 1200 °C for 5 h.

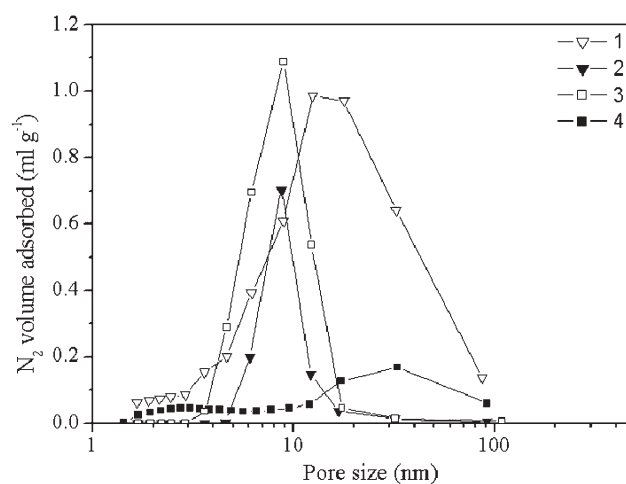


Fig. 2 Pore size distributions (PSD) of the samples: 1— aerogel; 2— calcined SCD sample; 3— xerogel; 4— calcined CD sample.

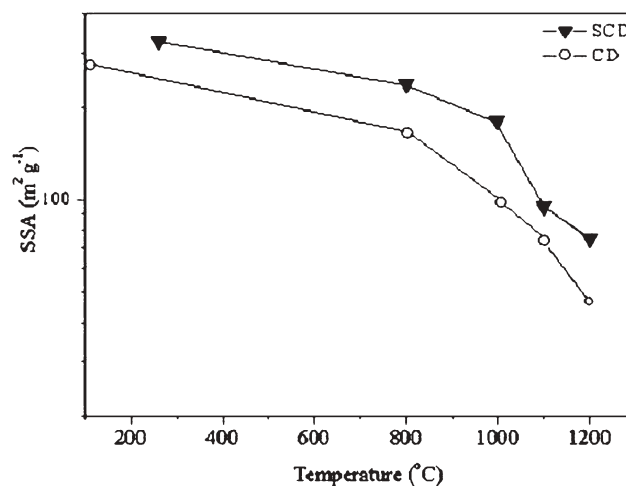


Fig. 3 Changes of specific surface area (SSA) of the $\text{BaMnAl}_{11}\text{O}_{19}$ catalysts with calcination temperature.

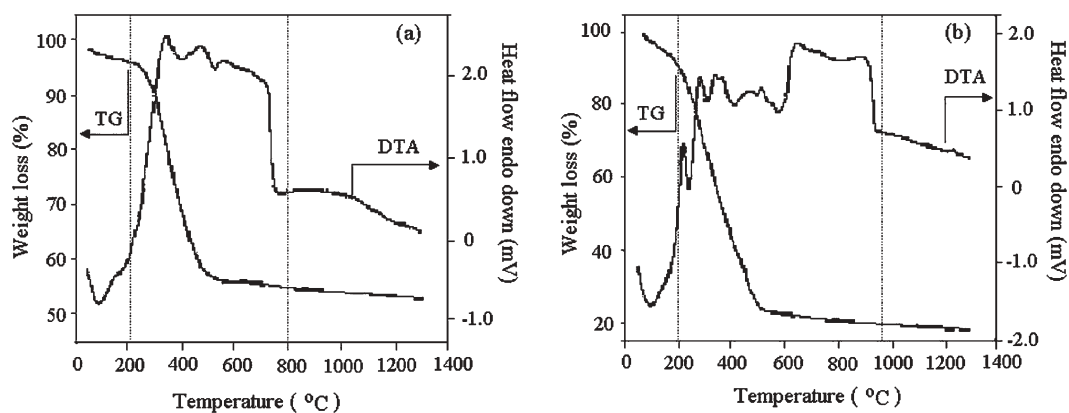


Fig. 4 TGA-DTA curves of the samples prepared in the reverse microemulsions ($W_0 = 0.10$) by different drying methods: (a) aerogel, (b) xerogel.

first took place at the contact neck between the particles. Large pore volume means a small contact area between particles, and therefore, the aerogel has high resistant ability to sintering. It is well known that the most serious sintering process takes place at high temperatures. However, the advanced porous structure of aerogel could reduce the sintering rate and hinder grain growth on the boundary between the particles at elevated temperature.¹⁴ Poco *et al.*¹⁵ further reported that the alumina aerogel does not sinter until above 950 °C due to its highly advanced pore. Therefore, we believe the formation of aerogel microstructure is responsible for its high resistant ability to sintering below 1000 °C during calcination. Above 1000 °C, the specific surface areas of the sample markedly decrease (Fig. 3), which could be ascribed to the initial formation of hexaaluminate phase. Once the hexaaluminate crystalline structure forms, grain growth along (001) could be suppressed effectively due to its specific crystal structure.¹⁶ As a result, the hexaaluminate catalyst with high surface area could be obtained. In contrast, during the CD process, the particles would agglomerate severely into large particles under high capillary tension of water (an order of ~ 100 MPa).¹⁷ After high-temperature calcination, the particles sintered or grew severely, which leads to a small surface area.

3.3. The phase composition of the $\text{BaMnAl}_{11}\text{O}_{19}$ catalysts

TG-DTA results are shown in Fig. 4. For the aerogel, the TG curve presents two stages of weight loss in the range of room temperature to 800 °C. Below 200 °C, the weight loss of the sample is about 5%, which is caused by the dehydration; and an endothermic peak at about 100 °C appears in the DTA curve. Above 200 °C, the weight loss of the sample is about 40%. This may be mainly caused by the removal of the organic chemicals and the hydroxyl, and the decomposition of the carbonates. During the stage, the combustion of the organic chemicals is exothermic; but the hydroxylation and the decomposition of the carbonates are endothermic. As shown in Table 2 and Fig. 2, the aerogel has a large pore size and pore volume, and the organic chemicals may sufficiently contact with air. The organic chemicals would combust quickly and produce quantities of heat. Ultimately, an exothermic platform can be observed between 200 and 800 °C in the DTA curve.

Above 800 °C, no weight loss and exothermic peak can be observed in the TG curve and DTA curves, respectively. The formation of hexaaluminate phase may be a slow process, or the exothermic effect due to the decrease of surface energy may be small under the experiment conditions; therefore, it is difficult to determine accurately the formation temperature of the hexaaluminate phase. As can be observed from Fig. 3, however, the surface area of the aerogel sample decreases rapidly from 1000 °C; it is probable that the hexaaluminate crystallites begin to form at 1000 °C. In the range of room temperature to 1300 °C, the total weight loss of the aerogel is about 45%.

For the xerogel, there are also two stages of weight loss in the TG curve. Below 200 °C, the weight loss of the sample is 10%, which is higher than that (5%) of the aerogel. At the same time, an endothermic peak also appears at about 100 °C in the DTA curve. This indicates the xerogel contains more water than the aerogel. The reason may be that the drying temperature (260 °C) in the SCD process is higher than that (110 °C) in the CD one. In the range of 200 to 950 °C, the weight loss of the CD sample is about 70%, which is higher than that (40%) of the SCD sample. This indicates the xerogel sample contains more hydroxyls than the aerogel does. In the DTA curve, the exothermic peaks appear at 220, 290, 350 and 520 °C, and an exothermic platform between 580 and 950 °C can be observed. However, the flat temperature region of the xerogel extends to 950 °C, compared with that (750 °C) of the aerogel. This could be ascribed to the texture of the xerogel. As shown in Table 2 and Fig. 2, the xerogel has small pore size and pore volume. The organic chemicals may not be in contact with air sufficiently, and therefore the organic chemicals will combust slowly. Due to the slow combustion model, the exothermic platform is extended up to a temperature of 950 °C. Above 950 °C, no weight loss in the TG curve and no exothermic peak in the DTA curve can be observed. In the range of room temperature to 1300 °C, the total weight loss of the xerogel is about 80%, which is more than that (45%) of the aerogel. This means that the xerogel contains more water and hydroxyl than the aerogel. Therefore, the CD sample would aggregate and sinter severely, compared with the SCD one. As shown in Table 2, the surface area of the SCD catalyst is higher than that of the CD one. From the DTA curve,

however, it is very difficult to determine the initial formation temperature of hexaaluminate crystalline phase. The surface area of the xerogel sample decreases rapidly from 1100 °C (in Fig. 3). It is possible that the hexaaluminate crystallites begin to form at about 1100 °C, which is higher than that (1000 °C) of the aerogel sample. The difference could be ascribed to the homogeneity of the precursors, which can be demonstrated by the XRD patterns.

As observed from Fig. 5, before calcination, both xerogel and aerogel are amorphous. No diffraction peaks of carbonates or hydroxides (Al, Mn and Ba) appear, indicating that the constituents were highly dispersed in the samples. Because the whole reaction is predominated by the matter exchange process between the micelles, the Al, Mn and Ba species would react with carbonate homogeneously, although the Mn, Ba, Al species have different precipitating rates. Therefore, through processing with the reverse microemulsion, the precursors can achieve the homogeneity at a molecular level. After calcination at 800 °C, the SCD sample is still amorphous. For the CD sample, however, the diffraction peaks of carbonates or oxides (Ba, Mn and Al) are observed. This could be caused by the drying method. In the SCD process, since the interface between liquid and vapor disappeared, the migration of the active species from inner to surface of the pores is eliminated effectively. As a result, the homogeneity of the precursor could be maintained. The high homogeneity could promote the reactions among Ba, Mn and Al, and the hexaaluminate crystalline phase could form at a low temperature.¹⁶ Therefore, the SCD catalyst may maintain small particle size and high surface area. Although the differences in reactivity of the Ba, Mn and Al species could be eliminated through the reverse microemulsion method, during the CD process, the active components would migrate while the water flows from the inner to the surface of the pores. As a result, the obtained precursor by CD method is not homogeneous, and the hexaaluminate phase would form at a high temperature.

After calcination at 1200 °C, the hexaaluminate phase, together with amounts of α -Al₂O₃ and BaAl₂O₄, formed (shown in Fig. 5b). It seems that phase transformation pathways for the two samples are different. For the SCD catalyst, the hexaaluminate phase formed directly from the amorphous precursor. For the CD sample, the BaCO₃ and BaAl₂O₄ crystallites formed before the formation of the hexaaluminate crystallites. This means that the hexaaluminate crystallites formed *via* the BaAl₂O₄ intermediate.

In our previous study,⁸ we reported that the texture properties of the precursor had a significant influence on the formation of La-hexaaluminate. We believed that the formation of La-hexaaluminate phase was delayed to some extent by SCD. In this study, it seems that the influence of the precursor homogeneity on the formation of Ba-hexaaluminate is more significant than that of its textural properties. To our knowledge, Lanthanum carbonate can decompose at about 800 °C, while barium carbonate can only decompose above 1100 °C. Since the homogeneity of the SCD precursor is superior to that of the CD precursor, the high homogeneity of the precursor would be beneficial to the solid-state reactions ($\text{BaCO}_3 + \text{Al}_2\text{O}_3 \rightarrow \text{BaAl}_2\text{O}_4$, $\text{BaAl}_2\text{O}_4 + \text{MnO} + \text{Al}_2\text{O}_3 \rightarrow \text{BaMnAl}_{11}\text{O}_{19}$).¹⁸ As a result, the hexaaluminate phase would form at low temperatures, supported by the TG-DTA curves and XRD patterns. Although the ultrafine particles are more apt to sinter than the large ones, the highly homogeneous precursor is beneficial to the formation of hexaaluminate because the diffusion and rearrangement of the ion could be promoted. Therefore, we believe that the homogeneity of the precursor may play a more important role in the formation of the Ba-hexaaluminate than in that of the La-hexaaluminate.

3.4. Effect of Ce introduction on the catalysts

Since ceria possesses the high storage capability of oxygen,¹⁹ we have attempted to introduce Ce into the hexaaluminate

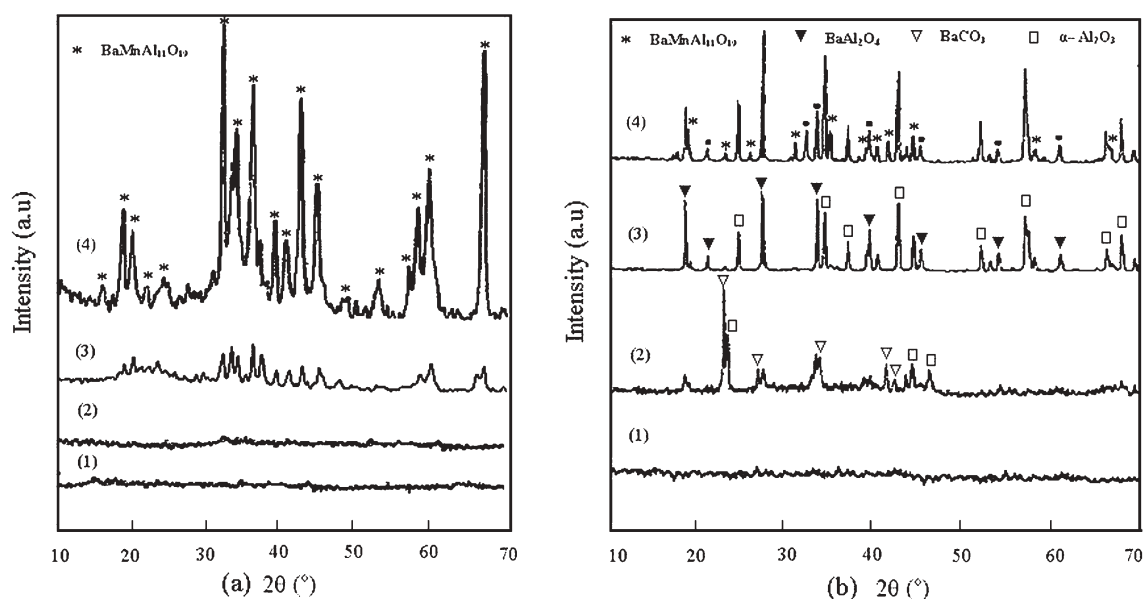


Fig. 5 The XRD patterns of the BaMnAl₁₁O₁₉ catalysts prepared in the reverse microemulsions ($W_0 = 0.10$) by different drying methods (a): 1—xerogel, 2—800 °C, 3—1100 °C, 4—1200 °C; (b): 1—xerogel, 2—800 °C, 3—1100 °C, 4—1200 °C.

crystal lattice. Iyi *et al.*²⁰ reported that only the mono-, di- and trivalent ions with radius above 1.10 Å could be accommodated in the mirror plane of hexaaluminate crystal. Since the radius of the Ce(III) ion is 1.18 Å, it seems that it could be accommodated in the hexaaluminate lattice. However, during the calcination process at 1200 °C in flowing air, the Ce(III) ions would be oxidized into the Ce(IV) ions. The radius of the Ce(IV) ion is 0.92 Å, so Ce would be excluded from the hexaaluminate lattice.

Fig. 6 presents the XRD patterns of the $Ce_xBa_{1-x}MnAl_{11}O_y$ catalysts. At $x = 0.1$, no characteristic peaks of the CeO_2 phase could be observed, which indicates the CeO_2 crystallites may highly disperse in the hexaaluminate matrix. Zarur and Ying⁷ also observed the similar phenomenon when they synthesized the $CeO_2/BaAl_{12}O_{19}$ catalyst. At $x = 0.2$, the CeO_2 phase appears as a separate impurity phase, and the hexaaluminate phase is still present. The reason is that the hexaaluminate could form in a wide range of Ba/Al ratios.²¹ When $x = 0.3$, the diffraction peaks of CeO_2 crystallites are strong, and the diffraction peaks of $\alpha-Al_2O_3$ appear; but the diffraction peaks of the hexaaluminate crystallites are very weak. This suggests that the presence of Ce could prevent the formation of hexaaluminate to some extent. On the other hand, compared with pure $\alpha-Al_2O_3$, the diffraction peaks of $\alpha-Al_2O_3$ in the $Ce_xBa_{1-x}MnAl_{11}O_y$ sample ($x = 0.3$) are weak, indicating that

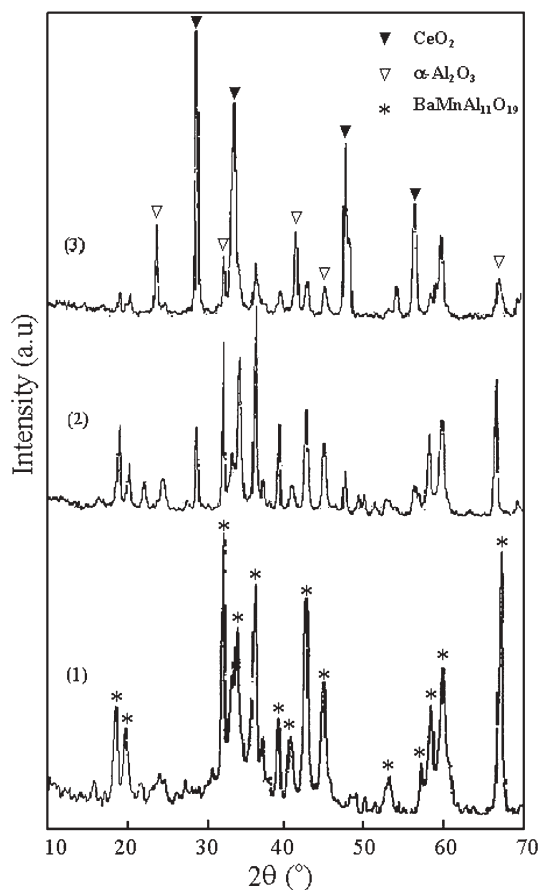


Fig. 6 The XRD patterns of the $Ce_xBa_{1-x}MnAl_{11}O_y$ catalysts prepared in the reverse microemulsions ($W_0 = 0.10$) under supercritical drying (SCD): (1) $x = 0.1$; (2) $x = 0.2$; (3) $x = 0.3$.

Table 3 The catalytic activity for methane combustion over the $Ce_xBa_{1-x}MnAl_{11}O_y$ catalysts prepared in reverse microemulsions ($W_0 = 0.10$)

Catalyst ^a	Ce content (x)	Drying	SSA/m ² g ⁻¹	$T_{10}/^{\circ}C$ ^b	$T_{90}/^{\circ}C$ ^b
C ₀ -SCD	0.0	SCD	72.4	445	770
C ₀ -CD	0.0	CD	43.3	520	810
C ₁ -SCD	0.1	SCD	74.2	430	730
C ₂ -SCD	0.2	SCD	47.1	510	820
C ₃ -SCD	0.3	SCD	25.5	550	850

^a The $Ce_xBa_{1-x}MnAl_{11}O_y$ catalysts prepared by SCD are designated as C_x-SCD ($x = 0, 0.1, 0.2$ and 0.3); the $Ce_xBa_{1-x}MnAl_{11}O_y$ catalysts prepared by CD were designated as C_x-CD. ^b T_{10} the temperature at 10% methane conversion, T_{90} the temperature at 90% methane conversion.

the phase transition from $\gamma-Al_2O_3$ to $\alpha-Al_2O_3$ could be restrained to some extent in the presence of CeO_2 crystallites. The phenomenon probably may be ascribed to the separating effect of ceria crystallites.²²

When Ce was introduced, the $Ce_xBa_{1-x}MnAl_{11}O_y$ catalyst had a large surface area at $x = 0.1$ (Table 3), although Ce could not enter the hexaaluminate lattice; when $x > 0.1$, the surface area of the $Ce_xBa_{1-x}MnAl_{11}O_y$ catalysts decreased due to the formation of CeO_2 phase. The results also show that the hexaaluminate structure is stable at high temperature. Therefore, the formation of pure hexaaluminate phase is very important to obtain the materials with large surface area.

3.5 Methane combustion over the $Ce_xBa_{1-x}MnAl_{11}O_y$ catalysts

The activities of methane combustion over the $Ce_xBa_{1-x}MnAl_{11}O_y$ catalysts are shown in Fig. 7, and summarized in Table 3.

At $x = 0$, T_{10} (the temperature at 10% methane conversion) of methane combustion over the SCD catalyst is 445 °C, lower than that (520 °C) over the CD one. At the low temperatures, the combustion reaction is mainly controlled by surface

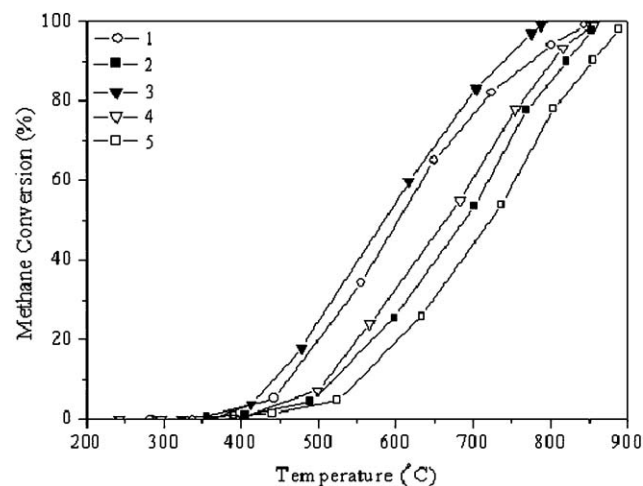


Fig. 7 Catalytic activities for methane combustion over the $Ce_xBa_{1-x}MnAl_{11}O_y$ catalysts prepared in the reverse microemulsions ($W_0 = 0.10$): (1) $x = 0$, SCD; (2) $x = 0$, CD; (3) $x = 0.1$, SCD; (4) $x = 0.2$, SCD; (5) $x = 0.3$, SCD.

reaction.⁸ Compared with the CD catalyst, the SCD catalyst has higher surface area; and the SCD catalyst could provide larger reacting surface. T_{90} (the temperature at 90% methane conversion) over the SCD catalyst is 770 °C, lower than those over the CD one (810 °C). At the high temperatures, the combustion reaction of methane is mainly controlled by mass transfer process.⁸ The high surface area of the SCD catalyst favors gas diffusivity. Therefore, the SCD catalyst shows higher activity than the CD one. When $x = 0.1$, the $\text{Ce}_{0.1}\text{Ba}_{0.9}\text{MnAl}_{11}\text{O}_y$ catalyst has a slightly higher activity ($T_{10} = 430$ °C, $T_{90} = 730$ °C) than the $\text{BaMnAl}_{11}\text{O}_{19}$ catalyst. The high activity of the $\text{Ce}_{0.1}\text{Ba}_{0.9}\text{MnAl}_{11}\text{O}_y$ catalyst could be ascribed to its high reactive surface, although the direct proof was not obtained. Machida *et al.*²³ concluded that the high catalytic activity for methane combustion over the $\text{BaMnAl}_{11}\text{O}_{19}$ catalyst resulted from the fast redox couple between Mn^{2+} and Mn^{3+} . It is well known that Ce can transform between Ce(III) and Ce(IV).¹⁹ We believe that there may exist a synergic effect between Ce and Mn, which could improve the catalyst activity. Yan and Thompson²⁴ also reported the synergic effect between Mn and Co, when they introduced Mn and Co into the Ba-hexaaluminate catalyst. When $x > 0.1$, the activities of the $\text{Ce}_x\text{Ba}_{1-x}\text{MnAl}_{11}\text{O}_y$ catalysts are low due to their low surface area.

4. Conclusions

In this study, the high-surface-area $\text{Ce}_x\text{Ba}_{1-x}\text{MnAl}_{11}\text{O}_y$ catalysts were synthesized by the reverse microemulsion method, using the nontoxic and inexpensive inorganic salts, instead of the alkoxides, as reactants. Therefore, the preparation is environmentally friendly and low-cost. The study shows that the catalyst morphology could be controlled effectively by the microemulsion microstructure; the homogeneity of precursor could be enhanced greatly by the reverse microemulsion method and the supercritical drying method. As a result, the hexaaluminate phase could form at a relatively low temperature (lower than 1100 °C). The $\text{BaMnAl}_{11}\text{O}_{19}$ catalyst has high surface area ($72.4 \text{ m}^2 \text{ g}^{-1}$) and high activity ($T_{10} = 445$ °C). Although Ce could not enter the hexaaluminate lattice, the CeO_2 crystallites could highly disperse in the catalyst at moderate Ce concentration ($x \leq 1$). Compared with the $\text{BaMnAl}_{11}\text{O}_{19}$ catalyst, the $\text{Ce}_{0.1}\text{Ba}_{0.9}\text{MnAl}_{11}\text{O}_y$ catalyst shows higher activity ($T_{10} = 430$ °C) due to the synergic effect between Mn and Ce.

Acknowledgements

We would like to thank the Ministry of Science and Technology of China (G1999022401) for financial support.

Fei Teng,^{*ab} Ping Xu,^a Zhijian Tian,^{*a} Guoxing Xiong,^{*b} Yunpeng Xu,^a Zhusheng Xu^a and Liwu Lin^{ba}

^aLaboratory of Natural Gas conversion & utilization, Dalian Institute of Chemical Physics, Chinese Academy of Sciences, Dalian 116023, China. E-mail: tfwd@dicp.ac.cn; tianz@dicp.ac.cn; Fax: +86-411-84379151; Tel: +86-411-84379151

^bState Key Laboratory of Catalysis, Dalian Institute of Chemical Physics, Chinese Academy of Sciences, Dalian 116023, China. E-mail: gxxiong@dicp.ac.cn; Fax: +86-411-84379182; Tel: +86-411-84379182

References

- 1 J. G. McCarty, *Nature*, 2000, **403**, 35.
- 2 E. M. Johansson, K. M. J. Danielsson, E. Pocaroba, E. D. Haralson and S. G. Järås, *Appl. Catal. A*, 1999, **182**, 199.
- 3 M. Machida, K. Eguchi and H. Arai, *J. Catal.*, 1987, **103**, 385.
- 4 Y. Mizushima and M. Hori, *J. Mater. Res.*, 1994, **9**, 2272.
- 5 G. Groppi, M. Bellotto, C. Cristiani, P. Forzatti and P. L. Villa, *Appl. Catal. A*, 1993, **104**, 101.
- 6 B. W.-L. Jang, R. M. Nelson, J. J. Spivey, M. Ocal, R. Oukaci and G. Marcelin, *Catal. Today*, 1999, **47**, 103.
- 7 A. J. Zarur and J. Y. Ying, *Nature*, 2000, **403**, 65.
- 8 J. Wang, Z. Tian, J. Xu, Y. Xu, Z. Xu and L. Lin, *Catal. Today*, 2003, **83**, 213.
- 9 F. Teng, Z. Tian, J. Xu, G. Xiong and L. Lin, *Stud. Surf. Sci. Catal.*, 2004, **147**, 493.
- 10 D. O. Shah and R. M. Jr. Hamlin, *Science*, 1971, **171**, 483.
- 11 M. Bellotto, G. Artioli, C. Cristiani, P. Forzatti and G. Groppi, *J. Catal.*, 1998, **179**, 597.
- 12 K. S. W. Sing, D. H. Everett, R. A. W. Haul, L. Moscou, R. A. Pierotti, J. Rouquerol and T. Siemieniewska, *Pure Appl. Chem.*, 1985, **57**, 603.
- 13 T. Ishikawa, R. Ohashi, H. Nakabayashi, N. Kakuta, A. Ueno and A. Furuta, *J. Catal.*, 1992, **134**, 87.
- 14 J. White, *The sintering of industrial powders*, in *Sintering processes*, ed. G. C. Kuczynski, P377, Plenum press, 1980.
- 15 J. F. Poco, J. H. Satcher, Jr. and L. W. Hrubesh, *J. Non-Cryst. Solids*, 2001, **285**, 57.
- 16 M. Machida, K. Eguchi and H. Arai, *Bull. Chem. Soc. Jpn.*, 1988, 3659.
- 17 L. L. Hench and J. K. West, *Chem. Rev.*, 1990, **90**, 33.
- 18 M. Machida, K. Eguchi and H. Arai, *J. Am. Ceram. Soc.*, 1998, **71**, 12, 1142.
- 19 A. Trovarelli, *Catal. Rev. Sci. Eng.*, 1996, **38**, 439.
- 20 N. Iyi, S. Takekawa and S. Kimura, *J. Solid State Chem.*, 1989, **83**, 8.
- 21 S. Kimura, E. Bannai and I. Shindo, *Mater. Res. Bull.*, 1982, **17**, 209.
- 22 A. Kato, *J. Am. Ceram. Soc.*, 1987, **70**, 7, C157.
- 23 M. Machida, K. Eguchi and H. Arai, *J. Catal.*, 1989, **120**, 377.
- 24 L. Yan and L. T. Thompson, *Appl. Catal. A*, 1998, **171**, 219.

Markedly improving lipase-mediated asymmetric ammonolysis of D,L-*p*-hydroxyphenylglycine methyl ester by using an ionic liquid as the reaction medium

Wen-Yong Lou,^{ab} Min-Hua Zong,^{*a} Hong Wu,^a Ruo Xu^a and Ju-Fang Wang^a

Received 22nd February 2005, Accepted 4th April 2005

First published as an Advance Article on the web 22nd April 2005

DOI: 10.1039/b502716k

A comparative study was made of lipase-catalyzed asymmetric ammonolysis of D,L-*p*-hydroxyphenylglycine methyl ester (D,L-HPGME) with ammonium carbamate as the ammonia donor in nine ionic liquids (ILs) and four organic solvents. An obvious enhancement in the enantioselectivity (E value) of the ammonolysis was observed using ILs as the reaction media when compared to the organic solvents tested. However, the rate of ammonolysis in the IL 1-hexyl-3-methylimidazolium tetrafluoroborate ($C_6MIm \cdot BF_4$), which was the best IL medium for the reaction, was much lower than that achieved in *tert*-butanol. It was also found that both the cation and the anion of ILs have a significant effect on the reaction. *Candida antarctica* lipase B immobilized on an acrylic resin (CAL-B, *i.e.*, Novozym 435) displayed no ammonolysis activity toward D,L-HPGME in two ILs, 1-butyl-3-methylimidazolium bromide ($C_4MIm \cdot Br$) and 1-butyl-3-methylimidazolium nitrate ($C_4MIm \cdot NO_3$). When an IL-*tert*-butanol co-solvent system was adopted as the solvent for the enzymatic ammonolysis, the initial rate and enantioselectivity were enhanced markedly. It was noticed that the ammonolysis was dependent on the water activity (a_w) in the co-solvent systems, and an a_w of 0.75 was optimal. Among the six co-solvent systems examined, the lowest apparent K_m and activation energy (E_a), and the highest V_{max} of the ammonolysis were achieved with the co-solvent mixture of $C_6MIm \cdot BF_4$ and *tert*-butanol (20 : 80, v/v), in which the lipase CAL-B also exhibited good stability.

Introduction

Enantiomerically pure unnatural amino acids are widely used as key intermediates for the synthesis of semisynthetic antibiotics, peptide hormones, pyrethroids and pesticides.¹ Among such intermediates, enantiopure *p*-hydroxyphenylglycine (HPG) and its derivatives, which play a crucial role in the manufacture of amoxicillin, aspoxicillin, cefpyramide, complestatin and vancomycin,² are some of the most important. Currently, enantiomerically pure HPG is commercially produced by a chemoenzymatic route using D-hydantoinase. In this procedure, chemically synthesized 5-hydroxyphenyl hydantoin is stereoselectively hydrolyzed to *N*-carbamoyl-D-HPG by D-hydantoinase, followed by the chemical conversion of the product to D-HPG under acidic conditions. However, the approach needs several additional operations and may generate a large amount of process waste.³ Consequently, more efficient methodologies for the production of enantiopure HPG are of great industrial importance. From a practical standpoint, enzymatic kinetic resolution of racemates is a favorable option. The enzymatic ammonolysis of carboxylic esters was discovered in the mid-1990s and provides a mild procedure for the preparation of carboxylic amides as well as an attractive method for the resolution of racemates.⁴⁻⁶ Some efforts have been made on the enzymatic ammonolysis of racemic phenylglycine methyl ester in

organic solvents to achieve the *R*-enantiomer, using ammonia as the acyl acceptor.⁷⁻⁹ It has been found, however, that excess ammonia is detrimental to the enzymatic reaction, especially for long-term operation, and thus ammonium carbamate has been employed in place of ammonia gas.^{10,11} Unfortunately, ammonolysis carried out in organic solvents showed only moderate enantioselectivity. Additionally, serious environmental problems are associated with the use of volatile organic solvents, particularly when they are employed on a large scale. Accordingly, there is a compelling need for a reaction medium that would minimize harm to the environment at the same time as permitting highly enantioselective catalysis.

Ionic liquids (ILs), typically consisting of organic cations and inorganic anions, have recently emerged as a promising replacement for volatile organic solvents in a wide variety of synthetic reactions, due to their advantageous properties including negligible vapor pressure, high thermal and chemical stability, recoverability and recyclability.¹² Also, ILs exhibit an excellent ability to dissolve polar and apolar organic, organometallic and inorganic compounds. ILs are also very versatile in that their properties can be manipulated to suit the requirements of a particular process by changing the nature of the cation and anion and the length of the side chain attached to the cation. All these unique characteristics make ILs promising for biocatalytic processes as well as chemical processes.¹³

In recent years, many enzymatic transformations in ILs or other systems containing ILs have been conducted successfully

*bhmhzong@scut.edu.cn

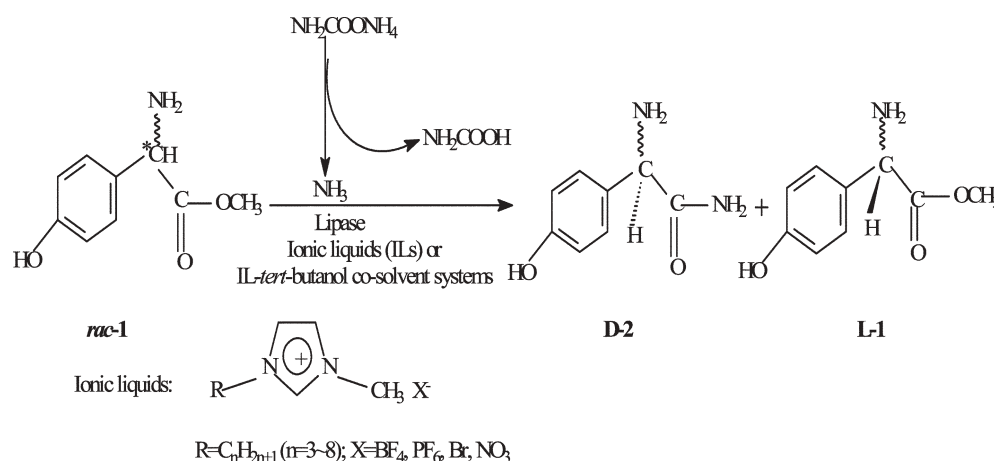
and in many cases, with remarkably improved results.^{14–21} For instance, we have recently reported papain-mediated enantioselective hydrolysis of D,L-*p*-hydroxyphenylglycine ester in a co-solvent mixture of IL and phosphate buffer for the preparation of enantiopure *p*-hydroxyphenylglycine (HPG).²² Papain displayed much higher hydrolytic activity and enantioselectivity in a buffer solution containing 12.5% (v/v) 1-butyl-3-methylimidazolium tetrafluoroborate (C₄MIm·BF₄) than in other co-solvent systems examined. Moreover, markedly enhanced stability of the enzyme was observed in the IL-buffer co-solvent systems. The reaction was subsequently carried out under reduced pressure to remove the product methanol *in situ*, resulting in further raised yield and enantiomeric excess (*e.e.*) of HPG.²³ As an extension of our ongoing research program on enzyme-catalyzed asymmetric reactions in ILs, we herein describe the successful lipase-mediated asymmetric ammonolysis of D,L-*p*-hydroxyphenylglycine methyl ester (D,L-HPGME, *rac*-1) to enantiopure D-hydroxyphenylglycine amide (D-HPGA, D-2) in ILs and IL-*tert*-butanol co-solvent systems (Scheme 1) and we describe the influence of the cation and the anion component of the IL on the reaction as well as the enzyme stability.

Results and discussion

Recent studies have shown that the activity, stability and even, in some cases, enantioselectivity of lipase-catalysed reaction can be considerably enhanced by switching the reaction media from organic solvents to ILs or systems containing ILs.^{24–27} However, the effect of different ionic liquids on lipase-mediated reactions has been found to vary widely. Consequently, we initially focused on the influence of the cations and anions of nine ILs on the asymmetric ammonolysis of *rac*-1 with ammonium carbamate by immobilized lipase from *Candida antarctica* B (CAL-B) (Novozym 435) (Table 1, entries 1–9), which displays good ammonolysis activity towards other substrates like carboxylic acid esters.⁶ In the case of 1-alkyl-3-methylimidazolium tetrafluoroborate (C_{*n*}MIm·BF₄, *n* = 3–8), both the hydrophobicity and the viscosity of ILs increase with increasing length of the alkyl group (*i.e.* increasing *n* value), while the polarity decreases to

some extent.^{28,29} As shown in Table 1, the reaction became faster and more enantioselective (expressed in terms of the enantiomeric ratio *E* unless specified otherwise) with the elongation of the alkyl chain (Table 1, entries 1–4). However, further extension of the alkyl chain, to seven carbon atoms and longer, resulted in lowered initial rate and minor variation in *E* value (Table 1, entries 4–6). In addition, CAL-B showed relatively high ammonolysis activity and low enantioselectivity in C₄MIm·BF₄ compared to C₄MIm·PF₆. No ammonolysis reaction was observed in C₄MIm·NO₃ or C₄MIm·Br. These results suggested that the activity and the enantioselectivity of CAL-B-mediated ammonolysis is anion-dependent. The anions NO₃[–] and Br[–] are more nucleophilic than BF₄[–] and PF₆[–], and may coordinate strongly to positively charged sites in the structure of lipase, resulting in conformational changes and thus inactivation of the enzyme.^{30,31} Also, BF₄[–] and PF₆[–] anions spread their negative charge over four and six fluorine atoms, respectively and thus weaken hydrogen-bond basicity of the ILs C₄MIm·BF₄ and C₄MIm·PF₆. Lower hydrogen-bond basicity minimizes interference with the internal hydrogen bonds of an enzyme and so consistent with this notion, enzymes are inactive in C₄MIm·NO₃ and C₄MIm·Br, which have high hydrogen-bond basicity. Surprisingly, CAL-B incubated for 48 h in C₄MIm·NO₃ retained around 85% of its original activity, while CAL-B incubated for the same period in C₄MIm·Br displayed no detectable activity. The reasons for this unexpected result are the subject of an ongoing investigation in our laboratory.

It is of particular interest to compare the reactions carried out in ILs with those in organic solvents. Table 1 illustrates that CAL-B-mediated ammonolysis of *rac*-1 proceeded in *tert*-butanol (BuOH) and *tert*-amyl alcohol (AmOH) with dramatically higher initial rates than those observed in 1,2-dichloroethane (DCIE), tetrahydrofuran (THF) or any of the ILs that were investigated. However, the enzyme was less enantioselective (*E* = 8–22) in all the organic solvents tested compared to the ILs. We tried to correlate the activity and the enantioselectivity of the reaction with parameters such as hydrophobicity, polarity, dielectric constant and viscosity of the medium, but no such correlation was detected.



Scheme 1 Lipase-mediated asymmetric ammonolysis of D,L-HPGE (*rac*-1) in ILs or IL-*tert*-butanol co-solvent systems

Table 1 Lipase-mediated asymmetric ammonolysis of *rac*-1

Entry	Lipase ^a	Medium ^a	Initial rate ($\mu\text{M}\cdot\text{min}^{-1}\cdot\text{mg}^{-1}$)	Time / h	Yield ^b (%)	<i>e.e.</i> _p (%)	<i>e.e.</i> _s (%)	<i>E</i>
1	CAL-B	C ₃ MIm·BF ₄	0.38	48	33.2	88.2	48.4	25
2	CAL-B	C ₄ MIm·BF ₄	0.57	48	42.4	90.6	72.5	43
3	CAL-B	C ₅ MIm·BF ₄	0.63	48	43.8	92.4	78.7	59
4	CAL-B	C ₆ MIm·BF ₄	0.78	48	46.5	94.1	86.3	67
5	CAL-B	C ₇ MIm·BF ₄	0.45	48	38.3	94.7	61.5	68
6	CAL-B	C ₈ MIm·BF ₄	0.31	68	26.6	95.4	35.7	63
7	CAL-B	C ₄ MIm·PF ₆	0.19	86	23.5	94.8	30.1	50
8	CAL-B	C ₄ MIm·Br	n.r.	48	n.r.	n.r.	n.r.	n.r.
9	CAL-B	C ₄ MIm·NO ₃	n.r.	48	n.r.	n.r.	n.r.	n.r.
10	CAL-B	BuOH	1.83	4	38.6	71.4	57.5	12
11	CAL-B	AmOH ^c	1.74	4	36.1	85.7	54.5	22
12	CAL-B	DCIE ^c	0.54	40	35.2	76.5	50.4	13
13	CAL-B	THF ^c	0.32	60	24.3	70.7	28.2	8
14	CAL-B	30% (v/v) C ₅ MIm·BF ₄ -BuOH	2.66	4	45.5	89.9	82.7	48
15	CAL-B	15% (v/v) C ₇ MIm·BF ₄ -BuOH	2.42	4	42.7	91.7	74.7	52
16	CAL-B	20% (v/v) C ₆ MIm·BF ₄ -BuOH	3.18	4	46.8	92.6	87.6	63
17	CAL-B	50% (v/v) AmOH-BuOH	2.45	4	44.4	83.9	78.5	27
18	CAL-B	10% (v/v) DCIE-BuOH	2.24	4	40.3	79.8	65.0	19
19	CAL-B	20% (v/v) THF-BuOH	1.56	4	34.0	78.2	47.7	15
20	TLL-IM	20% (v/v) C ₆ MIm·BF ₄ -BuOH	0.29	24	23.1	65.0	25.9	7
21	RML-IM	20% (v/v) C ₆ MIm·BF ₄ -BuOH	n.r.	24	n.r.	n.r.	n.r.	n.r.
22	CCL	20% (v/v) C ₆ MIm·BF ₄ -BuOH	2.17	6	31.3	28.6	35.7	3
23	CRL	20% (v/v) C ₆ MIm·BF ₄ -BuOH	n.r.	24	n.r.	n.r.	n.r.	n.r.
24	MML-IM	20% (v/v) C ₆ MIm·BF ₄ -BuOH	n.r.	24	n.r.	n.r.	n.r.	n.r.

^a The a_w in the reaction systems is 0.75. ^b Yield of the product **2** on a mole basis. ^c BuOH (*tert*-butanol) was added to AmOH (*tert*-Amyl alcohol), DCIE (1,2-Dichloroethane) and THF (Tetrahydrofuran) as co-solvent (20%, v/v) to dissolve the substrate *rac*-1. ^d n.r. = no reaction.

Unlike the other three organic solvents, BuOH dissolves the substrate *rac*-1 and the product **2** well. Furthermore, it is also miscible with C₅MIm·BF₄, C₆MIm·BF₄, and C₇MIm·BF₄ in all proportions. To enhance the initial rate of the ammonolysis performed in the ILs, mixtures of BuOH and ILs (C₅MIm·BF₄, C₆MIm·BF₄ or C₇MIm·BF₄) were used as the reaction media. Fig. 1 depicts the obvious effect of IL content in the co-solvent mixture on the reaction. As expected, the initial rate was strongly dependent on IL concentration. The initial rate and the *E* value went up markedly with increasing

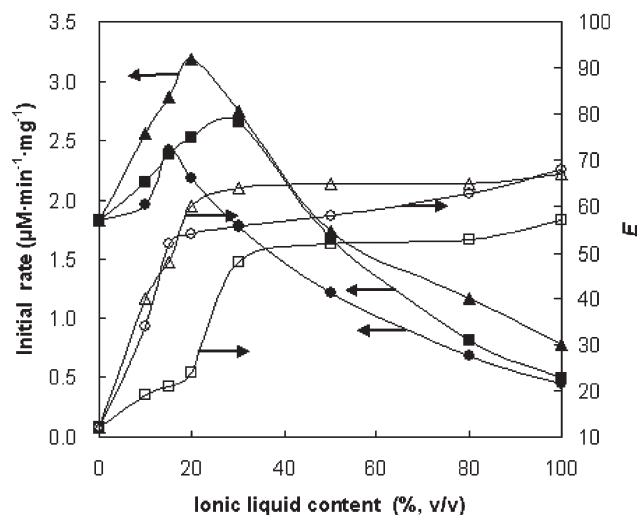


Fig. 1 Effect of ionic liquid content on lipase-catalyzed asymmetric ammonolysis of *rac*-1. Open symbols refer to *E* value; Full symbols refer to the initial rate. Symbols: (■ □) C₃MIm·BF₄; (▲ △) C₆MIm·BF₄; (● ○) C₇MIm·BF₄.

concentrations of C₅MIm·BF₄, C₆MIm·BF₄ and C₇MIm·BF₄ up to 30%, 20% and 15% (v/v), respectively, although further increase in IL content led to a sharp drop in the initial rate and a minor rise in the *E* value. High concentrations of IL cause high ionic strength in the reaction medium that might partially inactivate the enzyme. Also, the high viscosity of the reaction mixture caused by high concentrations of IL may limit the mass transfer of the substrate and product to and from the active sites of the enzyme, and may contribute to the fall in the initial rate seen at high IL concentrations. The results of a comparative study of CAL-B-mediated ammonolysis of *rac*-1 in different co-solvent mixtures are summarized in Table 1 (entries 14–19). A remarkable enhancement in the initial rate and the enantioselectivity was observed when the reaction was performed in the co-solvent mixtures containing the optimal concentration of each IL in BuOH. This is possibly because the presence of the optimal concentration of IL causes subtle changes in the enzyme conformation and the ionization state of the substrate that enhance their interaction. Of the co-solvent mixtures assayed, 20% (v/v) C₆MIm·BF₄-BuOH gave both the highest initial rate and enantioselectivity.

To get a better insight into the effect of the IL in the co-solvent mixtures on CAL-B-mediated ammonolysis of *rac*-1, a comparative study of the kinetic parameters of this reaction was conducted in 20% (v/v) C₆MIm·BF₄-BuOH, 50% (v/v) AmOH-BuOH, pure BuOH and 20% (v/v) THF-BuOH. In all four media the ammonolysis reaction followed Michaelis-Menten kinetics when ammonium carbamate, the ammonia donor, was in great excess. The values of apparent V_{max} and K_m are listed in Table 2. As expected, the highest V_{max} and lowest K_m were achieved when the reaction was carried out in the 20% (v/v) C₆MIm·BF₄-BuOH mixture. The value of V_{max}/K_m in 20% (v/v) C₆MIm·BF₄-BuOH was 2.2-, 2.9- and

Table 2 The apparent kinetic parameters and activation energy of CAL-B-mediated ammonolysis of *rac*-1 in various media

Media	K_m^a /mM	V_{max}^a / μ M min ⁻¹ mg ⁻¹	V_{max}/K_m (10^{-3} min ⁻¹ mg ⁻¹)	E_a^b /kJ mol ⁻¹
20% (v/v) C ₆ MIm·BF ₄ -BuOH	42.2	12.29	0.29	11.1
50% (v/v) AmOH-BuOH	69.5	9.34	0.13	26.2
BuOH	83.4	8.23	0.10	38.6
20% (v/v) THF-BuOH	108.3	7.50	0.07	52.8

^a The apparent kinetic parameters (V_{max} and K_m) were estimated by fitting the data to a standard Michaelis-Menten equation using the Eadie-Hofstee plot ($V = V_{max} - K_m \cdot V/C_s$, V : reaction rate; C_s : substrate concentration). ^b The apparent activation energy (E_a) values were determined by the linear regression analysis of the Arrhenius plots.

4.2-fold higher, respectively, than those observed in 50% (v/v) AmOH-BuOH, BuOH and 20% (v/v) THF-BuOH. Thus, it appears that the IL C₆MIm·BF₄ gives rise to an improvement in the affinity of the enzyme towards the substrate, which could partly account for the increased activity and enantioselectivity exhibited by CAL-B in 20% (v/v) C₆MIm·BF₄-BuOH in comparison with other media, as was demonstrated in Table 1 (entries 10, 16, 17 and 19). An increase in enzyme activity might also result from a decrease in activation energy (E_a) of the enzymatic reaction. As shown in Table 2, the E_a value of the reaction conducted in 20% (v/v) C₆MIm·BF₄-BuOH was much lower than those with 50% (v/v) AmOH-BuOH, pure BuOH and 20% THF-BuOH, suggesting that C₆MIm·BF₄ could make the "enzyme-substrate" transition state more stable due to its ionic nature.

Several other commercially available lipases were also investigated for their potential in catalyzing the asymmetric ammonolysis of *rac*-1 with ammonium carbamate in the co-solvent mixture of 20% (v/v) C₆MIm·BF₄ and BuOH (Table 1, entries 20–24). Among them, three lipases, namely RML-IM, CRL and MML-IM, exhibited no ammonolysis activity towards *rac*-1 (Table 1, entries 21, 23, 24) since the product was not detectable and no decline of the substrate concentration was observed after incubation of the reaction mixture for 24 h. In spite of the good ammonolysis activity, CCL showed no significant enantioselectivity to *rac*-1 ($E = 3$, Table 1, entry 22). TLL-IM exhibited low activity towards *rac*-1 (Table 1, entry 20), but interestingly had a slight preference of L-1 over D-1, which is in contrast to CAL-B. Among all the lipases tested, CAL-B displayed the highest activity and enantioselectivity. After a reaction time of 4 h, the yield, the product *e.e.* (*e.e.*_p) and the remaining substrate *e.e.* (*e.e.*_s) of the reaction with CAL-B were 46.8%, 92.6% and 87.6%, respectively (Table 1, entry 16).

It is well known that water activity (a_w) plays a crucial role in enzymatic reactions in non-aqueous media. In our case, it is of great significance to optimize the amount of water in the IL-*tert*-butanol co-solvent system since the presence of water may promote the competitive hydrolysis of *rac*-1. Two methods have been used to control a_w in ILs, including equilibration over saturated salt solutions,^{32–34} and the use of salt hydrate pairs.³⁵ The former is a well-established and effective approach for a_w studies, and the latter is not suitable for some ILs with good salt solubilities. Hence the pre-equilibration over saturated salt solutions for a_w control was chosen for this work. Table 3 shows the effect of a_w in the C₆MIm·BF₄-BuOH co-solvent system on the CAL-B-mediated asymmetric ammonolysis of *rac*-1. When the a_w

value was below 0.75, both the rate and the E value of the ammonolysis increased with increasing a_w . Further increase in a_w , however, led to lower reaction rates and lower enantioselectivity. Although hydrolysis of the substrate could be inhibited, the enzyme was hydrated incompletely and thus showed lower ammonolysis activity when a_w was below the optimum. On the other hand, an a_w above the optimum presumably allowed the enzyme to become completely hydrated, but competitive hydrolysis of the substrate *rac*-1 limited the ammonolysis reaction. It was also observed that too much water in the co-solvent system caused aggregation of the enzyme, which was clearly related to the decline in the reaction rate and the enantioselectivity at high a_w .

From both a practical and a theoretical viewpoint, it was of considerable importance to understand the influence of ILs on the stability of the enzyme. Accordingly, the operational stability of CAL-B was studied by incubating it in 20% (v/v) C₆MIm·BF₄-BuOH, 50% (v/v) AmOH-BuOH, pure BuOH and 20% (v/v) THF-BuOH, respectively, for a specified period of time at 35 °C, followed by the measurement of its relative activity. After operating repeatedly for eight batches (6 h each batch) in 20% (v/v) C₆MIm·BF₄-BuOH, 50% (v/v) AmOH-BuOH, pure BuOH and 20% (v/v) THF-BuOH CAL-B retained, respectively, approximately 83%, 37%, 25% and 5% of its original activity (Fig. 2). Fig. 3 illustrates the deactivation profile of CAL-B at various temperatures and in various media under the ammonolysis conditions. The much higher enzymatic activity after incubation in 20% (v/v) C₆MIm·BF₄-BuOH for 4 h at 90 °C than those in other media demonstrated that C₆MIm·BF₄ increased the thermal stability of CAL-B markedly. The coating and protection of the essential water surrounding the lipase by the IL could partly account for this.³⁶ Also, a greatly enhanced interaction of the substrate

Table 3 Influence of water activity on CAL-B-catalyzed asymmetric ammonolysis of D,L-HPGME in the IL-*tert*-butanol co-solvent mixture

a_w	V_0 / μ M min ⁻¹ mg ⁻¹	Yield of		$E.e._s$ (%)	$E.e._p$ (%)	E
		D-HPGA (4 h, %)	Conversion (4 h, %)			
0.12	1.60	34.7	35.8	52.2	94.2	51
0.33	2.69	44.5	46.4	79.2	92.4	55
0.55	3.03	45.4	47.6	83.5	91.3	57
0.75	3.18	46.8	48.9	87.6	92.6	65
0.85	3.07	45.9	49.5	83.4	84.6	32
0.97	2.62	41.8	45.3	67.3	81.5	22

^a Reaction conditions: 20 mM D,L-HPGME; 120 mM ammonium carbamate; 40 °C; 250 rpm; 50 mg Novozym 435; 1 mL C₆MIm·BF₄ (20%,v/v)-*tert*-butanol co-solvent.

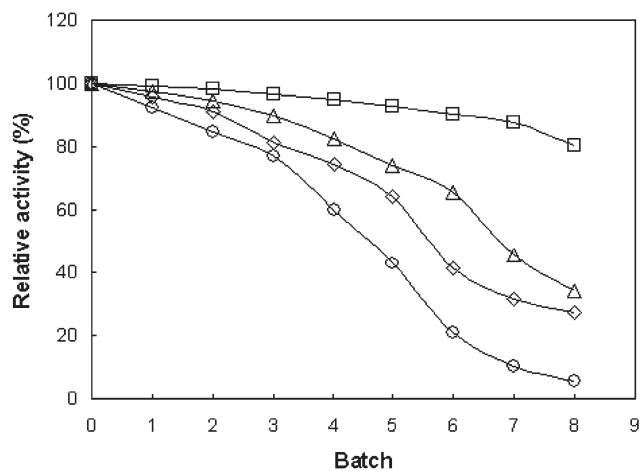


Fig. 2 Operational stability of CAL-B in 20% (v/v) C₆MIm·BF₄-BuOH c (□), 50% (v/v) AmOH-BuOH (Δ), BuOH (◇) and 20% THF-BuOH (○).

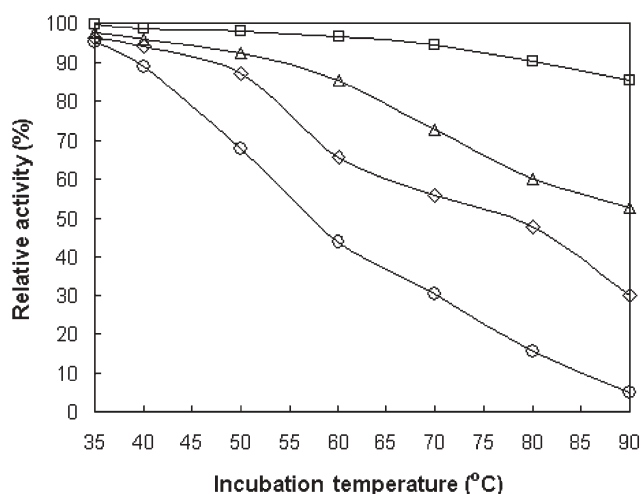


Fig. 3 Thermal stability of CAL-B in 20% (v/v) C₆MIm·BF₄-BuOH (□), 50% (v/v) AmOH-BuOH (Δ), BuOH (◇) and 20% THF-BuOH (○).

with the active site of CAL-B in the presence of the IL C₆MIm·BF₄ may be important in explaining these results. Furthermore, enzyme-solvent interactions in different media constitute an important factor in maintaining the active conformation of the protein. Thus, the observable improvement in the stability of CAL-B in C₆MIm·BF₄-BuOH mixture is possibly due to the electrostatic interaction between the IL and the protein, leading to a more rigid protein, which needs to overcome a higher kinetic barrier to unfold in comparison with the cases when the enzyme is incubated in non-ionic organic solvents.³⁷

Conclusions

The results described in this paper clearly demonstrate that the ILs in the co-solvent systems can boost markedly the activity, the enantioselectivity and the stability of CAL-B in asymmetric ammonolysis of *rac*-1 with ammonium carbamate. It has been

found that the water activity and IL content in the co-solvent systems have a significant impact on enzymatic ammonolysis. Further detailed investigations, however, will be necessary to gain sufficient knowledge about the impact of ILs on enzymes in general, and especially the interactions of various types of ILs with a wide variety of enzymes.

Experimental

Materials

Racemic *p*-hydroxyphenylglycine methyl ester (D,L-HPGME, 98% purity) and *p*-hydroxyphenylglycine (D,L-HPG, 99% purity) were kindly donated by Hebei Xinji Taida Petrochemical Co., Ltd. (Xinji, Hebei Province, China). Enantiopure HPGME (97% purity), HPG (98% purity) and ammonium carbamate (99%) were obtained from Aldrich-Fluka (USA). Enantiopure *p*-hydroxyphenylglycine amide (HPGA, over 97% purity) was obtained from DSM (Geleen, The Netherlands). Immobilized *Candida antarctica* lipase B (CAL-B) (*i.e.* Novozym 435, 10000 U g⁻¹), immobilized *Thermomyces lanuginosus* lipase (TLL-IM) (*i.e.* Lipozyme^{IM} TL, 50000 U g⁻¹), immobilized *Rhizomucor miehei* lipase (RML-IM) (*i.e.* Lipozyme^{IM} RM, 20000 U g⁻¹) and immobilized *Mucor miehei* lipase (MML-IM) (*i.e.* Lipozyme^{IM}, 9100 U g⁻¹) were kindly donated by Novozymes (Denmark). *Candida cylindracea* lipase (CCL, 360 U mg⁻¹) and *Candida rugosa* type VII lipase (CRL, 950 U mg⁻¹) were purchased from Sigma (USA). The nine ionic liquids used during this work {1-alkyl-3-methylimidazolium tetrafluoroborate (C_nMIm·BF₄, *n* = 3–8), 1-butyl-3-methylimidazolium hexafluorophosphate (C₄MIm·PF₆), 1-butyl-3-methylimidazolium nitrate (C₄MIm·NO₃) and 1-butyl-3-methylimidazolium bromide (C₄MIm·Br)} were supplied as gifts by Dr Li Xue-Hui (Department of Chemical Engineering, South China University of Technology, Guangzhou, China) and were all of over 98% purity. ILs were dried at 200 °C for 48 h before use. Solvents were dried over Zeolite CaA (Uetikon, activated at 400 °C for 24 h before use). All other chemicals were from commercial sources and were of analytical grade.

Water activity control

The pure solvents (ILs, organic solvents) and the substrate solutions (in ILs, organic solvents or IL-*tert*-butanol co-solvent mixtures) were equilibrated to fixed water activities (*a_w*) over saturated salt solutions in a closed container at 25 °C. The following salts were used: LiCl (*a_w* = 0.11), MgCl₂ (*a_w* = 0.33), Mg(NO₃)₂ (*a_w* = 0.53), NaCl (*a_w* = 0.75), KCl (*a_w* = 0.85) and K₂SO₄ (*a_w* = 0.97).³² The equilibration was monitored by water analysis using Karl Fischer titration until constant water contents were observed. The enzyme was equilibrated in separate vessels for 24 h at 25 °C.

General procedure for enzymatic ammonolysis

In a typical experiment, *rac*-1 (0.02 mmol), ammonium carbamate (0.12 mmol) and the selected lipase (500 U, one unit corresponds to the amount of enzyme that produces 1 μmole of fatty acid from a triglyceride h⁻¹ at pH 7.0 and 35 °C) were added to the reaction medium (IL or organic

solvent or the co-solvent mixture of IL and organic solvent, 1 mL) with specified a_w value. The resulting mixture was shaken reciprocally (250 rpm) at 40 °C. Aliquots were withdrawn at specified time intervals from the reaction mixture and the reactions were stopped by adding concentrated HClO₄. Then, the aliquots were diluted 20 times with water or methanol (when immiscible-water ILs such as C₆MIm·BF₄, C₇MIm·BF₄, C₈MIm·BF₄ and C₄MIm·PF₆ were used as solvents, methanol was added to dilute the samples) before HPLC analysis. To assay kinetic parameters, the reactions were carried out with *rac*-**1** concentrations between 5 and 120 mM. To investigate activation energy (E_a), the reactions were performed at various temperatures between 30 °C and 50 °C.

Enzyme stability

In order to assess the operational stability of the enzyme, the re-use of the CAL-B (Novozym 435) was investigated over 8 reaction cycles. Initially 50 mg aliquots of the immobilized enzyme were added into separate screw-capped vials each containing 1 mL of each of the appropriate medium {20% (v/v) C₆MIm·BF₄-*tert*-butanol co-solvent, 50% (v/v) *tert*-amyl alcohol-*tert*-butanol co-solvent, *tert*-butanol, or 20% (v/v) tetrahydrofuran-*tert*-butanol co-solvent}, together with *rac*-**1** (0.02 mmol) and ammonium carbamate (0.12 mmol). The reaction was then repeated over 8 cycles (6 h per batch) at 35 °C and 250 rpm. Between cycles the immobilized enzyme was filtered from the reaction mixture, then washed twice with fresh solvent, and added to a fresh batch of substrate solution. Additionally, the thermal stability of enzyme was studied by incubating it in the various media described above for 4 h at various temperatures from 35 to 90 °C, followed by the assay of its activity in the ammonolysis reaction.

Isolation of the product D-HPGA

Upon completion of the reaction, the reaction mixture was filtered to remove the immobilized enzyme and remaining ammonium carbamate. The unreacted substrate L-HPGME was extracted twice with ethyl acetate from the reaction mixture. Then, water was added to the reaction mixture, followed by dropwise addition of concentrated HCl (8.0 M) until the pH value was lowered to about 3.0 to precipitate the product D-HPGA. D-HPGA was filtered off and dried in vacuum at 70 °C. The separation yield of D-HPGA is over 90%. ¹H NMR (400 MHz, DMSO, ppm): δ = 4.17 (s, 1H, CHCONH₂), 6.68 and 7.16 (d, 4H, HOC₆H₄CH), 6.94 (s, 2H, CONH₂), 7.36 (s, 2H, CHNH₂), 9.28 (s, 1H, HOC₆H₄).

HPLC analysis

The reaction mixture was analyzed by chiral HPLC on a 4 × 150 mm 5 μ Crownpak CR (+) column from Daicel Chemical Industries Co., Ltd. (Tokyo, Japan) using a Waters 600 pump and a Waters 996 Photodiode Array Detector at 226 nm. The mobile phase was an aqueous solution of HClO₄ (0.011 M, pH 2.0) at 0.8 mL min⁻¹. The retention times for D-HPGA (D-2), D-HPGME (D-1), L-HPGA (L-2) and L-HPGME (L-1) were 2.18, 4.21, 6.95 and 17.35 min,

respectively. The initial rate (V_0), the enantiomeric excess (*e.e.*) of D-2 (*e.e.*_p), the *e.e.* of residual L-1 (*e.e.*_s), the yield of D-2 (on a mole basis unless specified), the substrate conversion (*c*) and the enantiomeric ratio ($E = \ln [(1 - c)(1 - e.e._s)] / \ln [(1 - c)(1 + e.e._s)]$) were calculated from the HPLC data. The average error for this determination was less than 0.7%. All reported data are averages of experiments performed at least in duplicate.

Acknowledgements

The authors wish to thank the National Natural Science Foundation of China (Grant No.20406006), the Natural Science Foundation of Guangdong Province (Grant No. 020839) and the State Key Laboratory of Bioreactor Engineering, East China University of Science and Technology for financial support. Dr Li Xue-Hui, South China University of Technology, is gratefully acknowledged for the generous gifts of ionic liquids. The authors are grateful to Dr Thomas J. Smith (Sheffield Hallam University) for his suggestions on improving English usage of the manuscript.

Wen-Yong Lou,^{ab} Min-Hua Zong,^{*a} Hong Wu,^a Ruo Xu^a and Ju-Fang Wang^a

^aDepartment of Biotechnology, South China University of Technology, Guangzhou 51640, China. E-mail: btmhzong@scut.edu.cn;

Fax: +86 20 2223 6669; Tel: +86 20 8711 1452

^bThe State Key Laboratory of Bioreactor Engineering, East China University of Science and Technology, Shanghai 200237, China

References

- 1 B. K. Hubbard, M. G. Thomas and C. T. Walsh, *Chem. Biol.*, 2000, **7**, 931–942.
- 2 A. Bruggink, E. C. Roos and E. de Vroom, *Org. Process Res. Dev.*, 1998, **2**, 128–133.
- 3 G. J. Kim and H. S. Kim, *Enzyme Microb. Technol.*, 1995, **17**, 63–67.
- 4 R. A. Sheldon, M. C. de Zoete, A. C. Kock-Van Dalen and F. van Rantwijk, *J. Mol. Catal. B: Enzym.*, 1996, **2**, 141–145.
- 5 M. J. J. Litjens, M. Sha, A. J. J. Straathof, J. A. Jongejan and J. J. Heijnen, *Biotechnol. Bioeng.*, 1999, **65**, 347–356.
- 6 I. Alfonso and V. Gotor, *Chem. Soc. Rev.*, 2004, **33**, 201–209.
- 7 M. A. P. J. Hacking, M. A. Wegman, J. Rops, F. van Rantwijk and R. A. Sheldon, *J. Mol. Catal. B: Enzym.*, 1998, **5**, 155–157.
- 8 M. A. Wegman, M. A. P. J. Hacking, J. Rops, P. Pereira, F. van Rantwijk and R. A. Sheldon, *Tetrahedron Asymmetry*, 1999, **10**, 1739–1750.
- 9 P. Lopez-Serrano, M. A. Wegman, F. van Rantwijk and R. A. Sheldon, *Tetrahedron Asymmetry*, 2001, **12**, 235–240.
- 10 W. Du, M. H. Zong, Y. Guo and D. H. Liu, *Biotechnol. Lett.*, 2003, **25**, 461–464.
- 11 W. Du, M. H. Zong, Y. Guo and D. H. Liu, *Biotechnol. Appl. Biochem.*, 2003, **38**, 107–110.
- 12 J. G. Huddleston, A. E. Visser, W. M. Reichert, H. D. Willauer, G. A. Broker and R. D. Rogers, *Green Chem.*, 2001, **3**, 156–164.
- 13 R. D. Rogers and K. R. Seddon, *Science*, 2003, **302**, 792–793.
- 14 K.-W. Kim, B. Song, M.-Y. Chio and M.-J. Kim, *Org. Lett.*, 2001, **3**, 1507–1509.
- 15 U. Kragl, M. Eckstein and N. Kaftzik, *Curr. Opin. Biotechnol.*, 2002, **13**, 565–571.
- 16 S. J. Nara, J. R. Harjani and M. M. Salunkhe, *Tetrahedron Lett.*, 2002, **43**, 2979–2982.
- 17 F. van Rantwijk, R. M. Lau and R. A. Sheldon, *Trends Biotechnol.*, 2003, **21**, 131–138.
- 18 T. Itoh, S. Han, Y. Matsushita and S. Hayase, *Green Chem.*, 2004, **6**, 437–439.
- 19 S. J. Nara, J. R. Harjani, M. M. Salunkhe, A. T. Mane and P. P. Wadgaonkar, *Tetrahedron Lett.*, 2003, **44**, 1371–1373.

- 20 S. Garcia, N. M. T. Lourenco, D. Lousa, A. F. Sequeira, P. Mimoso, J. M. S. Cabral, C. A. M. Afonso and S. Barreiros, *Green Chem.*, 2004, **6**, 466–470.
- 21 R. Irimescu and K. Kato, *Tetrahedron Lett.*, 2004, **45**, 523–525.
- 22 W.-Y. Lou, M.-H. Zong and H. Wu, *Biocatal. Biotransform.*, 2004, **22**, 171–176.
- 23 W.-Y. Lou, M.-H. Zong and H. Wu, *Biotechnol. Appl. Biochem.*, 2005, **41**, 151–156.
- 24 R. M. Lau, F. van Rantwijk, K. R. Seddon and R. A. Sheldon, *Org. Lett.*, 2000, **2**, 4189–4191.
- 25 M. S. Rasalkar, M. K. Potdar and M. M. Salunkhe, *J. Mol. Catal. B: Enzym.*, 2004, **27**, 267–270.
- 26 M.-J. Kim, H. M. Kim, D. Kim, Y. Ahe and J. Park, *Green Chem.*, 2004, **6**, 471–474.
- 27 P. Lozano, T. de Diego, S. Gmouh, M. Vaultier and J. L. Iborra, *Biotechnol. Prog.*, 2004, **20**, 661–669.
- 28 H. Zhao, *Phys. Chem. Liq.*, 2003, **41**, 545–557.
- 29 S. V. Dzyuba and R. A. Bartsch, *Chem. Phys. Chem.*, 2002, **3**, 161–166.
- 30 J. L. Kaar, A. M. Jesionowski, J. A. Berberich, R. Moulton and A. J. Russell, *J. Am. Chem. Soc.*, 2003, **125**, 4125–4131.
- 31 R. M. Lau, M. J. Sorgedragger, G. Carrea, F. van Rantwijk, F. Secundo and R. A. Sheldon, *Green Chem.*, 2004, **6**, 483–487.
- 32 M. Eckstein, M. Sesing, U. Kragl and P. Adlercreutz, *Biotechnol. Lett.*, 2002, **24**, 867–872.
- 33 M. Noël, P. Lozano, M. Vaultier and J. L. Iborra, *Biotechnol. Lett.*, 2004, **26**, 301–306.
- 34 M. Eckstein, P. Wasserscheid and U. Kragl, *Biotechnol. Lett.*, 2002, **24**, 763–767.
- 35 J. A. Berberich, J. L. Kaar and A. J. Russell, *Biotechnol. Prog.*, 2003, **19**, 1029–1032.
- 36 R. A. Sheldon, R. M. Lau, M. J. Sorgedragger and F. van Rantwijk, *Green Chem.*, 2002, **4**, 147–151.
- 37 M. Persson and U. T. Bornscheuer, *J. Mol. Catal. B: Enzym.*, 2003, **22**, 21–27.

Preparation of water soluble poly(aniline) and its gas-sensitivity

Xingfa Ma,^{*a} Mang Wang,^a Hongzheng Chen,^a Guang Li,^b Jingzhi Sun^a and Ru Bai^a

Received 11th February 2005, Accepted 4th April 2005

First published as an Advance Article on the web 22nd April 2005

DOI: 10.1039/b502192h

Water soluble poly(aniline) was prepared using the chemical oxide method by adding a small amount of poly(sodium-*p*-styrenesulfonate). Poly(aniline) composite film on interdigital electrodes of carbon was formed *via* the spin-coating approach. After pretreatment of exposure in an alkalescence atmosphere and desorption with high-purity N₂, the film showed an excellent sensitivity to trimethylamine of 5.14×10^{-7} mol mL⁻¹. Moreover, this film also had a good selectivity to analogous gases and a fast response while exhibiting a good reproducibility. It was easily recovered by high-purity N₂.

Introduction

Although a large number of studies on conductive polymers have been reported for several decades, this is still a hot research field. One of the main reasons is that devices with excellent properties would be expected to be obtained *via* tailoring the nano-structure of conductive polymers with template, non-template and seeding approaches.^{1–6}

Currently most of the research on conductive polymers is still focusing on the preparation of materials and morphology characterization,^{2,5,7–11} only a few reports have touched upon device properties. According to most research results, the sensitivity was very low and the response was very slow.^{12–14}

In our opinion, there are two main problems obstructing the progress development. One is that there are too many processes involved from the functional material to the device fabrication, and some of them are difficult to overcome in the near future. The other is that the conductivity of poly(aniline) strongly depends upon the doping and undoping. Because there are so many factors affecting the doping and undoping, and because it is too difficult to achieve the effect of doping *in-situ* polymerization using common doping methods, the excellent properties of the material are not easily realized on the devices.

Recently, Huang and co-workers^{15–17} investigated the sensitive properties of sensors based on nanostructured poly(aniline) prepared with interface polymerization and interdigital gold electrodes and obtained good results, which encouraged us to develop organic sensors with high sensitivity.

Poly(aniline) is one kind of typical conductive polymers. Due to its good mechanical flexibility, environmental stability and controllable conductivity by acid/base (doping/undoping), poly(aniline) has potential applications in many fields, such as lightweight battery electrodes, electromagnetic shielding devices, anticorrosion coatings, and sensors.^{2,3} In the sensor field, poly(aniline) and some other conductive polymers play the part of sensitive materials around room temperature and are an attractive developmental prospect.

Due to the poor solubility of poly(aniline), it is difficult to form films with general methods whereas many modifications

of poly(aniline) would affect some properties. Electropolymerization is a reasonable approach to prepare such a film, but it is difficult to carry out on the device with interdigital electrodes. Although a few papers reported that some poly(aniline)s could be dissolved in strong polar solvents, such as *N*-methylpyrrolidone, *m*-cresol, *etc.*, several disadvantages still need to be overcome. One problem is that the bp of *N*-methylpyrrolidone, *m*-cresol, *etc.*, are too high to make the film-forming extremely difficult. Another problem is that the volatile solvent would cause serious pollution. Therefore, the water soluble poly(aniline) obtained by adding a small amount of poly(sodium-*p*-styrenesulfonate) as described in this paper can overcome the problem mentioned above before it becomes significant.

Trimethylamine is an important organic ammonia, which is produced *via* metabolic processes of animal organs and protein. It is also an important toxic gas in biological fields and the food industry. At present, it is usually determined using sensors fabricated from metal oxide. To improve its sensitivity and speed of response, a poly(aniline) composite film is designed to determine the concentration of trimethylamine in our experiments.

The screen printing technique, which provides a method of rapid, economic and reproducible manufacture of sensor electrodes, has become a common method of electrode fabrication. Considering the low cost for future applications, we studied the poly(aniline) composite film formed by spin-coating or an immersion method on the screen-printed interdigital carbon paste electrodes in this paper.

The experimental results indicated that a device with high-sensitivity, rapid response, low-cost, reversible at room temperature and conveniently prepared was obtained after the pretreatment of poly(aniline).

Experimental

Materials

Aniline (AR) was freshly distilled in vacuum before use, ammonium peroxydisulfate (AR), hydrochloride (AR), poly(sodium-*p*-styrenesulfonate), 30% aqueous trimethylamine solution (C.P.), triethylamine (A.R.) are commercially

*xingfamazju@yahoo.com.cn

available. Deionized filtered water was used in all the studies. Carbon paste (Jelcon CH-10) was purchased from Jujo Chemical Co., Ltd., Japan.

The electrode is made of carbon paste, which is prepared using screen-printing technology. The gap and length of interdigital electrodes are 0.5 mm and 1.0 mm, respectively, and the substrate of the devices comprises a 0.5 mm thick polypropylene plate.

Preparation of sensing film

The coating mixture was prepared by adding equimolar aniline and ammonium peroxydisulfate in hydrochloride solution, and a small amount of poly(sodium-*p*-styrenesulfonate) was added. The blue-black solution of poly(aniline) in water was obtained after standing for 24 h. The gas-sensor was fabricated either by immersing the carbon electrode in the mixture or using a spin-coating method, and then dried at room temperature.

The pretreatment of poly(aniline) film

The device was put into an airproof test box (2.5 L), and desorbed with high-purity N₂. A certain amount of trimethylamine or other base volatile solvent (about 0.2 mL) was injected into the test chamber with a syringe for deprotonation.

Gas-sensitivity characterization of sensor

The gas-sensitivity characterization of sensor to vapors was the same as ref. 18. The details of the procedure are described as follows. The device was put into an airproof test box (2.5 L), which was connected to a vacuum and a high purity N₂ system with three-way valves. While 10 V DC voltage was applied on the interdigital electrodes, the DC current response was measured using a Keithley 236 Source Measure Unit. The DC current was measured continuously under N₂ atmosphere with arbitrary time intervals, such as 1 s, for evaluating the programmed detection time, and the current value was recorded automatically by an IBM PC compatible computer. The test box was flushed with high purity N₂ repeatedly until the current slowly reached the steady value without variation. At this moment, a certain amount of trimethylamine or other volatile solvent (about 0.2 mL) was injected into the test chamber with a syringe. Definition of gas-sensitivity (*R*) of the film is the ratio of $I_{\text{gas}}/I_{\text{N}_2}$, in which, I_{gas} and I_{N_2} represent the responsive currents of the sensor on exposure to measured gas and N₂, respectively.

The FTIR spectra measurement

The FTIR spectra were taken in silicon disks, and recorded on an IFS 66 V/S Fourier transform infrared spectrometer (made by the Bruker Company). Water soluble poly(aniline) was coated on the surface of silicon disks and dried at room temperature while insoluble poly(aniline) was coated on the surface of silicon disks *via in-situ* polymerization for comparison.

The UV-vis absorption measurement

The UV-vis absorption was recorded by a CARY Bio100 spectrophotometer. The water soluble poly(aniline) was coated

on the quartz glass, and then dried at room temperature, while insoluble poly(aniline) was coated on the quartz glass *via in-situ* polymerization for comparison.

Morphology observation with SEM

Scanning electron microscopy (SEM) was performed on a JSM-5510 Microscope. The water soluble poly(aniline) was coated on the glass and then dried at room temperature, while insoluble poly(aniline) was coated on the glass *via in-situ* polymerization for comparison.

Results and discussion

The FTIR spectra of poly(aniline) composite film

The FTIR spectra of poly(aniline) composite film was shown in Fig. 1.

Fig. 1 shows that, 3248 cm⁻¹ is attributed to the stretching peak of N–H, 1594 cm⁻¹ to the stretching peak of C=C of quinoid ring in emeraldine base and emeraldine salt, and 1318 cm⁻¹, 1171 cm⁻¹ to the stretching peak of C–N, C=N respectively. This illustrated that this composite film contained poly(aniline). Because the amount of poly(sodium-*p*-styrenesulfonate) added in our experiment is very small, no obvious difference was observed between the FTIR spectra of poly(aniline) composite film with and without poly(sodium-*p*-styrenesulfonate).

Since the poly(aniline) is easily prepared with the chemical oxide method and a number of publications have reported its synthesis and characterization, the details are not discussed in this paper.

The sensitivity of poly(aniline) composite film after pretreatment to trimethylamine and hydrochloride

The structure of the sensor is illustrated in Scheme 1.

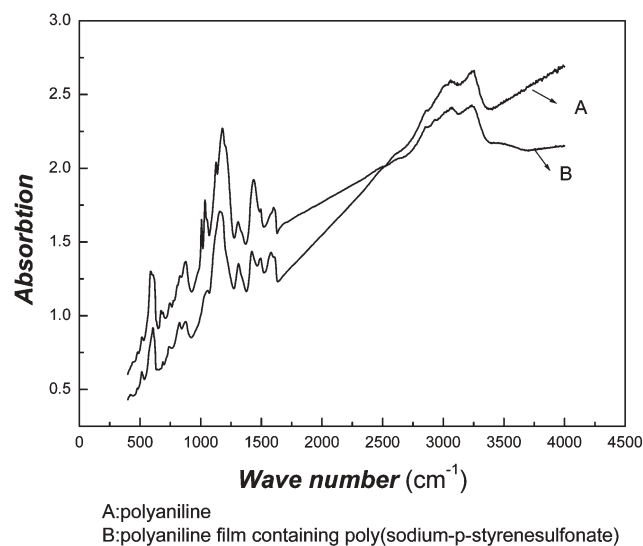
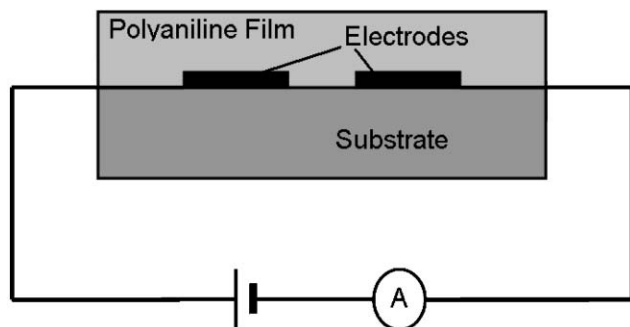


Fig. 1 The effect of a small amount of poly(sodium-*p*-styrenesulfonate) on the feature peaks of FTIR spectra of poly(aniline) composite film.



Scheme 1 The structure of the sensor in our experiments.

It is commonly known from previous publications already mentioned that most sensors made of poly(aniline) are based on the reversible reaction of acid/base, *i.e.* the conductivity of poly(aniline) is increased along with the amount of acid, and contrarily decreased with the amount of base. In our experiments, we observed an interesting and unusual phenomena, which is that when the film of protonated poly(aniline) is exposed to the atmosphere of the base, the responsive current of the film decreased sharply at the beginning, and then increased greatly. At this time, the film could be easily desorbed with high-purity N_2 , and can be utilized repeatedly. This film is not only sensitive to the atmosphere of the acid (the current of the film increased), but also sensitive to the ambience of the base (the current of the film also increased). The essential difference is that the film on exposure to acid cannot be desorbed with N_2 , which must be recovered in the atmosphere of the base. This inspired us to a new idea that the conductivity of the de-protonated poly(aniline) film is increased with the quantity of adsorbed gas of base. Based on this feature, a novel kind of gas-sensor, which has good reproducibility, convenient operating, and could be recovered with N_2 , may be developed. In this way, we believe that poly(aniline) can be fabricated into two kinds of sensor for the base atmosphere. The first kind is based on the reversible reaction of acid/base (the responsive current of the film increased on exposure to the acid atmosphere, and decreased on exposure to the base atmosphere); the other is based on the reversible process of polar vapors/ N_2 (the responsive current of the film increased on exposure to the base atmosphere, and decreased on exposure to the N_2 atmosphere). It was also found that the sensitivity of the latter one was much higher than that of the previous.

Generally, the preparation of poly(aniline) is carried out in an acid media. Consequently, the product obtained is usually emeraldine salt, which has good conductivity. In the process of de-protonation, it would contain several redox forms of poly(aniline), such as leucoemeraldine base (fully reduced form), emeraldine base (half-oxidized form), conducting emeraldine salt (half-oxidized and protonated form), and pernigraniline base (fully oxidized form).¹⁹ Therefore, the mechanism of its gas-sensitivity to vapors should be complex,¹⁶ including doping, dedoping, reduction, swelling, conformational changes of polymer chains, and so on.

The main reasons for the gas-sensitivity of the chemical sensor could be attributed to the interaction between the

sensitive film and the adsorbed molecular gas, which means both strong interaction (chemical bond) and weak interaction (such as hydrogen bonding, van der Waals force, and so on). For strong interacting systems, its recovery is generally very difficult; while for weak interaction systems, its recovery is relatively easier at room temperature with high-purity N_2 . Moreover, we had even carried out some comparison tests under similar conditions through a series of different polar vapors. It was found that, the increasing degree of electrical response of poly(aniline) after pretreatment strongly depended on the polarity of adsorbed vapors. The stronger the polarity of the vapor, the larger the increase of the conductivity. For the non-polar or weak-polar vapors (such as: *n*-hexane, toluene), there was little response. All of these phenomena showed that, the sensor, is based on the reversible acid/base reaction of poly(aniline), its mechanism involves protonation and de-protonation processes; and the unusual electrical conductivity response of poly(aniline) pretreated in our studies should be attributed to van der Waals' interactions. The latter is very similar to that of the system of polymers filled with carbon black.^{20–23} According to previous reports, although the separation of amino acids has been carried out based on the feature of weak interaction of poly(aniline) with chromatographic technology,²⁴ which acted as a stationary phase, some very similar amino acids can be identified. So, it is meaningful to obtain a great measurable physical signal based on this weak interaction. Until now, there has been no report on the electrical response increase on exposure to a base atmosphere.

The gas-sensitivity of poly(aniline) composite film after pretreatment to trimethylamine and hydrochloride is shown in Figs. 2 and 3 respectively. There is no response for blank interdigital electrodes.

It can be seen from Fig. 2 that the poly(aniline) composite film has a high gas-sensitivity of $5.14 \times 10^{-7} \text{ mol mL}^{-1}$ and a rapid response to trimethylamine. The responsive current took about 100 s to reach 3 orders and 800 s to 6 orders.

It is well illustrated in Fig. 3 that this composite film also has a good sensitivity of $5.14 \times 10^{-7} \text{ mol mL}^{-1}$ and rapid response to hydrochloride. The responsive current took about 140 s to reach 5 orders and 500 s to 6 orders.

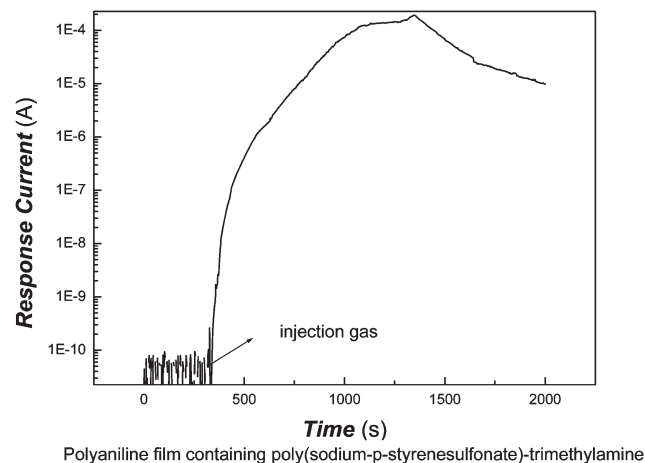


Fig. 2 Dependence of gas-sensitivity of poly(aniline) composite film to trimethylamine ($5.14 \times 10^{-7} \text{ mol mL}^{-1}$) on time.

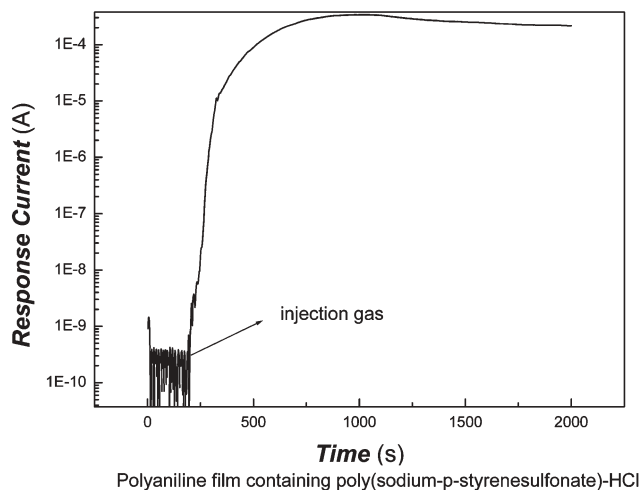


Fig. 3 Dependence of gas-sensitivity of poly(aniline) composite film to HCl ($5.14 \times 10^{-7} \text{ mol mL}^{-1}$) on time.

Contrasted with the atmosphere of base, it is very difficult to desorb with N_2 completely for the film on exposure to acid. In order to desorb with N_2 completely, the film must first be put into an atmosphere of base and then desorbs with N_2 .

The device absorbing base gas could be recovered completely with high-purity N_2 at room temperature so that the device can be utilized repeatedly though the speed of desorption, which can be quickened by increasing the flux of N_2 , is slower than that of absorption in general. The curves of desorption are shown in Figs. 4 and 5.

It can also be seen in Figs. 4 and 5 that the baselines of current are different after desorption with N_2 . This indicates that the protonation in part poly(aniline) is difficult to desorb with N_2 .

The comparisons of sensitivity of common organic sensitive materials

Among the organic sensitive materials, the phthalocyanine, porphyrin compounds, *etc.* and their derivatives are a few kinds of important sensitive materials, which showed good sensitivity to many gases.¹⁸ It is believed that the chemical

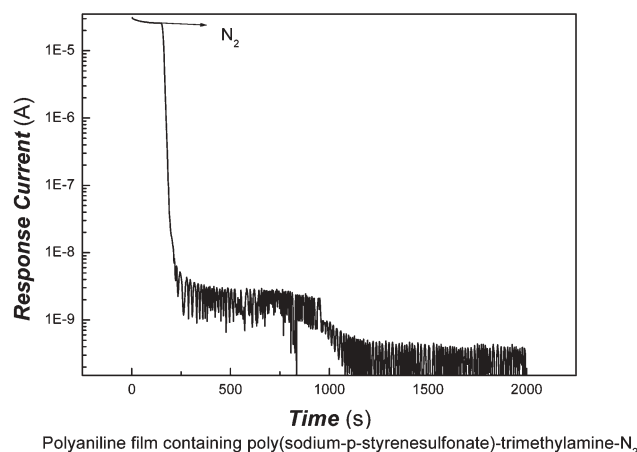


Fig. 4 Curve of desorption of poly(aniline) film with high-purity N_2 .

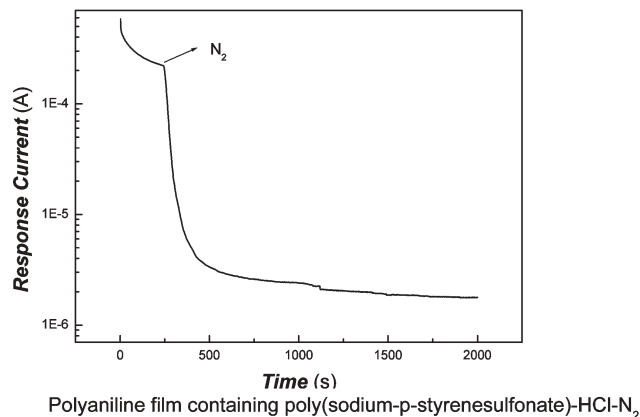


Fig. 5 Curve of desorption of poly(aniline) film with high-purity N_2 .

modification to these compounds is important to enhance their sensitivity and selectivity for many years. If we could obtain an organic film device with good sensitivity *via* a simple preparation method, it would be a meaningful event. Therefore, a series of tests were carried out utilizing some organic films for comparison under the same conditions. When we used zinc phthalocyanine, zinc porphyrin, perylene and their fluorination derivative-based films instead of poly(aniline) in the experiments, we observed similar results as described in the literature,¹⁸ which showed relatively low sensitivity and slow response rates. The results for these organic compounds were consistent with ref. 18. This illustrated that it is feasible to improve the speed of response of sensors *via* a simple method. The comparison of results with different sensitive materials is shown in Fig. 6.

Fig. 6 shows that the gas-sensitivity and response rates of the poly(aniline) composite film in our experiments are much higher than those of common organic sensitive materials and modification compounds. This illustrates that this simple method is very effective in obtaining film sensors with high sensitivity.

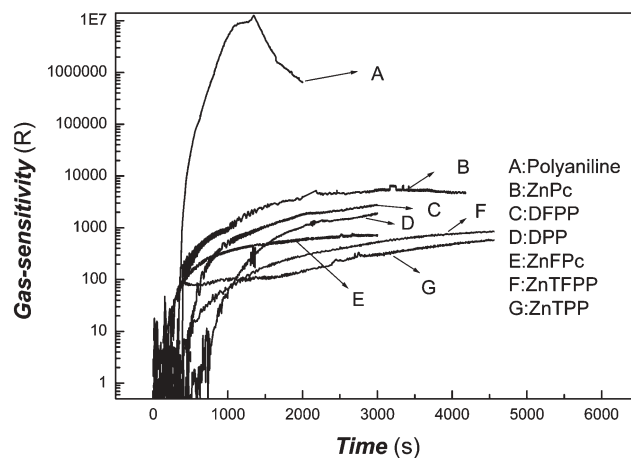


Fig. 6 Comparisons of gas-sensitivity of some common organic compounds under the same conditions (A: poly(aniline); B: zinc phthalocyanine; C: fluorination biphenyl perylene diimide; D: biphenyl perylene diimide; E: fluorination zinc phthalocyanine; F: fluorination tetraphenyl zinc porphyrin; G: tetraphenyl zinc porphyrin).

The gas-sensitivity and selectivity of poly(aniline) composite film to analogous and interferent gases

Unlike enzyme sensors, normally a single chemical sensor has no specific character to distinguish between gases although some gas sensor arrays can be used to identify different gases with the aid of a sensor array and an artificial neural network system. Therefore the gas-sensitivity of poly(aniline) composite film to a series of vapors (trimethylamine and triethylamine) was examined, and a blank comparison test was also carried out by considering the effect of moisture on the sensitivity by H₂O injection instead of trimethylamine. The results are shown in Fig. 7.

Distinct differences of the gas-sensitivity and response speed to some similar gases can be observed in Fig. 7. The value of gas-sensitivity and the response speed of triethylamine are much lower than those of trimethylamine so that the composite film can be used to distinguish between trimethylamine and triethylamine.

It is well known that trimethylamine and triethylamine are materials with electron donors, and the ability of electron donors of methyl and ethyl groups is different, thus the interaction force between sensitive films and adsorbed vapors would be different, which led to a variation of gas-sensitivity and response rate to different vapors.

Regarding the effect of moisture on the gas-sensitivity, the influence is very small although the baseline shifts a little. With comparison to the response to trimethylamine, this influence could be neglected.

The effect of a small amount of poly(sodium-*p*-styrenesulfonate) on the gas-sensitivity and other properties of poly(aniline) composite film

The purpose of adding a small amount of poly(sodium-*p*-styrenesulfonate) is to improve the solubility and film-forming technology of poly(aniline). Does it affect the gas-sensitivity? To answer this question, comparison tests of gas-sensitivity were carried out with insoluble poly(aniline) *in-situ* polymerization and soluble poly(aniline) in organic

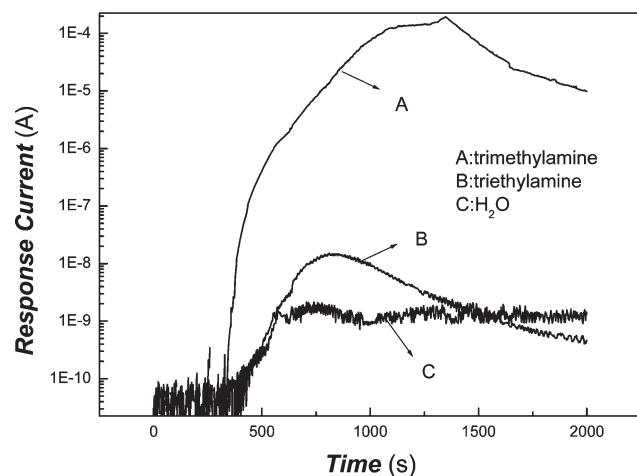


Fig. 7 The gas-sensitivity of poly(aniline) composite film to a series of vapors.

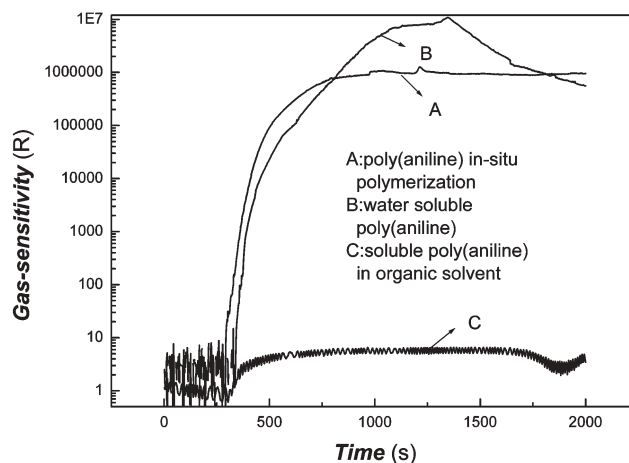


Fig. 8 The effect of a small amount of poly(sodium-*p*-styrenesulfonate) on the gas-sensitivity of the composite film.

solvent (*N*-methylpyrrolidone) under the same conditions. The results are shown in Fig. 8.

Fig. 8 shows that the effect of a small amount of poly(sodium-*p*-styrenesulfonate) on the gas-sensitivity of poly(aniline) composite film is small. Otherwise, the value of gas-sensitivity and response rate are much higher than that of poly(aniline) film obtained *via* conventional spin-coating [poly(aniline) was dissolved in *N*-methylpyrrolidone].

The UV-vis spectra of the poly(aniline) composite film is shown in Fig. 9.

Although the effects of a small amount of poly(sodium-*p*-styrenesulfonate) on the characteristic peaks in the FTIR spectra of the poly(aniline) composite (see Fig. 1) is small, an approximate 10 nm red shift was observed in the UV-vis spectra of poly(aniline), which was due to the interaction between poly(aniline) and poly(sodium-*p*-styrenesulfonate), as shown in Fig. 9.

Comparing with the results of Huang and Kaner,² the characteristic peaks of poly(aniline) at 340, 440, and 800 nm in

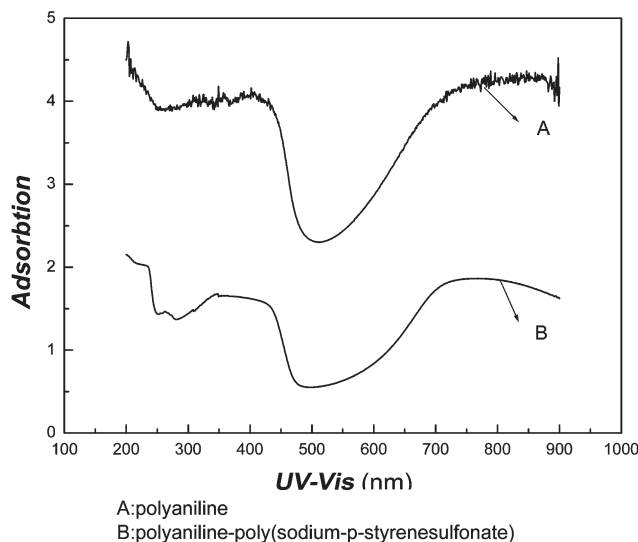
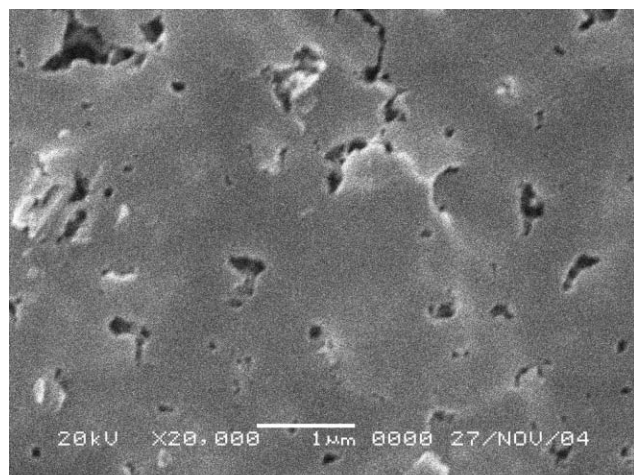
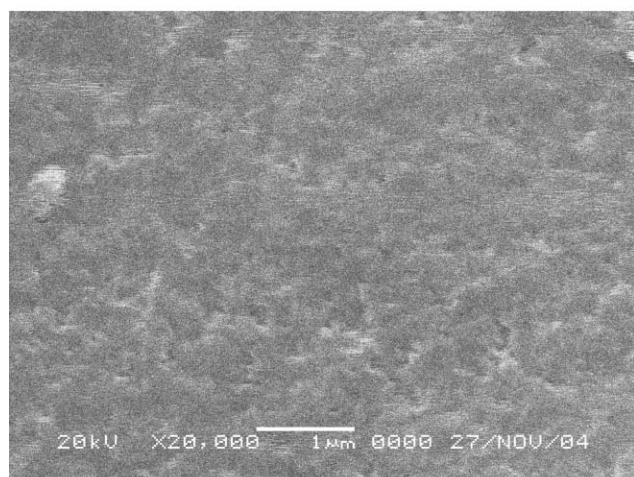


Fig. 9 The effect of a small amount of poly(sodium-*p*-styrenesulfonate) on the UV/vis spectra of the poly(aniline) composite film.



(A) poly(aniline) composite film via an in-situ polymerization



(B) poly(aniline) of water-soluble composite film

Fig. 10 The effect of a small amount of poly(sodium-*p*-styrenesulfonate) on the morphology of SEM of the poly(aniline) composite film.

UV-vis spectra in our experiments are consistent with ref. 2 but some peaks are widened (as shown in Fig. 9). This is possibly as a result of interaction of the poly(aniline) composite film.

Although the effect of a small amount of poly(sodium-*p*-styrenesulfonate) on the gas-sensitivity of the poly(aniline) composite film is small, the film-forming technique is improved greatly. The film can be coated with simple methods, such as spin-coating and so on. This water soluble poly(aniline) obtained is attributed to the effect of inducement of polyelectrolyte. The improvement of the film-forming technique can also be seen in Fig. 10.

As shown in Fig. 10, we can see that, the surface of water soluble poly(aniline) is more uniform than that of insoluble poly(aniline). This indicates that the morphology of poly(aniline) can be controlled by adding a small amount of poly(sodium-*p*-styrenesulfonate).

The circle reproducibility of composite film

The results of circle reproducibility of composite film are shown in Fig. 11.

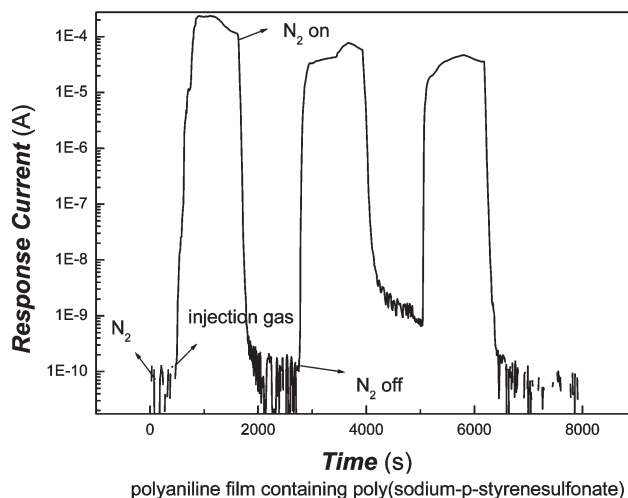


Fig. 11 The circle test examination of poly(aniline) composite film to trimethylamine ($5.14 \times 10^{-7} \text{ mol mL}^{-1}$).

Fig. 11 shows that the composite film in our experiment has an excellent reproducibility.

Conclusion

In summary, water soluble poly(aniline) was prepared by addition of a small amount of poly(sodium-*p*-styrenesulfonate). The film-forming technology was improved greatly by adding a small amount of polyelectrolyte, though the gas-sensitivity was affected slightly. In addition, the film exhibited an excellent sensitivity and a circle reproducibility to trimethylamine of $5.14 \times 10^{-7} \text{ mol mL}^{-1}$, the film was easily recovered with N_2 , and had a good selectivity to analogous and interferent gases. Therefore, the film has good potential applications to gas sensors, such as electronic noses.

This composite film was sensitive not only to the atmosphere of base, but also equivalently to the atmosphere of acid.

The method used to prepare the devices was very simple and feasible. It is suitable for mass production at low cost without any environmental pollution.

Acknowledgements

This project was supported by the National Basic Research Program of China (973 Program, project No. 2002CCA01800).

Xingfa Ma,^{*a} Mang Wang,^a Hongzheng Chen,^a Guang Li,^b Jingzhi Sun^a and Ru Bai^a

^aDepartment of Polymer Science and Engineering, State Key Lab of Silicon Materials, Zhejiang University, Hangzhou 310027, China.

E-mail: xingfamazju@yahoo.com.cn; xingfazju@163.com;

Fax: +86 571 87951635; Tel: +86 571 87952557

^bDepartment of Biomedical Engineering, State Key Lab of Biosensors, Key Lab of Biomedical Engineering of Ministry of Education of China, Zhejiang University, Hangzhou 310027, China.

E-mail: guangli@cbeis.zju.edu.cn; Fax: +86 571 87951676;

Tel: +86-13858068126

References

- 1 Y. Ma, J. Zhang, G. Zhang and H. He, *J. Am. Chem. Soc.*, 2004, **126**, 7097.
- 2 J. Huang and R. Kaner, *J. Am. Chem. Soc.*, 2004, **126**, 851.

- 3 X. Zhang, W. Goux and S. Manohar, *J. Am. Chem. Soc.*, 2004, **126**, 4502.
- 4 S. Han, A. Briseno, X. Shi, D. Mah and F. Zhou, *J. Phys. Chem. B*, 2002, **106**, 6465.
- 5 A. Carswell, E. O'Rear and B. Grady, *J. Am. Chem. Soc.*, 2003, **125**, 14793.
- 6 J. Huang and R. Kaner, *Angew. Chem., Int. Ed.*, 2004, **43**, 5817.
- 7 M. Ayad, N. Salahuddin and M. Sheneshin, *Synth. Met.*, 2003, **132**, 185.
- 8 A. Göka, B. Saryb and M. Talu, *Synth. Met.*, 2004, **142**, 41.
- 9 O. Raitman, E. Katz, A. Bückmann and I. Willner, *J. Am. Chem. Soc.*, 2002, **124**, 6487.
- 10 J. Avlyanov, J. Josefowicz and A. MaceDiarmid, *Synth. Met.*, 1995, **73**, 205.
- 11 I. Sapurina, A. Riede and J. Stejskal, *Synth. Met.*, 2001, **123**, 503.
- 12 M. Matsuguchi, J. Io, G. Sugiyama and Y. Sakai, *Synth. Met.*, 2002, **128**, 15.
- 13 A. Riul, Jr., A. Soto, S. Mello, S. Bone, D. Taylor and L. Mattoso, *Synth. Met.*, 2003, **132**, 109.
- 14 V. Chabukswar, S. Pethkar and A. Athawale, *Sens. Actuators*, 2001, **B77**, 657.
- 15 J. Huang, S. Virji, B. Weiller and R. Kaner, *J. Am. Chem. Soc.*, 2003, **125**, 314.
- 16 S. Virji, J. Huang, R. Kaner and B. Weiller, *Nano Lett.*, 2004, **4**, 491.
- 17 J. Huang, S. Virji, B. Weiller and R. Kaner, *Chem. Eur. J.*, 2004, **10**, 1314.
- 18 S. Gupta and T. Misra, *Sens. Actuators*, 1997, **B41**, 199.
- 19 V. Milind, K. Annamraju, R. Marimuthu and S. Tanay, *J. Polym. Sci., Part A: Polym. Chem.*, 2004, **42**, 2043.
- 20 S. Chen, J. Hu, M. Zhang, M. Li and M. Rong, *Carbon*, 2004, **42**, 645.
- 21 X. Dong, R. Fu, M. Zhang, B. Zhang, J. Li and M. Rong, *Carbon*, 2003, **41**, 369.
- 22 J. Li, J. Xu, M. Zhang and M. Rong, *Carbon*, 2003, **41**, 2353.
- 23 X. Dong, R. Fu, M. Zhang, B. Zhang and M. Rong, *Carbon*, 2004, **42**, 2551.
- 24 G. Gordon and A. Leon, *Adv. Mater.*, 2002, **14**, 953.

Direct aldol reactions catalyzed by 1,1,3,3-tetramethylguanidine lactate without solvent

Anlian Zhu, Tao Jiang,* Dong Wang, Buxing Han, Li Liu, Jun Huang, Jicheng Zhang and Donghai Sun

Received 8th February 2005, Accepted 1st April 2005

First published as an Advance Article on the web 22nd April 2005

DOI: 10.1039/b501925g

The ionic liquid, 1,1,3,3-tetramethylguanidine lactate ([TMG][Lac]), was used as a recyclable catalyst for direct aldol reactions at room temperature without any solvent. The results demonstrated that good chemo- and regio-selectivity could be achieved, and the ionic liquid can be easily recovered and recycled without considerable decrease of activity. The protocol is green and effective for producing β -hydroxyl ketones.

Aldol reactions are effective C–C bond forming reactions and the products of β -hydroxy ketones are frequently found in complex polyol architectures of natural products. These reactions have been studied extensively.^{1,2} The classical aldol reactions are highly atom-economic but suffer from problems of low selectivity. A common method to improve the selectivity is the use of enol silyl ether in the presence of Lewis acid (Mukaiyama aldol reaction).³ However, this method is inconvenient because it requires the masked enolates to be prepared from the corresponding ketones in advance and then decreases the atom-efficiency of aldol addition itself. Alternatively, a one-pot Reformatsky-type reaction promoted by Ba in THF between haloketone and aldehyde at $-78\text{ }^{\circ}\text{C}$ was developed by Yanagisawa *et al.*⁴ While this route produces the aldol adducts in good yields, it still leads to the atom waste. The other promising alternative is the direct aldol reactions⁵ between an unmodified ketone and an aldehyde, which is the most efficient approach from the atom-economy point of view.^{6–8}

Aldol reactions can be catalyzed by organic or inorganic bases. The reactions catalyzed by inorganic bases are not easily controlled and the dehydration of the product is often unavoidable. Organic molecules such as proline,⁶ cinchona-derived chemicals⁹ and guanidines have also been used as the catalysts. List and coworkers^{6a} developed an elegant proline-mediated aldol reaction based on the class I aldolases between acetone and aldehydes. Schuchardt *et al.*^{10a} used the encapsulation of cycloguanidine in zeolite Y to catalyze aldol reaction between acetone and benzaldehyde with the 4-phenyl-4-hydroxybutan-2-one as the principle product, but the byproduct from dehydration was still as high as 14%. They also used guanidines encapsulated in zeolite Y or anchored to MCM-41 as the heterogeneous catalysts to carry out the aldol reaction between acetone and benzaldehyde, and the homogeneous reaction using guanidines (unsupported) as the catalyst.^{10b} When guanidine–MCM-41 and guanidine–zeolite Y were used, the addition products were produced with reasonable yields, while the homogeneous reaction produced 90–94% condensation product.

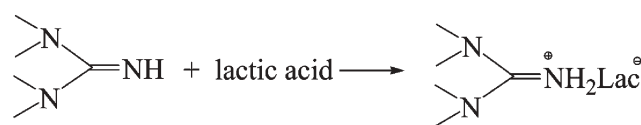
As we know, ionic liquids (ILs) are organic salts, which have been investigated extensively in organic synthesis as solvents or

catalysts.^{11,12} They possess advantages, such as undetectable vapor pressure and excellent reusability. In recent years, a great number of new functional ILs has been synthesized.¹³ In previous work, we reported the preparation and characterization of guanidine (TMG)-based ILs.^{13b} The IL, 1,1,3,3-tetramethylguanidine lactate ([TMG][Lac]) could be prepared by neutralizing TMG with lactic acid (Scheme 1). They have been applied in carrying out Henry reactions¹⁴ and preparing immobilized catalyst for hydrogenation of olefins.¹⁵

In this work, we used [TMG][Lac] as the basic catalyst for the direct aldol reactions at room temperature, and no solvent was used. It was demonstrated that for each reaction only the aldol adduct was produced when the molar ratio of the IL and substrate was smaller than 1.

The successful results of [TMG][Lac] catalyzed aldol reactions are given in Table 1. The reactions of 4-nitrobenzaldehyde with acetone, cyclopentanone, cyclohexanone, and acetophenone showed moderate to high yields. However, the reactions of 4-nitrobenzaldehyde with 2-butanone and 2-pentanone gave low yields even after 72 or 96 hours, respectively. The reason is that each of the ketones has two different α -hydrogens. Each of the two reactions afforded a sole product because one of the α -hydrogens is more active than the other, showing a perfect regioselectivity. Table 1 shows that 3-nitrobenzaldehyde can also readily react with acetone to give good yield (entry 7). When terephthalic aldehyde reacted with acetone, the reaction had good chemoselectivity, only producing hydroxyl ketone **8** as the product in moderate yields, and leaving another aldehyde group unreacted (entry 8).

It should be mentioned that a ketone possessing an alkyl substituent at the α -position is an interesting substrate from the view of *syn/anti* diastereoselectivity. As shown in Table 1, the corresponding aldol adducts were more *syn*-diastereoselective when the present IL was used to catalyze the reactions.



Scheme 1 Synthesis of the [TMG][Lac] ionic liquid.

*Jiangt@iccas.ac.cn

Table 1 The direct aldol reactions catalyzed by [TMG][Lac]

Entry	Aldehyde	Ketone	Product	Time/h	Yield (%) (<i>syn/anti</i>)
1		Acetone		24	93
2		2-Butanone		72	25 (68/32)
3		2-Pentanone		96	28 ^a (54/46)
4		Cyclopentanone		24	97 ^a (68/32)
5		Cyclohexanone		24	85 (60/40)
6		Acetophenone		50	70
7		Acetone		24	85
8		Acetone		24	73
9		Cyclopentanone 2nd run		24	97 ^a (70/30)
10		Cyclopentanone 3rd run		24	95 ^a (64/36)
11		Cyclopentanone 4th run		24	93 ^a (68/32)

^a The yields were determined by ¹H-NMR analysis.

From the industrial point of view, one of the most intriguing aspects for the utilization of ILs is that they can be recycled easily. In this work, we tested the reusability of the IL by using the reaction of cyclopentanone and 4-nitroaldehyde. After the reaction was completed, the reaction mixture was extracted with water and diethyl ether to form the IL-in-water layer and the organic layer. Analysis showed that the amount of IL leaching into the ether layer was negligible. Pure IL was obtained after drying the water-rich layer, and the IL was reused directly. As shown in Table 1, no considerable decrease in reactivity and diastereoselectivity was observed after four cycles (entries 4, 9, 10, 11).

In conclusion, our work presents successful examples of direct aldol reactions catalyzed by a basic IL under solvent-free conditions, and good chemo- and regio-selectivity can be achieved. Moreover, after the reaction, the ionic liquid can be easily recovered and recycled without considerably decrease of activity, and the yield and the diastereoselectivity remains at a comparable level as in the case of the fresh IL. This protocol gives a greener and effective alternative for direct aldol reactions over other reported methods.

Experimental

All starting materials (A. R. grade) were purchased from Beijing chemical reagents company and purified before use. In a typical experiment, 0.5 mmol aldehyde, 0.15 mmol IL, and 10 mmol ketone were mixed in a flask and stirred for the desired time at room temperature. The reactions were monitored by TLC. At the end of the reaction, water and diethyl ether were added and the reaction mixture was separated into two layers. As the IL was soluble in water, pure IL was obtained after drying the water-IL layer, which could be reused. The crude hydroxyl ketones were obtained from the upper diethyl ether layer and then were purified by flash chromatography on silica gel (eluent: ethyl acetate-petroleum ether (bp 60–90 °C)). The product and the ratio of *syn/anti* were analyzed by ¹H-NMR spectroscopy.

¹H NMR spectra were recorded as solutions in CDCl₃ at room temperature on a Bruker spectrometer at 300 MHz.

Product of entry 1: ¹H-NMR (300 MHz, CDCl₃) (ppm): 2.21 (s, 3H), 2.84 (m, 2H), 3.5 (bs, 1H), 5.25 (m, 1H), 7.52 (d, *J* = 6Hz, 2H), 8.19 (d, *J* = 6Hz, 2H).

Product of entry 2: ¹H-NMR (300 MHz, CDCl₃; *syn*) (ppm): 1.08 (d, *J* = 6Hz, 3H), 2.26 (s, 3H), 2.84 (bs, 1H), 5.29 (d, *J* = 3Hz, 1H), 7.52–8.25 (m, 4H); ¹H-NMR (300 MHz, CDCl₃; *anti*) (ppm): 1.03 (d, *J* = 6Hz, 3H), 2.23 (s, 3H), 2.91 (bs, 1H), 4.88 (d, *J* = 6Hz, 1H), 7.52–8.25 (m, 4H).

Product of entry 3: ¹H-NMR (300 MHz, CDCl₃; *syn*) (ppm): 0.82 (t, *J* = 6Hz, 3H), 1.68–1.75 (m, 2H), 2.18 (s, 1H), 2.79 (m, 1H), 3.24 (bs, 1H), 5.10 (d, *J* = 3Hz, 1H), 7.51–8.22 (m, 4H); ¹H-NMR (300 MHz, CDCl₃; *anti*) (ppm): 0.90 (t, *J* = 6Hz, 3H), 1.48–1.55 (m, 2H), 2.14 (s, 3H), 2.84 (m, 1H), 3.27 (bs, 1H), 4.92 (d, *J* = 6Hz, 1H), 7.51–8.24 (m, 4H).

Product of entry 4: ¹H-NMR (300 MHz, CDCl₃; *syn*) (ppm): 1.55–2.76 (m, 7H), 3.01 (bs, 1H), 5.42 (s, 1H), 7.73–8.32 (m, 4H); ¹H-NMR (300 MHz, CDCl₃; *anti*) (ppm): 1.55–2.76 (m, 7H), 4.78 (bs, 1H), 4.83 (d, *J* = 9Hz, 1H), 7.73–8.32 (m, 4H).

Product of entry 5: ¹H-NMR (300 MHz, CDCl₃; *syn*) (ppm): 1.30–2.61 (m, 9H), 3.23 (bs, 1H), 5.49 (s, 1H), 7.51–8.23 (m, 4H); ¹H-NMR (300 MHz, CDCl₃; *anti*) (ppm): 1.30–2.61 (m, 9H), 4.12 (bs, 1H), 4.89 (d, *J* = 9Hz, 1H), 7.51–8.23 (m, 4H).

Product of entry 6: ¹H-NMR (300 MHz, CDCl₃) (ppm): 3.38 (m, 1H), 3.8 (bs, 1H), 5.45 (m, 1H), 7.47–8.42 (m, 9H).

Product of entry 7: ¹H-NMR (300 MHz, CDCl₃) (ppm): 2.24 (s, 3H), 2.89 (d, *J* = 6Hz, 2H), 3.6 (bs, 1H), 5.25 (t, *J* = 6Hz, 1H), 7.50–8.24 (m, 4H).

Product of entry 8: ¹H-NMR (300 MHz, CDCl₃) (ppm): 2.21 (s, 3H), 2.85 (d, *J* = 6Hz, 2H), 3.53 (bs, 1H), 5.22 (m, 1H), 7.52–7.88 (m, 4H), 10.00 (s, 1H).

Acknowledgements

This work was supported by the National Natural Science Foundation of China (20332030, 20473105) and Chinese Academy of Sciences.

Anlian Zhu, Tao Jiang,* Dong Wang, Buxing Han, Li Liu, Jun Huang, Jicheng Zhang and Donghai Sun

Center for Molecular Science, Institute of Chemistry, Chinese Academy of Sciences, Beijing 100080, China. E-mail: Jiangt@iccas.ac.cn; Fax: 86-10-62562821

References

- C. H. Heathcock, in *Comprehensive Organic Synthesis*, Vol. 2, ed. B. M. Trost and I. Fleming, Pergamon Press, Oxford, 1991.
- (a) S. D. Rychonvsky, *Chem. Rev.*, 1995, **95**, 2021; (b) K. C. Nicklaw, D. Vourlouinis, N. Winssinger and P. S. Baran, *Angew. Chem., Int. Ed.*, 2000, **37**, 44.
- (a) T. K. Hollis and B. J. Bosnich, *J. Am. Chem. Soc.*, 1995, **117**, 4570; (b) S. E. Denmark and W. J. Lee, *Org. Chem.*, 1994, **59**, 707; (c) H. Li, H. Tian, Y. Chen, D. Wang and C. Li, *Chem. Commun.*, 2002, 2994.
- A. Yanagisawa, H. Takahashi and T. Arai, *Chem. Commun.*, 2004, 580.
- For reviews of direct catalytic aldol reactions: (a) B. Alcaide and P. Almendros, *Eur. J. Org. Chem.*, 2002, 1595; (b) B. List, *Tetrahedron*, 2002, **58**, 5573; (c) M. Shibasaki and N. Yashikawa, *Chem. Rev.*, 2002, **102**, 2187.
- For aldol reactions catalyzed by amino acid, see: (a) B. List, R. A. Lerner and C. F. Barbas, III, *J. Am. Chem. Soc.*, 2000, **122**, 2395; (b) S. Chandrasekhar, C. Narsihmulu, N. R. Reddy and S. S. Sultana, *Chem. Commun.*, 2004, 2450; (c) K. Sakthivel, W. Notz, T. Bui and C. F. Barbas, III, *J. Am. Chem. Soc.*, 2001, **123**, 5260; (d) T. Loh, L. Feng, H. Yang and J. Yang, *Tetrahedron Lett.*, 2002, **42**, 8741.
- For aldol reactions catalyzed by complex based on alkaline or alkaline earth metal, see: (a) Y. Wu, W. Shao, C. Zheng, Z. Huang, J. Cai and Q. Deng, *Helv. Chim. Acta*, 2004, **87**, 1377; (b) H. Wei, R. L. Jasoni, H. Shao, J. Hu and D. W. Paré, *Tetrahedron*, 2004, **60**, 11829.
- For aldol reaction promoted by Zn or Zn-proline, see: (a) N. Kumagai, S. Matsunaga, T. Kinoshita, S. Harada, S. Okada, S. Sakamoto, K. Yamaguchi and M. Shibasaki, *J. Am. Chem. Soc.*, 2003, **125**, 2169; (b) T. Darbre and M. Machuqueiro, *Chem. Commun.*, 2003, 1090.
- (a) C. M. Gasparsk and M. J. Miller, *Tetrahedron*, 1991, **29**, 5367; (b) M. Horikawa, J. Busch-Petersen and E. J. Corey, *Tetrahedron Lett.*, 1999, **40**, 3843.
- (a) R. Sercheli, A. L. B. Ferreira, M. C. Guerreiro, R. M. Vargas, R. A. Sheldon and U. Schuchardt, *Tetrahedron Lett.*, 1997, **38**, 1325; (b) R. Sercheli, R. M. Vargas, R. A. Sheldon and U. Schuchardt, *J. Mol. Catal. A: Chem.*, 1999, **148**, 173.
- For reviews for the utilization of ionic liquid in organic synthesis, see: (a) T. Welton, *Chem. Rev.*, 1999, **99**, 2071; (b) P. Wasserscheid

- and W. Keim, *Angew. Chem., Int. Ed.*, 2000, **39**, 3772; (c) R. Sheldon, *Chem. Commun.*, 2001, 2399; (d) J. Dupont, R. F. de Souza and P. A. Z. Alvarez, *Chem. Rev.*, 2002, **102**, 3667.
- 12 (a) W. A. Herrenmann, *Angew. Chem., Int. Ed.*, 2001, **41**, 1290; (b) C. P. Mehnert, N. C. Dispenziere and R. A. Cook, *Chem. Commun.*, 2002, 1610.
- 13 (a) D. Zhao, Z. Fei, T. J. Geldbach, R. Scopelliti and P. J. Dyson, *J. Am. Chem. Soc.*, 2004, **126**, 15876; (b) H. X. Gao, B. X. Han, J. C. Li, T. Jiang, Z. M. Liu, W. Z. Wu, Y. H. Chang and J. M. Zhang, *Synth. Commun.*, 2004, **34**, 17, 3083; (c) N. M. M. Mateus, L. C. Branco, M. M. T. Lourenco and C. A. M. Afonso, *Green Chem.*, 2003, **5**, 347.
- 14 T. Jiang, H. Gao, B. Han, G. Zhao, Y. Chang, W. Wu, L. Gao and G. Yang, *Tetrahedron Lett.*, 2004, **45**, 2699.
- 15 J. Huang, T. Jiang, H. Gao, B. Han, Z. Liu, W. Wu, Y. Chang and G. Zhao, *Angew. Chem., Int. Ed.*, 2004, **43**, 1397.

Organic solvent-free process for the synthesis of propylene carbonate from supercritical carbon dioxide and propylene oxide catalyzed by insoluble ion exchange resins

Ya Du, Fei Cai, De-Lin Kong and Liang-Nian He*

Received 4th January 2005, Accepted 11th April 2005

First published as an Advance Article on the web 13th May 2005

DOI: 10.1039/b500074b

Insoluble ion exchange resins, one type of polystyryl supported catalysts containing an ammonium salt or amino group, and the polar macroporous adsorption resin, are efficient and reusable heterogeneous basic catalysts for the synthesis of propylene carbonate from propylene oxide and CO₂ under supercritical CO₂ conditions (373 K, 8 MPa), which requires no additional organic solvents either for the reaction or for the separation of product. Various parameters affecting the reaction were examined. A quantitative yield (>99%) together with excellent selectivity (>99%) was obtained. The purity of product separated directly by filtration from the reaction mixture, reached more than 99.3% without further purification processes. The catalyst can be easily recovered and reused without significant loss of its catalytic activity. The process represents a simple, ecologically safer, cost-effective route to cyclic carbonates with high product quality, as well as easy product recovery and catalyst recycling.

Introduction

The development of a truly environmentally friendly process utilizing CO₂, which is the most abundant greenhouse gas and can be also regarded as a typical renewable natural resource, has led to the current interest in synthetic chemistry from the viewpoint of environmental protection and resource utilization. Chemical fixation of CO₂ into industrially useful materials is one of the most attractive methods because there are many possibilities for CO₂ to be used as a safe and cheap C₁ building block in organic synthesis.¹ Synthesis of cyclic carbonates such as ethylene carbonate and propylene carbonate *via* the coupling of CO₂ with epoxides is one of the most promising methodologies in this area since CO₂ can be incorporated without forming any co-products in view of green chemistry and atom economy.^{1b,1d} Moreover, cyclic carbonates have been widely used for various purposes, such as electrolytic elements of lithium secondary batteries, polar aprotic solvents, monomers for synthesizing polycarbonate (a biodegradable polymer), chemical ingredients for preparing medicines or agricultural chemicals, and alkylating agents.² Very recently, a phosgene-free process for the manufacture of polycarbonates starting from CO₂ and ethylene oxide, *via* consecutive formation of ethylene carbonate, dimethyl carbonate, diphenyl carbonate, has been commercialized.³ Therefore, there is an increasing demand for cyclic carbonates.

Since cyclic carbonates (*e.g.* ethylene carbonate and propylene carbonate) were produced on an industrial scale more than 40 years ago,⁴ many organic and inorganic compounds have been developed to catalyze carbon dioxide insertion into oxiranes for the synthesis of cyclic carbonates, such as amines,⁵ phosphines,⁵ quaternary ammonium

salts,^{2c,4,5} polymer supported onium salts,^{4,6} alkali metal salts,^{2c,5,7} halostannanes,⁸ antimony compounds,⁹ and porphyrin,¹⁰ and transition-metal compounds,¹¹ manganese,¹² calcinated hydrotalcites,¹³ and metal phthalocyanines,¹⁴ Cs-loaded zeolite and alumina,¹⁵ lanthanide oxychloride,¹⁶ polyoxometalate,¹⁷ and other types of homogeneous catalysts.¹⁸ Recently, ionic liquids such as imidazolium salts, molten tetrabutyl ammonium halides,¹⁹ and the salen-type metal complexes²⁰ were reported to be most effective catalysts for cyclic carbonate synthesis under mild conditions. However, in addition to more expensive catalysts used in those cases, organic solvents were needed for the reaction or were in fact used in the work-up in order to isolate the products, which defeated the original purpose.

In current processes employed by industry, a homogeneous catalyst is undesirably dissolved in a phase containing cyclic carbonate. Thus, it is necessary to separate the catalyst from the product through a purification process such as distillation after completion of the reaction, resulting in complicated production processes, and decomposition of the catalyst or formation of by-products during the separation step. In order to facilitate the separation of the catalyst, a number of solid catalysts have been proposed (*vide supra*), for example, calcinated hydrotalcites,¹³ Cs-loaded zeolite,¹⁵ and lanthanide oxychloride.¹⁶ More recently, niobium (V) oxide^{21a,b} and other heterogeneous catalyst systems^{21c-g} have been found to be efficient catalysts for the carboxylation of epoxides with CO₂. Unfortunately, these solid catalysts have insufficient activity and most of them are essentially required to contain a polar solvent as an additive for realizing activity and selectivity. Typically, polymer supported onium salts,^{4,6} exhibited moderate activity for propylene carbonate synthesis from CO₂ (gas) even in the presence of large amounts of organic solvent (*e.g.* DMF, toluene), which may have caused

*heln@nankai.edu.cn

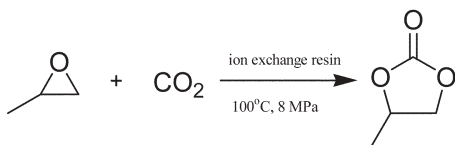
catalyst leaching and required additional processes for product separation.

Solid supported catalysts have received much more attention, because they may offer several advantages in preparative procedures, *e.g.* simplifying work-up and separation and recycling of the catalyst.²² These features may lead to economical automation and may effectively reduce pollution by hazardous compounds, advancing to an environmentally benign process. Proper use of supercritical CO₂ in heterogeneous catalysis may afford enhancement of the reaction rate, control of selectivity, and increasing catalyst lifetime, facilitating easier separation as well.²³ In other words, in heterogeneous catalysis, supercritical CO₂ properties can help reduce mass and heat transfer limitations and avoid coke formation or catalyst poisoning. Therefore, heterogeneous catalysis performed under supercritical CO₂ conditions may allow the construction of a fixed-bed continuous flow reactor and provide interesting advantages concerning the process safety and space requirement of chemical plants.

We attempted to carry out heterogeneous catalysis for propylene carbonate synthesis under supercritical CO₂ conditions, where CO₂ could act not only as a reagent but also as a solvent, in order to promote the reactivity of CO₂ and simplify product separation. Herein, we wish to report an efficient and environmentally benign process²⁴ for a highly selective synthesis of propylene carbonate from supercritical carbon dioxide and propylene oxide using insoluble ion exchange resins, as shown in Scheme 1. The reaction was carried out in the presence of the insoluble ion exchange resins, one type of polystyryl supported catalysts containing an ammonium salt or amino group, and a polar macroporous adsorption resin, under supercritical CO₂ conditions (373 K, 8 MPa) without any organic solvent or additive. An almost quantitative yield together with excellent selectivity was obtained. The purity of the product directly separated by simple filtration without any other purification process, reached more than 99.3%. Furthermore, the ion exchange resins used as solid catalysts in this study can be easily recovered and reused over five runs without significant loss of activity.

Experimental

The ion exchange resins were supplied from the Chemical Plant of Nankai University. Characteristics of the ion exchange resins are given in Table 1, entries 1–14. Prior to the reaction, all of the ion exchange resins used in this study were evacuated at 373 K for 3 h. SmOCl was prepared according to the published procedure,¹⁶ and was evacuated at 573 K for 3 h before use. Other reagents were of analytic grade and were used as received. The reaction was carried out in a stainless-steel autoclave reactor with an inner volume of 25 ml.



Scheme 1

A typical procedure for the synthesis of propylene carbonate from propylene oxide and CO₂ catalyzed by insoluble ion exchange resin (D201) is as follows: in an autoclave equipped with a magnetic stirrer, CO₂ (liquid, 5 MPa) was added to a mixture of propylene oxide (57.2 mmol), an ion exchange resin (D201, 5 mmol%), and biphenyl (60 mg, as internal standard for GC analysis) at room temperature. The initial pressure was generally adjusted to 8 MPa at 373 K. The autoclave was heated at that temperature for 12 h, and the pressure was kept constant during the reaction. The vessel was then cooled to ambient temperature by placement in an ice–water bath. The excess gases were vented. The product yield was determined by GC with a flame ionization detector and were further identified using GC-MS by comparing retention times and fragmentation patterns with authentic samples.†

Results and discussion

The insoluble ion exchange resins containing an ammonium salt or amino group, and the polar macroporous adsorption resin catalyzed the cycloaddition reaction of supercritical CO₂ with propylene oxide at 373 K for 24 h to afford propylene carbonate (Scheme 1). Table 1 summarizes the characteristics of ion exchange resins, the yield and the selectivity of propylene carbonate for the various ion exchange resins and other catalysts for comparison. Without a catalyst, the coupling of supercritical CO₂ with propylene oxide afforded no product (Table 1, entry 23); while in the presence of catalytic amounts (5 mmol%) of ion exchange resins, such as entries 1–10 in Table 1, quantitative yields (Table 1 entries 5 and 10) together with excellent selectivities were obtained. The products other than propylene carbonate were isomers of propylene oxide, such as acetone, propionaldehyde and 1,2-propanediol (Scheme 2), or oligomers of propylene oxide and their derivatives, such as 2-ethyl-4-methyl-1,3-dioxolane and 2-(1-methylethoxy)-1-propanol. It is noteworthy that no chlorinated organic compounds were detected by GC-MS.

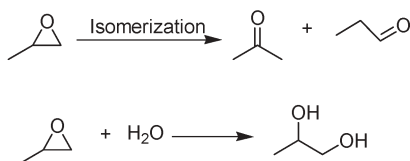
Notably, the catalytic activity strongly depended on the pendant functional group at the polymeric backbone of ion exchange resins. Several kinds of insoluble ion exchange resins, *e.g.* basic anion exchange resin containing quaternary ammonium salt or amino group, the macroporous adsorption resin, acidic cation exchange resins, and chelate ion exchanger, were screened for this purpose. As expected, the acidic cation exchange resins (Table 1, entries 12 and 13), the chelate ion exchanger (Table 1, entry 14), and apolar macroporous adsorption resin (Table 1, entry 11), were found to be inactive for propylene carbonate synthesis under the reaction conditions. The basic anion exchange resins containing a quaternary ammonium salt or amino group (Table 1, entries 1–9) were very effective catalysts. Among them, with the same degree of bead crosslinking (Table 1 entries 6, 8, 9), the catalytic activity depended on the functional group. The order of activity was found to be tertiary amine (entry 9) > secondary amine (entry 8) > primary amine (entry 6), which is the order of the basic

† CAUTION: experiments using compressed gases such as supercritical fluids are potentially hazardous and must only be carried out using appropriate equipment and safety precautions.^{1f,1h}

Table 1 Organic solvent-free synthesis of propylene carbonate from propylene oxide and supercritical CO₂ catalyzed by insoluble ion exchange resins^a

Entry	Catalyst ^b	Functional group	Exchange capacity ^c /mmol g ⁻¹	DC ^d of bead (%)	PC ^e yield (%)	Selectivity (%)
1	D201 × 4	N ⁺ (CH ₃) ₃ Cl ⁻	3.8	4	64.6	99.7
2	D201GF	N ⁺ (CH ₃) ₃ Cl ⁻	4.0	3	75.8	98.8
3	D296	N ⁺ (CH ₃) ₃ Cl ⁻	3.6	2	82.6	99.6
4	D262	N ⁺ (CH ₃) ₃ Cl ⁻	2.0	2	84.6	99.4
5	D201	N ⁺ (CH ₃) ₃ Cl ⁻	3.7	1	99.2	99.8
6	D380	NH ₂	6.5	1	82.3	99.0
7	D392	NH ₂	4.8	2	84.5	98.4
8	D382	NHCH ₃	3.5	1	89.2	99.1
9	D301R	N(CH ₃) ₂	4.8	1	92.9	99.2
10	S-8 ^f	polar	—	0.6	98.1	99.5
11	D4020 ^f	apolar	—	0.6	1.2	20.6
12	D072	SO ₃ Na	4.2	—	2.9	75.4
13	D152	COOH	9.5	—	0.5	64.7
14	D418	NHCH ₂ PO ₃ Na ₂	14	—	2.9	63.2
15	SmOCl ^g	—	—	—	9.8	98.9
16	Et ₃ N	—	—	—	9.3	85.8
17	NH ₄ Cl	—	—	—	0	—
18	NMe ₄ Cl	—	—	—	3.4	90.6
19	Et ₄ NBr	—	—	—	5.7	90.8
20	Et ₄ NBr ^h	—	—	—	60.6	99.2
21	KI	—	—	—	8.1	87.8
22	KI ^h	—	—	—	56.4	99.5
23	None	—	—	—	0	—

^a Reaction conditions: propylene oxide (57.2 mmol), catalyst (5 mmol%), total pressure (8 MPa), 373 K, 24 h. ^b Trade names for ion exchange resins (entries 1–14), bead diameter: 0.3–1.25 mm. The ion exchange resins used in this study were commercially supplied by the Chemical Plant of Nankai University, Tianjin, China. ^c The exchange capacity for the functional group of N⁺(CH₃)₃Cl⁻ in entries 1–5 is equal to chlorine percentage in bead (mmol g⁻¹). ^d Degree of crosslinking. ^e Determined by GC analysis. ^f The surface areas for macroporous resin S-8 (entry 10) and D4020 (entry 11) are 110 m² g⁻¹ and 560 m² g⁻¹, respectively. ^g SmOCl with a surface area of 8.7 m² g⁻¹ was prepared according to the published procedure, see: ref. 16a. The specific surface area was measured by means of the BET method using N₂ adsorption at 77 K after evacuation of the sample at 573 K. ^h In the presence of *N,N*-dimethylformamide (2 ml).

**Scheme 2** Possible side reactions.

strength of the functional groups. The resin with quaternary ammonium is the most active (entry 5), presumably due to the synergistic effect of activation of the epoxide and CO₂ by both ammonium ion and halide anion.^{11,12,18a} Furthermore, in order to evaluate the effect of the halide, a series of tetrabutylammonium halides, including chloride, bromide and iodide, were used as catalysts. The order of activity under the same conditions as mentioned in Table 1 was found to be as follows: Bu₄NI (36.4%) < Bu₄NBr (55.8%) < Bu₄NCl (68.3%), which is in accord with the order of nucleophilicity of the anion.^{5,6a} Hence, the chloride anion was selected as the counter ion in the case of resins with quaternary ammonium ions.

It worth mentioning that a lower degree of crosslinking increases the catalytic activity for the strongly basic anion exchange resins (Table 1, entries 1–5), which is consistent with published results.⁶ The strongly basic anion exchanger D201 containing pendant trimethyl ammonium chloride with a degree crosslinking of 1% (Table 1, entry 6) is the best catalyst for this reaction under the conditions used. Hence, ion exchange resin D201 was chosen as a model catalyst for

further investigation. Surprisingly, the polar macroporous adsorption resin (Table 1, entry 10) with a surface area of 110 m² g⁻¹, exhibited comparable catalytic activity with D201, whereas the non-polar one (Table 1, entry 11) had no activity, which could probably be attributed to the “Lewis acid and Lewis base cocatalyzed mechanism”^{17,18a} in a broad sense.

Interestingly, for comparison with the polymer-supported catalysts, the catalytic activities of the corresponding lower molecular weight catalysts such as Et₃N, NH₄Cl, NMe₄Cl (Table 1, entries 16–18) were also examined for the reaction of propylene oxide and supercritical CO₂. The results indicate that polymer supported ammonium salts or amino groups have higher catalytic activities than such low molecular weight catalysts under the same reaction conditions. It is noteworthy that the activities of ion exchange resins containing ammonium salts and amino groups or of the polar macroporous adsorption resin (Table 1, entries 1–10) were much higher than those of conventional catalysts,²⁵ e.g. tetraethyl ammonium bromide or potassium iodide (Table 1, entries 19 and 21), even when the activity was compared in the presence of DMF (Table 1, entries 20 and 22).

We recently reported that the heterogeneous catalyst, such as lanthanide oxychloride, especially samarium oxychloride and SmOCl supported on zirconia,¹⁶ can efficiently catalyze the propylene carbonate synthesis from CO₂ and propylene oxide, where propylene carbonate is obtained in good yields even in the absence of any additional organic solvents. To our knowledge, samarium oxychloride is one of the most effective heterogeneous catalysts reported to date. Surprisingly, the

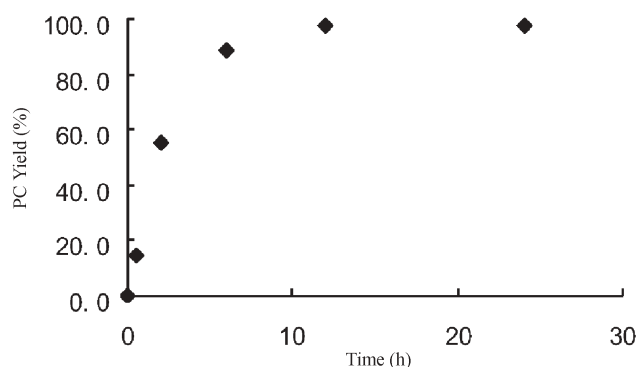


Fig. 1 Reaction time dependence of the yield of propylene carbonate for ion exchange resin D201. Reaction conditions: propylene oxide, 57.2 mmol, D201 (5 mmol%), CO₂, 8 MPa, 373 K.

catalytic activity of the ion exchange resin D201 (Table 1, entry 5) is much higher than that of SmOCl (Table 1, entry 15) under the same reaction conditions, even when the activity¹⁶ was compared in the presence of high catalyst loading (57.2 mmol propylene oxide per 1 g of SmOCl) at high reaction temperature (473 K) and high pressure (14 MPa).

Reaction time dependence of the yield of propylene carbonate for ion exchange resin (D201) is given in Fig. 1. The reactions were performed in the presence of 5 mol% of catalyst D201 at 373 K under 8 MPa, and were monitored for 24 h at regular intervals. The results indicated that the reaction proceeded rapidly within first 6 h. It is amazing to note that within 12 h, almost quantitative yield (97.4%) could be achieved with 99.4% selectivity, which is comparable to the result for the reaction time of 24 h (Table 1, entry 5). In other words, a reaction time of 12 h is required for complete propylene oxide conversion. Notably, selectivity remains more than 99% for the entire course of the reaction.

Fig. 2 shows the effect of CO₂ pressure on the yield of propylene carbonate for the catalyst D201. The selectivity is independent in CO₂ pressure range 1–14 MPa. However, the yield slightly changed with variation of CO₂ pressure, demonstrating the preferential effect of the supercritical conditions for promoting the reactivity of CO₂ as seen in Fig. 2. The isomerization to acetone increased at low CO₂ pressure, while too high CO₂ pressure may retard the

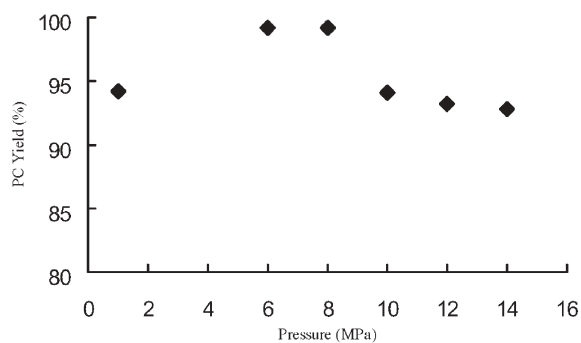


Fig. 2 Effect of CO₂ pressure on the yield of propylene carbonate for ion exchange resin D201. Reaction conditions: propylene oxide (57.2 mmol), D201 (5 mmol%), 373 K, 12 h.

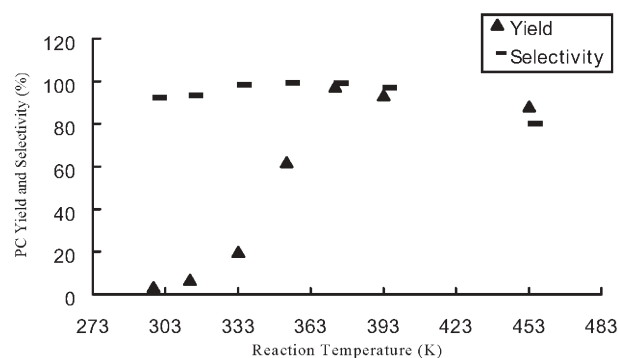


Fig. 3 Reaction temperature dependence of the yield and selectivity of propylene carbonate for ion exchange resin D201. Reaction conditions: propylene oxide (57.2 mmol), D201 (5 mmol%), CO₂, 8 MPa, 12 h.

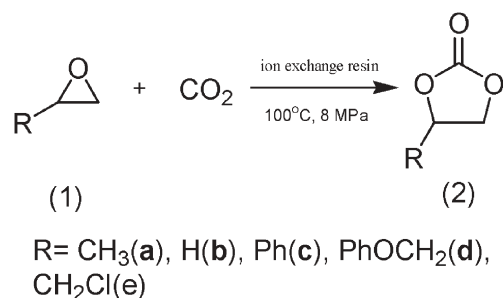
interaction^{21e} between epoxide and the catalyst, and may cause a low concentration of epoxide in the vicinity of the catalyst, thus resulting in a low yield.

The reaction in supercritical CO₂ was also advantageous in terms of product separation from the reaction media. Thus, the phase behaviour of the reaction visually inspected through a sapphire window attached to the autoclave revealed that propylene oxide and supercritical CO₂ initially formed a uniform phase while propylene carbonate was separated out and formed a new phase after the reaction. In addition, the catalyst D201 existed as a solid during the reaction. Therefore, CO₂ could be recycled, maintaining the high pressure. Accordingly, this procedure could be applied to the development of fixed-bed continuous flow reactors, avoiding the use of organic solvent to isolate the products.

The temperature dependence of the yield and selectivity of propylene carbonate is shown in Fig. 3 for catalyst D201. The yield increased with reaction temperature up to 373 K, whereas further increase in the temperature caused a decrease in the selectivity and catalytic activity, possibly due to decomposition of the catalyst and formation of more by-products at higher temperature. Surprisingly, the selectivity was found to be improved as temperature increased up to 333 K. In fact, acetone was readily formed as the main by-product at low temperature. The relatively low selectivity for the product is possibly due to the lower catalytic activity at lower temperature (below 333 K). Conclusively, 373 K could be the optimal temperature for the reaction.

Under the optimized reaction conditions, we examined the reactions of other terminal epoxides with CO₂ (Scheme 3), in order to survey the applicability of various epoxides to this process. The results are summarized in Table 2. The catalyst (D201) was found to be applicable to a variety of terminal epoxides, providing the corresponding cyclic carbonates in high yields and selectivities. Glycidyl phenyl ether (**1d**) was found to be the most reactive epoxide, while epichlorohydrin (**1e**) exhibited relatively low activity among the epoxides surveyed.

The ion exchange resin D201 as solid catalyst in this study can be easily recovered *via* simple filtration, followed by rinsing with ether and drying. Insolubility of the catalyst D201 in the product solution was confirmed by ion chromatography



Scheme 3

Table 2 The coupling of CO₂ and various epoxides catalyzed by ion exchange resin (D201)^a

Substrate	Product	Yield (%)	Selectivity (%)
		97.4	99.4
		98.2	99.5
		95.2	100
		99.5	100
		91.6	99.8

^a Reaction conditions: substrate (57.2 mmol), catalyst (5 mmol%), total pressure 8 MPa, 373 K, 12 h.

and elemental analyses of the resulting filtrate. Catalyst reusability was checked by performing reactions using the recovered catalyst (D201) under the optimized reaction conditions, that is 373 K, 8 MPa, 12 h. The results are summarized in Fig. 4. It is interesting to note that the results are similar to those of the fresh catalyst, suggesting that ion exchange resin D201 can be reused over 5 times without significant loss of its catalytic activity. More than 98% of selectivity for propylene carbonate was still maintained in the fifth run. Furthermore, judged by GC, the purities of the produced propylene carbonates are >99.3%.

In conclusion, the insoluble ion exchange resin containing ammonium salt or amino group, and the polar macroporous

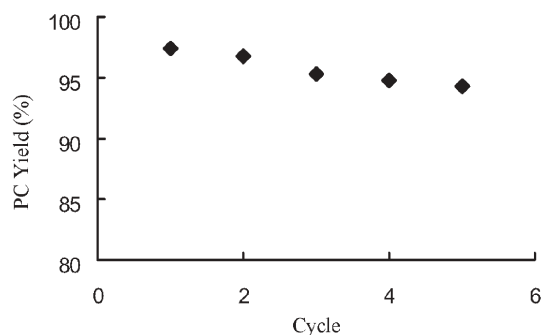


Fig. 4 Catalytic activity of the reused ion exchange resin D201. Reaction conditions: propylene oxide (57.2 mmol), D201 (5 mmol%), CO₂, 8 MPa, 12 h.

adsorption resin, are very effective for propylene carbonate synthesis under supercritical carbon dioxide conditions, where CO₂ could act not only as a reagent but also as a solvent. The process has notable advantages and remarkable environmentally benign features: 1) it requires no additional organic solvents either for the reaction or for the separation of products; 2) the catalyst is very effective at the mild conditions, a quantitative yield together with excellent selectivity was obtained; 3) the catalyst can be easily recovered and reused over 5 times without significant loss of its catalytic activity; 4) it is easy to get high purity (over 99.3%) of product without further purification processes, in a batch-wise reaction. It could be profitably applied to the development of continuous flow reactors, avoiding the use of solvent to isolate the products. The process disclosed here represents a simple, ecologically safer, cost-effective route to cyclic carbonates with high product quality, as well as easy product recovery and catalyst recycling.

Acknowledgements

The authors gratefully acknowledge No. 56 Quality Inspect Station for GC and GC-MS analyses. Gratitude is expressed to the National Natural Science Foundation of China (Grant No. 20472030), the Natural Science Foundation of Tianjin (Grant No. 033609311), Ministry of Education of China and Nankai University for financial support.

Ya Du, Fei Cai, De-Lin Kong and Liang-Nian He*

Institute of Elemento-Organic Chemistry, State Key Laboratory of Elemento-Organic Chemistry, Nankai University, Tianjin, 300071, P. R. China. E-mail: heln@nankai.edu.cn; Fax: +86-22-23503627; Tel: +86-22-23504216

References

- (a) H. Arakawa, M. Aresta, J. N. Armor, M. A. Barteau, E. J. Beckman, A. T. Bell, J. E. Bercaw, C. Creutz, E. Dinjus, D. A. Dixon, K. Domen, D. L. DuBois, J. Eckert, E. Fujita, D. H. Gibson, W. A. Goddard, D. W. Goodman, J. Keller, G. J. Kubas, H. H. Kung, J. E. Lyons, L. E. Manzer, T. J. Marks, K. Morokuma, K. M. Nicholas, R. Periana, L. Que, J. Rostrup-Nielson, W. M. H. Sachtler, L. D. Schmidt, A. Sen, G. A. Somorjai, P. C. Stair, B. R. Stults and W. Tumas, *Chem. Rev.*, 2001, **101**, 953; (b) P. T. Anastas and J. C. Warner, *Green Chemistry, Theory and Practice*, Oxford University Press, Oxford, 1998; (c) A. S. Matlack, in *Introduction to Green Chemistry*, Marcel Dekker, Basel, 2001; (d)

- B. M. Trost, *Science*, 1991, **254**, 1471; (e) W. Leitner, *Angew. Chem., Int. Ed. Engl.*, 1995, **34**, 2207; (f) *Chemical Synthesis Using Supercritical Fluids*, ed. P. G. Jessop, W. Leitner, Wiley-VCH, Weinheim, 1999; (g) M. Aresta and E. Quaranta, *CHEMTECH*, 1997, **32**; (h) W. Leitner, *Acc. Chem. Res.*, 2002, **35**, 746.
- 2 (a) A. G. Shaikh and S. Sivaram, *Chem. Rev.*, 1996, **96**, 951; (b) J. H. Clements, *Ind. Eng. Chem. Res.*, 2003, **42**, 663; (c) W. J. Peppel, *Ind. Eng. Chem.*, 1958, **50**, 767; (d) *Ullmann's Encyclopedia of Industrial Chemistry, Fifth*, ed. W. Gerhartz, et al., VCH, Weinheim, 1986, vol. A5.
- 3 S. Fukuoka, M. Kawamura, K. Komiyama, M. Tojo, H. Hachiya, K. Hasegawa, M. Aminaka, H. Okamoto, I. Fukawa and S. Konno, *Green Chem.*, 2003, **5**, 497.
- 4 (a) J. F. Cooper and M. Lichtenwalter, *US Pat.*, 2 773 070, 1956; (b) P. P. McClellan, *US Pat.*, 2 873 282, 1959.
- 5 N. Kihara, N. Hara and T. Endo, *J. Org. Chem.*, 1993, **58**, 6198.
- 6 (a) T. Nishikubo, A. Kameyama, J. Yamashita, M. Tomoi and W. Fukuda, *J. Polym. Sci., Part A: Polym. Chem.*, 1993, **31**, 939; (b) T. Nishikubo, A. Kameyama, J. Yamashita, T. Fukumitsu, C. Maejima and M. Tomoi, *J. Polym. Sci., Part A: Polym. Chem.*, 1995, **33**, 1011.
- 7 (a) G. Rokicki, W. Kuran and B. P. Marciniak, *Monatsh. Chem.*, 1984, **115**, 205; (b) T. S. Zhao, Y. Z. Han and Y. H. Sun, *Phys. Chem. Chem. Phys.*, 1999, **1**, 3047; (c) T. Iwasaki, N. Kihara and T. Endo, *Bull. Chem. Soc. Jpn.*, 2000, **73**, 713.
- 8 (a) A. Baba, T. Nodi and H. Matauda, *Bull. Chem. Soc. Jpn.*, 1987, **60**, 1552; (b) H. Matauda, A. Ninagawa, R. Nomura and T. Tsuchida, *Chem. Lett.*, 1979, 573.
- 9 H. Matauda, A. Ninagawa and R. Nomura, *Chem. Lett.*, 1979, 1261.
- 10 (a) N. Takeda and S. Inoue, *Bull. Chem. Soc. Jpn.*, 1978, **51**, 3564; (b) T. Aida and S. Inoue, *J. Am. Chem. Soc.*, 1983, **105**, 1304; (c) R. L. Paddock, Y. Hiyama, J. M. McKay and S. T. Nguyen, *Tetrahedron Lett.*, 2004, **45**, 2023.
- 11 (a) R. J. D. Pasquale, *J. Chem. Soc., Chem. Commun.*, 1973, 157; (b) T. Fujinami, T. Suzuki, M. Kamiya, S. Fukuzawa and S. Sakai, *Chem. Lett.*, 1985, 199; (c) M. Aresta, E. Quaranta and A. Ciccarese, *J. Mol. Catal.*, 1987, **41**, 355; (d) W. J. Kruper and D. V. Dellar, *J. Org. Chem.*, 1995, **60**, 725; (e) T. V. Magdesieva, S. V. Milovanov, B. V. Lokshin, Z. S. Klemenkova and L. G. Tomilova, *Russ. Chem. Bull.*, 1998, **47**, 2137; (f) H. S. Kim, J. J. Kim, B. G. Lee, O. S. Jung, H. G. Jang and S. O. Kang, *Angew. Chem., Int. Ed.*, 2000, **39**, 4096; (g) F. W. Li, C. G. Xia, L. W. Xu, W. Sun and G. X. Chen, *Chem. Commun.*, 2003, 2042; (h) M. Aresta and A. Dibenedetto, *J. Mol. Catal. A: Chem.*, 2002, **182–183**, 399; (i) M. Tu and R. J. Davis, *J. Catal.*, 2001, **199**, 85.
- 12 (a) T. Yano, H. Matsui, T. Koike, H. Ishiguro, H. Fujihara, M. Yoshikara and T. Maeshima, *Chem. Commun.*, 1997, 1129; (b) B. M. Bhanage, S. Fujita, Y. Ikushima and M. Arai, *Appl. Catal., A: Gen.*, 2001, **219**, 259.
- 13 K. Yamaguchi, K. Ebitani, T. Yoshida, H. Yoshida and K. Kaneda, *J. Am. Chem. Soc.*, 1999, **121**, 4526.
- 14 (a) X. B. Lu, Y. Z. Pan, D. F. Ji and R. He, *Chin. Chem. Lett.*, 2000, **11**, 589; (b) D. F. Ji, X. B. Lu and R. He, *Appl. Catal., A: Gen.*, 2000, **203**, 329.
- 15 (a) E. J. Doscocil, S. V. Bordawekar, B. G. Kaye and R. J. Davis, *J. Phys. Chem. B*, 1999, **103**, 6277; (b) M. Tu and R. J. Davis, *J. Catal.*, 2001, **199**, 85.
- 16 (a) H. Yasuda, L. N. He and T. Sakakura, *J. Catal.*, 2002, **209**, 547; (b) H. Yasuda, L.-N. He and T. Sakakura, *Stud. Surf. Sci. Catal.*, 2003, **145**, 259.
- 17 (a) H. Yasuda, C. Hu, L.-N. He and T. Sakakura, *JP Pat.*, 2004-250349, 2004, to AIST. Very recently, propylene carbonate synthesis using zinc-substituted polyoxometalate has been reported, however the selectivity of this reaction is unsatisfactory in the absence of dimethylaminopyridine, see: (b) M. Sankar, N. H. Tarte and P. Manikandan, *Appl. Catal., A*, 2004, **276**, 217.
- 18 (a) D. J. Darensbourg and M. W. Holtcamp, *Coord. Chem. Rev.*, 1996, **153**, 155; (b) L.-N. He, H. Yasuda and T. Sakakura, *Green Chem.*, 2003, **5**, 92; (c) Y.-M. Shen, W.-L. Duan and M. Shi, *Eur. J. Org. Chem.*, 2004, 3080; (d) F. Li, C. Xia, L. Sun and G. Chen, *Chem. Commun.*, 2003, 2042; (e) J.-W. Huang and M. Shi, *J. Org. Chem.*, 2003, **68**, 6705; (f) X.-B. Lu, Y.-J. Zhang, K. Jin, L.-M. Luo and H. Wang, *J. Catal.*, 2004, **227**, 537.
- 19 (a) V. Caló, A. Nacci, A. Monopoli and A. Fanizzi, *Org. Lett.*, 2002, **4**, 2561; (b) H. Yang, Y. Gu, Y. Deng and F. Shi, *Chem. Commun.*, 2002, 274; (c) H. Kawanami, A. Sasaki, K. Matsui and Y. Ikushima, *Chem. Commun.*, 2003, 896; (d) Y.-J. Kim and M. Cheong, *Bull. Korean Chem. Soc.*, 2002, **23**, 1027.
- 20 (a) R. L. Paddock and S. T. Nguyen, *J. Am. Chem. Soc.*, 2001, **121**, 11498; (b) Y. M. Shen, W. L. Duan and M. Shi, *J. Org. Chem.*, 2003, **68**, 1559; (c) X.-B. Lu, B. Liang, Y.-J. Zhang, Y.-Z. Tian, Y.-M. Wang, C.-X. Bai, H. Wang and R. Zhang, *J. Am. Chem. Soc.*, 2004, **126**, 3732; (d) M. Alvaro, C. Baleizao, D. Das, E. Carbonell and H. Garcia, *J. Catal.*, 2004, **228**, 254; (e) R. L. Paddock and S. T. Nguyen, *Chem. Commun.*, 2004, 1622; (f) X.-B. Lu, R. He and C.-X. Bai, *J. Mol. Catal. A: Chem.*, 2002, **186**, 1.
- 21 (a) M. Aresta, A. Dibenedetto, L. Gianfrate and C. Pastore, *Appl. Catal., A: Gen.*, 2003, **255**, 1, 5; (b) M. Aresta, A. Dibenedetto, L. Gianfrate and C. Pastore, *J. Mol. Catal. A: Chem.*, 2003, **204**, 245; (c) H. S. Kim, J. J. Kim, H. N. Kwon, M. J. Chung, B. G. Lee and H. G. Jang, *J. Catal.*, 2002, **205**, 226; (d) L.-F. Xiao, F.-W. Li and C.-G. Xia, *Appl. Catal., A: Gen.*, 2005, **279**, 125; (e) X.-B. Lu, J.-H. Xiu, R. He, K. Jin, L.-M. Luo and X.-J. Feng, *Appl. Catal., A: Gen.*, 2004, **275**, 73; (f) F. Shi, Q. Zhang, Y. He and Y. Deng, *J. Am. Chem. Soc.*, 2005, **127**, 4182.
- 22 R. F. Sammelson and M. J. Kurth, *Chem. Rev.*, 2001, **101**, 137.
- 23 A. Baiker, *Chem. Rev.*, 1999, **99**, 453–473.
- 24 L.-N. He, Y. Du, F. Cai and H.-X. Zhang, *CN Pat.*, 200410093952.9, to Nankai University, P. R. China.
- 25 (a) C. H. McMullen, J. R. Nelson, B. C. Ream and J. A. Sims, Jr., *US Pat.*, 4 314 945, 1982, to Union Carbide Corporation; (b) B. C. Ream, *US Pat.*, 4 877 886 1989, to Union Carbide Chemicals and Plastics Company Inc.; (c) S.-H. Wang, *PEP Review*, No. 92-1-1, SRI Consulting, Menlo Park, CA, 1993; and T. I. McMillan, *PEP Report No. 193*, SRI Consulting, Menlo Park, CA, 1991.

Effect of modifiers on the activity of a Cr₂O₃/Al₂O₃ catalyst in the dehydrogenation of ethylbenzene with CO₂

Xingnan Ye,^a Yinghong Yue,^a Changxi Miao,^b Zaiku Xie,^b Weiming Hua*^a and Zi Gao^a

Received 26th April 2005, Accepted 16th May 2005

First published as an Advance Article on the web 31st May 2005

DOI: 10.1039/b505781g

Chromium oxide supported on alumina was modified with various transition metal oxides by an incipient wetness method. The effect of modifiers on the activity of 20% Cr₂O₃/Al₂O₃ catalyst in the dehydrogenation of EB with CO₂ was investigated. The activity is enhanced for ceria and vanadia modified supported chromium oxide catalysts, whereas the activity is decreased for catalysts modified with cobalt, manganese, molybdenum and zinc oxides. Carbon monoxide was detected in the course of the reaction, suggesting that carbon dioxide, which is one of the most important greenhouse gases, could be utilized as a mild oxidant in the oxidative dehydrogenation of ethylbenzene to styrene over unmodified and modified Cr₂O₃/Al₂O₃ catalysts.

Introduction

Styrene is one of the most important basic chemicals in the petrochemical industry and is mainly used for the production of many different polymeric materials, such as polystyrene, styrene-acrylonitrile and acrylonitrile-butadiene-styrene (ABS). It is commercially produced mainly by the catalytic dehydrogenation of ethylbenzene (EB) using potassium-promoted iron oxide catalysts in the presence of a large amount of superheated steam as a diluent and heat carrier at high temperatures of 550–650 °C.^{1,2} The present commercial process is equilibrium limited and, moreover, it is very energy inefficient because all the latent heat of condensation of steam is not recovered in a liquid-gas separator following a reactor. Hence, a worldwide search for alternative processes is underway. The oxidative dehydrogenation of EB in the presence of oxygen has received much attention, because this reaction is free from thermodynamic constraints regarding conversion and can be operated at lower temperatures.^{3–5} However, a considerable decrease in styrene selectivity due to deep oxidation of hydrocarbons to carbon monoxide or carbon dioxide makes it uneconomical in view of industrial application.

In contrast to the present commercial process using steam, EB dehydrogenation using CO₂ as a non-traditional (mild) oxidant can substantially decrease the energy consumed and provide a higher equilibrium yield of styrene. It was estimated that the energies required for producing styrene by a present commercial process using steam and by a new process using CO₂ were 1.5×10^9 and 1.9×10^8 cal (ton-styrene)⁻¹, respectively.⁶ High selectivity to styrene for this new process can also be maintained. Moreover, it provides a new route to solve the problem of emission of CO₂ which is one of the most important greenhouse gases. Therefore, the dehydrogenation of EB in the presence of CO₂ has attracted much attention after the pioneering works of Sato *et al.*⁷ and Matsui *et al.*⁸ Unfortunately, potassium-promoted iron oxide catalysts used for the present commercial dehydrogenation process do not

work effectively in the dehydrogenation of EB with CO₂. Thus, the development of catalysts with improved dehydrogenation activity for the new process using CO₂ is required. The dehydrogenation of EB in the presence of CO₂ has been studied over a variety of metal oxide catalysts such as iron oxide,^{9–13} vanadium oxide,^{14–17} chromium oxide,^{18–20} cerium oxide^{14,18} and zirconium oxide.^{21,22} Among these catalysts, vanadia and chromia give better performance in the dehydrogenation of EB with CO₂. In our previous work,^{19,20} we investigated the dehydrogenation of EB to styrene in the presence of CO₂ over supported chromia catalysts. It was found that Cr₂O₃/Al₂O₃ catalysts exhibit the best catalytic performance when the Cr₂O₃ loading is 20–25 wt%.

In the present work, the supported 20% Cr₂O₃/Al₂O₃ catalyst was modified with various transition metal oxides by an incipient wetness method. The effect of modifiers on the activity of 20% Cr₂O₃/Al₂O₃ catalyst in the dehydrogenation of EB with CO₂ has been studied. The aim of this work is to improve the catalytic behavior of 20% Cr₂O₃/Al₂O₃ catalyst through modification.

Results and discussion

The dehydrogenation of EB was performed in the presence of CO₂ at 500 °C. The major product of the reaction is styrene, whereas benzene and toluene are minor by-products. As the reaction goes on, a slow decrease in activity was observed and meanwhile the selectivity to styrene rose very slightly. As an example, the effect of reaction time on EB conversion and styrene selectivity over the ceria modified 20% Cr/Al catalyst is shown in Fig. 1. The catalytic behavior of the 20% Cr/Al catalyst modified with various transition metal oxides after 6 h on stream is summarized in Table 1, along with their surface areas. The catalytic activities for EB dehydrogenation are obviously different. The EB conversions of modified 20% Cr/Al catalysts decrease in the order of 5% Ce/20% Cr/Al > 5% V/20% Cr/Al > 20% Cr/Al > 5% Co/20% Cr/Al > 5% Mo/20% Cr/Al > 5% Zn/20% Cr/Al > 5% Mn/20% Cr/Al. This suggests that the effect of modifiers on the reactivity of

*wmhua@fudan.edu.cn

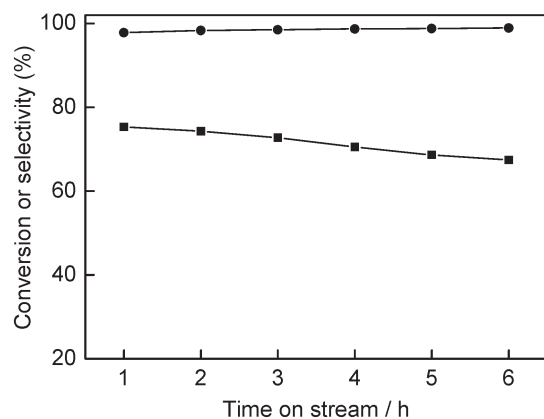


Fig. 1 Effect of reaction time on EB conversion (■) and styrene selectivity (●) at 500 °C over the 5% Ce/20% Cr/Al catalyst.

Table 1 Effect of modifiers on the catalytic property of 20% Cr/Al catalyst for the dehydrogenation of ethylbenzene in the presence of CO₂

Catalyst	S _{BET} /m ² g ⁻¹	Conv. (%)	Selectivity (%) ^a		
			STY	T	B
20% Cr/Al	173	57.5	99	0.8	0.2
5% Ce/20% Cr/Al	148	67.4	98.9	0.8	0.3
5% Co/20% Cr/Al	163	55.5	99.3	0.5	0.2
5% Mn/20% Cr/Al	144	41.1	98.9	0.9	0.2
5% Mo/20% Cr/Al	171	52.6	99.3	0.5	0.2
5% V/20% Cr/Al	142	65.7	98.8	0.7	0.5
5% Zn/20% Cr/Al	146	48.1	99.8	0.2	0

^a STY = styrene, T = toluene, B = benzene.

20% Cr/Al catalyst for the dehydrogenation of EB is different. The activity of 20% Cr/Al catalyst is promoted by the addition of cerium and vanadium oxides, whereas addition of other transition metal oxides to the 20% Cr/Al catalyst results in a decrease in activity. The inhibiting effect of manganese oxide on the reactivity of 20% Cr/Al catalyst for the dehydrogenation of EB is most evident. All the catalysts display a similar selectivity to styrene, which means that the influence of the investigated modifiers on styrene selectivity is relatively small. The influence of EB conversion on the styrene selectivity over the 5% Ce/20% Cr/Al catalyst is shown in Table 2. The conversion was adjusted through changing the catalyst loading. In general, the selectivity declines with an increase in conversion. However, this variation is very small when the EB conversion is below 67%. The above result suggests that there is no need to consider the change in selectivity with conversion when the influence of the selected modifiers on styrene selectivity is investigated. The BET surface area of the 20% Cr/Al catalyst decreases to different extents after modification with various transition metal oxides. Hirano discovered that the addition of CeO₂ to potassium-promoted iron oxide increased the catalytic activity for EB dehydrogenation.²³ Cherian *et al.* reported that

Table 2 Influence of EB conversion on the styrene selectivity over the 5% Ce/20% Cr/Al catalyst

	Conversion (%)	Styrene selectivity (%)	EB conversion (%)	Styrene selectivity (%)
Conversion (%)	15.0	39.7	67.4	77.3
Selectivity (%)	99.2	99.1	98.9	98.1

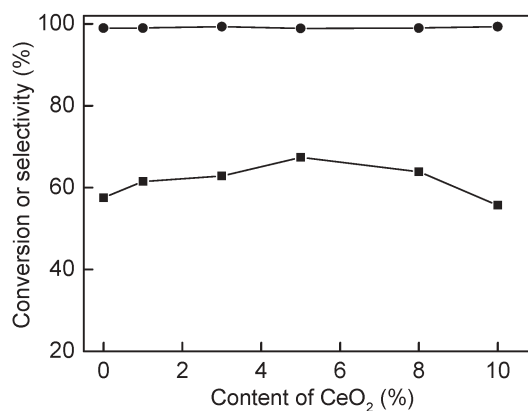


Fig. 2 Effect of CeO₂ content on the conversion of EB (■) and selectivity to styrene (●) over Ce/20% Cr/Al catalysts at 500 °C.

modification of Cr₂O₃/Al₂O₃ and Cr₂O₃/TiO₂ catalysts with vanadium oxide caused an increase in activity for the oxidative dehydrogenation of propane.²⁴ Our results are in agreement with the phenomena reported in the literature,^{23,24} albeit the catalyst system and the catalytic reaction are different.

The dehydrogenation activities of Ce/20% Cr/Al catalysts in the presence of CO₂ after 6 h on stream as a function of ceria loading are illustrated in Fig. 2. As the CeO₂ loading is increased, the conversion of EB on Ce/20% Cr/Al catalysts first increases and then decreases. A maximum of 67.4% conversion appears at a CeO₂ loading of 5 wt%. The selectivity to styrene at the maximum conversion is 98.9%. Under the same reaction conditions, the conversion of EB after 6 h on stream over the 5% Ce/Al catalyst is only 2%. Activated carbon-supported ceria catalyst was reported to be effective for EB dehydrogenation in the presence of CO₂.^{14,18} This discrepancy is probably caused by the different support employed in our work and in the literature.

Table 3 shows the catalytic properties of unmodified and ceria modified supported chromium oxide catalysts for the dehydrogenation of EB in the presence of CO₂ as well as in the absence of CO₂ after 6 h on stream. It is observed that the selectivity to styrene is the same for both reaction atmospheres. For both catalysts, the activity in the presence of CO₂ is obviously higher than that in the absence of CO₂, indicating that CO₂ plays a positive role in the reaction. The promoting effect of CO₂ on the dehydrogenation of EB can be attributed to both the oxidative dehydrogenation of EB by the oxygen species originating from CO₂^{9,15,19,21} and the coupling of EB dehydrogenation with the reverse water–gas shift reaction.^{10,25} A single reverse water–gas shift reaction was conducted at 500 °C by feeding a mixed gas of CO₂ and H₂ over the 5% Ce/20% Cr/Al catalyst, and the result is given in Table 4. It is

Table 3 Comparison of catalytic behavior for the dehydrogenation of ethylbenzene in the presence of CO₂ and in the absence of CO₂

Catalyst	With CO ₂ (%)		Without CO ₂ (%)	
	Conv.	Select.	Conv.	Select.
20% Cr/Al	57.5	99.0	48.9	98.9
5% Ce/20% Cr/Al	67.4	98.9	61.0	98.9

Table 4 Reverse water–gas shift reaction over the 5% Ce/20% Cr/Al catalyst at 500 °C^a

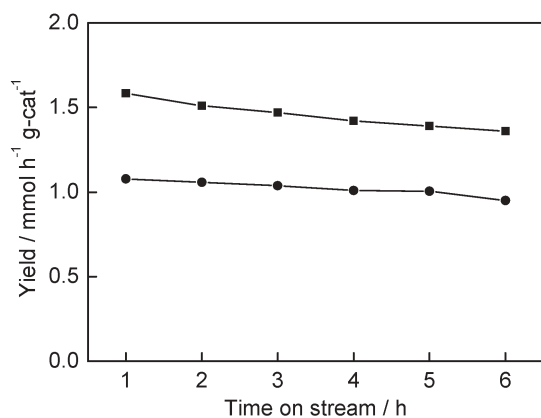
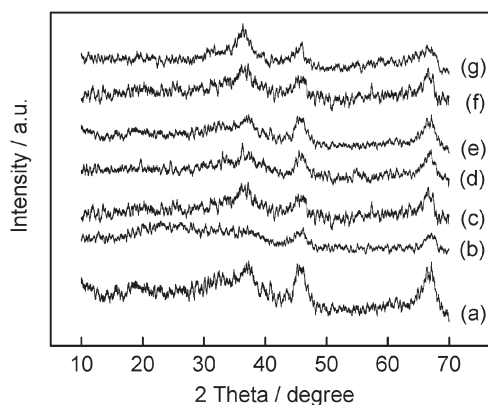
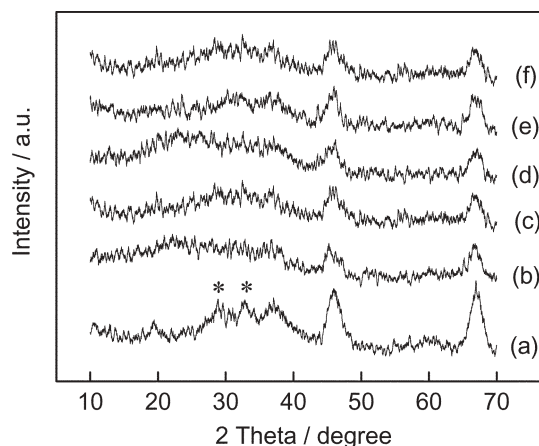
Reaction time/h	CO formation/ mmol min ⁻¹	H ₂ consumption/ mmol min ⁻¹
2	0.0147	0.0145
6	0.0143	0.0141

^a Catalyst loading: 150 mg; pre-treatment at 500 °C in N₂ for 2 h; reaction at 500 °C under the mixed gas flow of N₂ : CO₂ : H₂ at 25 : 4 : 1 ml min⁻¹.

clear that the catalyst is active for the reverse water–gas shift reaction. Carbon monoxide was detected in the effluent gases, suggesting that CO₂ was converted into CO during the reaction. Carbon monoxide is formed through the reverse water–gas shift reaction and the direct reaction of CO₂ and EB.^{9,15,19,21,26} This implies that CO₂ can be used as a mild oxidant in the oxidative dehydrogenation of EB over unmodified and modified Cr₂O₃/Al₂O₃ catalysts. In order to understand the role of CO₂ in the reaction, the variation of the amount of CO in the reaction product as a function of reaction time on the 5% Ce/20% Cr/Al catalyst at 500 °C was tested and is given in Fig. 3. The amount of CO formed in the reaction is always lower than the amount of styrene, and it is *ca.* 70% of the styrene yield. This suggests that both oxidative dehydrogenation and simple dehydrogenation reactions are probably present on the catalyst,^{26,27} as shown below:



Fig. 4 shows the XRD patterns of various transition metal oxide modified 20% Cr/Al catalysts calcined at 550 °C. All the catalysts display a similar X-ray diffractogram to γ -Al₂O₃. No distinct diffraction peaks corresponding to crystalline modifiers and Cr₂O₃ appear when the loadings of modifiers and Cr₂O₃ are 5 and 20 wt%, respectively, suggesting that both modifiers and chromia are highly dispersed on the γ -Al₂O₃ support. Fig. 5 shows the XRD patterns of a series of Ce/20% Cr/Al catalysts with various content of CeO₂ calcined at 550 °C. The catalysts do not display distinct diffraction peaks due to crystalline ceria, even if a CeO₂ loading as high as

**Fig. 3** Yield of styrene (■) and CO (●) in the course of the reaction on the 5% Ce/20% Cr/Al catalyst at 500 °C.**Fig. 4** XRD patterns of various transition metal oxide modified 20% Cr/Al catalysts calcined at 550 °C. (a) γ -Al₂O₃, (b) 5% Ce, (c) 5% Co, (d) 5% Mn, (e) 5% Mo, (f) 5% V, (g) 5% Zn.**Fig. 5** XRD patterns of a series of Ce/20% Cr/Al catalysts with various CeO₂ contents calcined at 550 °C. (a) 5% Ce/Al, (b) 1% Ce/20% Cr/Al, (c) 3% Ce/20% Cr/Al, (d) 5% Ce/20% Cr/Al, (e) 8% Ce/20% Cr/Al, (f) 10% Ce/20% Cr/Al. (*) CeO₂.

10 wt% is reached. In contrast, diffraction peaks of crystalline CeO₂ were observed on the 5% Ce/Al catalyst with a 5 wt% CeO₂ loading, indicating that sole ceria is poorly dispersed on the γ -Al₂O₃ support. There is probably a strong interaction between CeO₂ and Cr₂O₃, which leads to the formation of smaller CeO₂ crystals. Consequently, an improvement in the dispersion of ceria on the γ -Al₂O₃ support for Ce/20% Cr/Al catalysts was observed.

The TPR profiles of some representative catalysts are depicted in Fig. 6. For the 5% Ce/Al catalyst, there are two very small peaks centered at 434 and 545 °C indicative of the reduction of surface Ce⁴⁺, suggesting that CeO₂ can be only partially reduced under the experimental conditions employed in this work. This is consistent with the results reported by other authors.²⁸ There is one strong reduction peak centered at 334 °C on the profile of the 20% Cr/Al catalyst, corresponding to the reduction of Cr⁶⁺ to Cr³⁺.^{19,29,30} There is also one reduction peak on the TPR profile of the 5% Ce/20% Cr/Al catalyst, but the peak temperature is slightly shifted towards lower temperature, suggesting that the oxygen is more weakly bound in the dispersed chromia on the ceria modified catalyst.

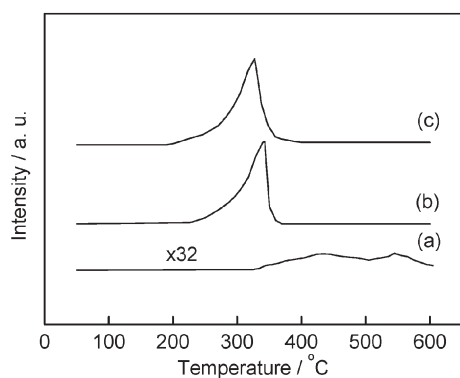


Fig. 6 TPR profiles of the catalysts: (a) 5% Ce/Al, (b) 20% Cr/Al, (c) 5% Ce/20% Cr/Al.

The disappearance of the very small peak corresponding to the reduction of CeO₂ in the 5% Ce/20% Cr/Al catalyst is probably caused by the overlap between chromia and ceria reduction peaks. The TPR data and the amount of Cr⁶⁺ in the catalysts calculated from the H₂ consumption are listed in Table 5. It is observed that the amount of Cr⁶⁺ in the 5% Ce/20% Cr/Al catalyst is higher than that in the 20% Cr/Al catalyst. In previous literature,^{31,32} the *n*-butane or isobutane dehydrogenation activity of Cr₂O₃/Al₂O₃ catalysts increased in line with the amount of Cr⁶⁺ in the fresh catalyst. The high oxidation state Cr species were proposed to be the precursors of the active sites, which have a higher activity for the dehydrogenation reaction. Our previous work on the dehydrogenation of EB in the presence of CO₂ over chromia-based catalysts seems to support this suggestion.¹⁹ The TPR results reveal that the addition of ceria to the 20% Cr/Al catalyst increases the reducibility of chromia and the amount of Cr⁶⁺ species in the fresh catalyst. This is probably the main reason for the promoting effect of ceria on the reactivity of the 20% Cr/Al catalyst for EB dehydrogenation with CO₂.

Conclusion

In the present work we have shown that carbon dioxide can be used as a selective oxidant in the oxidative dehydrogenation of ethylbenzene to styrene over unmodified and modified Cr₂O₃/Al₂O₃ catalysts. The 5% CeO₂/20% Cr₂O₃/Al₂O₃ catalyst exhibits the best catalytic performance for the dehydrogenation of ethylbenzene with CO₂, a much more energy efficient process in comparison with the present commercial process using steam. A higher styrene yield of 66.7% at high styrene selectivity of 98.9% is achieved on this catalyst. The promoting effect of ceria on the 20% Cr₂O₃/Al₂O₃ catalyst for ethylbenzene dehydrogenation in the presence of CO₂ can be ascribed

Table 5 TPR data for the catalysts

Catalyst	Peak temp./°C	H ₂ consumption/ mmol (g cat) ⁻¹	Cr ⁶⁺ /mmol (g cat) ⁻¹
5% Ce/Al	434, 545	0.024	—
20% Cr/Al	334	0.78	0.52
5% Ce/20% Cr/Al	227	0.86	0.57

to the improved reducibility of chromia and the increased amount of Cr⁶⁺ species in the fresh catalyst.

Experimental

Catalyst preparation

The γ -Al₂O₃ support used in this work has a BET surface area of 214 m² g⁻¹. To prepare alumina supported chromium oxide catalysts doped with M_mO_n (M = Ce, Co, Mn, Mo, V or Zn), a certain amount of Ce(NO₃)₃, Co(NO₃)₂, Mn(NO₃)₂, (NH₄)₂MoO₄, NH₄VO₃ or Zn(NO₃)₂ was mixed with Cr(NO₃)₃ and dissolved in a small amount of water, then the aqueous solution was applied to the γ -Al₂O₃ support until incipient wetness, followed by drying at 110 °C overnight. After calcination in air at 550 °C for 5 h, the catalysts were obtained. They are denoted as x% M/20% Cr/Al, where x% represents the weight percentage of M_mO_n in the catalysts, the weight percentage of Cr₂O₃ in all catalysts was 20%. For comparison, 20% Cr₂O₃/Al₂O₃ and 5% CeO₂/Al₂O₃ catalysts were also prepared in the same way as the above catalysts. They are labeled as 20% Cr/Al and 5% Ce/Al, respectively.

Characterization of catalysts

The BET surface areas of the support and catalysts were measured by N₂ adsorption at -196 °C on a Micromeritics ASAP 2000 instrument. X-Ray powder diffraction (XRD) patterns were recorded on a Rigaku D/MAX-IIA diffractometer with Ni-filtered Cu K α radiation operated at 30 kV and 20 mA. Temperature programmed reduction (TPR) experiments were carried out using a Micromeritics TPD/TPR 2900 instrument. After pretreating 200 mg of catalyst in N₂ at 300 °C for 3 h, a reduction run was performed from 50 to 600 °C at a heating rate of 10 °C min⁻¹ under a gas flow (40 ml min⁻¹) of hydrogen (10 vol%) and argon (90 vol%).

Activity measurement

The oxidative dehydrogenation of EB in the presence of CO₂ was carried out in a flow-type fixed-bed microreactor under atmospheric pressure. To supply the reactant, a gas mixture of N₂ and CO₂ (19 : 1 molar ratio) at a flow rate of 60 ml min⁻¹ was passed through a glass evaporator filled with liquid EB maintained at 0 °C. The catalyst load was 100 mg, and the reaction temperature was 500 °C. The molar ratio of CO₂ to EB was kept at a constant of 19. Prior to the reaction, the catalyst was pretreated at 500 °C in N₂ for 2 h. The hydrocarbon products were analyzed with a gas chromatograph equipped with a flame ionization detector and a 2 m long stainless steel column packed with 15% DNP. The effluent from the reactor was also collected in a gas bag and analyzed for CO and CO₂ content with a gas chromatograph equipped with a thermal conductivity detector and a 6 m long stainless steel column packed with porapak Q.

Acknowledgements

This work was financially supported by the Chinese Major State Basic Research Development Program (2000077507), the Shanghai Major Basic Research Program (03DJ14004),

Shanghai Research Institute of Petrochemical Technology, the National Natural Science Foundation of China (20303004) and the Shanghai Natural Science Foundation (03ZR14013).

Xingnan Ye,^a Yinghong Yue,^a Changxi Miao,^b Zaiku Xie,^b Weiming Hua*^a and Zi Gao^a

^aDepartment of Chemistry and Shanghai Key Laboratory of Molecular Catalysis and Innovative Materials, Fudan University, Shanghai 200433, P. R. China. E-mail: wmhua@fudan.edu.cn; Fax: +862165641740; Tel: +862165642409

^bShanghai Research Institute of Petrochemical Technology, Shanghai 201208, P. R. China

References

- H. Lee, *Catal. Rev.*, 1973, **8**, 285.
- W. D. Mross, *Catal. Rev. Sci. Eng.*, 1983, **25**, 591.
- F. Cavani and F. Trifiro, *Appl. Catal., A*, 1995, **133**, 219.
- W. S. Chang, Y. Z. Chen and B. L. Yang, *Appl. Catal., A*, 1995, **124**, 221.
- W. Oganowski, J. Hanuza and L. Kepinski, *Appl. Catal., A*, 1998, **171**, 145.
- N. Mimura, I. Takahara, M. Saito, T. Hattori, K. Ohkuma and M. Ando, *Catal. Today*, 1998, **45**, 61.
- S. Sato, M. Ohhara, T. Sodesawa and F. Nozaki, *Appl. Catal.*, 1988, **37**, 207.
- J. Matsui, T. Sodesawa and F. Nozaki, *Appl. Catal.*, 1991, **67**, 179.
- M. Sugino, H. Shimada, T. Turuda, H. Miura, N. Ikenaga and T. Suzuki, *Appl. Catal., A*, 1995, **121**, 125.
- N. Mimura and M. Saito, *Catal. Lett.*, 1999, **58**, 59.
- T. Badstube, H. Papp, R. Dziembaj and P. Kustrowski, *Appl. Catal., A*, 2000, **204**, 153.
- M. Saito, H. Kimura, N. Mimura, J. Wu and K. Murata, *Appl. Catal., A*, 2003, **239**, 71.
- A. L. Sun, Z. F. Qin, S. W. Chen and J. G. Wang, *J. Mol. Catal. A: Chem.*, 2004, **210**, 189.
- Y. Sakurai, T. Suzaki, N. Ikenaga and T. Suzuki, *Appl. Catal., A*, 2000, **192**, 281.
- Y. Sakurai, T. Suzaki, K. Nakagawa, N. Ikenaga, H. Aota and T. Suzuki, *J. Catal.*, 2002, **209**, 16.
- M. S. Park, V. P. Vislovskiy, J. S. Chang, Y. G. Shul, J. S. Yoo and S. E. Park, *Catal. Today*, 2003, **87**, 205.
- J. S. Chang, V. P. Vislovskiy, M. S. Park, D. Y. Hong, J. S. Yoo and S. E. Park, *Green Chem.*, 2003, **5**, 587.
- N. Ikenaga, T. Tsuruda, K. Senma, T. Yamaguchi, Y. Sakurai and T. Suzuki, *Ind. Eng. Chem. Res.*, 2000, **39**, 1228.
- X. N. Ye, W. M. Hua, Y. H. Yue, W. L. Dai, C. X. Miao, Z. K. Xie and Z. Gao, *New J. Chem.*, 2004, **28**, 373.
- X. N. Ye, W. M. Hua, Y. H. Yue, C. X. Miao, Z. K. Xie and Z. Gao, *Chin. J. Catal.*, 2004, **25**, 581.
- J. N. Park, J. Noh, J. S. Chang and S. E. Park, *Catal. Lett.*, 2000, **65**, 75.
- J. Noh, J. S. Chang, J. N. Park, K. Y. Lee and S. E. Park, *Appl. Organomet. Chem.*, 2000, **14**, 815.
- T. Hirano, *Appl. Catal.*, 1986, **28**, 119.
- M. Cherian, R. Gupta, M. S. Rao and G. Deo, *Catal. Lett.*, 2003, **86**, 179.
- A. L. Sun, Z. F. Qin and J. G. Wang, *Appl. Catal., A*, 2002, **234**, 179.
- Y. Ohishi, T. Kawabata, T. Shishido, K. Takaki, Q. H. Zhang, Y. Wang and K. Takehira, *J. Mol. Catal. A: Chem.*, 2005, **230**, 49.
- X. N. Ye, N. Ma, W. M. Hua, Y. H. Yue, C. X. Miao, Z. K. Xie and Z. Gao, *J. Mol. Catal. A: Chem.*, 2004, **217**, 103.
- E. Rocchini, A. Trovarelli, J. Llorca, G. W. Graham, W. H. Weber, M. Maciejewski and A. Baiker, *J. Catal.*, 2000, **194**, 461.
- A. Zecchina, E. Garrone, G. Ghiotti, C. Morterra and E. Borello, *J. Phys. Chem.*, 1975, **79**, 966.
- A. Hakuli, M. E. Harlin, L. B. Backman and A. O. Krause, *J. Catal.*, 1999, **184**, 349.
- S. Rossi, M. Casaletto, G. Ferraris, A. Cimino and G. Minelli, *Appl. Catal., A*, 1998, **167**, 257.
- A. Hakuli, A. Kytokivi, A. O. Krause and T. Suntola, *J. Catal.*, 1996, **161**, 393.

Hyperbranched aliphatic polyethers obtained from environmentally benign monomer: glycerol carbonate

Gabriel Rokicki,* Paweł Rakoczy, Paweł Parzuchowski and Marcin Sobiecki

Received 31st January 2005, Accepted 12th April 2005

First published as an Advance Article on the web 10th May 2005

DOI: 10.1039/b501597a

A hyperbranched aliphatic polyether with hydroxyl end groups was produced from glycerol carbonate (4-hydroxymethyl-1,3-dioxolan-2-one)—the benign monomer obtained from renewable starting materials: glycerol and dimethyl carbonate. Anionic polymerization of glycerol carbonate, which proceeds with simultaneous decarboxylation, was performed using partially deprotonated trimethylolpropane (TMP) as an initiator. Pendant hydroxyl groups facilitate the ring-opening multibranching polymerization leading to a hyperbranched polyether. ^{13}C NMR analysis of the polymerization products confirmed the presence of linear, dendritic, and terminal repeating units. MALDI-TOF mass spectrum analysis confirmed the presence of TMP and glycerol core containing branched structures as well as a relatively small amount of macromolecules with cyclic groups. The polymers were soluble in water, THF, methanol and DMSO.

Introduction

Dendrimers represent a new class of polymeric compounds which are distinguished from traditional linear polymers by their unusual fractal-like architecture.¹ Dendrimers are highly branched entities with repeating units emanating from a central core in a regular three-dimensional structure. The perfect branched dendrimers are usually obtained in a stepwise procedure and represent monodispersed polymers.² Due to their unique characteristic features they appear attractive for applications in the fields of biology and materials sciences as well as for use in homogeneous catalysis.³ However, the synthesis of dendrimers often involves tedious multiple steps of protection/deprotection procedure and complicated purification. For these reasons they are not commonly used.

In contrast to dendrimers, hyperbranched polymers can be prepared according to one synthetic step only.⁴ This type of polymer structure has been known from natural polysaccharides such as dextran, amylopectin.

In a synthetic route leading to hyperbranched polymers AB_n -type monomers are used. Such monomers contain one A functionality and n complementary B groups. The only possible reaction is that between the A and B groups. In the majority of monomers used $n = 2$. The reaction leading to a hyperbranched polymer proceeds according to polycondensation or polymerization modes. In the case of polymerization, mainly monomers containing oxirane or oxetane rings are used. This class of monomers is considered as latent AB_2 -type monomers due to the release of the second B functionality upon reaction with group A.^{5,6}

Two different types of aliphatic hyperbranched polyethers have been obtained from latent AB_2 -type monomers. The polymerization of glycidol, which can be carried out according to anionic^{7,8} or cationic^{1,9–11} mechanisms, leads to

polyglycerol, and cationic polymerization of 3-ethyl-3-(hydroxymethyl)oxetane^{12–14} to polytrimethylolpropane. However, the anionic polymerization of substituted oxetane has been recently reported.¹⁵

Polymers obtained *via* cationic polymerization exhibited relatively low molecular weight and products of both polymerization types have an irregular structure.

Sunder *et al.*^{16–18} developed a convenient reaction pathway to well-defined hyperbranched polyglycerol, based on the anionic polymerization of glycidol under slow monomer addition conditions using partially dehydrogenated 1,1,1-tris(hydroxymethyl)propane as an initiator-starter. Proton exchange equilibrium maintains all hydroxyl groups present in the growing polymer molecule as potentially active propagation centers, thus leading to random branching. Due to this procedure it is possible to incorporate a di-, tri- or polyfunctional unit as a core of branched macromolecules and control their molecular weight by monomer/starter ratio.

However, glycidol is produced according to non-environmentally friendly methods. An industrial method of glycidol production is accomplished by the hydrolysis of an epichlorohydrin epoxy group, followed by the dehydrochlorination of 3-chloropropane-1,2-diol. Another method involves the epoxidation of allyl alcohol. Both methods originate from unrecoverable petrochemical resources. In the first method, besides propylene, toxic chlorine is used in the process of epichlorohydrin production. Epichlorohydrin and alkali metal chlorides generated in the process are the main pollutants of this method. Alkali metal chlorides are also generated in a stoichiometric amount as side products in the process of glycidol production.

As far as the method comprising the epoxidation process is concerned, the hazardous compound H_2O_2 and a toxic tungsten catalyst are usually used.

Moreover, it is well known that glycidol has a big impact on the environment. Glycidol is *reasonably anticipated to be a*

*gabro@ch.pw.edu.pl

human carcinogen based on sufficient evidence of carcinogenicity in experimental animals.^{19,20} Glycidol is soluble in water and in case of leakage can be harmful to fish. The LC₅₀ (14 day) determined for guppy was in the level of 50 mg l⁻¹.

A low molecular oligoglycerol moiety can be produced by heating glycerol at 200 °C under vacuum with potassium hydroxide as a catalyst. Carbon dioxide should be bubbled through the reaction vessel to prevent oxidation.²¹

Very recently we have found that in the synthesis of the hyperbranched polyether, glycerol carbonate (4-hydroxymethyl-1,3-dioxolan-2-one) can be used. This latent cyclic AB₂-type monomer containing a 1,3-dioxolan-2-one ring and hydroxyl group in a single molecule can be easily obtained from glycerol and dimethyl carbonate under mild conditions.

Glycerol carbonate is a stable, colorless liquid that is used as a solvent, additive and chemical intermediate. As a chemical intermediate it reacts readily with alcohols, phenols and carboxylic acids with loss of CO₂ as well as with aliphatic amine with carbon dioxide recovery. Glycerol carbonate can be obtained according to various methods, using epoxy compounds as well as glycerol as raw materials.

It was reported that glycerol carbonate can be formed in the reaction of epichlorohydrin with KHCO₃ carried out at 80 °C in the presence of 18-crown ether.²² Nevertheless, more attractive methods are those utilising glycerol as a renewable and cheap raw material. Taking into consideration that biofuels for diesel engines are being introduced on the market in increasing amounts, a large amount of glycerol will be available as a side-product of the plant oils methanolysis.

A typical method of obtaining carbonate derivatives of glycerol is its transesterification with ethylene carbonate or dialkyl carbonate. In the reaction with ethylene carbonate carried out at 125 °C in the presence of sodium bicarbonate the product was formed in a yield of 81%.²³ Recently, in the patent literature, a glycerol carbonate synthesis was reported in which urea was used in the reaction with glycerol to give the product with a good selectivity (92%).^{24,25}

Very promising methods of glycerol carbonate preparation comprise the reaction of glycerol with CO₂ or carbon monoxide and oxygen in the presence of Cu(I) catalysts.²⁶ The reaction of glycerol with carbon dioxide was carried out in a scCO₂ medium in the presence of zeolite and ethylene carbonate as a co-source of carbonate groups.²⁷ Nevertheless, according to all the above mentioned methods glycerol carbonate should be purified by distillation under reduced pressure at a relatively high temperature (125–150 °C).

In our approach, the glycerol carbonate synthesis was carried out under mild conditions without any solvent, using glycerol and dimethyl carbonate as environmentally benign and renewable reagents. Due to the almost quantitative reaction yield there is no need for product purification by distillation at high temperature and recovery of unreacted glycerol.

In this paper we describe the anionic ring-opening polymerization of the obtained glycerol carbonate, which proceeds with CO₂ liberation leading to a branched polyether. 1,1,1-Tris(hydroxymethyl)propane was used as a trifunctional initiator-starter and central core of the polyether. The

hyperbranched polyglycerol structure was obtained by slow addition of the cyclic carbonate monomer at above 150 °C.

Results and discussion

Glycerol carbonate synthesis

We have developed a convenient method of glycerol carbonate (4-hydroxymethyl-1,3-dioxolan-2-one) (**1**) synthesis from glycerol and dimethyl carbonate under mild conditions. Dimethyl carbonate was used in a molar excess (3 : 1) to shift the reaction equilibrium towards the product. When glycerol, containing less than 2% water, was used for the reaction carried out at 60–70 °C in the presence of K₂CO₃ as a catalyst, the resulting glycerol carbonate was obtained in an almost quantitative yield (Scheme 1). To suppress side product formation, the reaction was carried out for 3 h under reflux, and then methanol and unreacted dimethyl carbonate were distilled off at 40 °C under reduced pressure. In the ¹H NMR spectrum of the product no signals were present in the range 3.0–3.5 ppm, which could be assigned to glycerol protons (Fig. 1).

Under such conditions no reaction of dimethyl carbonate with the third OH group of glycerol was observed. Due to the proximity of the carbonate group in **1**, the reactivity of the third OH group was much lower than that of the first one.

No mixed methyl-glycerol carbonates (**4** and **5**, Scheme 2) were observed in the product. The intramolecular reaction with the second OH group (eqn. (a), Scheme 2) proceeds much faster than the intermolecular one with the next dimethyl carbonate molecule (eqn. (b) or (c), Scheme 2) and thermodynamically stable five-membered cyclic carbonate **1** is formed exclusively.

It was shown that when using dimethyl carbonate in a much larger (10-fold) excess and for a longer reaction time (48 h), diglycerol tricarboxylate (**2**) was formed with relatively low yield (18%) (Scheme 1). To involve the third OH group of glycerol, the reaction with dimethyl carbonate should be carried out at higher temperature (above 90 °C) with progressive methanol removal from the reaction system and using a very large excess of dimethyl carbonate. Crystals of glycerol dicarbonate (4-(methoxycarbonyloxymethyl)-1,3-dioxolan-2-one) (**3**) were obtained with 34% yield. In the ¹H NMR spectrum of **3** there is a signal at 3.7 ppm corresponding to the CH₃ group protons (Fig. 2).

The signal at 5.2 ppm, which was assigned to the OH group proton, disappeared. In the FTIR spectrum two absorption bands corresponding to the carbonyl group of linear (1761 cm⁻¹) and cyclic carbonate (1788 cm⁻¹) were present and no absorption band of the hydroxyl group was observed.

Synthesis of hyperbranched polyglycerol

It was found that glycerol carbonate can be used to obtain a hyperbranched polyether. Similarly to the procedure of Sunder *et al.*,¹⁶ partially deprotonated 1,1,1-tris(hydroxymethyl)propane (TMP) was used as a central core and initiator for anionic polymerization. The deprotonation of TMP was carried out with potassium methanolate. About 10% of the hydroxyl groups were converted into alkoxide ones.

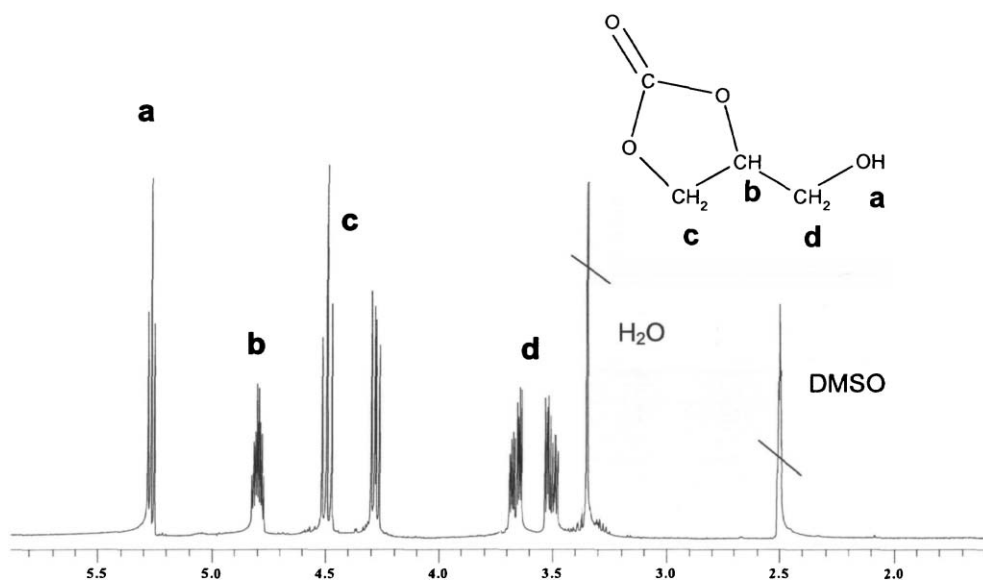
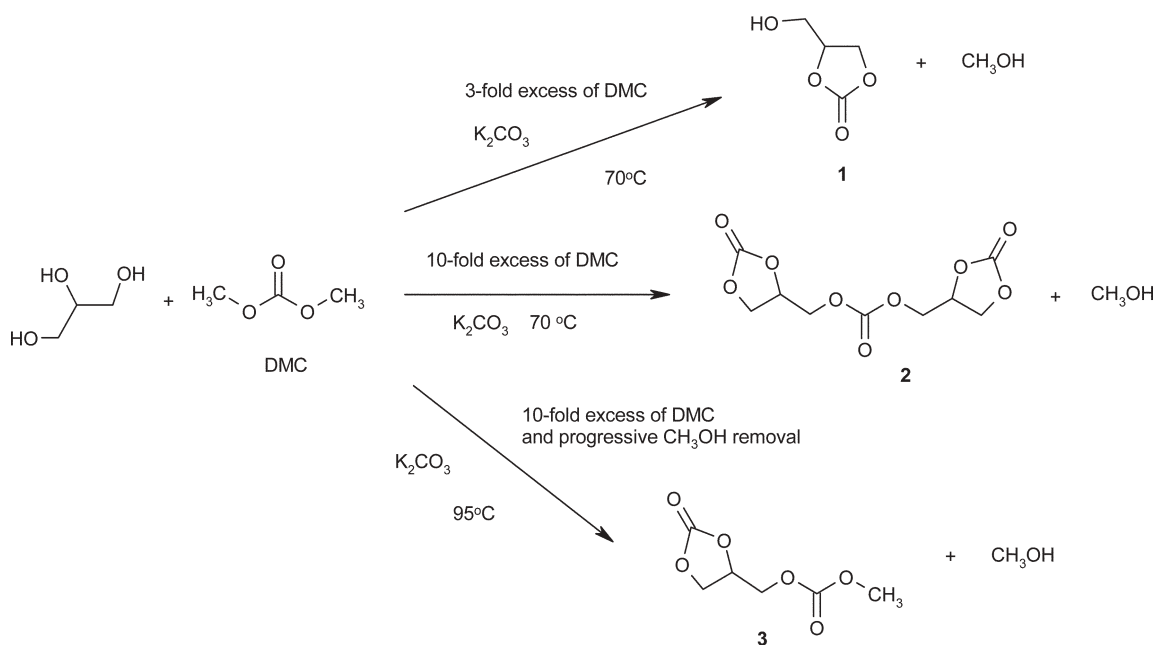


Fig. 1 ^1H NMR (400 MHz, DMSO-d_6) spectrum of glycerol carbonate (4-hydroxymethyl-1,3-dioxolan-2-one).

According to this procedure, the concentration of active sites (alkoxides) and simultaneous intramolecular ion transfer can be controlled. To reduce the possibility of the formation of cyclic polyethers, glycerol carbonate should be added very slowly in a dropwise manner to the anionic initiator. Moreover, slow addition of the cyclic carbonate monomer enables complete decarboxylation of the intermediate products.

It is known^{28,29} that the reaction of alkoxide with five-membered cyclic carbonate can proceed according to two reaction pathways. The alkoxide can attack at the carbonyl carbon atom leading to a linear carbonate or at alkyl carbon atom and an ether linkage is formed (Scheme 3). The central feature of the ring-opening process is that the carbonyl group attack is favored kinetically, over the methylene group attack;

however, the carbonyl group attack is reversible, whereas the methylene group attack is not, due to rapid decarboxylation of the terminal carbonate groups (Scheme 3, eqn. 2).

The product of reaction 1 cannot react with another molecule of glycerol carbonate for thermodynamic reasons³⁰ and no oligocarbonate structures were observed in the product (Scheme 4).

The intramolecular attack of the secondary alkoxide at CH carbon atom in product (I) leads to secondary–secondary ether unit formation (eqn. (a), Scheme 5). The reaction proceeds irreversibly with carbon dioxide liberation. According to this mechanism the terminal units with two primary hydroxyl groups can be formed by proton exchange or acid addition.

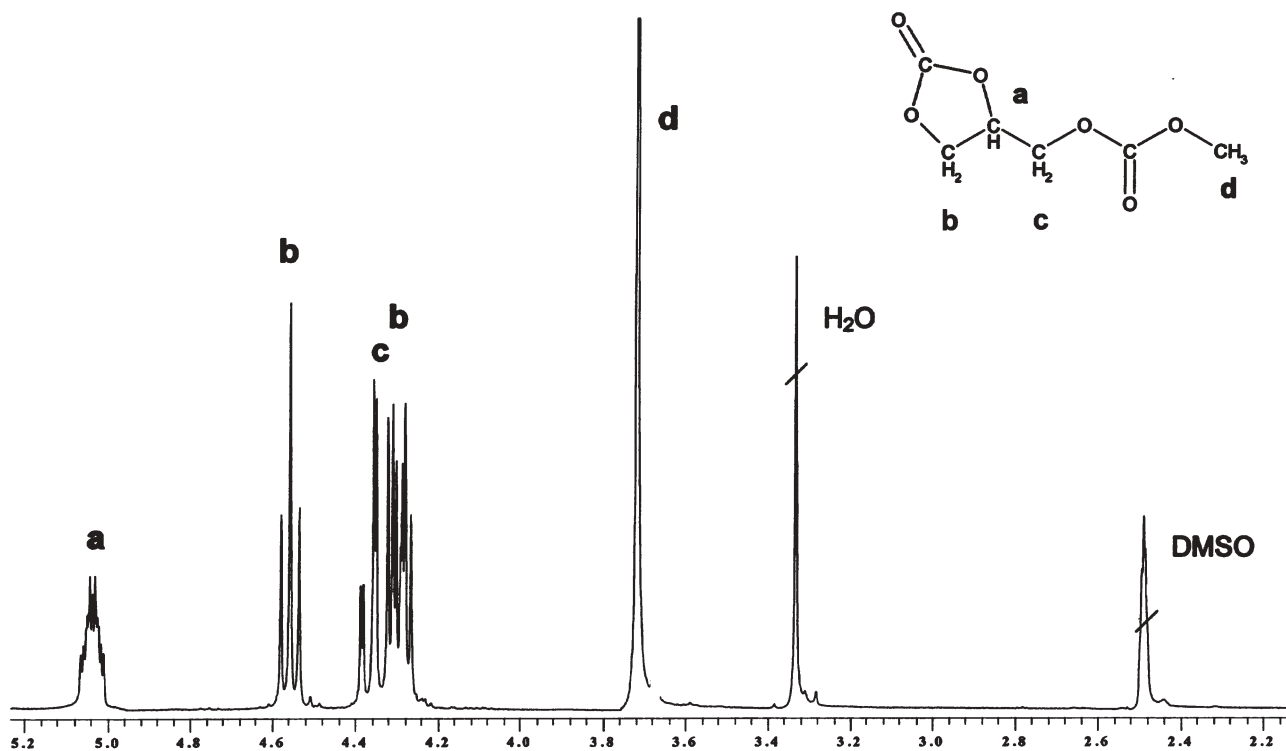
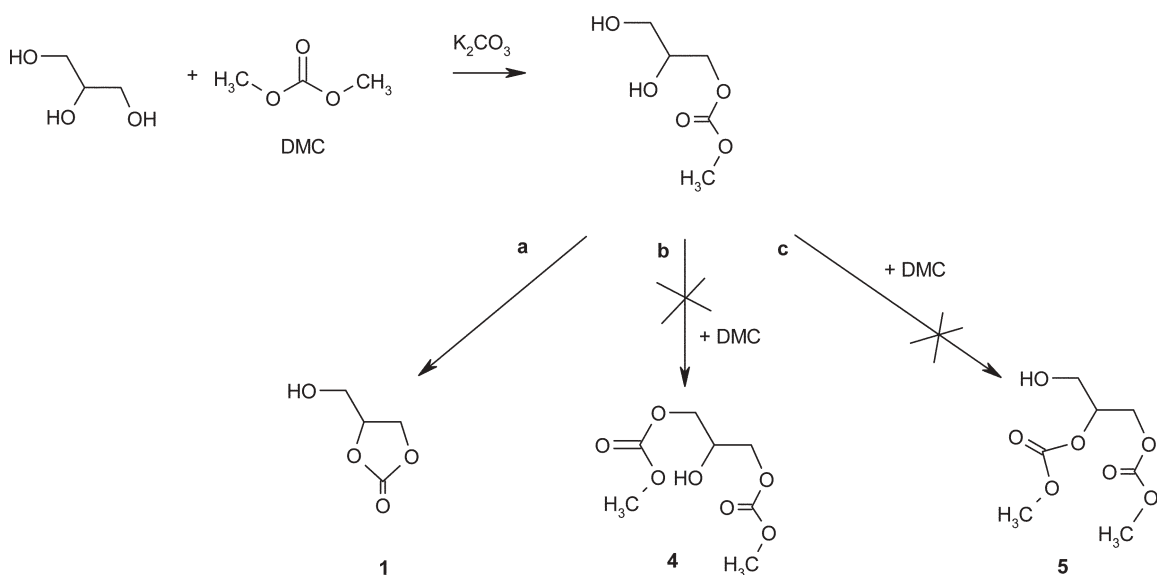


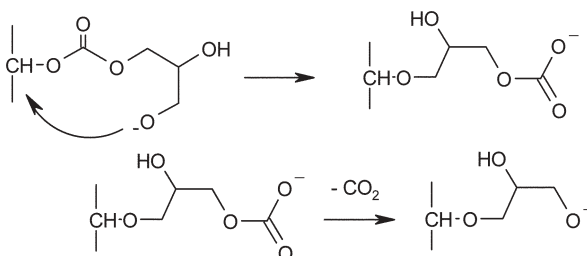
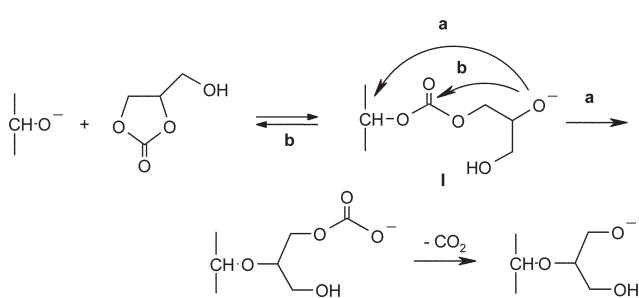
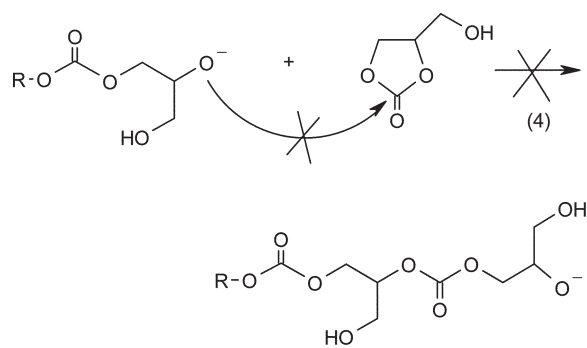
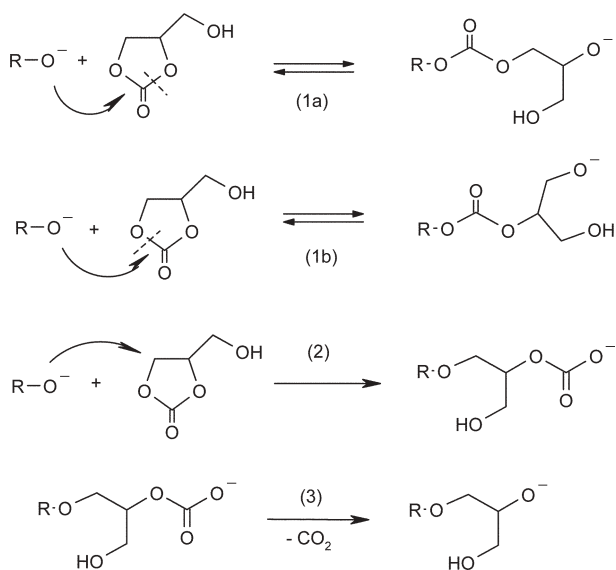
Fig. 2 ^1H NMR (400 MHz, DMSO-d_6) spectrum of glycerol dicarbonate [4-(methoxycarbonyloxymethyl)-1,3-dioxolan-2-one].

It is worth mentioning that these ether units were not observed during the glycidol polymerization reported by Sunder *et al.*¹⁶ In the case of glycidol polymerization, in the propagation step the alkoxide initiator reacts with the epoxide group on its unsubstituted end and thereby generates secondary–primary or primary–primary ether units.

When the primary alkoxide attacks intramolecularly the carbon atom of the CH group, secondary–primary ether units are formed (Scheme 6). These ether units are observed in the product of glycidol polymerization as well as being formed in reaction 2 (Scheme 3).

It should be added that in the intramolecular attack of the secondary alkoxide at the carbonyl carbon atom (eqn. (b), Scheme 5) the glycerol carbonate molecule is restored.

Thus, taking into account that all hydroxyl groups are potentially active in the reaction with glycerol carbonate and the above discussed reactions can proceed, the resulting structure of branched polyether consists of dendritic (D), linear (L) and terminal (T) units. In dendritic units all hydroxyl groups, in linear ones two OH groups, and in terminal ones only one OH group are reacted. Depending on which OH groups are engaged, linear 1,3 or 1,4 units and terminal units



with 1,2-dihydroxyl or 1,3-dihydroxyl groups can be formed (Fig. 3).

The DEPT ^{13}C NMR spectrum of the hyperbranched polyether obtained by polymerization of glycerol carbonate by slow addition of the monomer to the partially deprotonated TMP is presented in Fig. 4.

Only a few representative standards of oligoglycerols are described in the literature.^{31–34} Signal assignments for ^{13}C NMR spectra of polyglycerol were reported by Vandenberg,⁸ Penczek *et al.*,¹⁰ Dworak *et al.*¹¹ and Plusquellec *et al.*³⁴

In the ^{13}C NMR spectrum of the product the signals corresponding to carbon atoms of dendritic as well as linear and terminal units can be observed (Fig. 4).

The signals at 70.4 ppm can be assigned to CH_2 and at 77.0 ppm to CH carbon atoms of dendritic units; at 60.8–61.1 and 69.4 ppm to the CH_2 and 78.2 ppm to the CH carbon atoms of linear 1,3 units; at 72.2 ppm to the CH_2 and 68.8 ppm to CH carbon atoms of linear 1,4 units; at 62.7 and 70.3 ppm to CH_2 and 70.5 ppm to CH carbon atoms of terminal 1,2 units.

Thus, the ^{13}C NMR spectrum of the product obtained from glycerol carbonate is very similar to that obtained from glycidol.¹⁶ However, a new signal appeared, which can be assigned to primary carbon atoms of CH_2 terminal 1,3-dihydroxy units (61.1 ppm). The chemical shifts of the carbon atoms for these structures were established based on the standards of oligoglycerols reported by Plusquellec *et al.*³⁴ and Penczek *et al.*¹⁰ The polyether obtained by cationic polymerization of glycidol contained terminal units with 1,3-dihydroxyl groups.

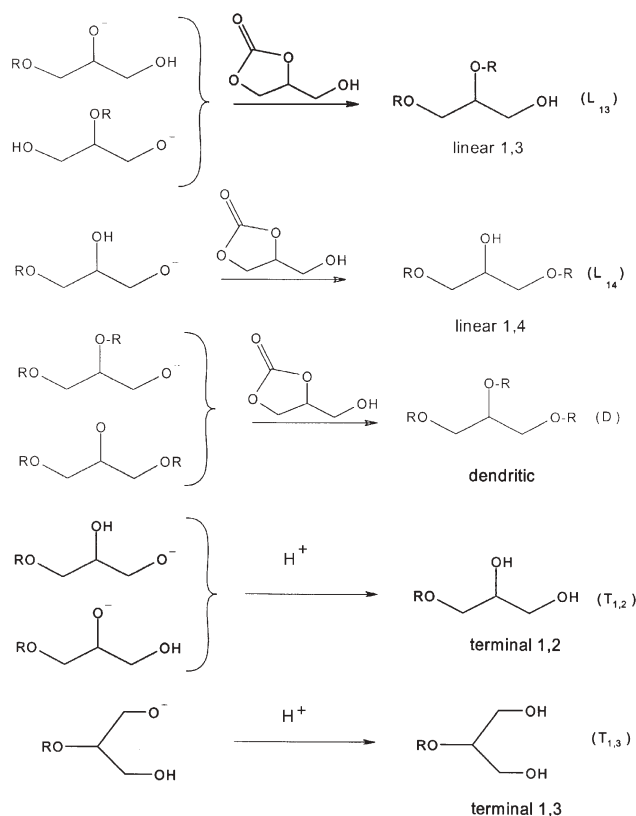


Fig. 3 Formation of different structural units from glycerol carbonate.

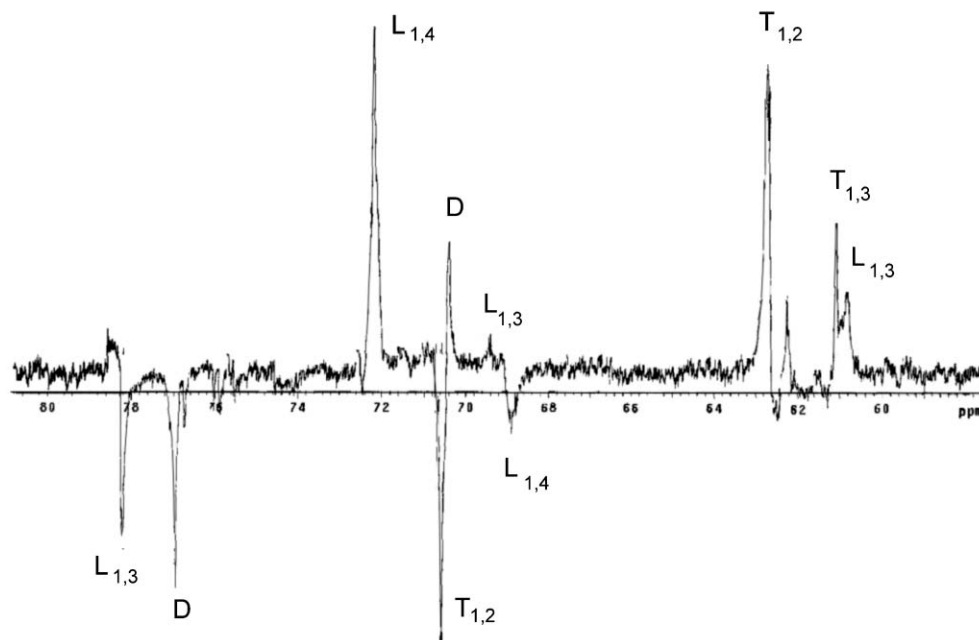


Fig. 4 ^{13}C NMR (400 MHz, D_2O) spectrum of polyglycerol obtained at 170°C from partially deprotonated TMP and glycerol carbonate by slow addition of the monomer.

It should be underlined that the intensity of the signals at 60.9–61.1 ppm corresponding to CH_2OH carbon atoms of linear 1,3 units is higher than that of signals at 78.2 ppm corresponding to CH carbon atoms of these units. In the same region (60–61 ppm), signals corresponding to carbon atoms of terminal 1,3-dihydroxyl units are also present. Thus, the relatively high intensity of these signals confirm the formation of terminal units with 1,3-dihydroxyl groups.

The ^1H NMR spectrum of the polyether obtained from TMP and glycerol carbonate confirms the incorporation of TMP into the polymer structure (Fig. 5). The signals corresponding to the methyl and methylene groups of TMP are present at 0.9 and 1.3 ppm, respectively. The methylene and methine protons of polyether appeared as a broad resonance pattern between 3.3 and 4.0 ppm.

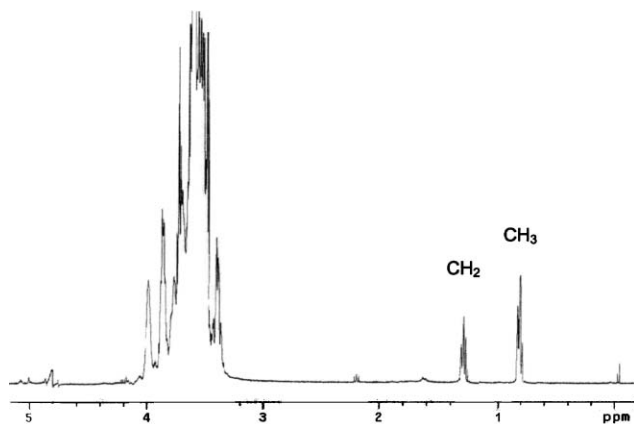


Fig. 5 ^1H NMR (400 MHz, D_2O) spectrum of polyglycerol obtained at 170°C from partially deprotonated TMP and glycerol carbonate by slow addition of the monomer.

To establish whether TMP was incorporated into the polymer macromolecules and the extent of cyclization as well as the molecular weight of polyglycerol, MALDI-TOF mass spectrometry was used.

In Fig. 6 the MALDI-TOF mass spectrum of the polymer obtained from TMP and glycerol carbonate at 170°C with slow addition of the monomer is shown. In the spectrum there are 5 series of signals corresponding to polyether macromolecules. The peaks of each series are characterized by a mass increment of 74 Da. This mass increment equals the mass of the repeating unit in polyglycidol. The most intensive series of signals (a) can be assigned to the potassium cation adduct of macromolecules containing TMP as the core (134.2) and the respective number of glycidol repeating units. A less intensive series of signals (b) corresponds to macromolecules containing glycerol as the core unit (92.1). The average molecular weight of these macromolecules was distinctively smaller than that of macromolecules with the TMP core. These macromolecules were formed due to the presence of traces of glycerol in the monomer. The smaller molecular weight of these macromolecules may be caused by lower reactivity of the secondary OH group of glycerol in the reaction with glycerol carbonate. In accordance with Vanderberg's report,⁸ the lower reactivity is due to higher sterical hindrance and lower stability of the secondary alkoxide.

The third series of peaks (c) corresponds to macromolecules containing a dimer of the TMP core.

At a relatively high reaction temperature (170°C) and under basic conditions, dimerization of TMP can take place similarly to that reported by Wilson *et al.*²¹ for glycerol. The much less intense series of signals (d) corresponds to macromolecules with a cyclic structure resulting from the polymerization initiated by a glycerol carbonate alkoxide (Scheme 7). The last

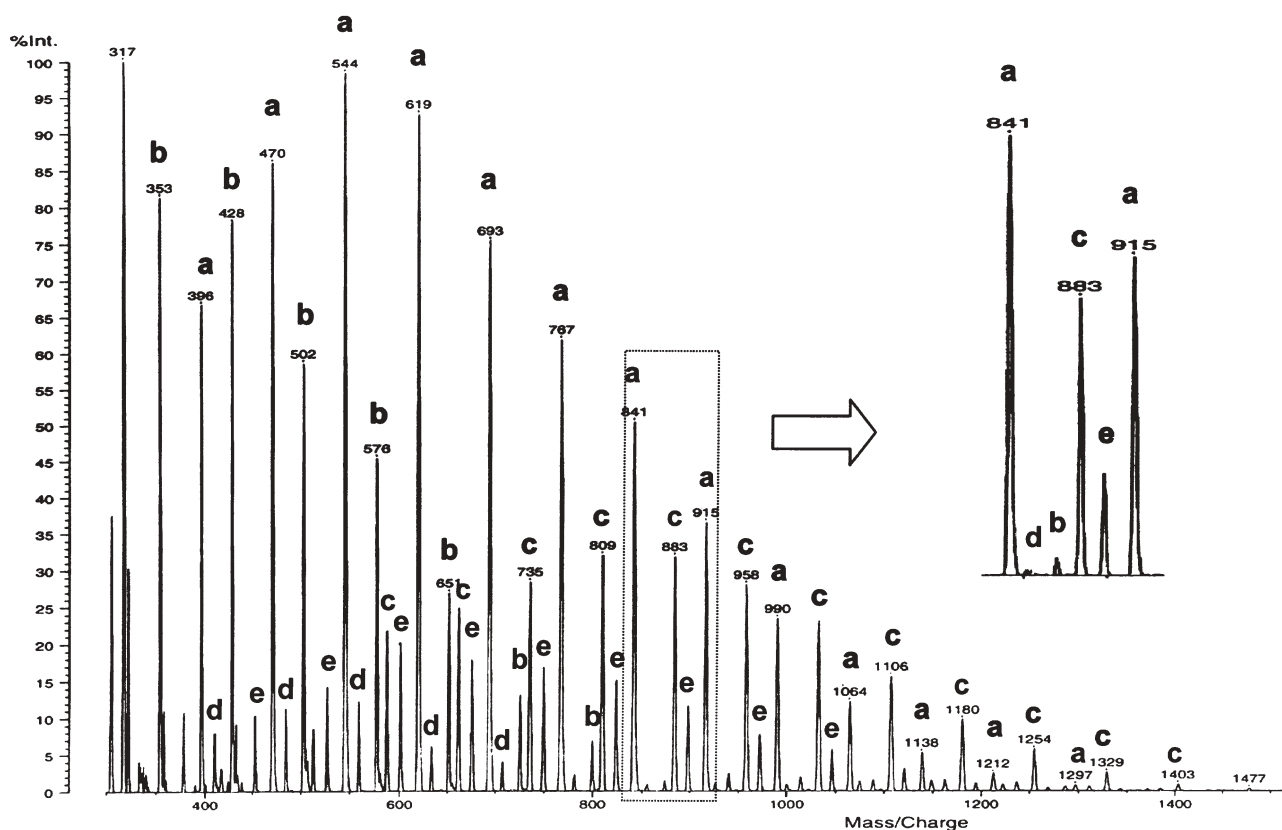


Fig. 6 MALDI-TOF mass spectrum of polyglycerol obtained at 170 °C from partially deprotonated TMP and glycerol carbonate by slow addition of the monomer.

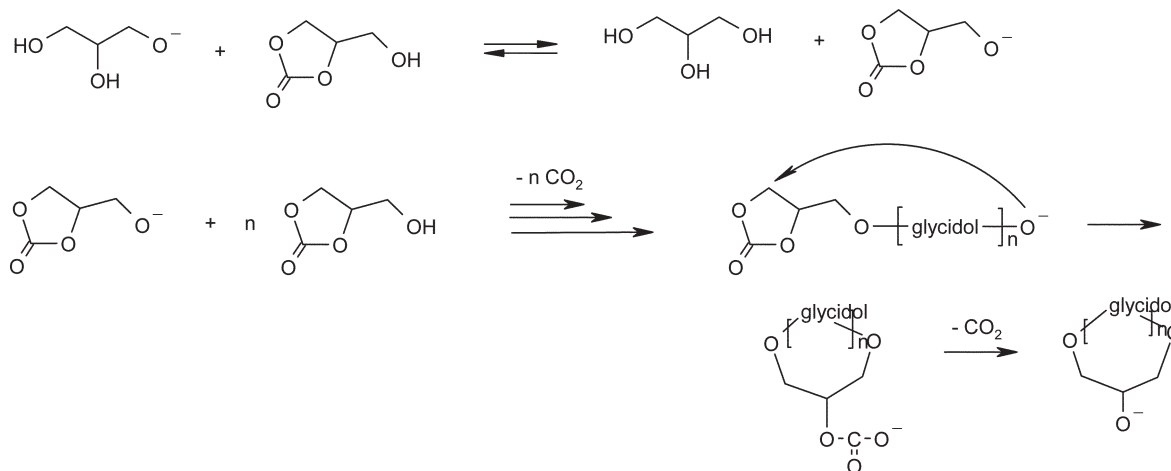
series of signals (e) can be assigned to macromolecules containing the TMP core and cyclic ether group.

In the case of rapid addition of glycerol carbonate at 160 °C to the partially deprotonated glycerol used as the core, a series of peaks of high intensity, which can be assigned to cyclic macromolecules, is observed in the MALDI-TOF mass spectrum of the product (Fig. 7).

The cyclic structures of polyglycerol were formed by an intramolecular ring-opening process when a large molar ratio

of glycerol carbonate to initiator was present in the reaction medium (Scheme 7).

Under such conditions a hydrogen transfer from OH groups of glycerol carbonate, the concentration of which is higher than that of the initiator, proceeds with a higher probability and deprotonated glycerol carbonate can initiate the ring-opening polymerization of glycerol carbonate. When an intramolecular attack at the cyclic carbonate group takes place, macromolecules of a cyclic structure are formed.



Scheme 7

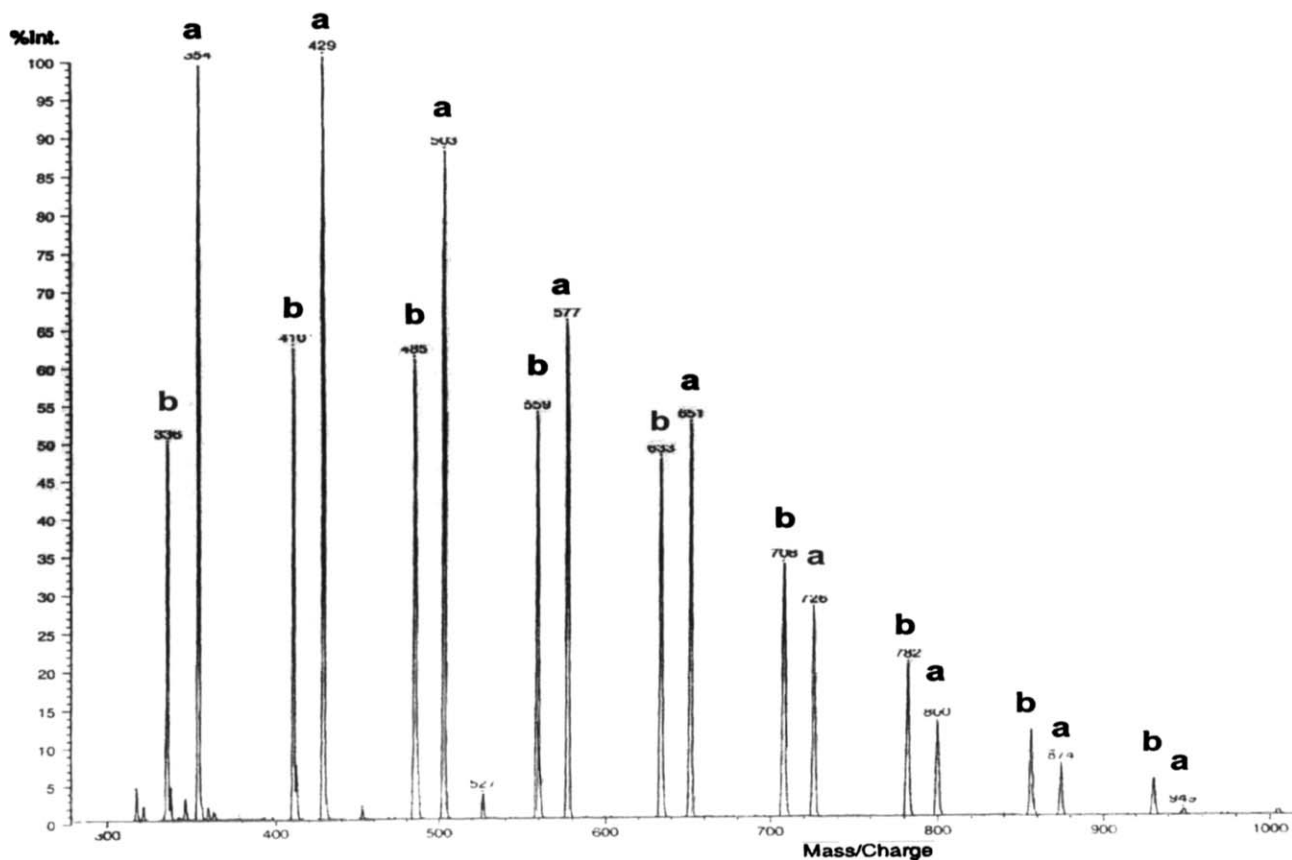


Fig. 7 MALDI-TOF mass spectrum of polyglycerol obtained at 170 °C from partially deprotonated glycerol and glycerol carbonate by rapid addition of the monomer.

When glycerol carbonate was added rapidly, at below 160 °C, linear carbonate units were observed in the product. In the FTIR spectrum of the product the absorption band at 1745 cm^{-1} was present. This absorption band confirmed the reaction pathway comprising an attack at the carbonyl group of 1,3-dioxolane-2-one and intermediate linear carbonate formation (Scheme 3).

The molar weights of the obtained polyglycerols measured by the GPC method were a few times higher than those obtained from MALDI-TOF (Table 1). The explanation of the over-estimated molecular weight cannot be limited to the fact that hyperbranched polyols, due to a high concentration of hydroxyl groups in the molecule outer sphere, exhibit aggregation. In the case of hyperbranched polymers, it is difficult to calibrate the GPC apparatus in order to obtain quantitative results due to their undefined hydrodynamic volume which depends on the

Table 1 Characteristics of the hyperbranched polyglycerols obtained in the anionic polymerization of glycerol carbonate at 170 °C, initiated with partially deprotonated 1,1,1-tris(hydroxymethyl)propane (10%)

Polymer	GC/ TMP	^{13}C NMR DP ^a	MALDI-TOF		Viscosity/ Pa s (50 °C)	DSC, $T_g/^\circ\text{C}$
			M_n	M_w/M_n		
Pgly 1	10/1	9	850	1.2	30.5	-18
Pgly 2	10/1	9	830	1.2	29.1	—
Pgly 3	12/1	11	1020	1.3	50.3	-19

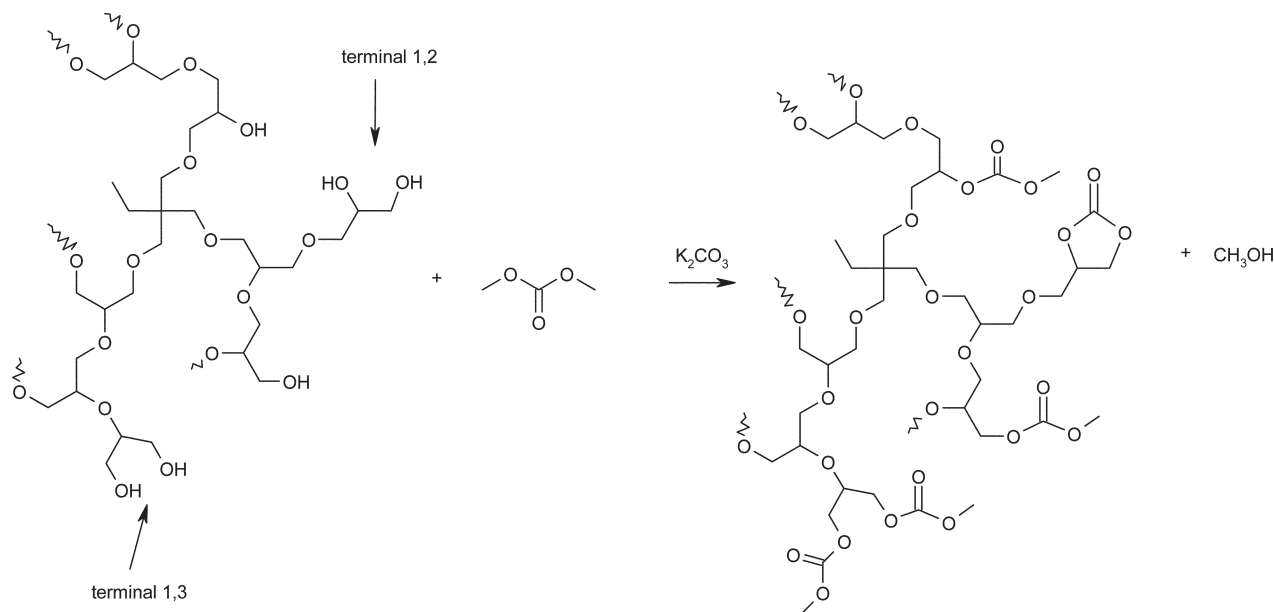
^a calculated from the ^{13}C NMR spectrum according to Frey.³⁷

degree of polymerization, degree of branching, solvent–polymer interactions *etc.* Therefore, GPC measurements can lead to erroneous molecular weight characterization.¹⁶ Similar observations were reported by the Frey's group.^{35,36}

Taking into consideration that the terminal units with vicinal OH groups can be selectively transformed into five-membered cyclic carbonate, as was discussed above for glycerol carbonate synthesis, the obtained polyglycerol (Pgly 1) was treated with an excess of dimethyl carbonate in the presence of K_2CO_3 as a catalyst to transform all OH groups into carbonate ones (Scheme 8). In the FTIR spectrum of the product, two absorption bands of carbonyl groups of the linear carbonate (1745 cm^{-1}) as well as the five-membered cyclic carbonate (1790 cm^{-1}) were present (Fig. 8).

No absorption band in the region 3400–3600 cm^{-1} characteristic of hydroxyl groups was present. Using the calibration curve, the molar ratio of linear carbonate to cyclic carbonate groups was estimated as 83 : 17. In contrast, in the FTIR spectrum of the polyglycerol of the same molecular weight obtained from glycidol, a smaller molar ratio of linear carbonate to cyclic carbonate groups (65 : 35) was observed.

Taking into account that only terminal units with vicinal OH groups can form five-membered cyclic carbonates and that in both ^{13}C NMR spectra the intensity of the signals which can be assigned to linear units are similar, the formation of terminal units with two primary hydroxyl groups is additionally confirmed.



Scheme 8

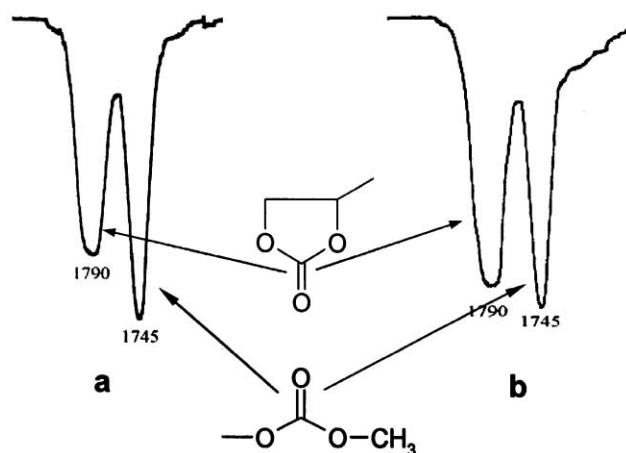


Fig. 8 Fragments of IR spectra of the reaction products of polyglycerol (Pgly 1) (a) and polyglycidol (b) with an excess of dimethyl carbonate.

This method can be used for the determination of the degree of branching of a polyglycerol obtained by polyglycidol polymerization, in which only one type of terminal unit is present.

Conclusions

A hyperbranched aliphatic polyether with hydroxyl end groups can be produced from glycerol carbonate—the benign monomer was obtained from renewable starting materials: glycerol and dimethyl carbonate.

The convenient method of glycerol carbonate synthesis developed leads, under mild conditions, to a product with almost quantitative yield and there is no need for its additional purification by distillation.

The ring-opening polymerization of glycerol carbonate initiated with alkoxide can proceed according to two reaction

pathways in which attack at carbonyl or alkyl carbon atoms of the cyclic carbonate group takes place. In the reaction involving intermediate linear carbonate formation, terminal units with two primary hydroxyl groups can be formed.

The chemical structure of the hyperbranched polyether obtained from glycerol carbonate was very similar to that obtained from glycidol and thus the various derivatization reactions for modification of the end OH groups used for glycidol based polyether can be applied to this polymer.

The high concentration of hydrophilic OH groups, which can be easily transformed into hydrophobic ester groups, enable the use of such hyperbranched polyglycerol in the generation of new amphiphilic materials for biomedical applications such as drug carriers, molecular labels or probe moieties,^{37–39} and hydrogels.⁴⁰

Experimental

Materials

Glycerol (POCh-Gliwice) was pretreated by azeotropic water removal. 1,1,1-Tris(hydroxymethyl)propane, dimethyl carbonate (Aldrich), K_2CO_3 (POCh-Gliwice) were used as received.

Monomer synthesis

Synthesis of glycerol carbonate (1). In a 100 cm³ flask equipped with a magnetic stirrer, condenser and thermometer, glycerol (99%) (40.05 g, 0.435 mol), dimethyl carbonate (117.45 g, 1.305 mol) and K_2CO_3 as a catalyst (1.8 g, 13.05 mmol) were placed. The reaction was carried out under reflux (73–75 °C) for 3 h. The transesterification reaction progress was monitored by collecting samples of the reaction mixture and observing the changes of the signal derived from the cyclic carbonate carbonyl group (1796 cm⁻¹) by means of infrared spectroscopy. Then, methanol and the excess of dimethyl carbonate were distilled off at 40 °C under reduced

pressure (0.5 mmHg). The crude product was filtrated over a cation-exchanging resin (Amberlit IR 120) to remove the catalyst (K_2CO_3). 48.8 g (yield 97%) of colorless liquid glycerol carbonate was obtained.

1H NMR (400 MHz, DMSO- d_6): δ (ppm) = 5.29 (t, 1H, OH, J = 5.6 Hz), 4.81–4.76 (m, 1H, CH), 4.48 (dd, 1H, OCH_2 , J_1 = 8.0 Hz, J_2 = 8.4 Hz), 4.28 (dd, 1H, OCH_2CH , J_1 = 8.0 Hz, J_2 = 6.0 Hz), 3.65 (ddd, 1H, CH_2OH , J_1 = 12.4 Hz, J_2 = 5.6 Hz, J_3 = 2.8 Hz), 3.50 (ddd, 1H, CH_2OH , J_1 = 12.4 Hz, J_2 = 5.6 Hz, J_3 = 3.2 Hz).

FTIR (film): 3401 (s. OH), 2931 (v. CH_2), 1796 (v. $OC(O)O$), 1403 (s. CH_2), 1181 (s. CH), 1054 cm^{-1} (s. OH).

Synthesis of diglycerol tricarbonate (2). In a 50 cm^3 flask equipped with a magnetic stirrer, condenser and thermometer, glycerol (99%) (4.8 g, 0.0425 mol), dimethyl carbonate (38.3 g, 0.424 mol) and K_2CO_3 as a catalyst (0.12 g, 0.85 mmol) were placed. The reaction was carried out at 70 $^\circ C$ for 48 h. Then, methanol and the excess of dimethyl carbonate were distilled off at 40 $^\circ C$ under reduced pressure (0.5 mmHg). The crystalline product was purified by recrystallization from THF. 0.98 g of product 2 (yield 18%) was obtained. Mp 140.5–141.5 $^\circ C$.

1H NMR (400 MHz, DMSO- d_6): δ (ppm) = 5.09–5.02 (m, 2H, CH), 4.56 (dd, 1H, OCH_2CHCH_2O , J_1 = 8.6 Hz, J_2 = 8.7 Hz), 4.40 (dd, 1H, OCH_2CHCH_2O , J_1 = 12.4 Hz, J_2 = 2.8 Hz), 4.34 (dd, 1H, OCH_2CHCH_2O , J_1 = 12.4 Hz, J_2 = 5.6 Hz), 4.29 (dd, 1H, OCH_2CHCH_2O , J_1 = 8.6 Hz, J_2 = 6.2 Hz).

FTIR (KBr): 1790 (v. $C=O$ cyclic), 1760 (v. $OC(O)O$ linear), 1401 (s. CH_2), 1176 cm^{-1} (s. CH).

Synthesis of glycerol dicarbonate (3). In a 150 cm^3 flask equipped with a magnetic stirrer, thermometer, dropping funnel and distillation column, glycerol (99%) (10.5 g, 0.089 mol), dimethyl carbonate (80.1 g, 0.89 mol) and K_2CO_3 as a catalyst (0.37 g, 2.67 mmol) were placed. The reaction was carried out at 95 $^\circ C$ for 10 h with continuously removing methanol from the reaction medium. Then, residual methanol and the excess of dimethyl carbonate were distilled off at 40 $^\circ C$ under reduced pressure (0.5 mmHg). The crystalline product was purified by recrystallization from THF. 5.32 g of product 3 (yield 34%) was obtained. Mp 83.5–85.5 $^\circ C$.

1H NMR (400 MHz, DMSO- d_6): δ (ppm) = 5.08–4.99 (m, 1H, CH), 4.56 (dd, 1H, OCH_2CHCH_2O , J_1 = J_2 = 8.6 Hz), 4.37 (dd, 1H, OCH_2CHCH_2O , J_1 = 12.4 Hz, J_2 = 2.4 Hz), 4.30 (dd, 1H, OCH_2CHCH_2O , J_1 = 12.4 Hz, J_2 = 4.4 Hz), 4.28 (dd, 1H, OCH_2CHCH_2O , J_1 = 8.6 Hz, J_2 = 5.8 Hz), 3.72 (s, 3H, CH_3).

FTIR (KBr): 1788 (s. $C=O$ cyclic), 1761 (s. $C=O$ linear), 1451 (w. OCH_3), 1397 (s. CH_2), 1175 cm^{-1} (s. CH).

Synthesis of hyperbranched polyether

The anionic ring-opening polymerization of glycerol carbonate was carried out in a reactor equipped with a mechanical stirrer and dosing pump under nitrogen atmosphere. Potassium methanolate solution (25%) in methanol was used to partially

deprotonate 1,1,1-tris(hydroxymethyl)propane. An excess of methanol was removed under reduced pressure at 50 $^\circ C$. Glycerol carbonate (molar ratio 12 : 1) was slowly (2 $mL h^{-1}$) added by means of a dosing pump to the reaction system at 170 $^\circ C$ over 12 hours. The reaction was carried out until no absorption band, corresponding to the carbonyl group, was present in the IR spectrum. Then, the product was dissolved in methanol and neutralized by filtration over a cation-exchange resin. The polyether was obtained as a highly viscous liquid (dynamic viscosity at 50 $^\circ C$ 29.1 Pa s).

1H NMR (400 MHz, D_2O): δ (ppm) = 0.9 (t, CH_2CH_3), 1.3 (q, CH_2CH_3), 3.3–4.0 (m polyglycerol protons).

^{13}C NMR (400 MHz, D_2O): δ (ppm) 69.4, 70.3–70.5, 72.2 (CH_2O); 78.2, 77.0 (CHO); 60.8–61.1 (CH_2OH); 68.8, 70.5 (CHOH).

Reaction of dimethyl carbonate with hyperbranched polyether.

In a 100 cm^3 flask equipped with a magnetic stirrer, condenser and thermometer, hyperbranched polyether (6.07 g, 4.87 mmol), dimethyl carbonate (23.86 g, 0.265 mol) and K_2CO_3 as a catalyst (0.31 g, 2.20 mmol) were placed. The reaction was carried out at 80 $^\circ C$ for 3 h. Then, the second portion of dimethyl carbonate (23.86 g, 0.265 mol) was added. The reaction was carried out with simultaneous distillation of methanol. After 3.5 h, when no more methanol was generated, the residual amount of dimethyl carbonate was distilled off under reduced pressure. The product was dissolved in CH_2Cl_2 and the catalyst was filtrated off. 12.1 g of hyperbranched polyether with cyclic and linear carbonate groups was obtained. The viscosity of the polymer was 17.5 Pa s at 50 $^\circ C$.

FTIR (KBr): 1795 cm^{-1} ($C=O$ cyclic carbonate), 1745 cm^{-1} ($C=O$ linear carbonate), 1100 cm^{-1} ($C-O-C$), 1050 cm^{-1} ($C-O$).

Measurements

IR spectra were recorded on a Biorad FTIR spectrometer (KBr pellets or film). 1H NMR and ^{13}C NMR spectra were recorded on a Varian VXR 400 MHz spectrometer. Deuterated solvents were used and tetramethylsilane served as internal standard. MALDI-TOF spectra were recorded on a Kratos Kompact MALDI 4 V5.2.1 apparatus equipped with a 337 nm nitrogen laser with a 3 ns pulse duration. The measurements were carried out in the linear mode of the instrument at an acceleration voltage of +20 kV. For each sample, spectra were averaged over 200 laser shots. The samples were dissolved in isopropanol (5 $mg mL^{-1}$) and mixed with a solution of the MALDI-TOF matrix (2,5-dihydroxybenzoic acid (DHB)), 0.2 M in *iso*-PrOH. The laser power was moderated in the range 120–130 units characteristic of this apparatus in order to avoid distortion of the mass spectrum. Measurements of the molecular weight were performed with a GPC LabAlliance apparatus using water as an eluent at 35 $^\circ C$. Poly(oxyethylene) glycol was used for calibration. Dynamic viscosity of hyperbranched polyglycerol was measured with METTLER RM180 Rheomat at 50 $^\circ C$. DSC thermograms were recorded over the temperature range –150 to 250 $^\circ C$ on a Perkin Elmer Pyris 1 DSC apparatus. The samples were dried at 80 $^\circ C$ for 48 h under vacuum (0.1 Torr) to remove moisture

prior to recording the thermograms. The experiments were carried out at a heating rate of $20\text{ }^{\circ}\text{C min}^{-1}$ under a nitrogen purge of 20 mL min^{-1} . Sample weights were 15–25 mg.

Acknowledgements

This paper is based upon work supported by the Polish State Committee for Scientific Research (PBZ-KBN-070/T09/2001/8; 2003-2006).

Gabriel Rokicki,* Paweł Rakoczy, Paweł Parzuchowski and Marcin Sobiecki

Warsaw University of Technology, Faculty of Chemistry, Noakowskiego 3, Warsaw, Poland. E-mail: gabro@ch.pw.edu.pl; Fax: +48 22 6282741; Tel: +48 22 6607562

References

- G. R. Newkome, C. N. Moorefield and F. Vögtle, *Dendritic Macromolecules: Concepts, Syntheses, Perspectives*, VCH, Weinheim, 1996.
- D. A. Tomalia and J.-M. J. Fréchet, *J. Polym. Sci., Part A: Polym. Chem.*, 2002, **40**, 2719.
- P. Kolhe, E. Misra, R. M. Kannan, S. Kannan and M. Lieh-Lai, *Int. J. Pharm.*, 2003, **259**, 143.
- B. Voit, *J. Polym. Sci., Part A: Polym. Chem.*, 2000, **38**, 2505.
- A. Sunder, J. Heinemann and H. Frey, *Chem. Eur. J.*, 2000, **6**, 2499.
- K. Inoue, *Prog. Polym. Sci.*, 2000, **25**, 453.
- S. R. Sandler and F. R. Berg, *J. Polym. Sci., Polym. Chem. Ed.*, 1966, **4**, 1253.
- E. J. Vanderberg, *J. Polym. Sci., Polym. Chem. Ed.*, 1985, **23**, 915.
- E. J. Goethals, H. C. De Clercq and P. J. Hartmann, *Makromol. Chem. Macromol. Symp.*, 1991, **47**, 151.
- R. Tokar, P. Kubisa, S. Penczek and A. Dworak, *Macromolecules*, 1994, **27**, 320.
- A. Dworak, W. Wałach and B. Trzebicka, *Macromol. Chem. Phys.*, 1995, **196**, 1963.
- M. Bednarek, T. Biedron, J. Helinski, K. Kaluzynski, P. Kubisa and S. Penczek, *Macromol. Rapid Commun.*, 1999, **20**, 369.
- H. Magnusson, E. Malmstrom and A. Hult, *Macromol. Rapid Commun.*, 1999, **20**, 453.
- Y. Mai, Y. Zhou, D. Yan and H. Lu, *Macromolecules*, 2003, **36**, 9667.
- T. J. Smith and L. J. Mathias, *Polymer*, 2002, **43**, 7275.
- A. Sunder, R. Hanselmann, H. Frey and R. Mülhaupt, *Macromolecules*, 1999, **32**, 4240.
- A. Sunder, R. Mülhaupt, R. Haag and H. Frey, *Adv. Mater.*, 2000, **12**, 235.
- R. Haag, A. Sunder and J.-F. Stumbe, *J. Am. Chem. Soc.*, 2000, **122**, 2954.
- International Agency for Research on Cancer (IARC) Monographs on the Evaluation of Carcinogenic Risks to Humans; Some Industrial Chemicals, 2000, **77**, IARC, Lyon, France, <http://www-cie.iarc.fr/htdocs/monographs/vol77/77-14.html>.
- National Toxicology Program (NTP) Technical Report Series No. 374, 1990, Research Triangle Park, USA, <http://ntp.niehs.nih.gov/index.cfm?objectid=0708ED20-F329-7A3E-A4EF3BEDD5736C29>.
- R. Wilson, B. J. Van Schie and D. Howes, *Food Chem. Toxicol.*, 1998, **36**, 711.
- G. Rokicki and W. Kuran, *Bull. Chem. Soc. Jpn.*, 1984, **57**, 1662.
- J. B. Bell, V. A. Currier and J. D. Malkemus, *US Pat.* 2 915 529, 1959.
- M. Okutsu and T. Kitsuki, *US Pat.* 6 495 703, 2002.
- S. Claude, Z. Mouloungui, J.-W. Yoo and A. Gaset, *US Pat.* 6 025 504, 2000.
- J. H. Teles, N. Rieber and W. Harder, *US Pat.* 5 359 094, 1994.
- C. Vieville, J. W. Yoo, S. Pelet and Z. Mouloungui, *Catal. Lett.*, 1998, **56**, 245.
- G. Rokicki and T. Kowalczyk, *Polymer*, 2000, **41**, 9013.
- P. Pawłowski and G. Rokicki, *Polymer*, 2004, **45**, 3125.
- L. Vogdanis, B. Martens, H. Uchtmann, F. Henzel and W. Heitz, *Makromol. Chem.*, 1990, **191**, 465.
- H. J. Wright and R. N. Du Puis, *J. Am. Chem. Soc.*, 1946, **68**, 446.
- H. Wittcoff, J. R. Roach and S. E. Miller, *J. Am. Chem. Soc.*, 1947, **69**, 2655.
- H. Wittcoff, J. R. Roach and S. E. Miller, *J. Am. Chem. Soc.*, 1949, **71**, 2666.
- S. Cassel, C. Debaig, T. Benvegnu, P. Chaimbault, M. Lafosse, D. Plusquellec and P. Rollin, *Eur. J. Org. Chem.*, 2001, 875.
- A. Burgath, R. Hanselmann, D. Hölter and H. Frey, *Proc. Am. Chem. Soc. Div. Polym. Mater. Sci. Eng.*, 1994, **77**, 166.
- A. Sunder, H. Türk, R. Haag and H. Frey, *Macromolecules*, 2000, **33**, 7682.
- H. Frey and R. Haag, *Rev. Mol. Biotechnol.*, 2002, **90**, 257.
- A. Sunder, M. Kraemer, R. Hanselmann, R. Mülhaupt and H. Frey, *Angew. Chem., Int. Ed.*, 1999, **38**, 3552.
- R. Haag, A. Sunder, A. Hebel and S. Roller, *J. Comb. Chem.*, 2002, **4**, 112.
- R. Knischka, P. J. Lutz, A. Sunder, R. Mülhaupt and H. Frey, *Macromolecules*, 2000, **33**, 315.

Biological properties of arginine-based glycerolipidic cationic surfactants

Noemí Pérez,* Lourdes Pérez, M. Rosa Infante and M. Teresa García*

Received 23rd December 2004, Accepted 15th April 2005

First published as an Advance Article on the web 12th May 2005

DOI: 10.1039/b419204d

Amino acid-based surfactants have attracted much interest as environmentally friendly surfactants because of their biodegradability, low aquatic toxicity, and low haemolytic activity. Our group has recently developed a new family of arginine-based glycerolipidic surfactants: 1-acyl-3-*O*-(*L*-arginyl)-*rac*-glycerol·2HCl (XOR) and 1,2-diacyl-3-*O*-(*L*-arginyl)-*rac*-glycerol·2HCl (XXR) with alkyl chain lengths in the range of C₈–C₁₄. In this paper we study the biodegradability and aquatic toxicity of these recently developed arginine-based glycerolipidic cationic surfactants and compare these to conventional cationic surfactants.

Introduction

Surfactants are employed in large quantities every day on a worldwide scale. Since it is well known that surface-active compounds can adversely affect the aquatic environment, the biodegradability and biocompatibility of surfactants have become almost as important as their functional performance to the consumer.¹ In this regard, amino acid-based surfactants have attracted much interest as environmentally friendly surfactants because of their biodegradability, low aquatic toxicity, and low haemolytic activity.^{2,3} Their amphiphilic structures consist of one polar amino acid head group joined to a hydrophobic alkyl chain *via* a biodegradable acyl, amide, or ester linkage.^{4,5} Furthermore, they are prepared from renewable sources of raw materials.^{6–8} Preparation of surfactant molecules which mimic the structure of natural compounds such as lipoaminoacids,⁹ phospholipids¹⁰ and glycerolipids,¹¹ is becoming increasingly important because of their unique physicochemical and biological properties.

Our group has recently developed a new family of arginine-based glycerolipidic surfactants: 1-acyl-3-*O*-(*L*-arginyl)-*rac*-glycerol·2HCl (XOR) and 1,2-diacyl-3-*O*-(*L*-arginyl)-*rac*-glycerol·2HCl (XXR) (Fig. 1) with alkyl chain lengths in the range of C₈–C₁₄.^{12,13} Like the mono and diacylglycerides, these compounds have a glycerol backbone linked to one or two alkyl chains by ester bonds. Nevertheless, these surfactants possess cationic character due to the presence of the arginine in the polar head, which introduces antimicrobial activity in the molecule.^{13–15} In this paper we study the biodegradability and aquatic toxicity of these new arginine-based glycerolipidic cationic surfactants and compare them to conventional cationic surfactants and other arginine-based and glycerolipidic-based surfactants.

Results and discussion

Two types of arginine-based glycerolipidic surfactants were initially prepared. The 1-acyl-3-*O*-(*L*-arginyl)-*rac*-glycerol·2HCl (XOR) and 1,2-diacyl-3-*O*-(*L*-arginyl)-*rac*-glycerol·2HCl (XXR)

series (Fig. 1) with alkyl chains in the range of C₈–C₁₄ were prepared using the synthetic approach previously described.^{12,13}

The biological behaviour of the XOR and XXR surfactants is compared with that of conventional cationic surfactants and other surfactants with arginine or glycerolipidic-like structure. Conventional quaternary ammonium compounds and the non-ionic monoglyceride 1000 (Fig. 1), were commercially available. The arginine-based single chain surfactants (CAM and LAM) (Fig. 1) and the glycerolipidic arginine-based surfactant with one positive charge in the polar head (1-dodecyl-3-*O*-acetylarginyl-glycerol monochlorhydrate, 120RAc) (Fig. 1) were previously prepared by our group as reported in literature.^{3,12,16}

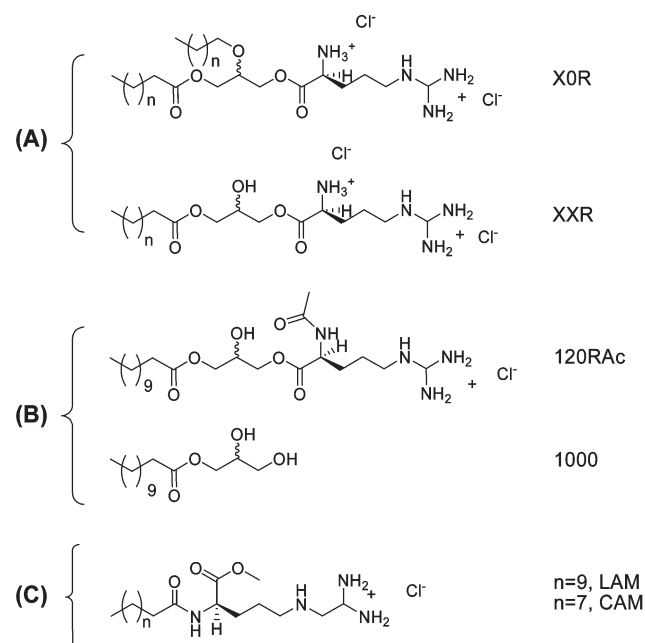


Fig. 1 Molecular structure of: (A) 1-acyl-3-*O*-(*L*-arginyl)-*rac*-glycerol·2HCl (XOR) and 1,2-diacyl-3-*O*-(*L*-arginyl)-*rac*-glycerol·2HCl (XXR); (B) 1-dodecyl-3-*O*-acetylarginyl-glycerol monochlorhydrate (120RAc) and 1-acyl-*rac*-glycerol (1000) and (C) *N*-acyl-L-arginine methyl esters (LAM and CAM).

*nplste@cid.csic.es (Noemí Pérez)
mtgbet@iiqab.csic.es (M. Teresa García)

Table 1 Aquatic toxicity values of X0R and XXR series on *Daphnia magna* and *Photobacterium phosphoreum* and critical micellar concentration (CMC) values of these surfactants in the aqueous media of the toxicity bioassays

Compound	<i>Daphnia magna</i> IC ₅₀ ^a /μM		<i>P. phosphoreum</i> EC ₅₀ ^b /μM		CMC ^c /mM	
	Mean	95% CI	Mean	95% CI	A	B
100R	200	(170–220)	10	(8–12)	0.25	0.40
120R	50	(40–60)	2	(1–3)	0.10	0.10
140R	30	(20–40)	2	(1–5)	0.03	0.02
88R	— ^d	—	2	(1–9)	— ^d	— ^d
1010R	30	(20–40)	5	(3–7)	— ^e	— ^e
1212R	40	(30–50)	— ^e	—	— ^e	— ^e
1414R	60	(50–80)	— ^e	—	— ^e	— ^e

^a Concentration values that cause 50% inhibition in the crustacean mobility after 24 h of exposure. ^b Concentration values that cause 50% reduction in the light emitted by the bacteria after 30 min of exposure. ^c CMC values obtained by fluorescence measurements in the *Daphnia magna* (A) and *Photobacterium phosphoreum* (B) test media. ^d Problems of solubility in the test medium. ^e Not enough available amount of surfactant.

Aquatic toxicity

Acute toxicity tests on freshwater crustaceans (*Daphnia magna*)¹⁷ as well as on saltwater bacteria (*Photobacterium phosphoreum*)¹⁸ were carried out to assess the aquatic toxicity of the new cationic surfactants. The result of both the *Daphnia magna* 24 h immobilisation test (IC₅₀) and *Photobacterium phosphoreum* 30 min luminiscent reduction test (EC₅₀) for the monoacyl and diacylglycerol arginine-based surfactants (X0R and XXR, respectively) are summarised in Table 1.

The data indicated that the bacteria population is more sensitive to toxic effects of these arginine-based cationic surfactants than *Daphnia*, since the concentration of the cationic surfactants able to reduce to 50% the light emitted by the bacteria is one order of magnitude less than the concentration required to immobilise 50% of the crustacean population.

To evaluate the relative toxicity of the arginine-based cationic surfactants investigated, the data obtained were compared with those corresponding to some conventional quaternary ammonium compounds and those corresponding both to other arginine-based surfactants (*N*^ω-acyl-arginine-methyl esters: CAM and LAM and acyl-acetylglyceryl-glycerol: 120Rac) and to surfactants with glycerolipidic-like structures (acyl-glycerols: X00). Tables 2 and 3 summarize toxicity data for the chosen set of surfactants.

Against *Daphnia magna*, arginine-based mono (X0R) and diglycerides (XXR) are much less toxic than the conventional

Table 2 Acute toxicity of quaternary ammonium surfactants on *Daphnia magna* and *Photobacterium phosphoreum*

Compound ^a	<i>D. magna</i> IC ₅₀ /μM	<i>P. phosphoreum</i> EC ₅₀ /μM
DT	1.23	0.78
TT	0.42	0.83
HT	0.36	1.73
BDD	0.34	0.47
BDT	0.35	0.41
BDH	0.56	1.39

^a DT, dodecyl trimethyl ammonium bromide; TT, tetradecyl trimethyl ammonium bromide; HT, hexadecyl trimethyl ammonium bromide; BDD dodecyl benzyl dimethyl ammonium bromide; BDT tetradecyl benzyl dimethyl ammonium chloride; BDH hexadecyl benzyl dimethyl ammonium chloride. Data reported by Garcia *et al.*¹⁹

Table 3 Acute toxicity of some arginine-based cationic surfactants and non-ionic glycerolipidic surfactants on *D. magna* and *P. phosphoreum*

Compound ^a	<i>D. magna</i> IC ₅₀ /μM	<i>P. phosphoreum</i> EC ₅₀ /μM
CAM	203 ^b	11 ^b
LAM	37 ^b	30 ^b
120Rac	60 ± 10	8 ± 2
1000	170 ± 20	29 ± 6
1200	—	8 ± 2

^a CAM, *N*^ω-caproyl-L-arginine methyl ester; LAM, *N*^ω-lauroyl-L-arginine methyl ester; 120Rac, 1-dodecyl-3-*O*-acetylglyceryl-glycerol monochlorhydrate; 1000, 1-acyl-*rac*-glycerol; 1200, 1-acyl-*rac*-glycerol. ^b Data reported by Perez *et al.*²⁰

quaternary ammonium-based surfactants (differences in IC₅₀ values about two orders of magnitude). Likewise, for *Photobacterium phosphoreum*, X0R and XXR arginine-based surfactants are clearly less toxic than quaternary ammonium compounds although the differences in the effective concentrations are not so striking as for the microcrustacea population.

It is interesting to compare the aquatic toxicity of these new arginine-based mono (X0R) and diglyceride (XXR) compounds with other structurally related surfactants such as *N*^ω-acyl-arginine-methyl esters (LAM and CAM), 1-acyl-3-*O*-acetylglyceryl-glycerols (120Rac) and acyl-glycerols (X00) (Tables 1 and 3). For the overall surfactants, the estimated concentration able to immobilise 50% of the crustacean population after a 24 hour exposure (IC₅₀) ranged from 30 up to 200 μmol L⁻¹ whereas the effective concentration required to reduce by 50% the light produced by the bacteria after a 30 min exposure (EC₅₀) ranged from 2 up to 10 μmol L⁻¹. These data indicate that bacteria are more sensitive than the microcrustacea population to the toxic effects of these surfactants and that, with the exception of the shorter homologues of each series, the potency of their biological activity is very similar.

In the *Daphnia magna* test, the shorter alkyl chain length homologue of both single chain arginine-based surfactants and monoglyceride surfactants (100R, CAM and 1000, respectively) proved to be clearly less toxic than their corresponding more hydrophobic homologues, as demonstrated by their effective concentrations being about 5 times higher than those corresponding to the longer alkyl chain length homologues.

Bearing in mind that biological membranes are essentially nonpolar interfaces, evidence exists that the toxicity of chemicals against the water-living species tested is caused by the ability of the molecules to disrupt the integral membrane by a hydrophobic/ionic adsorption phenomenon at the cell membrane–water interface.^{21,22} The more hydrophobic the molecule, the higher its ability to accumulate at the interfaces, exerting a toxic effect. Therefore, higher toxicity would be expected with increasing hydrophobicity in the molecule, as reported for anionic surfactants on *Daphnia magna*²³ and for alcohol ethoxylated surfactants on *Photobacterium phosphoreum*.²⁴ Accordingly, acute toxicity clearly grows with increasing alkyl chain length from C₁₀ to C₁₂ homologues for the single alkyl chain surfactants. Likewise, the introduction of a second alkyl chain in the surfactant molecule (from 100R to 1010R) increases the acute toxicity. However, an incremental difference in toxicity with increasing alkyl chain length or with introducing a second alkyl chain was not observed for the longer alkyl chain homologues. This could be attributed to the lower bioavailability of the longer alkyl chain homologues due to their poor solubility in the test medium. This assumption is enhanced by the results on antimicrobial activity, which shows that the less soluble compound, 1414R, exhibits the lower activity against the microorganisms tested.¹³

CMC values are consistent with the above comments on solubility and bio-availability of these surfactants. The results obtained show that the CMC depends on the alkyl chain length. The CMC values decreased as the number of methylene groups in the alkyl chain was raised, *i.e.*, the more hydrophobic the molecule, the lower the CMC value.

Biodegradability assessment

The biodegradability of the arginine-based glycerolipidic cationic surfactants prepared in this study was evaluated by applying two ready biodegradation tests, the Modified Screening Test²⁵ and the Closed Bottle Test.²⁶ In these tests, ultimate biodegradation or mineralisation of the surfactants, that is, the microbial transformation of the parent chemical into inorganic final products of the degradation process, such as carbon dioxide, water, and assimilated biomass, was determined.

In the Modified Screening Test, a determined amount of the cationic surfactant tested was dissolved in an inorganic medium, inoculated with a small number of microorganisms from a mixed population and aerated at 23 ± 1 °C in the dark. The biodegradation process was monitored through DOC measurements, as recommended by the standard procedure.²⁵ However, due to the possible adsorption of the cationic surfactants onto the filters used for DOC determination, TOC measurements were also carried out. Reaction vessels of all series were withdrawn in triplicate. The procedure was checked by means of a readily biodegradable surfactant, sodium *n*-dodecyl sulfate (SDS). Controls with inoculation, but without either test material or standard were run in parallel for the determination of DOC blanks. In the course of the biodegradation tests, the DOC concentrations were determined at the beginning and at regular time intervals during a 28 day period. Biodegradation was stated as the percentage of DOC or TOC removal within 28 days.

DOC removal values higher than 70% were obtained for X0R compounds from the first week of the test period and the biodegradation extent after a 28 day period of X0R surfactants ranged from 71 to 99% (Table 4). These results provide evidence for an excellent and very rapid ultimate biodegradation of X0R surfactants in this relatively stringent biodegradation test. Biodegradation of X0R compounds clearly exceeds the specified biodegradation pass level in the Modified Screening Test (70% DOC removal), allowing them to be classified as readily biodegradable compounds, *i.e.*, X0R surfactants would degrade readily and rapidly when discharged to the aerobic aquatic environment. The excellent biodegradation of X0R cationic surfactants is consistent with that expected regarding their molecular structure. Thus, the primary event in the degradation process is probably the hydrolytic cleavage of the ester bonds giving rise to the formation of compounds such as arginine, fatty acids, glycerol or acylglycerolipids, that are readily biodegradable.

In agreement with data available on biodegradability of quaternary ammonium-based surfactants,^{19,27} the biodegradation of X0R compounds decreased with increasing alkyl chain length. This fact could be due to the higher inhibitory effects of the more hydrophobic homologues on bacterial population. On the other hand, the biodegradation extent of the single-chain compounds X0R (Table 4) is higher than that reported for quaternary ammonium-based surfactants²⁸ and similar to the biodegradation extent reported for other arginine-based cationic surfactants.²⁰

For XXR surfactants, comparison of TOC and DOC values demonstrated a significant adsorption of these cationic surfactants on the filters used for DOC determination and led to the rejection of this method for the evaluation of their biodegradability. Thus, to assess the ultimate biodegradability of the XXR surfactants another ready biodegradability test, the Closed Bottle Test (OECD 301D),²⁶ was applied. In this method, the surfactant tested was added to an aerobic aqueous medium inoculated with wastewater microorganisms and the depletion of dissolved molecular oxygen was measured for a defined period of time and reported as a percentage of the theoretical maximum. Duplicate bottles of each series were analysed at the start of the test for dissolved oxygen and the remaining bottles were incubated at 20 °C ± 1 °C in the dark. Bottles of all series were withdrawn in duplicate for dissolved

Table 4 Ultimate biodegradation of X0R and XXR surfactant series, 1000 and 120RAc surfactants

	% Biodegradation Modified Screening Test ^a		% Biodegradation Closed Bottle Test ^b O ₂ consumption
	TOC	DOC	
100R	99	99	—
120R	86	71	—
140R	76	76	—
1010R	—	—	20
1212R	—	—	82
1414R	—	—	61
1000	—	—	71
120RAc	—	—	98

^a % of total and dissolved organic carbon (TOC and DOC) removal. ^b Dissolved oxygen depletion.

oxygen analysis over the 28 day incubation period. A control with inoculum, but without test chemicals was run in parallel for the determination of oxygen blanks. Sodium *n*-dodecyl sulfate (SDS) was used as reference substance. Compounds which reached a biodegradation level higher than 60% are referred to as “readily biodegradable”.

The biodegradation extent obtained for the diglycerolipidic cationic surfactants (1212R, 1414R), the monoglycerolipidic arginine-based cationic surfactant (120RAC) and the non-ionic monoglyceride surfactant (1000) after a 28 day period surpassed 60% (82, 61, 71 and 98%, respectively) while 1010R underwent only a modest amount of biodegradation (20%). The excellent biodegradation of all these surfactants, with the exception of 1010R, allows them to be regarded as readily biodegradable compounds which is consistent with the presence in the molecules of ester bonds susceptible to chemical or enzymatic hydrolysis that leads to the formation of easily biodegradable metabolites such as arginine, glycerol, acyl glycerol, *etc.* The poor degradation of 1010R could be attributed to its inhibitory effects on the bacterial population since, as reported elsewhere,²⁰ this homologue possesses the highest antimicrobial activity of the XXR surfactant series.

Conclusions

A series of the arginine-based glycerolipidic surfactants: 1-acyl-3-*O*-(L-arginyl)-*rac*-glycerol·2HCl (X0R) and 1,2-diacyl-3-*O*-(L-arginyl)-*rac*-glycerol·2HCl (XXR) were prepared and their aquatic toxicity evaluated using two short-term bioassays: the *Daphnia magna* test and the bioluminescent bacteria test. These new arginine-based cationic surfactants have proved to be much less toxic than conventional quaternary ammonium-based surfactants. Bacterial populations were more sensitive to the toxic effects of these surfactants than microcrustacea, which is consistent with their potential use as antimicrobial agents. To evaluate the biodegradability of these compounds two ready biodegradation tests were applied, the Modified Screening Test and the Closed Bottle Test. With the exception of the 1010R compound, all the arginine-based glycerolipidic surfactants were found to be excellently biodegradable and could be classified as “readily biodegradable”. The rapid and total biodegradation of these cationic surfactants is likely due to the presence in the molecule of easily breakable ester bonds that leads to the formation of compounds which are further readily biodegradable. The low biodegradation extent for the 1010R surfactant could be attributed to its inhibitory effects on the bacterial degraders due to the higher antimicrobial activity of this compound.

Experimental

Synthesis of cationic surfactants

The surfactants X0R and XXR were prepared following the chemical reactions described previously.^{12,13} Briefly, this involved a three-step procedure, starting from commercially available *N*-Cbz-L-arginine·HCl. The first step consists of the preparation of *O*-(*N*-Cbz-L-arginyl)-*rac*-glycerol·HCl (00RZ) by chemical esterification of the α -carboxyl group of

N-Cbz-L-arginine·HCl with the primary hydroxyl function of glycerol using boron trifluoroetherate as catalyst. The purification of 00RZ was carried out by ion exchange chromatography following the procedure described by Morán *et al.*²⁹ The next synthetic step consists of the preparation of 1-acyl-3-*O*-(*N*-Cbz-L-arginyl)-*rac*-glycerol·HCl (X0RZ) or 1,2-diacyl-3-*O*-(*N*-Cbz-L-arginyl)-*rac*-glycerol·HCl (XXRZ) by acylation of the remaining free hydroxyl groups of 00RZ with the corresponding long chain acid chloride, in a proportion depending on the compound (mono or diacylated) required. The isolation of the pure monoacyl and diacyl derivatives was carried out by silica gel chromatography. Silica (100 mL Chromagel 60 A CC, 70–230) was packed into a flash chromatography column. Then, XXRZ or X0RZ dissolved in chloroform was loaded into the column and was eluted with a gradient from chloroform to chloroform–methanol, 90 : 10 (v/v). The fractions containing the desired products were pooled and evaporated to dryness. The target compounds X0R or XXR were obtained by catalytic hydrogenation of the Cbz group using Pd over charcoal. Pure compounds were obtained after several crystallizations in methanol–acetonitrile. The purity of the products was established with HPLC, NMR and elemental analysis. All the results indicate that the purity was higher than 99%. The surfactants CAM, LAM and 120RAC were also previously prepared by our group.^{3,12,16}

1-decyl-3-*O*-(L-arginyl)-*rac*-glycerol·2HCl (100R).

$C_{19}H_{40}N_4O_5Cl_2$ *m/z* 403.3 Calc. Anal. (%) with 3.5 mol H₂O: C, 42.4; H, 8.7; N, 10.4; Cl, 13.2; Found: C, 42.2; H, 8.5; N, 10.3; Cl, 13.6.

¹H NMR: δ_H (CD₃OD), 0.91 [t, 3H, CH₃ of the alkyl chain], 1.31 [s, 12H, 6CH₂ of the alkyl chain], 1.67 [m, 2H, CH–CH₂–CH₂–CH₂–NH–], 1.8 [m, 2H, CH₂–CH₂–COO–], 2.1 [m, 2H, CH–CH₂–CH₂–CH₂–NH–], 2.4 [m, 2H, –CH₂–COO–], 3.4 [t, 2H, CH–CH₂–CH₂–CH₂–NH–], 4.1 [m, 1H, –CHOH–], 4.15 [m, 1H, –CH–NH₃–], 4.18 [m, 2H, –CH₂–CHOH–CH₂–arginine], 4.25 [m, 2H, –CH₂–CHOH–CH₂–arginine].

¹³C NMR: δ_C (CD₃OD), 14.46 [CH₃– alkyl chain], 23.76–41.74 [–CH₂– alkyl chain and CH–CH₂–CH₂–CH₂–NH], 53.69 [CH–CH₂–CH₂–CH₂–NH], 65.73 [–CH₂–CHOH–CH₂–arginine], 68.0 [–CH₂–CHOH–CH₂–arginine], 68.20 [–CH₂–CHOH–CH₂–arginine], 158.67 [C guanidine group], 170.10 [–COO– arginine group], 175.26 [–COO– alkyl chain].

1-dodecyl-3-*O*-(L-arginyl)-*rac*-glycerol·2HCl (120R).

$C_{21}H_{44}N_4O_5Cl_2$ *m/z* 431.3 Calc. Anal. (%) with 2 mol H₂O: C, 46.8; H, 8.9; N, 10.4; Cl, 13.3. Found: C, 46.5; H, 8.8; N, 10.5; Cl, 13.7.

¹H NMR: δ_H (CD₃OD), 0.91 [t, 3H, CH₃ of the alkyl chain], 1.31 [s, 16H, 8CH₂ of the alkyl chain], 1.67 [m, 2H, CH–CH₂–CH₂–CH₂–NH–], 1.8 [m, 2H, CH₂–CH₂–COO–], 2.1 [m, 2H, CH–CH₂–CH₂–CH₂–NH–], 2.4 [m, 2H, –CH₂–COO–], 3.4 [t, 2H, CH–CH₂–CH₂–CH₂–NH–], 4.1 [m, 1H, –CHOH–], 4.15 [m, 1H, –CH–NH₃–], 4.18 [m, 2H, –CH₂–CHOH–CH₂–arginine], 4.25 [m, 2H, –CH₂–CHOH–CH₂–arginine].

¹³C NMR: δ_C (CD₃OD), 14.46 [CH₃– alkyl chain], 23.76–41.74 [–CH₂– alkyl chain and CH–CH₂–CH₂–CH₂–NH], 53.69 [CH–CH₂–CH₂–CH₂–NH], 65.73 [–CH₂–CHOH–CH₂–arginine], 68.0 [–CH₂–CHOH–CH₂–arginine], 68.20

[$-\text{CH}_2-\text{CHOH}-\text{CH}_2-\text{arginine}$], 158.67 [C guanidine group], 170.10 [$-\text{COO}-$ arginine group], 175.26 [$-\text{COO}-$ alkyl chain].

1-tetradecyl-3-O-(L-arginyl)-rac-glycerol·2HCl (140R). $\text{C}_{23}\text{H}_{48}\text{N}_4\text{O}_5\text{Cl}_2$ *m/z* 459.3 Calc. Anal. (%) with 2.5 mol H_2O : C, 47.9; H, 9.2; N, 9.7; Cl, 12.3. Found: C, 47.9; H, 9.5; N, 9.6; Cl, 12.5.

^1H NMR: δ_{H} (CD_3OD), 0.91 [t, 3H, CH_3 of the alkyl chain], 1.31 [s, 20H, 10CH_2 of the alkyl chain], 1.67 [m, 2H, $\text{CH}-\text{CH}_2-\text{CH}_2-\text{CH}_2-\text{NH}-$], 1.8 [m, 2H, $\text{CH}_2-\text{CH}_2-\text{COO}-$], 2.1 [m, 2H, $\text{CH}-\text{CH}_2-\text{CH}_2-\text{CH}_2-\text{NH}-$], 2.4 [m, 2H, $-\text{CH}_2-\text{COO}-$], 3.4 [t, 2H, $\text{CH}-\text{CH}_2-\text{CH}_2-\text{CH}_2-\text{NH}-$], 4.1 [m, 1H, $-\text{CHOH}-$], 4.15 [m, 1H, $-\text{CH}-\text{NH}_3-$], 4.18 [m, 2H, $-\text{CH}_2-\text{CHOH}-\text{CH}_2-\text{arginine}$], 4.25 [m, 2H, $-\text{CH}_2-\text{CHOH}-\text{CH}_2-\text{arginine}$].

^{13}C NMR: δ_{C} (CD_3OD), 14.46 [CH_3- alkyl chain], 23.76–41.74 [$-\text{CH}_2-$ alkyl chain and $\text{CH}-\text{CH}_2-\text{CH}_2-\text{CH}_2-\text{NH}$], 53.69 [$\text{CH}-\text{CH}_2-\text{CH}_2-\text{CH}_2-\text{NH}$], 65.73 [$-\text{CH}_2-\text{CHOH}-\text{CH}_2-\text{arginine}$], 68.0 [$-\text{CH}_2-\text{CHOH}-\text{CH}_2-\text{arginine}$], 68.20 [$-\text{CH}_2-\text{CHOH}-\text{CH}_2-\text{arginine}$], 158.67 [C guanidine group], 170.10 [$-\text{COO}-$ arginine group], 175.26 [$-\text{COO}-$ alkyl chain].

1,2-dioctyl-3-O-(L-arginyl)-rac-glycerol·2HCl (88R). $\text{C}_{25}\text{H}_{52}\text{N}_4\text{O}_6\text{Cl}_2$ *m/z* 501.2 Calc. Anal. (%) with 1 mol H_2O : C, 48.5; H, 8.9; N, 9.05; Cl, 11.5. Found: C, 48.3; H, 8.8; N, 9.3; Cl, 11.7.

^1H NMR: δ_{H} (DMSO), 0.90 [m, 6H, 2CH_3 of the alkyl chain], 1.31 [s, 16H, 8CH_2 of the alkyl chain], 1.59–2.01 [m, 8H, $2(-\text{CH}_2-\text{CH}_2-\text{COO}-)$, $\text{CH}-\text{CH}_2-\text{CH}_2-\text{CH}_2-\text{NH}-$], 2.31–2.38 [2t, 4H, $2(-\text{CH}_2-\text{COO}-)$], 3.25–3.31 [m, 2H, $\text{CH}-\text{CH}_2-\text{CH}_2-\text{CH}_2-\text{NH}-$], 4.12–4.61 [m, 5H, $\text{CH}_2-\text{CHOH}-\text{CH}_2\text{OCO}-\text{CH}-$], 5.32–5.36 [m, 1H, $-\text{CHOH}-$].

^{13}C NMR: δ_{C} (DMSO), 14.43 [CH_3- alkyl chain], 23.68–41.75 [$-\text{CH}_2-$ alkyl chain and $\text{CH}-\text{CH}_2-\text{CH}_2-\text{CH}_2-\text{NH}$], 53.57 [$\text{CH}-\text{CH}_2-\text{CH}_2-\text{CH}_2-\text{NH}$], 63.17 [$\text{CH}_2-\text{CHOH}-\text{CH}_2\text{OCO}-\text{CH}$], 65.42 [$\text{CH}_2-\text{CHOH}-\text{CH}_2\text{OCO}-\text{CH}$], 70.30 [$\text{CH}_2-\text{CHOH}-\text{CH}_2\text{OCO}-\text{CH}$], 158.64 [C guanidine group], 170.09 [$-\text{OCO}-$ arginine], 174.44 [alkylchain $\text{COO}-\text{CH}$], 174.80 [alkylchain $\text{COO}-\text{CH}_2$].

1,2-didodecyl-3-O-(L-arginyl)-rac-glycerol·2HCl (1010R). $\text{C}_{29}\text{H}_{58}\text{N}_4\text{O}_6\text{Cl}_2$ *m/z* 557.4 Calc. Anal. (%) with 2 mol H_2O : C, 52.3; H, 9.3; N, 8.4; Cl, 10.7; Found: C, 52.8; H, 9.5; N, 8.7; Cl, 10.5.

^1H NMR: δ_{H} (DMSO), 0.86 [m, 6H, 2CH_3 of the alkyl chain], 1.26 [s, 24H, 12CH_2 of the alkyl chain] 1.59–2.02 [m, 8H, $2(-\text{CH}_2-\text{CH}_2-\text{COO}-)$, $\text{CH}-\text{CH}_2-\text{CH}_2-\text{CH}_2-\text{NH}-$], 2.27–2.33 [2t, 4H, $2(-\text{CH}_2-\text{COO}-)$], 3.25–3.31 [m, 2H, $\text{CH}-\text{CH}_2-\text{CH}_2-\text{CH}_2-\text{NH}-$], 4.02–4.55 [m, 5H, $\text{CH}_2-\text{CHOH}-\text{CH}_2\text{OCO}-\text{CH}-$], 5.32–5.36 [m, 1H, $-\text{CHOH}-$].

^{13}C NMR: δ_{C} (DMSO), 14.46 [CH_3- alkyl chain], 23.73–41.78 [$-\text{CH}_2-$ alkyl chain and $\text{CH}-\text{CH}_2-\text{CH}_2-\text{CH}_2-\text{NH}$], 53.68 [$\text{CH}-\text{CH}_2-\text{CH}_2-\text{CH}_2-\text{NH}$], 63.19 [$\text{CH}_2-\text{CHOH}-\text{CH}_2\text{OCO}-\text{CH}$], 65.424 [$\text{CH}_2-\text{CHOH}-\text{CH}_2\text{OCO}-\text{CH}$], 70.33 [$\text{CH}_2-\text{CHOH}-\text{CH}_2\text{OCO}-\text{CH}$], 158.63 [C guanidine group], 170.62 [$-\text{OCO}$ arginine], 174.45 [alkylchain $\text{COO}-\text{CH}$], 174.81 [alkylchain $\text{COO}-\text{CH}_2$].

1,2-didodecyl-3-O-(L-arginyl)-rac-glycerol·2HCl (1212R). $\text{C}_{33}\text{H}_{66}\text{N}_4\text{O}_6\text{Cl}_2$ *m/z* 613.7 Calc. Anal. (%) with 1 mol H_2O :

C, 56.3; H, 9.7; N, 8.0; Cl, 10.1. Found: C, 56.0; H, 9.7; N, 8.3; Cl, 10.4.

^1H NMR: δ_{H} (DMSO), 0.90 [m, 6H, 2CH_3 of the alkyl chain], 1.29 [s, 32H, 16CH_2 of the alkyl chain], 1.57–2.03 [m, 8H, $2(-\text{CH}_2-\text{CH}_2-\text{COO}-)$, $\text{CH}-\text{CH}_2-\text{CH}_2-\text{CH}_2-\text{NH}-$], 2.31–2.38 [2t, 4H, $2(-\text{CH}_2-\text{COO}-)$], 3.27–3.31 [m, 2H, $\text{CH}-\text{CH}_2-\text{CH}_2-\text{CH}_2-\text{NH}-$], 4.12–4.60 [m, 5H, $\text{CH}_2-\text{CHOH}-\text{CH}_2\text{OCO}-\text{CH}-$], 5.31–5.39 [m, 1H, $-\text{CHOH}-$].

^{13}C NMR: δ_{C} (DMSO), 14.48 [CH_3- alkyl chain], 23.75–41.73 [$-\text{CH}_2-$ alkyl chain and $\text{CH}-\text{CH}_2-\text{CH}_2-\text{CH}_2-\text{NH}$], 53.56 [$\text{CH}-\text{CH}_2-\text{CH}_2-\text{CH}_2-\text{NH}$], 63.19 [$\text{CH}_2-\text{CHOH}-\text{CH}_2\text{OCO}-\text{CH}$], 65.29 [$\text{CH}_2-\text{CHOH}-\text{CH}_2\text{OCO}-\text{CH}$], 70.29 [$\text{CH}_2-\text{CHOH}-\text{CH}_2\text{OCO}-\text{CH}$], 158.61 [C guanidine group], 170.01 [$-\text{OCO}$ arginine], 174.35 [alkylchain $\text{COO}-\text{CH}$], 174.76 [alkylchain $\text{COO}-\text{CH}_2$].

1,2-ditetradecyl-3-O-(L-arginyl)-rac-glycerol·2HCl (1414R). $\text{C}_{37}\text{H}_{74}\text{N}_4\text{O}_6\text{Cl}_2$ *m/z* 669.7 Calc. Anal. (%) with 2 mol H_2O : C, 57.0; H, 10.0; N, 7.2; Cl, 9.2; Found: C, 57.4; H, 9.9; N, 6.8; Cl, 9.2.

^1H NMR: δ_{H} (DMSO), 0.90 [m, 6H, 2CH_3 of the alkyl chain], 1.29 [s, 40H, 20CH_2 of the alkyl chain], 1.57–2.33 [m, 8H, $2(-\text{CH}_2-\text{CH}_2-\text{COO}-)$, $\text{CH}-\text{CH}_2-\text{CH}_2-\text{CH}_2-\text{NH}-$], 2.31–2.37 [2t, 4H, $2(-\text{CH}_2-\text{COO}-)$], 3.31–3.37 [m, 2H, $\text{CH}-\text{CH}_2-\text{CH}_2-\text{CH}_2-\text{NH}-$], 4.12–4.60 [m, 5H, $\text{CH}_2-\text{CHOH}-\text{CH}_2\text{OCO}-\text{CH}-$], 5.32–5.39 [m, 1H, $-\text{CHOH}-$].

^{13}C NMR: δ_{C} (DMSO), 14.48 [CH_3- alkyl chain], 23.76–41.74 [$-\text{CH}_2-$ alkyl chain and $\text{CH}-\text{CH}_2-\text{CH}_2-\text{CH}_2-\text{NH}$], 53.57 [$\text{CH}-\text{CH}_2-\text{CH}_2-\text{CH}_2-\text{NH}$], 63.21 [$\text{CH}_2-\text{CHOH}-\text{CH}_2\text{OCO}-\text{CH}$], 65.39 [$\text{CH}_2-\text{CHOH}-\text{CH}_2\text{OCO}-\text{CH}$], 70.30 [$\text{CH}_2-\text{CHOH}-\text{CH}_2\text{OCO}-\text{CH}$], 158.63 [C guanidine group], 170.06 [$-\text{OCO}$ arginine], 174.43 [alkylchain $\text{COO}-\text{CH}$], 174.78 [alkylchain $\text{COO}-\text{CH}_2$].

1-dodecyl-3-O-acetylarginil-glycerolmonochlorhydrate (120RAc). $\text{C}_{23}\text{H}_{45}\text{N}_4\text{O}_6\text{Cl}_2$ *m/z* 669.7 Calc. Anal. (%) with 1 mol H_2O : C, 52.42; H, 8.92; N, 10.66; Cl, 6.74. Found: C, 52.13; H, 8.83; N, 10.42; Cl, 6.53.

^1H NMR: δ_{H} (DMSO), 0.84 [CH_3 , alkyl chain], 1.23 [CH_2 , alkyl chain], 1.28 [$-\text{CH}_2\text{O}-$, alkyl chain], 1.84 [CH_3-CO , acetyl group], 3.15 [CH_2-NH -arginine group], 3.9–4.2 [$\text{O}-\text{CH}_2-\text{CH}_2-\text{OH}-\text{CH}_2\text{O}$ and $-\text{CH}-$ in the arginine group], 5.2 [$-\text{CH}_2\text{OH}-$], 7.1 [2NH_2 , guanidine group], 7.71 [$-\text{NH}-\text{C}$, guanidine group], 8.25 [$-\text{CH}-\text{NH}-\text{CO}$, amide group].

^{13}C NMR: δ_{C} (DMSO), 13.87 [CH_3- alkyl chain], 22.17 [CH_3- acetyl group], 22.04–33.43 [$-\text{CH}_2-$ alkyl chain and arginine group], 51.76 [$-\text{CH}-$ arginine group], 64.68 [$-\text{COO}-\text{CH}_2-\text{CHOH}$], 65.38 [$-\text{O}-\text{CH}_2-\text{CHOH}-\text{CH}_2-\text{O}$ -arginine], 66.17 [$-\text{O}-\text{CH}_2-\text{CHOH}-\text{CH}_2-\text{O}-$], 156.98 [C guanidine group], 169.75 [$-\text{CO}-$ amide group], 171.81 and 172.86 [$\text{COO}-$ ester groups].

Aquatic toxicity

Two acute toxicity tests were carried out, the *Daphnia magna* Immobilisation Test¹⁷ and the *Photobacterium phosphoreum* Luminescence Reduction Test, Microtox[®] Test.¹⁸

***Daphnia magna* Immobilization Test¹⁷.** *Daphnia magna*, laboratory bred, not more than 24 h old were used in this

test, where the swimming incapability is the end point. The pH of the medium was 8.0 and the total hardness was 250 mg L⁻¹ (as CaCO₃), with a Ca : Mg ratio of 4 : 1. Tests were performed in the dark at 20 °C. Twenty *Daphnia*, divided into four groups of five animals each, were used at each test concentration. For each surfactant, 10 concentrations in a geometric series were tested in the concentration range first established in a preliminary test. The percentage immobility at 24 h was plotted against concentration on logarithmic-probability paper, a linear relationship was obtained and the EC₅₀ was calculated from the corresponding equation.

Photobacterium phosphoreum Luminescence Reduction Test (Microtox[®] Test)¹⁸. *Photobacterium phosphoreum* is a marine luminescent bacterium naturally adapted to a saline environment. These bacteria liberate energy in the form of visible light (intensity maximum at 490 nm) as a consequence of the series of metabolic reactions. On exposure to toxic substances, the light output is reduced and this reduction is proportional to the toxicity of the sample. Therefore, the toxicity bioassay is based on the light emission of these bacteria, as a measurement of their metabolic activity. In the Microtox bioassay the concentration of an aqueous solution of a chemical that causes a 50% reduction of the light emitted by the bacteria (EC₅₀) is calculated from a concentration–response curve by regression analysis. The osmotic pressure of the samples was adjusted by NaCl addition (2%). Toxicity data were based on a 30 min exposure of bacteria to the surfactant solution at 15 °C.

Biodegradation tests

Assays based on the Modified Screening Test and Closed Bottle Test, described in the Organization for Economic Cooperation and Development (OECD) Guidelines were applied.^{25,26} A mixture of equal volumes of secondary effluent from a wastewater treatment plant and garden soil aqueous suspension was used as inoculum for both biodegradation tests.

Modified Screening Test (OECD 301E)²⁵. In the Modified Screening Test, biodegradation is studied by the organic carbon depletion. A surfactant concentration of 10 mg L⁻¹ dissolved in an inorganic medium and inoculated with microorganisms was tested. Because of the high capacity of adsorption of these surfactants, biodegradation was monitored by the dissolved organic carbon (DOC) and total organic carbon (TOC) removal over a 28 day period. Both TOC and DOC were determined by the combustion infrared method in a total organic carbon analyser (Shimadzu TOC-5050, Tokyo, Japan) after decarbonation by acidification with HCl and stirring for 15 min. For DOC determination, samples were subjected to membrane filtration (0.22 µm porous size). Measurements were periodically performed and ultimate biodegradation was stated as the percentage of DOC removal.

Closed Bottle Test (OECD 301D)²⁶. In this method, the chemical being evaluated is added to an aerobic aqueous medium inoculated with wastewater microorganisms and the depletion of dissolved molecular oxygen is measured for a

defined period of time and reported as a percentage of the theoretical maximum. Compounds which reach a biodegradation level higher than 60% are referred to as “readily biodegradable”. Sodium *n*-dodecyl sulfate (SDS) was used as reference substance. Solutions containing 2 mg L⁻¹ of the test surfactants and the reference chemical as sole sources of organic carbon were prepared, separately, in previously aerated mineral medium. The solutions were then inoculated with secondary effluent collected from an activated sludge treatment plant and each well-mixed solution was carefully dispensed into a series of BOD bottles so that all the bottles were completely full. A control with inoculum, but without test chemicals was run parallel for the determination of oxygen blanks. Duplicate bottles of each series were analysed immediately for dissolved oxygen and the remaining bottles were incubated at 20 ± 1 °C in the dark. Bottles of all series were withdrawn in duplicate for dissolved oxygen analysis over the 28 day incubation period. The biodegradation after *n* days was expressed as the ratio of the biochemical oxygen demand (BOD) to the chemical oxygen demand (COD), both of them expressed as mg O₂ per mg compound. The chemical oxygen demand was determined by the dichromate reflux method.³⁰ For the calculation of the biochemical oxygen demand the determined oxygen depletions were divided by the concentration of surfactant.

Fluorescence measurements

The fluorescence spectrum of micelle-bound pyrene is sensitive to the polarity of the microenvironment at the site of solubilisation of the fluorophore. The CMC of the surfactant solutions were determined from the plots of the intensity ratio II : III versus concentration. II and III were, respectively, the first and third vibronic peaks in the fluorescence emission spectrum of pyrene solubilised at 10⁻⁵ M in the surfactant solutions.³¹ The fluorescence spectra were recorded using a Shimadzu RF 540 spectrofluorometer at the excitation wavelength 335 nm and a bandwidth of 1.5 nm.

Acknowledgements

This research was supported by the Spanish Ministerio de Ciencia y Tecnología (MCyT), project PPQ2003-01834.

Noemí Pérez,* Lourdes Pérez, M. Rosa Infante and M. Teresa García*
 Department of Surfactant Technology, IIQAB-CSIC, Jordi Girona 18-26, 08034 Barcelona, Spain. E-mail: nplste@cid.csic.es; lpmste@iiqab.csic.es; rimste@iiqab.csic.es; mtgbet@iiqab.csic.es;
 Fax: +34 93 2045904; Tel: +34 93 4006100

References

- 1 K. Holmberg, *Novel Surfactants. Preparation, Applications and Biodegradability*, ed. K. Holmberg, Marcel Dekker, New York, 2nd edn., revised and expanded, 2004, Surfactant Science Series K.
- 2 M. Macián, J. Seguer, M. R. Infante, C. Selve and M. P. Vinardell, *Toxicology*, 1996, **106**, 1.
- 3 M. R. Infante, A. Pinazo and J. Seguer, *Colloids Surf., A*, 1997, **49**, 123.
- 4 M. C. Morán, A. Pinazo, L. Pérez, P. Clapés, M. Angelet, M. T. García, M. P. Vinardell and M. R. Infante, *Green Chem.*, 2004, **6**, 166.

- 5 J. Xia, J. Nnanna and K. Sakamoto, *Amino acid based Surfactants, Protein based Surfactants*, ed. Ifendu A. Nnanna and Jiding Xia, Marcel Dekker, New York, 2001, Surfactant Science Series, vol. 101.
- 6 T. Furutani, H. Ooshima and J. Kato, *Enzyme Microb. Technol.*, 1997, **20**, 214.
- 7 B. Gallot and H. H. Hassan, *Mol. Cryst. Liq. Cryst.*, 1989, **170**, 195.
- 8 A. Nagao and M. Kito, *J. Am. Oil Chem. Soc.*, 1989, **66**, 710.
- 9 M. R. Infante, J. Molinero, P. Erra, R. Juliá, J. J. García Domínguez and M. Robert, *Fette Seifen Anstrichm.*, 1986, **88**, 108.
- 10 Y. Okahata, S. Tammamachi, M. Magai and T. Kunitake, *J. Colloid Interface Sci.*, 1981, **82**, 401.
- 11 T. Kida, N. Morishima, A. Masuyama and Y. Nakatsuji, *J. Am. Oil Chem. Soc.*, 1994, **71**, 705.
- 12 L. Pérez, A. Pinazo, M. T. García and M. R. Infante, *New J. Chem.*, 2004, **28**, 1326.
- 13 L. Pérez, A. Pinazo, M. P. Vinardell, P. Clapés, M. Angelet and M. R. Infante, *New J. Chem.*, 2002, **26**, 1221.
- 14 M. R. Infante, J. Molinero, P. Erra, M. R. Juliá and J. J. García Domínguez, *Fett Wiss. Technol.*, 1998, **87**, 309.
- 15 H. Gibson and J. T. Holah, *Preservation of Surfactant Formulations*, ed. F. F. Morpeth, Blackie Academic and Professional, Glasgow, 1995, p. 30.
- 16 M. R. Infante, J. J. García Domínguez, P. Erra, M. R. Juliá and M. Prats, *Int. J. Cosmet. Sci.*, 1984, **6**, 275.
- 17 OECD Guidelines for testing of Chemicals, Method 202: Daphnia sp. Acute Immobilisation test and Reproduction test, OECD, Paris, 1981.
- 18 DIN (Deutsches Institut für Normung), German standard methods for the examination of water, waste water and sludge, Bio-assays (group L9 Part-37. Determination of the inhibitory effect of waste water on the light emission of Photobacterium phosphoreum: luminescent bacteria waste water test using conserved bacteria (L-34)), DIN 38412-34, Beuth Verlag, Berlin, Germany, 1997.
- 19 M. T. García, I. Ribosa, T. Guindulain, J. Sánchez-Leal and J. Vives-Rego, *Environ. Pollut.*, 2001, **111**, 169.
- 20 L. Pérez, M. T. García, I. Ribosa, M. P. Vinardell, A. Manresa and M. R. Infante, *Environ. Toxicol. Chem.*, 2002, **21**, 6.
- 21 L. L. Uppgard, A. Lindgren, M. Sjöstrom and S. Wold, *J. Surfactants Deterg.*, 2000, **3**, 33.
- 22 S. D. Dyer, D. T. Santon, J. R. Laugh and D. S. Cherry, *Environ. Toxicol. Chem.*, 2000, **19**, 608.
- 23 H. A. Painter, in *The Handbook of Environmental Chemistry*, Springer-Verlag, Berlin-Heidelberg, 1992, 3 Part F.
- 24 I. Ribosa, M. T. García, J. Sánchez-Leal and J. J. Gonzalez, *Toxicol. Environ. Chem.*, 1993, **39**, 237.
- 25 OECD Chemical group, Ready Biodegradability: Modified Screening Test, Method 301 E, OECD Revised Guidelines for ready biodegradability, OECDParis, France, 1993.
- 26 OECD Chemical group, Ready Biodegradability: Closed Bottle Test, Method 301 D, OECD Revised Guidelines for ready biodegradability, OECDParis, France, 1993.
- 27 G. C. Van Ginkel, *Biodegradability of surfactants.*, ed. D. R. Karsa and M. R. Porter, Blackie Academic Professional, Chapman & Hall, London, UK, 1995.
- 28 J. Sánchez-Leal, J. J. González, K. L. Kaiser, V. S. Palabrica, F. Comelles and M. T. Garcia, *Acta Hydrochim. Hydrobiol.*, 1994, **22**, 13.
- 29 C. Morán, M. R. Infante and P. Clapés, *J. Chem. Soc., Perkin Trans. 1.*, 2002, 1124.
- 30 APHA (American Public Health Association), Method 5220C, Standard Methods for the Examination of Water and Wastewater, APHA, Washington, 20th edn., 1998, 5–13, 5–16.
- 31 K. Kalyanasunderam and J. K. Thomas, *J. Am. Chem. Soc.*, 1977, **99**, 2039.

Optimal lipase-catalyzed formation of hexyl laurate

Shu-Wei Chang,^a Jei-Fu Shaw,^{abc} Kun-Hsiang Yang,^d Ing-Lung Shih,^e Chih-Han Hsieh^f and Chwen-Jen Shieh^{*f}

Received 2nd February 2005, Accepted 4th April 2005

First published as an Advance Article on the web 25th April 2005

DOI: 10.1039/b501724f

A medium-chain ester, hexyl laurate, with a fruity flavor is primarily used in personal care formulations as an important emollient for cosmetic applications. In order to conform to the “natural” interests of consumers, the ability for immobilized lipase from *Rhizomucor miehei* (Lipozyme IM-77) to catalyze the direct esterification of hexanol and lauric acid was investigated in this study. Response surface methodology (RSM) and 4-factor-5-level central composite rotatable design (CCRD) were employed to evaluate the effects of synthesis parameters, such as reaction time (20 to 100 min), temperature (25 to 65 °C), enzyme amount (10 to 50%), and substrate molar ratio of hexanol to lauric acid (1 : 1 to 3 : 1) on percentage molar conversion of hexyl laurate by direct esterification. Reaction time and enzyme amount had significant effects on percent molar conversion. Based on ridge max analysis, the optimum conditions for synthesis were: reaction time 74.8 min, temperature 47.5 °C, enzyme amount 45.5%, and substrate molar ratio 1 : 1.5. The predicted value was 90.0% and the actual experimental value 92.2% molar conversion.

Introduction

Hexyl esters with a “green note” flavor, derived from medium-chain carboxylic acids such as hexyl laurate, are used as important emollient materials in many cosmetic industrial applications.¹ Customarily, they are produced by chemical synthesis or extracted from natural sources. However, with the steadily growing “natural” demand, the biosynthesis of such esters by lipase-catalyzed chemical reactions under mild conditions has been receiving much attention for producing these valuable products. In particular, the development of optimum enzymatic synthesis procedure to improve the yield conversion of hexyl esters and to reduce the production costs would be more attractive for the manufacturers and consumers.

Ester synthesis catalyzed by lipase was first described by Inada *et al.* in 1984;² and some relevant researches (*e.g.* the effect of experimental variables on the thermodynamic parameters and optimization of esterification reactions) were issued successively.^{3–5} Carvalho *et al.*⁶ reported that hexyl acetate was synthesized by the cutinase-catalyzed transesterification reaction of butyl acetate with hexanol in reversed micelles system. Bourg-Garros *et al.*⁷ synthesized (*Z*)-3-hexenyl laurate by direct esterification using lipases *Mucor miehei* (Lipozyme IM) and *Candida antarctica* (Novozym 435) in *n*-hexane and solvent-free systems. However, until to date the enzymatic synthesis of hexyl laurate by esterification has not been investigated in detail.

The present work focuses on the parameters that affect lipase from *Rhizomucor miehei* (Lipozyme IM-77) to catalyze the direct esterification of hexyl laurate using lauric acid as acyl donor in *n*-hexane. Our purpose was to better understand

the relationships between the factors (reaction time, temperature, enzyme amount, and substrate molar ratio) and the response (percent molar conversion); and to determine the optimal conditions for hexyl laurate synthesis using central composite rotatable design (CCRD) and response surface methodology (RSM).

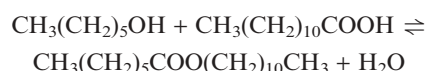
Experimental

Reagents

Immobilized lipase (triacylglycerol hydrolase, EC 3.1.1.3; Lipozyme IM-77, 7.7 Batch Acidolysis Units of Novo (BAUN)/g, water 5.4% w/w) from *R. miehei* supported on macroporous weak anionic resin beads was purchased from Novo Nordisk Bioindustrials, Inc. (Bagsvaerd, Denmark). Hexanol (98% pure), lauric acid (99% pure) and glyceryl tributyrates (99% pure) were purchased from Sigma Chemical Co. (St. Louis, MO, USA). Molecular sieve 4 Å was purchased from Davison Chemical (Baltimore, MD, USA) and *n*-hexane was obtained from Merck Chemical Co. (Darmstadt, Germany). All other chemicals were of analytical reagent grade.

Esterification

Lipozyme IM-77 was employed as a biocatalyst to perform the direct esterification of hexanol by lauric acid:



Lipozyme IM-77 was dehydrated for 24 h by a freeze-drier (Eyela, FD-1000, Japan), then was equilibrated in desiccators containing a saturated salt solution (CH_3COOK , $a_w = 0.23$) for at least 7 days at 25 °C. The water content was measured using a Karl–Fisher titrator (Mettler-Toledo, DL31, USA).

*cjsieh@mail.dyu.edu.tw

The initial water content in Lipozyme IM-77 was 5.1% in this study. Molecular sieve 4 Å (10% w/w of substrate and *n*-hexane) was added to all chemicals for at least 24 h before reaction in order to remove all water. Hexanol (0.1 M, 0.31 g) and different molar ratios of lauric acid were added to *n*-hexane, followed by different amounts of lipase. The mixtures of hexanol, lauric acid and Lipozyme IM-77 were stirred in an orbital shaking water bath (200 rpm) at different reaction temperatures and reaction times, as shown in Table 1.

Determination of hexyl laurate

Immobilized Lipozyme IM-77 and any residual water were removed by passing reaction media through an anhydrous sodium sulfate column. Then, hexyl laurate formation was determined by injecting a 1 µL aliquot in a splitless mode into a gas chromatograph (GC) (Hewlett Packard 6890, Avondale, PA, USA) equipped with a flame-ionization detector (FID) and a DB-5 fused-silica capillary column (30 m × 0.32 mm i.d.; film thickness 1 µm; J&W Scientific, Folsom, CA, USA). Tributyrin was employed as an internal standard. Injector and FID temperatures were set at 280 °C and 300 °C, respectively. Oven temperature was maintained at 70 °C for 2 min, elevated to 120 °C at a rate of 70 °C min⁻¹, held for 1 min, and then increased to 230 °C at a rate of 70 °C min⁻¹. Nitrogen was used as carrier gas. The percentage yield (molar conversion) was defined as (mmol hexyl laurate/mmol initial hexanol) × 100% and was estimated using the peak area integrated by on-line software—Hewlett Packard 3365 Series II ChemStation (Avondale, PA, USA).

Experimental design and statistical analysis

A 4-factor-5-level CCRD was employed in this study, requiring 27 experiments.⁸ To avoid bias, 27 runs were performed in a totally random order. The central composite rotatable design consists of 16 factorial points, 8 axial points (two axial points on the axis of each design variable at a distance of 2 from the design center), and 3 center points. The parameters and their levels selected for the study of hexyl laurate synthesis were: reaction time, 20–100 min; temperature, 25–65 °C; lipase amount, 10–50% (0.24–1.18 BAUN) by weight of hexanol; substrate molar ratio, 1 : 1–1 : 3 (hexanol : lauric acid). Table 1 shows the independent factors (x_i), levels and experimental design in terms of coded and uncoded. The experimental data were analyzed by the response surface regression (RSREG) procedure to fit the following second-order polynomial equation:⁹

$$Y = \beta_{k0} + \sum_{i=1}^4 \beta_{ki}x_i + \sum_{i=1}^4 \beta_{kii}x_i^2 + \sum_{i=1}^3 \sum_{j=i+1}^4 \beta_{kij}x_i x_j \quad (1)$$

Where Y is response (% molar conversion); β_{k0} , β_{ki} , β_{kii} , and β_{kij} are constant coefficients and x_i the uncoded independent variables. The ridge max option was used to compute the estimated ridge of maximum response for increasing radii from the center of the original design.

Results and discussion

Effect of reaction time

Fig. 1 shows the time course for the direct esterification of hexanol with lauric acid by Lipozyme IM-77 at 30 °C.

Table 1 Central composite rotatable second-order design, experimental data, and predicted values for 4-factor-5-level response surface analysis

Treatment no. ^a	Time/min x_1	Temperature/°C x_2	Enzyme (% by wt of hexanol) x_3	Substrate molar ratio (hexanol/lauric acid) x_4	Yield (% molar conversion) Y
1	-1(40) ^b	-1(35)	-1(20)	1(1 : 2.5)	58.83
2	-1(40)	-1(35)	1(40)	-1(1 : 1.5)	71.72
3	-1(40)	1(55)	-1(20)	-1(1 : 1.5)	52.75
4	-1(40)	1(55)	1(40)	1(1 : 2.5)	80.00
5	1(80)	-1(35)	-1(20)	-1(1 : 1.5)	68.07
6	1(80)	-1(35)	1(40)	1(1 : 2.5)	83.93
7	1(80)	1(55)	-1(20)	1(1 : 2.5)	71.25
8	1(80)	1(55)	1(40)	-1(1 : 1.5)	85.80
9	0(60)	0(45)	0(30)	0(1 : 2)	70.60
10	-1(40)	-1(35)	-1(20)	-1(1 : 1.5)	57.43
11	-1(40)	-1(35)	1(40)	1(1 : 2.5)	67.49
12	-1(40)	1(55)	-1(20)	1(1 : 2.5)	55.88
13	-1(40)	1(55)	1(40)	-1(1 : 1.5)	72.46
14	1(80)	-1(35)	-1(20)	1(1 : 2.5)	72.94
15	1(80)	-1(35)	1(40)	-1(1 : 1.5)	84.61
16	1(80)	1(55)	-1(20)	-1(1 : 1.5)	79.07
17	1(80)	1(55)	1(40)	1(1 : 2.5)	77.18
18	0(60)	0(45)	0(30)	0(1 : 2)	72.50
19	-2(20)	0(45)	0(30)	0(1 : 2)	42.39
20	2(100)	0(45)	0(30)	0(1 : 2)	82.57
21	0(60)	-2(25)	0(30)	0(1 : 2)	63.17
22	0(60)	2(65)	0(30)	0(1 : 2)	69.59
23	0(60)	0(45)	-2(10)	0(1 : 2)	59.67
24	0(60)	0(45)	2(50)	0(1 : 2)	84.73
25	0(60)	0(45)	0(30)	-2(1 : 1)	79.11
26	0(60)	0(45)	0(30)	2(1 : 3)	69.08
27	0(60)	0(45)	0(30)	0(1 : 2)	72.33

^a The treatments were run in a totally random order. ^b Numbers in parenthesis represent actual experimental amounts.

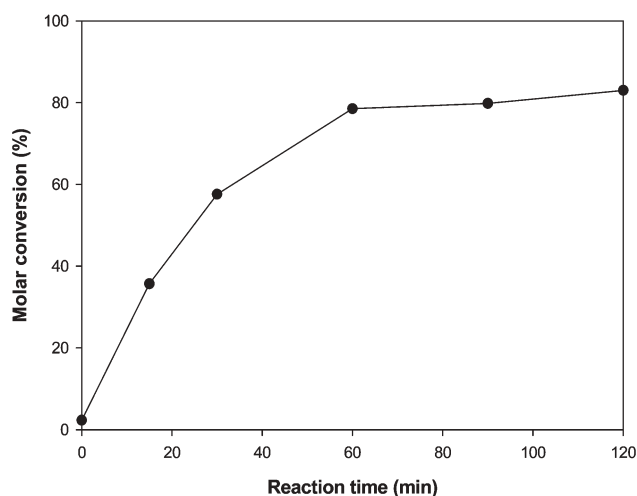


Fig. 1 Time course of the direct esterification of hexanol with lauric acid by Lipozyme IM-77. The reaction was carried out at 30 °C in hexane containing 0.1 M hexanol, 50% (wt. of hexanol) Lipozyme IM-77, substrate molar ratio of 1 : 1 (hexanol : lauric acid). The activity of 10% Lipozyme IM-77 is 0.24 BAUN.

The percent molar conversion of hexyl laurate increased to 79% at 60 min, therefore, the range of reaction time from 20 to 100 min was chosen in this study. The selection of reaction time range needs to be extremely precise in the study of CCRD, otherwise, the optimal condition of synthesis cannot be found inside the experimental region through the analyses of statistics and contour plots. Also, as shown in Fig. 1 the conversion was over 80% after 120 min, so the commercially immobilized Lipozyme IM-77 was directly added and pH was not controlled in the reaction system.

Model fitting

The major objective of this paper is the development and evaluation of a statistical approach to better understand the relationship between the variables of a lipase-catalyzed direct esterification reaction. In this way, the process can be optimized before the scaling-up procedure in order to save work, money, and time, allowing an economically important flavor of high quality with lower costs to be obtained. Compared with one-factor-at-a-time design, which has been adopted most often in the literature, RSM conjugated with 4-factor-5-level CCRD employed in this study was more efficient in reducing the experimental runs and time for investigating the optimized synthesis of hexyl laurate.

The RSREG procedure was employed to fit the second-order polynomial eqn. (1) to the experimental data—percent molar conversions (Table 1). Among the various treatments, the highest molar conversion (85.8%) was treatment no. 8 (80 min, 55 °C, substrate molar ratio 1 : 1.5, and 40% (0.96 BAUN) enzyme), and the lowest conversion (42.4%) was treatment no. 19 (20 min, 45 °C, substrate molar ratio 1 : 2, and 30% (0.72 BAUN) enzyme). From the SAS

output of RSREG, the second-order polynomial eqn. (2) is given below:

$$Y = -28.018 + 1.494 \times 1 + 1.051 \times 2 + 0.872 \times 3 - 3.261 \times 4 - 0.005 \times 1^2 - 0.001 \times 2 \times 1 - 0.01 \times 2^2 - 0.008 \times 3 \times 1 + 0.004 \times 3 \times 2 - 0.005 \times 3^2 - 0.126 \times 4 \times 1 - 0.089 \times 4 \times 2 - 0.095 \times 4 \times 3 + 3.901 \times 4^2 \quad (2)$$

Analysis of variance (Table 2) indicated that the second-order polynomial model was highly significant and adequate to represent the actual relationship between the response (percent molar conversion) and the significant variables with very small *p*-value (0.0001) and a satisfactory coefficient of determination ($R^2 = 0.903$). Furthermore, the overall effect of the four synthesis variables on the percent molar conversion of hexyl laurate was further analyzed by a joint test (data not shown). The results revealed that the reaction time (x_1), and enzyme amount (x_3) were the most important parameters, and exerting a statistically significant overall effect ($p < 0.01$) on the response molar conversion of hexyl laurate.

Mutual effect of parameters

Substrate molar ratio and reaction temperature were investigated in the range of 1 : 1–1 : 3 and 25–65 °C, respectively. Fig. 2A represents the effect of varying enzyme amount and reaction time on esterification at 45 °C and substrate molar ratio 1 : 2. With the highest enzyme amount (50%, 1.2 BAUN) and appropriate reaction time (85 min) environment, the maximum percent molar conversion (89.5%) of hexyl laurate was obtained. However, the lowest reaction time and enzyme amount significantly decreased the molar conversion to 30%, indicating that both the enzyme amount and reaction time are the most important parameters in the biosynthesis of hexyl laurate.

Fig. 2B shows the effect of enzyme amount, reaction temperature, and their mutual interaction on hexyl laurate synthesis at 60 min and substrate molar ratio 1 : 2. At any given reaction temperature, range from 25–65 °C, there is no significant effect on the molar conversion of hexyl laurate, whereas, the molar conversion was increased with an increase in the enzyme amount. This means that Lipozyme IM-77 possesses a broad range of temperature stability during the hexyl laurate esterification process. For slight difference in molar conversions, a reaction with enzyme amount 50% (1.2 BAUN) and moderate reaction temperature (48 °C) favored the maximum molar conversion (87%).

Table 2 Analysis of variance for synthetic variables pertaining to response percent molar conversion

Source	Degrees of freedom	Sum of squares	Prob > F
Model	14	2780.02	0.0005
Linear	4	2525.31	0.0001
Quadratic	4	176.05	0.1993
Cross product	6	78.65	0.7773
Total error	12	298.08	
R^2 (coefficient of determination)	0.903		

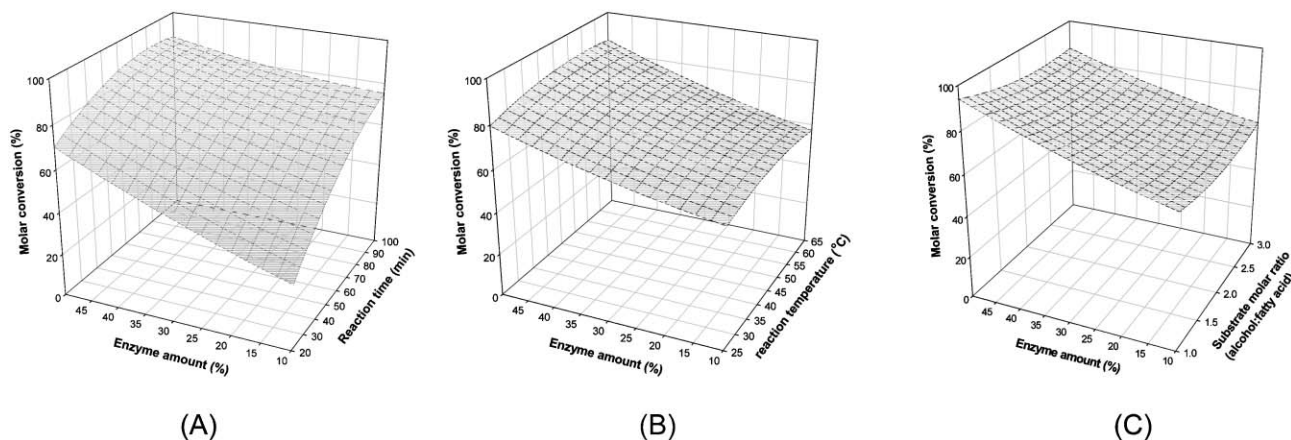


Fig. 2 Response surface plot showing the effect of (A) enzyme amount, reaction time, and their mutual interaction on hexyl laurate synthesis, (B) the effect of enzyme amount, reaction temperature, and their mutual interaction on hexyl laurate synthesis, and (C) the effect of substrate molar ratio, enzyme amount, and their mutual interaction on hexyl laurate synthesis.

The effect of varying enzyme amount and substrate molar ratio on esterification at constant reaction time (60 min) and reaction temperature (45 °C) is shown in Fig. 2C. At any given substrate molar ratio (1 : 1–1 : 3; alcohol : fatty acid), an increase in enzyme amount tends toward higher yields. Under reaction conditions of lowest substrate molar ratio (1 : 1) and highest enzyme amount (50%; 1.2 BAUN), the maximal yield (94%) was obtained, but an increase in substrate molar ratio from 1.0 to 3.0 resulted in slightly reduced esterification

efficiency at any given enzyme amount, indicating that the concentration of lauric acid wouldn't inhibit the activity of Lipozyme IM-77.

The relationships between reaction factors and response can be better understood by examining the planned series of contour plots (Fig. 3) generated from the predicted model (eqn. (2)) by holding constant enzyme amount (20, 30, 40%) and substrate molar ratio (1 : 1.5, 1 : 2, 1 : 2.5). Figs. 3(A–C) represent the same substrate molar ratio (1 : 1.5); and A, D,

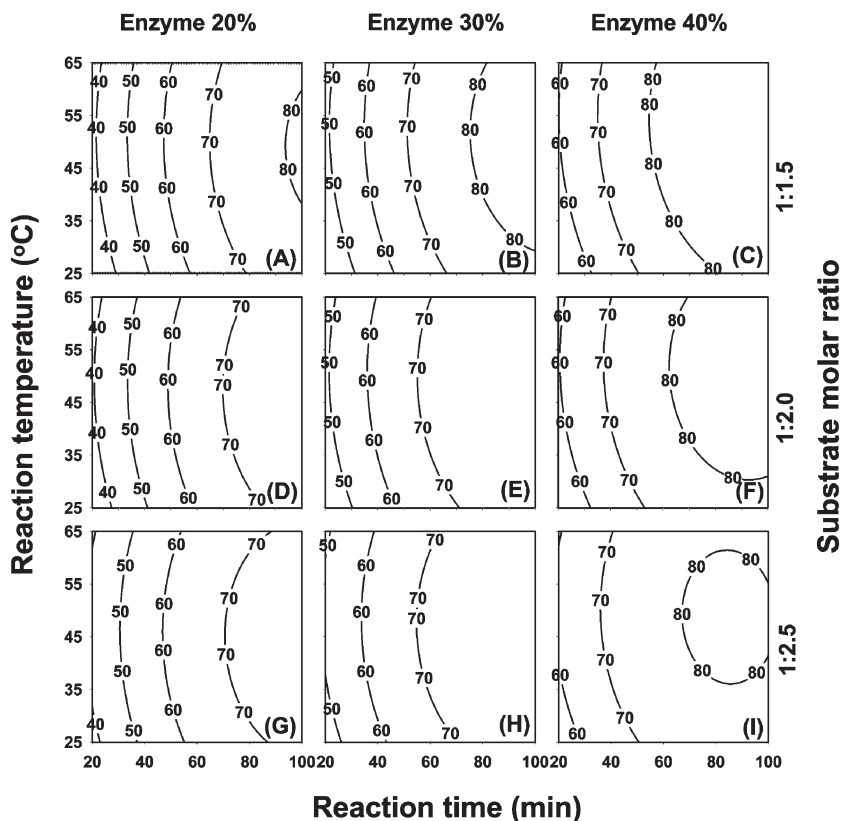


Fig. 3 Contour plots of percent molar conversion of hexyl laurate (the numbers inside the contour plots indicate molar conversions at given reaction conditions).

Table 3 Estimated ridge of maximum response for variable percent molar conversion

Coded radius	Estimated response (% conversion)	Standard error	x_1 /min	x_2 /°C	x_3 (%)	x_4 (hexanol/lauric acid)
0	71.81	2.88	60.00	45.00	30.00	2.00
0.2	75.70	2.80	65.50	45.41	32.78	1.96
0.4	79.26	2.60	69.56	45.93	35.96	1.89
0.6	82.72	2.49	72.17	46.52	39.27	1.78
0.8	86.27	2.82	73.77	47.15	42.49	1.65
1.0	90.00	3.81	74.80	47.78	45.51	1.51

and G represent the same enzyme amount (20%). Such an application could be adopted to study the synthesis variables simultaneously in a five-dimensional space. Reaction time (x_1) and enzyme temperature (x_2) were important variables for hexyl laurate synthesis and considered as indicators of effectiveness and economical performance. In general, all nine contour plots in Fig. 3 exhibited similar behavior in that predicted molar conversion increased with reaction time. Otherwise, the lower substrate molar ratio around 1 : 1.5 gave higher percent molar conversion in a shorter reaction time than 1 : 2 and 1 : 2.5. This means that the reaction with 40% (0.96 BAUN) enzyme and substrate molar ratio 1 : 1.5 (Fig. 3C) was suggested as the optimal condition for enzymatic biosynthesis of hexyl laurate which represented higher predicted molar conversion than the others in Fig. 3(C).

Attaining optimum conditions

The optimum point was determined by ridge max analysis.⁹ The method of ridge analysis computes the estimated ridge of maximum response for increasing radii from the center of original design. The ridge max analysis (Table 3) indicated that maximum molar conversion was $90\% \pm 3.8\%$ at 74.8 min, 47.8 °C, 1 : 1.5 substrate molar ratio, and 45.5% (0.96 BAUN) enzyme amount.

Model verification

The validity of the predicted model was examined by experiments at the suggested optimum synthesis conditions and 3 center points of CCRD (treatment no. 9, no. 18, and no. 27). The predicted value was 90% obtained by ridge max analysis and the actual value was $92.2 \pm 2.6\%$. Chi-square tests (p -value = 0.981, degrees of freedom = 5) indicated that observed values were significantly the same as the predicted values and the generated model adequately predicted the percent molar conversion.¹⁰ Thus, the optimization of

lipase-catalyzed synthesis of hexyl laurate by Lipozyme IM-77 was successfully developed by CCRD and RSM.

Acknowledgements

This research was supported by the National Science Council (NSC-89-2313-B-212-005), Taiwan, the Republic of China.

Shu-Wei Chang,^a Jei-Fu Shaw,^{abc} Kun-Hsiang Yang,^d Ing-Lung Shih,^e Chih-Han Hsieh^f and Chwen-Jen Shieh^g

^aInstitute of Bioscience and Biotechnology, National Taiwan Ocean University, Keelung, 202, Taiwan

^bDepartment of Food Science and Biotechnology, National Chung Hsing University, Taichung, 402, Taiwan

^cInstitute of Botany, Academia Sinica, Nankang, Taipei, 115, Taiwan

^dVedan Enterprise Corporation, Shalu, Taichung, 433, Taiwan

^eDepartment of Environmental Engineering, Dayeh University, Da-Tsuen, Chang-Hua, 515, Taiwan

^fDepartment of Bioindustry Technology, Dayeh University, Da-Tsuen, Chang-Hua, 515, Taiwan. E-mail: cjshieh@mail.dyu.edu.tw;

Fax: +886-4-851-1316

References

- 1 T. Mitsui, *New Cosmetic Science*, Elsevier Science, Amsterdam, 1998.
- 2 Y. Inada, H. Nishimura, K. Takahashi, T. Yoshimoto, A. R. Saha and Y. Saito, *Biochem. Biophys. Res. Commun.*, 1984, **122**, 845.
- 3 P. J. Halling, *Biotechnol. Bioeng.*, 1990, **35**, 691.
- 4 R. H. Valivety, G. A. Johnston, C. J. Sucking and P. J. Halling, *Biotechnol. Bioeng.*, 1991, **38**, 1137.
- 5 Y. K. Twu, I. L. Shih, Y. H. Yen, Y. F. Ling and C. J. Shieh, *J. Agric. Food Chem.*, 2005, **53**, 1012.
- 6 C. M. L. Carvalho, M. L. M. Serralheiro, J. M. S. Cabral and M. R. Aires-Barros, *Enzyme Microb. Technol.*, 1996, **21**, 117.
- 7 S. Bourg-Garros, N. Razafindramboa and A. A. Pavia, *J. Am. Oil Chem. Soc.*, 1997, **74**, 1471.
- 8 W. G. Cochran and G. M. Cox, *Experimental Designs*. Wiley, New York, 1992.
- 9 SAS, *SAS User Guide*, SAS Institute, Cary, 1990.
- 10 L. Ott, *An Introduction to Statistical Methods and Data Analysis*, PWS-Kent Publishing, Boston, 1988.

A novel highly active biomaterial supported palladium catalyst

Mark J. Gronnow,^a Rafael Luque,^b Duncan J. Macquarrie^a and James H. Clark^{*a}

Received 25th January 2005, Accepted 15th April 2005

First published as an Advance Article on the web 18th May 2005

DOI: 10.1039/b501130b

We have developed an expanded starch supported palladium catalyst which is highly active in Suzuki, Heck and Sonogashira reactions.

Introduction

Palladium catalysed methods of forming new C–C bonds are extremely useful to the chemical industry. Since their discovery in 1981¹ they have rapidly evolved into a general technique capable of coupling many different substrates under many conditions.

In the last few years, much work has been devoted to metal catalysed coupling reactions. The use of these reactions for synthesizing better and more complicated molecules suitable as intermediates for the preparation of natural compounds, pharmaceuticals and molecular organic materials has been widespread.^{2,3}

One of the most important advances in this area has been the immobilisation of ligands and highly active metal catalysts onto insoluble supports. The heterogeneous catalysts have been proven to offer similar levels of activity to their homogeneous counterparts whilst eliminating the need for an extensive work-up and preventing the metal from being found in the product. Much work in the area of carbon–carbon bond forming reactions has focused on using phosphine based ligand systems, as these tend to be more active. Phosphine ligands are notoriously difficult to manufacture as they are either air/moisture sensitive or have air/moisture sensitive intermediates in addition to being highly toxic. A further disadvantage, which represents a particularly serious drawback for supported complexes, is the propensity of the phosphine to oxidise, something which is, for practical purposes, irreversible. In this paper we propose a new support for a recently developed highly active bidentate nitrogen ligand.^{4–7}

Clay,⁸ silica,⁴ and mesoporous silicas such as MCM-41⁹ are well established supports for many catalysts including palladium, however we, and others, are beginning to study the use of porous biomaterials for this purpose. Biomaterials can make suitable supports for many reagents and catalysts; they offer the advantages of being renewable and biodegradable, as well as being relatively cheap and of low toxicity. To date chitosan derived from the shells of crustaceans has been proven to be a suitable support for palladium.^{10–15}

We have recently developed expanded starch as a novel catalyst support¹⁶ and as a chromatographic medium.^{17,18} Various surface modifications have been made to the starch, including attachment of amino-moieties. From this point we decided to build Schiff bases onto the surface for chelating

palladium.^{4,5,7} The proposed structure of the new catalyst, StarCat, is shown in Fig. 1.

In this paper, we describe the preparation and application of this catalyst in three of the most commonly used C–C bond forming reactions—the Suzuki,¹ the Heck^{19,20} and the Sonogashira reactions.²¹

Experimental

All chemicals were used as received from suppliers unless otherwise stated. Quantitative analysis was carried out with an internal standard method. Reactions were monitored at regular intervals by filtering a few drops of reaction mixture dissolved in 1 ml DCM through a tissue plug in a pasteur pipette and submitting them for analysis. Monitoring was carried out using a Varian 3800 GC with an 8200 autosampler and computer control. The microwave used was a CEM Discover system with PC control.

Catalyst preparation

The expanded starch was produced according to the procedure outlined in the literature.¹⁷

The expanded starch (4.23 g) was added to a round bottom flask containing 35 ml toluene (sodium dried) and stirred under argon. 4.82 g (5 mmol g⁻¹) 3-aminopropyltriethoxysilane were added and the slurry refluxed for 24 hours. After this time the vessel was cooled to room temperature and 135 ml ethanol were added. The modified starch was removed by filtration and washed with excess ethanol.

The amino-modified starch from the previous step was added to a round bottom flask containing 110 ml ethanol and 0.67 g (1.3 mmol g⁻¹) 2-acetyl pyridine and refluxed under argon for 24 hours. After this time the reaction was cooled, filtered and the solids washed with excess ethanol.

The immobilised Schiff base from the previous step was added to a round bottom flask containing 110 ml acetone and

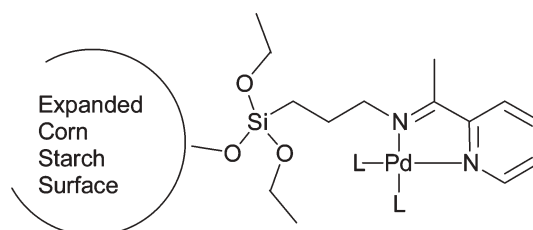


Fig. 1 StarCat.

*jhcl@york.ac.uk

1.33 g (1.3 mmol g⁻¹) palladium acetate, the mixture was stirred overnight at room temperature under argon. Following the reaction, the catalyst was filtered, washed with excess acetone and dried on a vacuum line at room temperature (4.51 g yield).

To remove any physisorbed palladium and ensure heterogeneous activity the catalyst was conditioned prior to use. This involved refluxing the catalyst in acetonitrile, ethanol and toluene for a total of 27 hours (3 × 3 hours per solvent).

Characterisation

Surface area analysis was carried out using a Micromeritics SA 3100 porosimeter. Degassing was carried out at 65 °C for 180 minutes for each sample. Elemental analysis was carried out using University of Newcastle ACMA ICP service. SEM images were obtained using a Sirian FEI microscope with EDAX analyser. TEM was carried out using a FEI Techna 12 BioTwin CIS MegaView III. Diffuse reflectance IR was carried out using a Bruker Equinox 55 with DRIFT optical configuration. A hot filtration test was carried out by stopping a standard Suzuki coupling after 10 minutes and passing the reaction mixture through a bed of celite in a jacketed pressure filter. The reaction liquors were returned to the reaction vessel and another charge of base added. The reaction was then allowed to continue with regular sampling. STA was carried out using a PL Thermal Sciences STA 625, ramping from room temperature to 625 °C at 10 °C min⁻¹.

Suzuki reaction

In a standard Suzuki coupling 0.2 g of StarCat, 0.79 g (1 mol equiv.) bromobenzene, 0.91 g (1.1 mol equiv.) benzene boronic acid, 1.38 g (7 mol equiv.) potassium carbonate and 13 ml mixed xylene were added to an appropriately sized 3 necked flask equipped with a condenser and suba seal through which argon was flowed over the reaction mixture. The mixture was stirred at 140 °C and sampled at regular intervals.

Heck reaction

In a standard Heck coupling 0.2 g of StarCat, 1.65 ml (1 mol equiv.) iodobenzene, 1.35 ml (1 mol equiv.) methyl acrylate, 2.1 ml (1 mol equiv.) triethylamine and 15 ml xylene were added to an appropriately sized 3 necked flask equipped with a condenser and suba seal through which argon was flowed over the reaction mixture. The mixture was stirred at 140 °C overnight and sampled at regular intervals.

Sonogashira reaction

A two-necked flask equipped with a condenser was charged with the alkyne (phenylacetylene, 1 mmol), DABCO (2 mmol, 224 mg), and the desired iodoarene (2 mmol). The mixture was pre-heated to 100 °C in an oil bath when StarCat (33 mg ~1 mol%) was added. The reaction was almost complete; after stirring for 30 minutes at 100 °C and the colour of the solution gradually turned to deep red–brown. After cooling, the catalyst was easily recovered by filtration and subsequently washed with methanol and gently dried under vacuum (70 °C) before reuse.

Results and discussion

Catalyst characterisation

The catalyst has been characterised using a number of different complementary techniques. Changes to the surface area were tracked through the preparation procedure. The initially supplied corn starch had a surface area less than 2 m² g⁻¹ (the limit of the instrument). Following the expansion procedure¹⁷ the surface area was increased to 196.1 m² g⁻¹. Subsequently, the surface area decreased in a stepwise fashion during the modification process, AMP-Starch (137.1 m² g⁻¹), Schiff-base on starch (57.9 m² g⁻¹) and StarCat (35.4 m² g⁻¹) and ultimately the conditioned StarCat (33.5 m² g⁻¹). During the modification the surface area is reduced due to the surface being covered with groups and to a lesser degree the pores collapsing as the solvent is removed as discussed in the literature.^{17,18} The surface area is also likely to have been reduced by the mechanical action of stirring the reaction, breaking down any fragile structures. The catalyst was found to maintain a surface area of around 30 m² g⁻¹ during use and reuse.

The IR spectrum of the catalyst was measured and is shown in Fig. 2. The spectrum is compared against a background of expanded starch to remove the contribution from the backbone. The spectrum shows the characteristic peaks at 1660 cm⁻¹ for the imine group.

The physical form of the catalyst was characterised using SEM—an image is shown in Fig. 3. StarCat is a fine

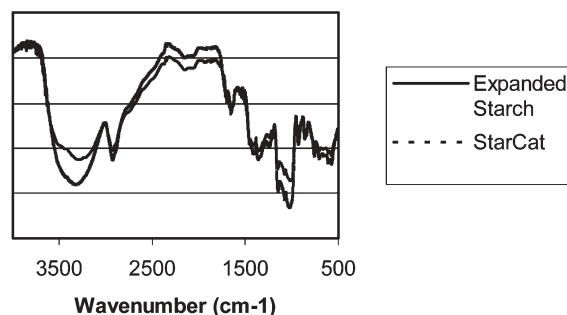


Fig. 2 DRIFT spectra of StarCat.

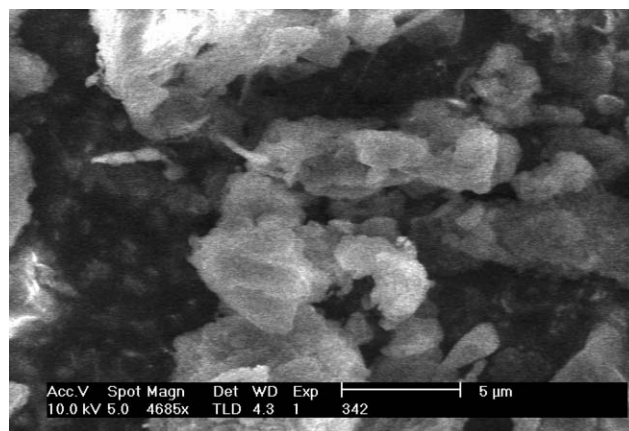


Fig. 3 SEM image of StarCat.

homogeneous powder, beige in colour. As can be seen from the image, the support has maintained the porous structure observed with the expanded starch.¹⁸ The TEM images of the catalyst (Fig. 4) showed it to contain dispersed nanoclusters of palladium around 10 nm across. This is in contrast to the silica-based materials, where no such Pd(0) component is seen. The silica catalysts have been proven by XPS to have all Pd(II) therefore the metal is bound into the ligand. Here in the starch catalyst loadings of ligand is much lower around 0.079 mmol g⁻¹, therefore the palladium is becoming reduced to Pd(0) during the conditioning or by the starch surface. The Pd(0) nanoclusters are then becoming stabilised by the support material and able to act catalytically, the binding of platinum group metals to polysaccharides has been observed by other workers.¹⁹ The EDX spectra of the powder was taken at random points on the surface. Due to the high carbon and hydrogen concentrations from the starch, integration of nitrogen proved to be difficult (as nitrogen lies between carbon and hydrogen). Therefore the loading was observed from looking at the ratio of silicon to palladium. The ratio varied from 1 : 1 to 2 : 1. This indicates in some areas of the catalyst every aminopropyl site has been fully modified to the desired catalyst and in others the modification stopped at the aminopropyl or Schiff base stage. The accurate palladium loading was obtained by ICP analysis, the loading was determined to be 0.079 mmol g⁻¹ Pd.

Conditioning

Conditioning is essential for removal of any physisorbed palladium on the starch surface. All three reactions afforded 100% yields in rapid times prior to the conditioning step, however, the reaction liquors were becoming visibly contaminated with palladium and the catalyst decoloured. A conditioning procedure previously successfully used in the literature for conditioning a similar catalyst⁶ was used. A slight deterioration (<10%) in surface area was observed, thus the three dimensional structure of the material at this stage is relatively stable.

The heterogeneous nature of the catalysis was proved using ICP analysis and a hot filtration test. The reaction mixture was

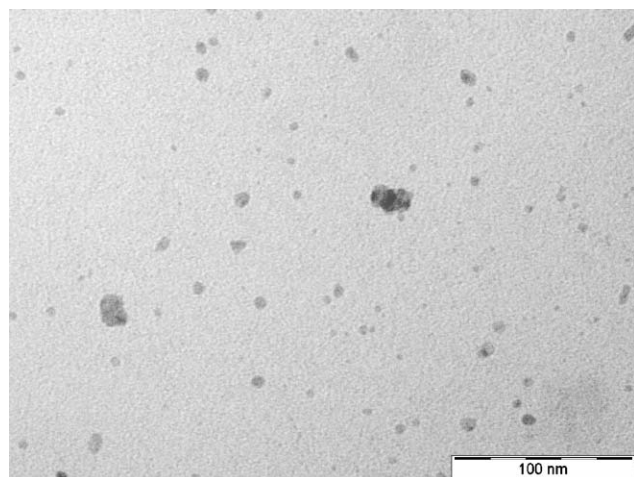


Fig. 4 TEM image of StarCat.

filtered and extracted into concentrated aqueous acid to extract any leached palladium. The acidic layer was analysed by ICP, no palladium was observed. Furthermore a hot filtration test was used to prove the catalyst was not leaching. The reaction profile for a Suzuki coupling is shown in Fig. 5, it can clearly be seen that with no catalyst in the reaction no further reaction is observed. Further hot filtration tests were carried out using the Heck and Sonogashira conditions, again no reaction was observed following the removal of the catalyst. This indicates that the palladium is strongly bound to the surface and no significant quantities of metal are lost to the reaction liquors during the process.

The STA analysis of StarCat shows the catalyst to contain 1–2% water and to be thermally stable to around 400 °C which correlates with the starch decomposition.

Suzuki reaction

The Suzuki reaction, shown in Fig. 6, is one of the classic routes to new C–C bonds *via* palladium catalysis.¹ The test reaction used was the synthesis of biphenyl (3) from bromobenzene (2 R = H X = Br) and benzene boronic acid (1). The reaction shown in Fig. 5 is usually carried out at a temperature of 90 °C⁶ however it was found that low (<10%) conversion was observed at this temperature. This unusual result has previously been observed with another biomaterial based catalyst, chitosan.¹² Increasing the temperature to 140 °C gave the observed yields. The yield at the higher temperature was 100% in 7 hours with no side products observed. The blank reaction of these two reagents gave no detectable yield of biphenyl after 24 hours.

Reuse of StarCat in the Suzuki reaction was very interesting and the results are shown below in Table 1. The reuses were carried out by running the coupling experiment for 24 hours then washing the catalyst thoroughly with dichloromethane then ethanol. The results show the catalyst does become deactivated with time. However the physical form of the catalyst had changed from a free-flowing powder to brittle flakes, indicating that the catalyst structure has collapsed. This

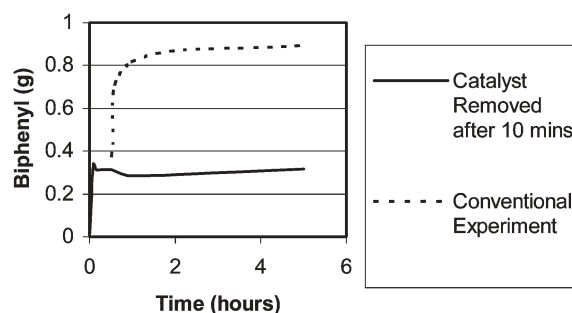


Fig. 5 Hot filtration reaction profile.

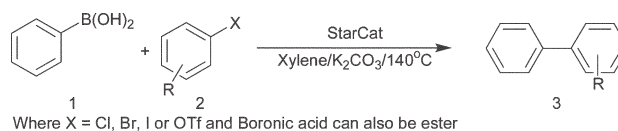


Fig. 6 A Suzuki coupling.

Table 1 Reuses of StarCat in a Suzuki coupling

Run	Initial yield ^a	Final yield ^b
1	95	100
2	100	100
3	80	45
4	17	24

^a Yield after 30 min. ^b Yield after 24 h.

is likely to be due to moisture entering the system and collapsing the structure of the support. The use of carbonate as base generates water. It is known that the reagents have water associated with them also. It is expected that use of rigorously anhydrous conditions would reduce this problem and permit further reuses.

Heck reaction

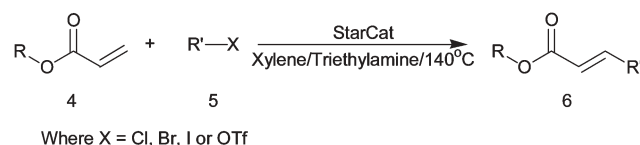
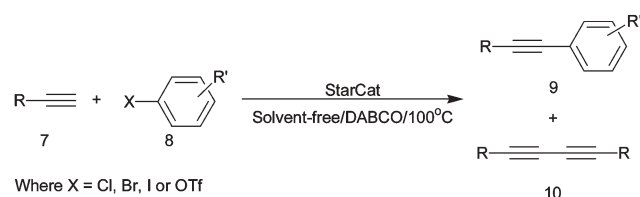
The Heck–Mizoroki reaction, shown in Fig. 7 predates the Suzuki methodology and is one of the most useful derivations of palladium chemistry.^{20,21} The Heck coupling gives us access to new larger alkenes *via* the addition of alkenes (**4**) to alkenes or arenes (**5**).

Using the test reaction system of methyl acrylate (**4** R = Me) and iodobenzene (**5** R' = phenyl X = I) StarCat again gave no yield of the desired product (**6**) at the conventional reaction temperature of 82 °C.⁶ The reaction solvent was changed from acetonitrile to xylene to allow the temperature to be increased to 140 °C as optimised in the Suzuki coupling. At this temperature the yield increased to 77% with 100% selectivity to *E*-methyl cinnamate and no side products or homo-coupling was observed. The blank reaction gave no reaction after 24 h.

The less reactive styrene couple (**4** is PhC=CH) was also carried out. A GC area yield of 65% conversion to stilbene. The selectivity was measured at 90% to the *trans* isomer.

Sonogashira reaction

The Sonogashira conditions developed the range of molecules which can be formed *via* palladium chemistry.²² In a typical Sonogashira reaction, the cross-coupling reaction of phenylacetylene (**7** R = phenyl) with different electron-poor reagents (**8**) under certain conditions was studied over StarCat (Fig. 8).

**Fig. 7** A Heck–Mizoroki coupling.**Fig. 8** A Sonogashira coupling.

Original Sonogashira methodology requires the use of a copper(I) co-catalyst and phosphine ligands. Here we propose the use of StarCat in a copper and phosphine-free route, analogous to that of Bandini *et al.*²³

Stability of the supported material was tested in the same reaction conditions (by hot filtration and ICP). Additionally, small portions of the reaction mixture were removed from the reaction from time to time and added to a solution containing only the starting materials (phenylacetylene and a second aryl halide). No coupling of these two reaction partners was observed. Through hot filtration and ICP analyses, we found that the Pd on starch catalyst was behaving as a heterogeneous catalyst irrespective of the reaction conditions (base, temperature, *etc*). In addition, as can be seen from Table 2, promising results in terms of catalytic activity (conversion and selectivity towards the selected product) were found when using this catalyst in the Sonogashira reaction (see entries 3 to 7). The coupling reaction takes place within an hour and conversion levels higher than 90% of the main coupling product were found for certain substrates. Likewise, no significant amount of homocoupling products were found in either of them (see entries 3 to 7).

The reaction is proven to require catalysis as when StarCat is not added to the reaction mixture a zero yield was observed over 2 hours.

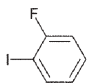
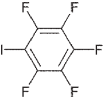
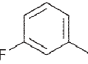
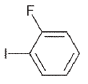
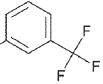
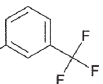
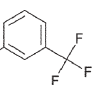
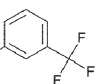
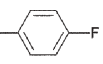
Moreover, the same reaction was carried out using microwave heating, Table 3. For the microwave reactions, several attempts were made in order to optimise all the microwave variables (temperature, power, pressure, time, *etc*). The common method for the microwave reactions was as follows: ramp time 3 min, hold time 5 min, temperature 80–170 °C with power being varied between 30–300 W. In this sense, we found interesting conversion values when using medium power (100–200 W) at a fixed temperature (170 °C) but lower yields were found when experiments were carried out at a lower power (30–100 W) and lower temperature (80–120 °C) (entries 3 to 6).

TON/TOF

The turnover numbers have been calculated in the traditional method (moles product per mole of palladium), subsequently turnover frequencies have been calculated *via* the TON per unit time. The results are shown in Table 4. For the Suzuki and Heck reactions the profile shows a rapid initial rate followed by a slowing of product formation up to the maximum yield; because of this we measured the TOF for the initial 53% (4 hours) when the product formation was rapid. The TON quoted for the Suzuki and Heck reaction is based on the final maximum product yield. The reaction profile for the Sonogashira reaction showed a more even build-up of product therefore the metrics quoted are for the end of the reaction. As indicated before, the TON is likely to be significantly higher when reuse is included, and especially if an optimised recovery and reactivation method is developed.

The Sonogashira TOF under microwave conditions is excellent due to the short reaction times employed to achieve high yields. The TON for all reactions are excellent, this is due to the low loaded catalyst. The starch support does not seem suited to extremely high loadings, 0.5 mmol g⁻¹ was attempted

Table 2 Sonogashira screening of electron poor reagents over StarCat catalyst^a

Run	Starting material (8)	Conversion (%)	Product ratio	
			9	10
1 ^b		35	100	—
	1-iodo 2-fluorobenzene			
2 ^b		25	75	25
	1-iodopentafluorobenzene			
3 ^{b,c}		45	98	2
	1-iodo 3-fluorobenzene			
4 ^c		53	98	2
	1-iodo 2-fluorobenzene			
5 ^c		80	98	2
	3-iodobenzotrifluoride			
6		>98	100	—
	3-iodobenzotrifluoride			
7 ^c		>95	100	—
	3-iodobenzotrifluoride			
8 ^{c,d}		80	100	—
	3-iodobenzotrifluoride			
9 ^c		65	98	2
	1-iodo 4-fluorobenzene			


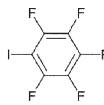

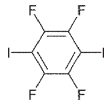
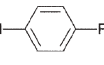
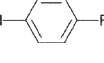
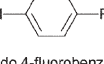
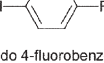
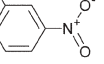
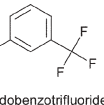
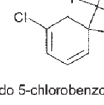
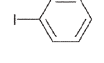
^a 1 equiv. phenylacetylene, 2 equiv. arylhalide, 2 equiv. DABCO, 1 mol% StarCat, 100 °C, <1 h. ^b TEA at 70 °C (12 h reaction time) was used instead of DABCO. ^c Phenylacetylene–arylhalide ratio 1 : 1. ^d DABCO at 70 °C.

but the final bound quantity of palladium was merely 0.079 mmol g⁻¹. The Suzuki reaction, which is very close to completion after only 30 minutes, gives an extremely high TOF of 310 h⁻¹ at this point.

Conclusion

In conclusion, we have demonstrated StarCat to be an active catalyst for a range of palladium mediated reactions. It is capable of performing well under microwave irradiation. The

Table 3 Microwave experiments with the Sonogashira system over StarCat^a

Run	Starting material (8)	Conversion (%)	Microwave conditions	Product ratio	
				9	10
1		90	Power 100 W Temp 170 °C Hold time 5 min	96	4
	1-iodopentafluorobenzene				
2 ^b		75	Power 30 W Temp 170 °C Hold time 5 min	73	27
	1-iodopentafluorobenzene				
3		25	Power 100 W Temp 80 °C Hold time 5 min	80	20
	1-iodopentafluorobenzene				
4		40	Power 100 W Temp 80 °C Hold time 15 min	84	16
	1-iodopentafluorobenzene				
5		<15	Power 100 W Temp 80 °C Hold time 5 min	100	—
	1-iodo 4-fluorobenzene				
6 ^c		50	Power 300 W Temp 80 °C Hold time 15 min	10 ^c	20 ^c
	1-iodo 4-fluorobenzene				
7		40	Power <50 W Temp 170 °C Hold time 5 min	80	20
	1-iodo 4-fluorobenzene				
8 ^b		75	Power 80 W Temp 170 °C Hold time 5 min	80	20
	1-iodo 4-fluorobenzene				
9 ^b		40	Power 30 W Temp 170 °C Hold time 5 min	10	90
	3-nitroiodobenzene				
10 ^b		85	Power 100 W Temp 120 °C Hold time 5 min	100	—
	3-iodobenzotrifluoride				
11 ^b		90	Power 70 W Temp 120 °C Hold time 5 min	100	—
	1-iodo 5-chlorobenzotrifluoride				
12 ^b		85	Power 120 W Temp 170 °C Hold time 5 min	98	2
	1-iodo 2-fluorobenzene				

^a 1 equiv. phenylacetylene, 1 equiv. arylhalide, 4 equiv TEA, 1 mol% StarCat, 5 min. ^b DABCO was used instead of TEA. ^c Dimer and crossed-coupling products were found extensively.

Table 4 Turnover numbers and frequencies for StarCat

Reaction	TON ^a	TOF/h ^{-1b}
Suzuki	378	310
Heck	639	109.8
Sonogashira ^c – microwave	326	3928
Sonogashira ^c – thermal	384	767

^a Maximum TON from reaction at 24 h. ^b TOF from initial rate, from change in slope of reaction profile. ^c Average TON, TOF from end of reaction.

catalyst offers significant advantages over inorganic supported catalysts as the palladium is considerably simpler to recover from the spent catalyst.

Acknowledgements

The authors would like to thank the biomaterials group of the Clean Technology Centre at York for provision of the expanded starch. Paul Elliott, Mark Harriman and Meg Stark are thanked for help with the analysis. MJG would like to thank GlaxoSmithKline P.L.C. for their financial support. RLA would like to thank Dirección General de Investigación (Project BQU2001-2605) and Ministerio de Educacion, Cultura y Deporte for financial assistance and also the Organic Chemistry department from Universidad de Cordoba (UCO).

Mark J. Gronnow,^a Rafael Luque,^b Duncan J. Macquarrie^a and James H. Clark^{*a}

^aClean Technology Centre, Department of Chemistry, University of York, Heslington, York, UK YO10 5DD. E-mail: jhc1@york.ac.uk; Fax: +44 1904 432705; Tel: +44 1904 432559

^bDepartamento de Química Organica, Universidad de Córdoba, Campus de Rabanales, Edificio Marie Curie (C-3), Ctra. N-IV Km. 396, 14014-Córdoba, Spain. E-mail: q62alsor@uco.es; Tel: +34 957218623

References

- N. Miyaura, T. Yanagi and A. Suzuki, *Synth. Commun.*, 1981, **11**, 513.
- N. E. Leadbeater and M. J. Marco, *Org. Chem.*, 2003, **68**, 5660.
- I. Patterson, R. D. Davies and R. Marquez, *Angew. Chem., Int. Ed.*, 2001, **40**, 603.
- J. H. Clark, D. J. Macquarrie and E. B. Mubofu, *Green Chem.*, 2000, **2**, 53.
- E. B. Mubofu, J. H. Clark and D. J. Macquarrie, *Green Chem.*, 2001, **3**, 23.
- E. B. Mubofu, *DPhil Thesis*, 2001, University of York.
- S. Paul and J. H. Clark, *Green Chem.*, 2003, **5**, 635.
- K. Ravi Kumar, B. M. Choudary, Z. Jamil and G. Thyagarajan, *J. Chem. Soc., Chem. Commun.*, 1986, 130.
- A. Corma, H. Garcia and A. Legua, *Appl. Catal., A: Gen.*, 2002, **236**, 179.
- F. Quignard, A. Choplin and A. Domard, *Langmuir*, 2000, **16**, 9106.
- P. Buisson and F. Quignard, *Aust. J. Chem.*, 2002, **55**, 73.
- J. J. E. Hardy, S. Hubert, D. J. Macquarrie and A. J. Wilson, *Green Chem.*, 2004, **6**, 53.
- M. Adlim, M. A. Bakar, K. Y. Liew and J. Ismail, *J. Mol. Catal. A: Chem.*, 2004, **212**, 141.
- T. Vincent and E. J. Guibal, *Environ. Manage.*, 2004, **71**, 15.
- D. J. Macquarrie, J. J. E. Hardy, S. Hubert, A. J. Deveaux, M. Bandini, R. L. Alvarez and M. Chabrel, *Feedstocks for the Future*, 2004, ACS Symposium Series, in press.
- S. Doi, J. H. Clark, D. J. Macquarrie and K. Milkowski, *Chem. Commun.*, 2002, 2632.
- J. H. Clark, F. E. I. Deswarte, J. J. E. Hardy, A. J. Hunt, F. M. Kerton and K. Milkowski, *PCT Patent Application*, PCT/GB2004/003276, 2004.
- V. Budarin, F. E. I. Deswarte, J. J. E. Hardy, A. J. Hunt, F. M. Kerton, K. Milkowski and J. H. Clark, *Chem. Commun.*, in press.
- D. S. Dos Santos, P. J. Goulet, N. P. Pieczonka, O. N. Oliveira and R. F. Aroca, *Langmuir*, 2004, **20**, 10273; H. Huang and X. Yang, *Biomacromolecules*, 2004, **5**, 2340; H. Huang and X. Yang, *Carbohydr. Res.*, 2004, **339**, 2627.
- T. Mizoroki, K. Mori and A. Ozaki, *Bull. Chem. Soc. Jpn.*, 1971, **44**, 581.
- R. F. Heck, *J. Am. Chem. Soc.*, 1971, **93**, 6896.
- K. Sonogashira, *J. Organomet. Chem.*, 2002, **653**, 46.
- M. Bandini, D. J. Macquarrie, R. Luque and V. Budarin, manuscript in preparation.

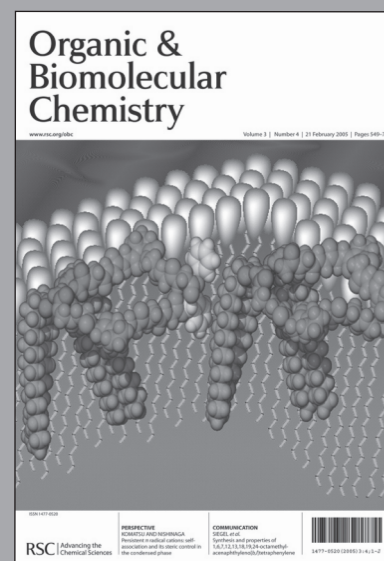
Call for papers

Organic & Biomolecular Chemistry

A major peer-reviewed international, high quality journal covering the full breadth of synthetic, physical and biomolecular organic chemistry.

Publish your review, article, or communication in OBC and benefit from:

- The fastest times to publication (80 days for full papers, 40 days for communications)
- High visibility (OBC is indexed in MEDLINE)
- Free colour (where scientifically justified)
- Electronic submission and manuscript tracking via ReSource (www.rsc.org/ReSource)
- A first class professional service
- No page charges



Submit today!

www.rsc.org/obc

RSC | Advancing the
Chemical Sciences

Find a SOLUTION

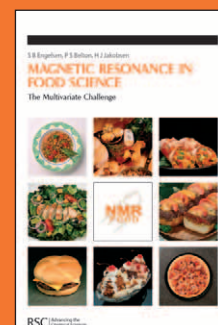
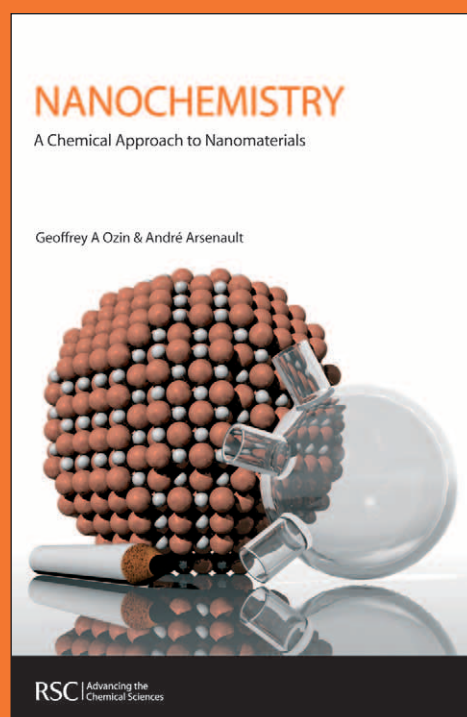
... with books from the RSC

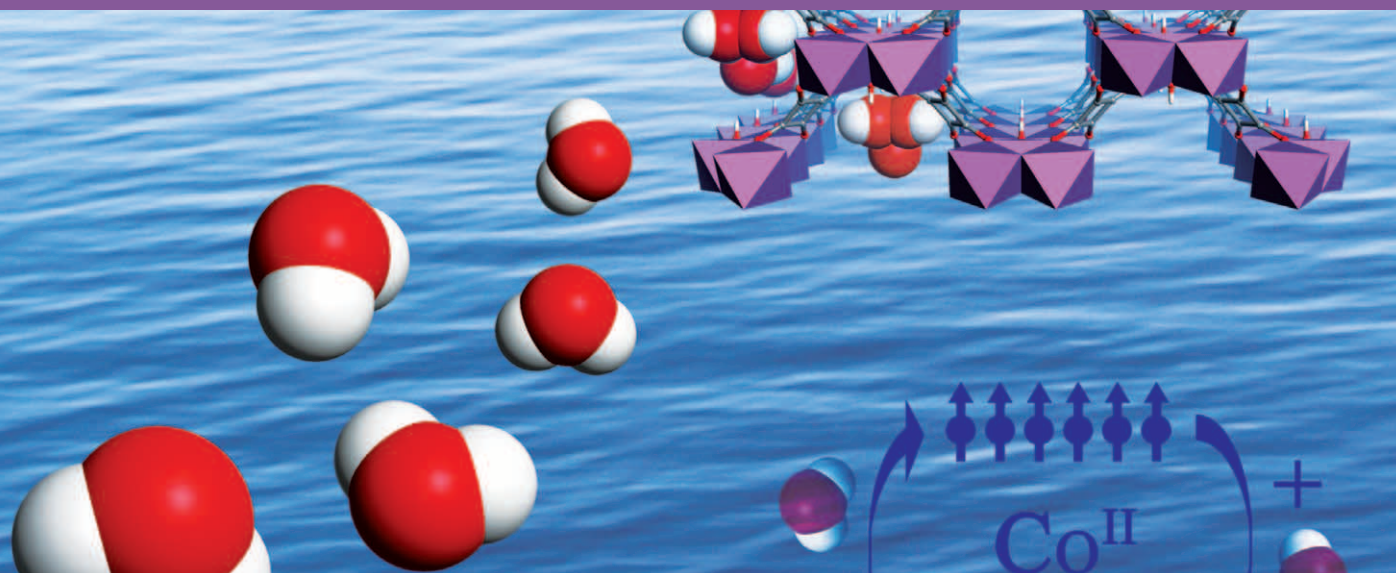
Choose from exciting textbooks, research level books or reference books in a wide range of subject areas, including:

- Biological science
- Food and nutrition
- Materials and nanoscience
- Analytical and environmental sciences
- Organic, inorganic and physical chemistry

Look out for 3 new series coming soon ...

- RSC Nanoscience & Nanotechnology Series
- Issues in Toxicology
- RSC Biomolecular Sciences Series





ChemComm

The leading international journal for the publication of communications on important new developments in the chemical sciences.

- Weekly publication
- Impact factor: 4.031
- Rapid publication – typically 60 days
- 3 page communications – providing authors with the flexibility to develop their results and discussion
- 40 years publishing excellent research
- High visibility – indexed in MEDLINE
- Host of the RSC's new journal, *Molecular BioSystems*

